Technical Report

CRWR 264

AN EVALUATION OF THE FACTORS AFFECTING THE QUALITY OF HIGHWAY RUNOFF IN THE AUSTIN, TEXAS AREA

by

LYNTON B. IRISH, JR., P.E.

WILLIAM G. LESSO, Ph.D.

and

MICHAEL E. BARRETT, M.S.,
Project Manager

JOSEPH F. MALINA, JR., P.E.
Principal Investigator

and

RANDALL J. CHARBENEAU, P.E.
GEORGE H. WARD, Ph.D.
Co-Principal Investigators

September 1995

CENTER FOR RESEARCH IN WATER RESOURCES

Bureau of Engineering Research • The University of Texas at Austin
J.J. Pickle Research Campus • Austin, TX 78712

ACKNOWLEDGMENTS

This research was funded by the Texas Department of Transportation (TxDOT) and the Civil Engineering Department at the University of Texas at Austin through grant number 7-1943, “Water Quantity and Quality Impacts Assessment of Highway Runoff and Construction in the Austin, Texas Area.”

TABLE OF CONTENTS

LIST OF TABLES

LIST OF FIGURES

1.0 Conclusions and Recommendations

The Center for Research in Water Resources at The University of Texas at Austin has conducted a four-year investigation of the quality of storm water runoff from existing highway pavements in and near the recharge zone of the Barton Springs segment of the Edwards Aquifer. The two goals of this research project were to identify the variables that affect the build-up and wash-off of constituents from highways in the Austin, Texas area and to develop a water quality model that incorporates these variables. The research was funded by the Texas Department of Transportation and the Department of Civil Engineering at The University of Texas at Austin through grant number 7-1943, "Water Quantity and Quality Impacts Assessment of Highway Construction in the Austin, Texas Area."

Isolation of the variables that influence highway runoff quality is facilitated during "steady-state" storm conditions (e.g., a constant rate of constituent input from rainfall and traffic). A unique rainfall simulator was used to produce steady-state storm events during this research. The rainfall simulator provided a uniform rainfall over a 230-meter length of 3-lane highway during periods of active traffic. The entirety of the runoff drained to a single curb inlet where water quality samples were collected throughout the simulation. The length of highway exposed to the artificial rainfall allowed for collection of water that had washed from the bottoms of the moving vehicles. This project marked the first scientific use of a rainfall simulator in conjunction with active traffic.

Thirty-five rainfall simulations were conducted between July 6, 1993 and July 14, 1994. Additionally, 23 natural storm events were sampled at the same location between September 14, 1993 and April 28, 1994. Statistical analysis showed no significant difference between the runoff generated by the rainfall simulator and the natural runoff. The samples collected during simulated and natural storm events combined to provide 423 storm water runoff observations. Furthermore, 21 variables were identified for each storm event, and multiple regression analysis was used to determine the relationship of each variable to the quality of the highway runoff. The variables found to be statistically significant were retained for use in a constituent-specific regression model.

The majority of variations observed in highway storm water loading in the Austin area may be explained by causal variables measured during the rain storm event, the antecedent dry period, and the previous rain storm event. Significant causal variables during the rainfall event include the duration of the event (min), the volume of runoff per area of watershed (L/m^2), the intensity of the runoff per area of watershed (L/m^2/min), and the average volume of traffic per lane. The significant causal variables from the antecedent dry period include the duration of the dry period (hrs) and the average volume of traffic per lane during the dry period. The significant causal variables from the preceding storm event include the duration of the event (min), the volume of runoff per area of watershed (L/m^2) and the intensity of the runoff per area of watershed (L/m^2/min).

The identification of the causal variables that significantly influence constituent loading is among the more important findings of this study. There are two major applications of this knowledge. First, recognition of the specific variables that influence a given constituent load may suggest constituent-specific mitigation procedures, and second, the applicability of the model is directly reflected in the causal variables.

Because the dependent variable in the regression analysis is expressed as load (g/m^2), the total volume of flow during the storm event will appear in every constituent model. Similarly, the intensity of the runoff and the duration of the runoff also will frequently appear in the models. The variables flow, intensity, and storm duration, therefore, offer little diagnostic information in the interpretation of the model specification. However, the appearance of the other variables in the model, such as the number of vehicles during the storm, the duration of the antecedent dry period, and the volume of runoff during the previous storm event, are variables that "control" the constituent loading. The examination of the controlling variables in each model adds insight into the applicability of the model and the mitigation of constituent loading. A summary of selected water quality constituents and their relevant causal variables is presented in Table 1.1.

Table 1.1 Variables Affecting Pollutant Runoff Loads

	Storm Duration	Storm Volume	Storm Intensity	Vehicles During Storm	Length of Antecedent Dry Period	Antecedent Traffic Count	Previous Storm Duration	Previous Storm Volume	Previous Storm Intensity
Iron		*	*		*				
TSS		*	*		*				*
Zinc	*	*				*	*	*	*
COD	*	*	*		*	*			
Phosphorus	*	*	*			*			
Nitrate		*	*			*			
BOD_5		*	*	*		*			
Lead		*	*	*					*
Copper	*	*		*					
Oil and Grease		*		*					

As an example, 93% of the variation observed in the storm water loadings of total suspended solids (TSS) is explained by the total volume of storm water runoff (L/m^2), intensity of the runoff ($L/m^2/min$), total duration of the antecedent dry period (hrs), and the intensity of the runoff during the previous storm event ($L/m^2/min$). This model formulation suggests that the conditions during the antecedent dry period (e.g., dustfall, pavement/right-of-way maintenance activities, etc.) and the intensity of the preceding storm event (e.g., the thoroughness of the previous wash-off) have a greater influence on TSS storm water loadings than any of the other variables examined, including the traffic volume during the storm event. Efforts to mitigate the storm water loading of TSS should therefore be directed at activities during the antecedent dry period that deposit dirt and debris on the highway surface. Consequently, street sweeping was found to be effective at reducing TSS loads. Street sweeping on a once every two-week schedule, as compared to no street sweeping, significantly reduced the average loads of TSS observed in the highway storm water runoff. However, no other constituent showed a significant change in loading during the street sweeping period.

Highway runoff constituents, in general, fall into one of three categories: (1) those constituents, such as TSS, which are influenced by conditions during the dry period and may be mitigated by dry period activities such as street sweeping and others; (2) those

constituents that are most influenced by conditions during the rainfall event and may only be mitigated through the use of runoff controls; and (3) those constituents that are influenced equally by both periods. The constituents that are significantly affected by conditions during the preceding storm event generally are those constituents that are controlled by the dry period variables.

The variables found to significantly affect the other highway runoff constituents are detailed below:

- **Nutrients:** The total duration of the storm event (min), total volume of storm water runoff (L/m^2), intensity of the runoff ($L/m^2/min$), and the total volume of traffic during the antecedent dry period (a measure of the length of the dry period) combine to explain 95% of the variation in nitrate load, and 90% of the variation in total phosphorus load, observed in the highway runoff. This regression formulation is strongly influenced by the quantity of these nutrients contained in the rainfall. The concentrations of nutrients observed in rainfall accounted for 50% to 100% of the nitrate load, and up to 22% of the total phosphorus load observed in the highway runoff. The mitigation of nutrients in highway runoff requires the use of runoff controls.

- **Organics:** The total duration of the storm event (min), total volume of storm water runoff (L/m^2), runoff intensity ($L/m^2/min$), total volume of traffic during the storm, and the total volume of traffic during the antecedent dry period combine to explain 86% of the biochemical oxygen demand (BOD_5) load, 95% of the chemical oxygen demand (COD) load, 94% of the total carbon load, and 91% of the dissolved total carbon load observed in the highway runoff. The mitigation of organics must be accomplished with runoff controls.

- **Oil and Grease**: The total volume of storm water runoff (L/m^2) and the total volume of traffic during the storm combine to explain 94% of the variation in the oil and grease loads observed in the highway runoff. The mitigation of oil and grease must be accomplished with runoff controls.

- **Copper:** The total duration of the storm event (min), total volume of storm water runoff (L/m^2), and total volume of vehicles during the storm combine to explain 90% of the variation in the copper load observed in the highway runoff. The mitigation of copper must be accomplished with runoff controls.

- **Lead:** The total volume of storm water runoff (L/m^2), runoff intensity ($L/m^2/min$), total volume of vehicles during the storm, and the intensity of the previous storm runoff ($L/m^2/min$) combine to explain 68% of the variation in the lead load observed in the highway runoff. The mitigation of lead must be accomplished with runoff controls.

- **Iron:** The total volume of storm water runoff (L/m^2), runoff intensity ($L/m^2/min$) and the total duration of the antecedent dry period (hrs) combine to explain 92% of the variation in the iron load observed in the highway runoff. The mitigation of iron must be accomplished with dry period practices.

- **Zinc:** The total duration of the storm event (min), total volume of storm water runoff (L/m^2), volume of vehicles during the antecedent dry period, total duration of the previous storm (min), and the total volume of storm water runoff in the previous storm (L/m^2) combine to explain 92% of the variation in the zinc load observed in the highway runoff. The mitigation of zinc must be accomplished with both runoff controls and dry period practices.

Although traffic volume during the storm does not appear as a "significant" variable in every model formulation, it is nevertheless an influential factor in all constituent loading. The storm water constituent wash-off patterns for high speed highway pavements were found to be different during periods when traffic is on the highway than during periods when there is no traffic. The runoff from pavements with high speed traffic does not exhibit as pronounced a "first flush" of constituent mass as the runoff of pavements without traffic. The continuous input of material from traffic insures a continual increase in the cumulative constituent load throughout the duration of the storm event. As a result, highway watersheds that contain large shoulder areas or other non-traffic bearing surfaces (e.g., > 35% of the total watershed) can be expected to produce less constituent loading per unit of surface area than other highway pavements.

2.0 Introduction

2.1 Research Area

The State of Texas, through the Texas Natural Resource Conservation Commission (TNRCC), regulates all activities that have the potential to cause pollution in the Edwards Aquifer (Chapter 313 entitled "Edwards Aquifer," Subchapter B, §313.27). This rule applies to any activity that alters or disturbs surface water quality and quantity characteristics within the recharge zone of the aquifer. The construction of highways, railroads, utility services, and residential/commercial developments are all regulated activities under Chapter 313. Consequently, the Texas Department of Transportation (TxDOT) is charged with the responsibility for the control of storm water runoff from highway construction sites and from existing highways located inside the Edwards Aquifer recharge zone. Exercising this responsibility has had a profound impact on the design and construction of area highways. During fiscal year 1993, the Austin District of TxDOT spent more than $10 million on the installation and construction of temporary and permanent runoff control facilities. The cost of storm water control now accounts for as much as 20% of the overall cost of highway construction in the Edwards Aquifer recharge zone. This financial burden has placed a new importance on understanding the role of the urban highway as a non-point source of water pollution in the Austin area.

2.2 Research Objective

Controlling the cost of storm water management along highways in the Edwards Aquifer recharge zone is a major concern of TxDOT. Cost-effective and efficient management practices to mitigate the transport of harmful constituents to the aquifer are dictated by fiscal and environmental concerns. The environmental concerns in the Edwards Aquifer, in conjunction with the high cost of complying with a pollution prevention policy whose goals are not easily understood, have motivated TxDOT to undertake an extensive investigation of the water quality aspects of storm water runoff from highways in or near the Barton Springs segment of the Edwards Aquifer recharge zone. Identification of the variables that determine constituent loads in highway runoff is

the first step in determining the most cost-effective mitigation methods. Development of predictive models will further assist cost-effective analyses of highway storm water management practices in the Edwards Aquifer recharge zone.

The objectives of this research are:

- the determination of the variables that affect the build-up and wash-off of constituents from highways in the Austin, TX area,
- the development of a predictive model that incorporates the variables that affect runoff quality.

The methodology of model development is the subject of this report. The underlying theory of the build-up and wash-off of materials from highway surfaces is presented in this chapter. The rationale for data collection and the manner in which data were collected is discussed in Chapter 3. A summary of the data is presented in Chapter 4. The formulation of the model is detailed in Chapter 5; the results of the model presented are given in Chapter 6. Appendices provide supporting data and documentation.

2.3 Highway Runoff Constituents

The bulk of the material on urban roadways consists of inert minerals such as quartz, feldspar, etc. (Sartor and Boyd, 1972). The quantities of these particles correlate well with the average daily traffic count (Hvitved-Jacobson and Yousef, 1991), although atmospheric dustfall also may be a major source (Gupta et al., 1981). Stormwater runoff that carries solids from highway surfaces is undesirable for several reasons:

1. High sediment loads increase the probability of transporting nutrients, pesticides, organic constituents, and microbial forms that may be attached to the particles (Svensson, 1987; Wagner and Mitchell, 1987; Sartor and Boyd, 1972).
2. The deposition of solids can clog recharge features and restrict the flow of water into the aquifer (Guadalupe-Blanco River Authority, 1988)
3. The Edwards Aquifer contains a number of invertebrates and at least one vertebrate. The build-up of silt in submerged caverns may interfere with organism metabolism (Guadalupe-Blanco River Authority, 1988).

Several classifications of solids have been observed for highway runoff. The total solids (TS) content of a sample is defined as the amount of material remaining after evaporation of the water or a steam bath followed by drying the sample to a constant weight at 103^{o} - 105^{o}C. Total suspended solids (TSS) is the fraction of total solids that is retained on a filter with a pore size of about 1.2 micrometers (μm). Volatile suspended solids (VSS) consists of the organic fraction of TSS. Highway runoff studies typically report values for both TSS and VSS.

Organic material is the next most common constituent in highway runoff. Biodegradable organics may stimulate the growth of bacteria in receiving watercourses. In the worse case, the oxygen consumed during the biochemical oxidation of organic matter can deplete the dissolved oxygen in the receiving stream to the point of causing septic conditions and destroying populations of fish and other aquatic species that require dissolved oxygen.

The organic content of runoff may be expressed as BOD, COD, and total organic carbon (TOC). The BOD analysis is a bioassay procedure that provides suitable living conditions for bacteria to function in an unhindered fashion (i.e., all necessary nutrients for bacteria growth must be present and there must be an absence of toxic substances). The test is a direct measure of the oxygen consumed by bacteria during the oxidation of organic matter in a measured time period. Five days is the typical test period, and the results are denoted as BOD_5. Durations of up to 20 days, however, are also employed.

The COD analysis measures the ability of organic material to be reduced by a strong oxidizing agent (potassium dichromate) at an elevated temperature. Organic matter is oxidized during the test regardless of the biological assimilability of the substances. COD values are therefore greater than BOD_5 values for most compounds. The COD may be much greater when the organic matter is resistant to biological degradation.

The TOC is the total amount of organic carbon in the runoff. Carbon in runoff is oxidized to carbon dioxide with a catalyst and oxygen as the carrier gas; carbon dioxide is then measured using an infrared analyzer. The TOC analysis is rapid and is applicable to low concentrations of organic matter.

The dissolved oxygen content in natural surface waters also is affected by the input of nutrients to the water body. Nitrogen and phosphorus are the primary nutrients observed in highway runoff that can stimulate algal blooms in receiving waters. The sources of nutrients typically include atmospheric deposition and the application of roadside fertilizers (Hvitved-Jacobson and Yousef, 1991). The concentration of nitrogen and phosphorus in highway runoff is a concern for two reasons; (1) these compounds stimulate the growth of aquatic plants in surface waters and (2) excessive nitrates (NO_3) in drinking water can cause methemoglobinemia in infants.

The enrichment of a surface water with nutrients, or eutrophication, is a natural aging process that results in the increased growth of planktonic and rooted aquatic plants. During the daylight hours, aquatic plants convert inorganic nutrients and CO_2 into organic plant material through the process of photosynthesis. The process will continue as long as nutrients are available to maintain plant growth. The dissolved oxygen (DO) produced during photosynthesis is generally beneficial to the surface water ecosystem, but an over-abundance of plant growth can result in severe DO problems. Excess vegetation, in the most extreme cases, can produce exaggerated diurnal variations in dissolved oxygen that results in supersaturated levels of DO during daylight hours and extremely low levels of DO as the plants respire at night. An additional oxygen demand is exerted as the plant matter dies and decays. Excessive aquatic plant growth also may be aesthetically objectionable and can interfere with the biological, recreational, and navigational use of the water.

Phosphorus is not known to be harmful outside of stimulating plant growth. The control of phosphorus, however, may be important in areas where natural surface waters contain low concentrations of phosphorus relative to the nitrogen concentration. Both phosphorus and nitrogen are required to sustain maximum growth of aquatic plants and the nutrient that is in short supply therefore limits the growth aquatic plants. If phosphorus is the “limiting” nutrient in the receiving stream, additional discharges of phosphorus may promote new plant growth.

Nitrogen compounds can cause problems other than aquatic plant growth. Un-ionized ammonia is toxic to several species of young freshwater fish (USEPA, 1981), but the greater concern is the contamination of drinking water sources with nitrates.

Excessive nitrates in drinking water can cause methemoglobinemia in very young infants. Nitrates have a negative charge (NO_3) and, therefore, are not attracted to soils, which also have negative charges. It is for this reason that nitrogen in the form of nitrate usually reaches the ground water, where it is very mobile due to its solubility and anionic form.

Metals are the most common toxicants found in highway runoff. The sources of metals in highway runoff include vehicles, atmospheric deposition, naturally occurring metals in soils, and highway-related sources such as paint and corrosion products (Gupta et al., 1981; Yousef et al., 1886). The two major concerns with trace metals are: (1) these elements may move through soils and enter ground water and (2) metals can accumulate in the food chain. It should be noted that metals are not necessarily toxic; however, unless the concentration causes toxicity (e.g., metals at low concentrations are essential to the human diet).

The most common metals found in highway runoff are copper, iron, lead, and zinc (Sartor and Boyd, 1972; Gupta et al., 1981; USEPA, 1983; Driscoll et al., 1990). Chromium, which is found in small concentrations, is most likely in the reduced form of the chromate ion (Cr^{3+}), which is much less toxic than the highly oxidized form (Cr^{6+}) found in plating shop wastes (Driscoll et al., 1990). Arsenic, cadmium, mercury, and nickel are found in relatively insignificant amounts (Sartor and Boyd, 1972; Gupta et al., 1981). Iron is not known to be harmful; however, the iron concentrations normally observed in highway runoff are higher than those reported in natural water systems (Driscoll et al., 1990).

Pathogenic organisms that potentially are responsible for waterborne diseases such as typhoid and paratyphoid fever, dysentery, diarrhea, and cholera, have been observed in highway runoff (Sartor and Boyd, 1972; Gupta et. al., 1981). The Barton Springs segment of the Edwards Aquifer is potentially sensitive to the presence of pathogenic organisms. The aquifer is used as a drinking water source, and Barton Creek is used by the public for swimming and boating.

It is difficult to identify specific pathogenic organisms in a water sample. The number of pathogens in a normal sample usually is very small and it is difficult to isolate the pathogens from the other bacteria in the sample. Water quality samples are analyzed for “indicator organisms” that signify the potential presence of pathogens. Total coliform

(TC), fecal coliform (FC), and fecal streptococci (FS) are indicators used in bacteriological analyses of water. Fecal coliforms and fecal streptococci are bacteria found in the digestive tract of warm-blooded animals. The presence of fecal coliforms and fecal streptococci may be an indication of pathogenic organisms. Additionally, the ratio of fecal coliforms to fecal streptococci may be used to determine the origin of the contamination. Domestic animals have a FC/FS ratio that is less than 1.0, whereas the ratio for humans is typically greater than 4.0 (Metcalf & Eddy, Inc., 1991). A total coliform count includes both the fecal coliforms and the coliforms found in soils.

Coliforms generally die off quite rapidly in receiving waters (Sartor and Boyd, 1972). Bacteria also are removed from runoff streams by filtration, adsorption, desiccation, radiation (sunlight), predation by other bacteria, and exposure to other adverse conditions (USEPA, 1981). Therefore, any relationship between the number of coliforms on the highway surface and the number that may be found in adjacent receiving streams is difficult at best.

Other parameters and constituents of concern in highway runoff include pH, temperature, total dissolved solids, oil and grease, and pesticides and herbicides. Values of pH reported by Driscoll et al. (1990) ranged from 5.5 to 7.5, with an average of 6.5. Discharges within this pH range are not known to cause water quality problems. Temperature is of concern only if runoff volumes are large enough to severely alter the temperature of the receiving stream. Total dissolved solids (TDS) may be a concern if the highway runoff results in an increase in the salinity of the receiving water. TDS could be a concern during snow melt in areas where highways are heavily salted to aid in ice removal.

Oil and grease concentrations reported by Driscoll et al. (1990) ranged from 5 mg/L to 10 mg/L. There is no evidence that oil and grease at these concentrations are harmful to human health and the environment.

Pesticides (chlorinated hydrocarbons) were found in significant quantities in street runoff by Sartor and Boyd (1972). However, this class of constituents was not addressed in this study.

The median constituent concentrations observed in highway runoff are summarized in Tables 2.3.1 and 2.3.2.

2.4 Highway Runoff Constituent Build-Up Mechanisms

Highway runoff characterization studies have been conducted in the United States for over 30 years. A massive amount of data relating to the quality of runoff from urban pavements has been generated. An evaluation of the available literature suggests that the sources of constituents in highway runoff can be categorized as: (1) vehicular contributions, (2) atmospheric deposition, and (3) the road bed material. The relationship of each source to the quality of the storm water runoff is very complex and not well understood.

Table 2.3.1 Reported Median Constituent Concentrations in Urban Runoff

Constituent	Median Concentration
pH	5.5 - 7.5 [(a)]
TSS	142 mg/L (0.62) [(a)]
VSS	39 mg/L (0.58) [(a)]
BOD_5	5 mg/L - 25 mg/L [(a)]
COD	114 mg/L (0.58) [(a)]
Total Carbon	25 mg/L (0.62) [(a)]
Kjeldahl Nitrogen	1.83 mg/L (0.45) [(a)]
$NO_2 + NO_3^-$	0.76 mg/L (0.56) [(a)]
PO_4 - P	0.40 mg/L (0.89) [(a)]
Total Coliform	260/100ml - 180,000/100ml [(b)]
Fecal Coliform	20/100ml - 1,900/100ml [(b)]
Fecal Streptococci	940/100ml - 27,000/100ml [(b)]
Oil & Grease	5 mg/L - 10 mg/L [(a)]

Number in parenthesis is the reported coefficient of variation
(a) - Driscoll et al. (1990); (b) - Gupta et al. (1981)

Table 2.3.2 Metals in Highway Runoff

Metal	Concentration in Highway Runoff (μγ/Λ)	% Dissolved	Drinking Water Standard (μγ/Λ)
Cadmium	1 - 30 [c]	72% [e]	10 [a]
Chromium	15 - 35 [c]	65% [e]	(Cr^{6+}) 50 [a]
Copper	54 (0.68) [c]	70% [e]	1,000 [b]
Iron	3,000 - 12,000 [c]	27% [e]	300 [b]
Lead	400 (1.46) [c]	21% [e]	50 [a]
Mercury	0.001 - 1.5 [c]	Not Reported	2 [a]
Nickel	150 [d]	76% [e]	Not Established
Zinc	329(0.44) [c]	57% [e]	5,000 [b]

Number in parenthesis is the reported coefficient of variation

(a) USEPA Primary Drinking Water Standards
(b) USEPA Secondary Drinking Water Standards
(c) Driscoll et al. (1990). A single value represents the site median EMC for all urban highway sites.
(d) Gupta et al. (1981)
(e) Yousef et al. (1986)

The source of the constituents in highway runoff is influenced by environmental conditions that are often difficult, if not impossible, to measure. Some of the constituents can be traced to more than one source, in which case it is often difficult to distinguish the dominant source. The build-up process of constituents in highway runoff is further complicated by a continuous and complex removal process. During dry weather, materials are continually blown on and off the highway, as well as on and off of vehicles by natural and vehicle induced winds. During wet weather, storm water washes constituents from both the highway surface and the vehicles. Although physical transport is thought to be the primary method of constituent removal, there is certainly some chemical or biological removal that occurs on the highway surface (i.e., volatilization, chemical decay, biodegradation, etc.).

Highway constituent loads are thought to be closely related to the average daily traffic (ADT) count of the highway. Sartor and Boyd (1972) identified the following list of vehicle contributions:

1) Leakage of fuel, lubricants, hydraulic fluids, and coolants;
2) Fine particles worn off of tires and clutch and brake linings;
3) Particulate exhaust emissions;

4) Dirt, rust, and decomposing coatings that drop off of fender linings and undercarriages;

5) Vehicle components broken by vibration or impact (glass, plastic, metals, etc.).

ADT is a measure of highway usage. The high ADT highways, such as urban expressways, typically produce higher constituent concentrations than the low ADT highways that are normally located in rural areas. Driscoll et al. (1990) found a statistically significant difference in the constituent concentrations at sites with an ADT greater than 30,000 and those with an ADT less than 30,000. However, it is difficult to segregate the influence of traffic from that of the surrounding land use since lighter traffic sites tend to be more rural than heavier traffic sites. A lack of a clear correlation with ADT within each group led Driscoll et al. (1990) to the conclusion that surrounding land use is a more important influence than traffic. Stotz (1987) and Mar et al. (1982) also reached the same conclusion.

ADT should not be confused with the number of vehicles that use the highway between storms, which for most highway traffic patterns is indistinguishable from the duration of the antecedent dry period (ADP) of a storm. Although not a true "source," the ADP is a commonly cited variable thought to affect runoff quality (Sartor and Boyd, 1972; Moe et al., 1978; Howell, 1978; Kent et al., 1982; Lord, 1987; Hewitt and Rashed, 1992). The ADP provides the opportunity for material to accumulate on the highway surface. The pattern of constituent build-up during the ADP is an important relationship used in many highway runoff models. Although linear build-up patterns have been observed (Moe et al., 1978), it is obvious that accumulations are limited by some upper bound. Sartor and Boyd (1972) and Pitt (1979) observed non-linear build-up patterns that approached asymptotic values.

Ordinary least squares (OLS) regression analysis is often used to identify the factors that influence constituent accumulation during the ADP. Correlation coefficient values for curves fit to the duration of the ADP are typically less than 0.30 (Sartor and Boyd, 1972; Driscoll et al., 1990), which suggests that there are additional parameters that influence material accumulation other than the duration of the ADP. The poor correlations may also reflect the difficulty involved in accurately measuring the amount of material that has accumulated on the highway surface during the ADP. Since the ADP

build-up washes off early in the rainfall event (during that time both vehicles and rainfall are contributing materials to the runoff), it is difficult to measure the dry period build-up during a natural rainfall event. Sartor and Boyd (1972) attempted to remedy this problem by using a rainfall simulator to wash the highway surface during a period of no traffic. The use of the simulator allowed the collection of runoff samples under ideally controlled conditions, which should have minimized the sampling error.

Some researchers (Horner et. al., 1979; Kerri et. al., 1985; Harrison and Wilson, 1985) have reported a weak correlation with ADP, which suggests that a net accumulation of material need not occur during a dry period. Constituents are continually being removed from the highway surface during the ADP. Natural and vehicle-induced winds have been observed to blow materials off the highway during dry weather. Constituents may also be removed during the ADP by volatilization, biodegradation, and chemical decay. Kerri et al. (1985) concluded that there is no statistical significance between the constituent load of a storm and the duration of the ADP of a storm. This finding was attributed to the traffic-generated winds that continually sweep the surface of the highway and the pick-up of materials by tires. Their study established a better correlation with the number of vehicles *during* the storm (VDS). It was suggested that constituents are more likely to be washed from vehicles during a storm than blown from vehicles during dry weather. Harrison and Wilson (1985) and Horner et al. (1979) also found a weak correlation between the duration of the ADP and constituent concentration in the storm runoff.

VDS is the total count of vehicles that actually travel the highway section during the rain storm. A related parameter, vehicle intensity during the storm (VIDS), is a density measure reported as number of vehicles per unit time or unit of discharge. Driscoll et al. (1990) suggests that neither VDS nor VIDS should be estimated from ADT counts. Traffic counts recorded on a 1 hour interval or less should be matched as close as possible to the duration of the runoff event.

The relationship between VDS and water quality suggest that vehicles are the major source of runoff constituents during a storm event, whereas VIDS may account for less obvious vehicle contributions. Both tires and undercarriage winds apply substantial energy to the surface of the road. These forces may dissolve or suspend many of the

constituents that have accumulated on the highway. Particulates in exhaust emissions are "scrubbed" from the air during a rain storm, adding constituents to the runoff that otherwise may have drifted from the highway (Gupta et al., 1981). Both of these phenomena are better represented with a density measure.

Regression analysis that uses VDS or VIDS as the single explanatory variable would be expected to fail for the same reasons as with ADP, described above. But many researchers have found a correlation between VDS and contaminate loading (Chui et al., 1981; Chui et al., 1982; Asplund et al., 1982; Horner and Mar, 1983). Vehicular traffic may dominate other sources under certain storm duration or intensity situations. Therefore, the concentrations of constituents would be expected to reach a "steady state" during a lengthy storm event with steady traffic flow. Gupta et al. (1981), however, observed decreasing concentrations of constituents after over two hours of rainfall. The average vehicle speed and vehicle mix (i.e., the distribution of cars, buses, tractor trailers, etc.) also would be expected to have an influence on runoff quality, but these parameters have not been widely studied.

Atmospheric fallout can contribute a considerable amount of constituents to the highway. Gupta et al. (1981) reported that typical dustfall loads in U.S. cities range from 2,600 to 26,000 kg/km^2-month. Solids, nutrients, metals, and biodegradable organics also may be contributed by atmospheric fallout (Sartor and Boyd, 1972; Gupta et al., 1981). The type and amount of constituents that collect on highways are influenced by the surrounding land use. Driscoll et al. (1990) concluded that surrounding land use is the most important factor that influences constituent loads in highway runoff. In general, the constituent loading in industrial areas is substantially higher than residential or commercial areas (Sartor and Boyd, 1972; Gupta et al., 1981; Driscoll et al., 1990).

The characteristics of the highway surface also may influence runoff quality. Such characteristics include the materials of construction, curbs and gutters, guard walls, age, configuration, and drainage features. There is little evidence to suggest that asphalt highways produce more or less constituents than concrete pavements. The age and condition of the pavement seems to be a more dominant factor than the material of construction (Sartor and Boyd, 1972; Driscoll et al., 1990). An older highway, or one in need of repair, can be expected to release a larger amount of aggregates regardless of the

base material. The presence of guard walls, curbs, and gutters tend to trap constituents that otherwise would be blown from the highway during dry periods (Wiland and Malina, 1976; Gupta et al., 1981; Driscoll et al., 1990).

2.5 Constituent Removal Mechanisms

Material is continually being removed from the highway surface by natural and vehicle-induced winds that constantly "sweep" the highway surface (Aye, 1979; Asplund, et al., 1980). This phenomenon clearly is demonstrated on curbed highways by the build-up of dirt and debris along the gutter and shoulder and the noticeable lack of material in the traffic lanes. Stormwater runoff also has been observed to deposit material along the curb. Therefore, it is not surprising that the majority of material on the highway surface is found within 3 feet of the curb (Sartor and Boyd, 1972; Laxen and Harrison, 1977).

Street sweeping is a commonly used municipal practice for the control of dirt, debris, litter, etc. along urban streets and highways. A regular schedule of street sweeping not only has the potential for reducing storm water constituent loads, but also has the additional benefits of improving air quality, aesthetic conditions, and public safety (Pitt, 1979). Unfortunately, street sweeping is not very effective in reducing the organic, nutrient, and metal loading in storm waterss because the largest percentage of these constituents is associated with materials less than 48 microns in size (Sartor and Boyd, 1972; Pitt, 1979; Gupta et al., 1981; USEPA, 1983). Modern street sweeping equipment is not a very effective collector of material this small.

Constituents are removed via storm water wash during rainfall events. The extent of constituent removal during a runoff event depends primarily on runoff volume, which is a function of rainfall intensity and duration. A positive correlation between rainfall intensity and highway runoff volume is expected and well documented (Driscoll et al., 1990). It is also reasonable to expect that a higher intensity rain storm would wash more constituents from the highway surface, in less time, than a smaller storm. Therefore, it is generally accepted that constituent loading (i.e., mass of constituent removed from highway per unit time and/or area) is positively correlated with rainfall intensity (USEPA, 1983). This correlation is important because the ultimate constituent

concentration in a receiving stream is determined by the constituent mass loading to that stream.

It would seem logical that the large amounts of water produced by high-intensity storms would dilute the finite amount of material present on the highway. However, intuition fails with respect to constituent concentrations within the storm event. Research has shown that constituent concentrations (i.e., mass of constituent per unit volume of runoff) are not only variable within a particular storm, but also from one storm to the next. Varying rainfall patterns result in runoff flows that vary considerably within the storm events. The work of Harrison and Wilson (1985) and Hoffmann et al. (1985) show that constituent concentrations generally follow the same trend as rainfall intensity during long-duration, light-intensity storms (i.e., storm duration to 8 hours with peak intensities less than 8 mm/hr). The National Urban Runoff Program (NURP) data analysis (USEPA, 1983) considered over 300 samples and found no correlation between concentration and storm volume or intensity. The NURP analysis is supported by over 250 samples collected during a Federal Highway Administration study (Shelley and Gaboury, 1986) and by the work of Driscoll et al. (1990).

There is also substantial evidence to suggest that a period of high concentration typically occurs early in the runoff event (Howell, 1978; Horner et al., 1979) This period is known as the "first flush" and has lead to the speculation that the majority of constituents are removed early in the event. It should be noted that some literature refers to "first flush" in terms of constituent loading, whereas others define "first flush" in terms of concentration.

The phenomenon of "first flush" was first demonstrated by Sartor and Boyd (1972) with the use of a rainfall simulator. The magnitude of the "first flush" was a function of rainfall intensity and the particle size of the constituent. Others have shown that dissolved constituents and the constituents associated with the smaller solids are more likely to show a "first flush" pattern (McKenzie and Irwin, 1983; Harrison and Wilson, 1985; Hewitt and Rashed, 1992).

Although the period of "first flush" is easily recognized by looking at a constituent loadograph (i.e., a plot of load vs. time), few researchers have attempted to define the boundaries, either time or magnitude, that constitute "first flush." This

ambiguity has lead to disagreement among the designers of water quality control structures regarding the volume of runoff that should be captured to meet a desired treatment level. The City of Austin has defined the "first flush concentration" as the mean concentration of a constituent in the first 0 to 3 mm of runoff. This concentration is generally found to be higher than the event mean concentration (Chang et al., 1990). It has also been shown in Austin that a water quality control structure that collects the first 13 millimeters of runoff will effectively capture 73% - 100% of the total annual load, depending on the degree of watershed imperviousness (Chang et al., 1990). However, the "13 millimeter rule" is highly site specific and dependent on the characteristics of the local annual rainfall.

2.6 Highway Constituent Discharge Theory

Analysis of the preceding literature review indicates the complexity of the constituent build-up process on the highway surface. During the dry period between storm events, material is continually being deposited onto the highway surface by vehicles and through atmospheric deposition. At the same time, many substances are removed from the road by natural and vehicle-induced winds, volatilization, biodegradation, and chemical decay. The complexity of constituent build-up on highway surfaces is illustrated in Figure 2.6.1a, using data collected during this research

Wash-off of accumulated substances, shown in Figure 2.6.1b, is more predictable than build-up. The materials accumulated during the dry period are removed early in the storm during the "first flush." Traffic and rainfall continue to introduce new substances throughout the storm. Rainfall may also "scrub" vehicle exhaust and other sources

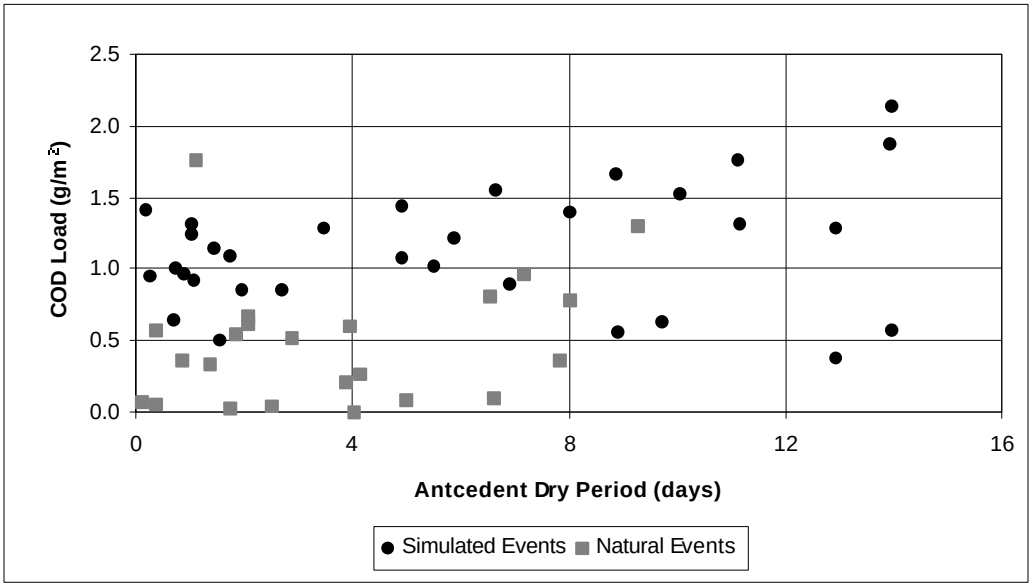

(a) Observed COD Build-Up

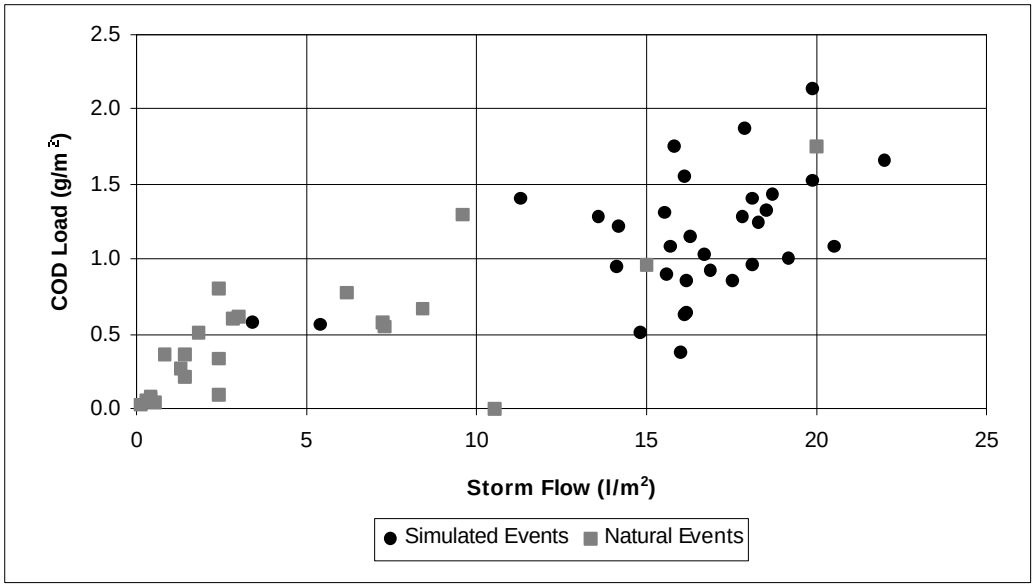

(b) Observed COD Wash-Off

Figure 2.6.1

associated with the highway environment. The commonly observed correlation between total storm runoff and constituent load is a result of the continual input of material throughout the storm and, of course, the inclusion of flow in the load calculation.

All rainfall events do not result in a net removal of constituents from the highway surface. Many storm events produce light rainfall (i.e., less than 0.25 mm in 15 min) that will produce little or no runoff; however, enough moisture is available to wash the bottoms of vehicles. Storm events of this magnitude, many lasting 6 hours or longer, frequently occur in the Austin area. Furthermore, storms are followed by a time of no rainfall during that vehicle bottoms continue to be washed but the runoff is insufficient to remove any material. Therefore, most naturally occurring storm events are not capable of completely removing all material from the surface of busy highways.

Constituent loads vary between storm events because each individual storm event is different. However, even if two storms were perfectly alike, the pollutant loads would differ. The fact that the two storms occurred at different times would cause the storms to be different. An endless number of differences between storm events is possible; however, only a few variables actually affect the quality of the runoff. The major variables that affect the constituent loading are the total volume of runoff, the average intensity of the runoff, the length of antecedent dry period, and the number of vehicles traveling through the storm. Ideally, holding these variables constant between storms should result in similar loads.

The total constituent load (or mass), M, produced during a storm event, is the product of the flow-weighted mean concentration of the constituent, $\bar{c}$, and the total volume of runoff, V, given as:

$$M = \bar{c}V = \int c(t)Q(t)dt \qquad (2.6.1)$$

where c is the instantaneous concentration and Q is the volumetric rate of runoff. Furthermore, the total volume of runoff, V, is equal to the total volume of rainfall, P, on the watershed, less any losses, L, such as storage, evaporation, infiltration, drift, etc. given as:

$$V = P - L = \int Q(t)dt \qquad (2.6.2)$$

Any two storm events of equal rainfall intensity and duration, over the same section of highway, under equivalent weather conditions (e.g., temperature and wind) *should* produce similar volumes of runoff. Since *L* is expected to be small and approximately constant for a 100% impervious surface, the total volume of runoff from any given storm should be predictable.

The flow-weighted mean concentration of a constituent is the amount of constituent mass, *M*, available during the storm divided by the volume of storm water runoff, *V*. The volume of runoff, *V*, varies primarily with the rainfall. However, the amount of constituent mass, *M*, that is available during the storm is considerably more complex. The total storm load can consist of the mass that has accumulated on the highway surface at the instant the storm begins, plus any pollutant mass introduced during the storm, plus or minus any production/decay of pollutant mass during the storm. However, the amount of dry material that has accumulated on the highway prior to the start of the storm, is influenced only by variables that precede the rainfall. These variables occur during the antecedent dry period (ADP), although the extent of pollutant wash-off (or accumulation) during the preceding storm event also may be important. Similarly, the amount of material input from traffic and rainfall is completely independent of the ADP and preceding storm. Finally, any production/decay (including settling) of material during the storm will depend on the total amount of material present, which, in turn, is a function of variables of the pre-rainfall and rainfall periods.

The changes in constituent load during a storm may be illustrated by considering a rainfall event over a segment of highway as analogous to the flushing of a dry stream bed. In this system, the pavement segment is the "stream bed," with rainfall providing the inflow and the point of outflow being at the curb inlet box. The stream bed is dry at the beginning of the storm but contains a specific mass of a constituent. As rain water enters the system, the available mass of constituent is mobilized and moved downstream toward the curb inlet. If there is no change in the inflow of water (i.e., the inflow is at steady state) a hydrograph recorded at the curb inlet will show a rising leg over the time of concentration, a plateau throughout the remainder of the storm, and a falling leg that is similar to the rising leg after the end of the rainfall. To an observer at the curb inlet, there is a "time release" of the dry mass of constituent that accumulated on the highway

surfaces. If the traffic across the highway segment is constant throughout the storm, and the storm completely flushes the dry accumulation from the highway, the outflow of constituent mass ultimately will equal the input of mass from the rainfall and the vehicles. The principal statement for the mass balance is:

Rate of change of mass of constituent =

the rate of input from rainfall into the system

\+ the rate of input from traffic into the system

\+ the mobilization rate of the dry accumulation

\+ the sum of all rates of output from the system

± rate of production/decay within the system

The mass balance is expressed mathematically as:

$$\frac{d(Vc)}{dt} = W + R - Qc \pm K_1 Vc \qquad (2.6.3)$$

Where the mass entering the system is:

$$W = Q_P c_P + M_v \qquad (2.6.4)$$

and the outflow Q at the curb inlet is:

$$Q = Q_P - Q_L \qquad (2.6.5)$$

where:

Q_P = flow provided by rainfall (L^3/T)

c_P = concentration of the constituent in rainfall (M/L^3)

M_V = mass input from vehicles (M/T)

Q_L = loss of flow resulting from watershed storage, evaporation, etc.

K_1 = constituent decay rate within the system

and

$$R \equiv \text{ mobilization rate of the dry accumulation } = f\left(P, \frac{dP}{dt}, \text{traffic rate}\right)$$

where during the storm:

$$\frac{dM}{dt} = -R \qquad (2.6.6)$$

(R would probably be first order, e.g., K_2M with $K_2 = f$[P, dp/dt, traffic rate])

and during the dry build-up period:

$$\frac{dM}{dt} = W_a + W_t + W_m - W_s \qquad (2.6.7)$$

and

$$M = \int_{t_0}^{t_s} (W_a + W_t + W_m - W_s)dt \qquad (2.6.8)$$

where:

W_a = net atmospheric load = f(wind, temperature, humidity, land use)

W_t = net traffic load = f(traffic rate, traffic mix, temperature)

W_m = net load from maintenance activities = f(guard rail repair, grass cutting, bridge sanding)

W_s = removal of constituent mass by street sweeping

t_0 = end of previous storm

t_s = start of current storm

Some rainfall is going to accumulate on the pavement during the early stages of the storm; therefore:

$$\frac{dV}{dt} = A\frac{dh}{dt} \qquad (2.6.9)$$

and expanding the derivative in equation 2.6.3 gives:

$$\frac{dVc}{dt} = V\frac{dc}{dt} + c\frac{dV}{dt} = V\frac{dc}{dt} + cA\frac{dh}{dt} \qquad (2.6.10)$$

that yields the general case equation:

$$cA\frac{dh}{dt} + V\frac{dc}{dt} = W + R - Qc \pm K_1Vc \qquad (2.6.11)$$

The maximum amount of time that a particle is mobilized on the highway segment (i.e., the time of concentration) is probably too short for any chemical transformation of the constituent to occur; therefore the decay/production rate, K_1, is approximately equal to zero. Furthermore, once all of the inputs have reached steady state (e.g., flow-in is equal to flow-out and the traffic flow is constant) then the

mobilization rate, R, is constant. Therefore, if the rainfall and traffic provided no constituent input into the system (i.e., $W = 0$), the only mass output of the system is the flushing of the material that originally resided on the dry road surface, and the concentration of constituent in the runoff, c_F, is given by:

$$c_F = c_0 \exp\left[-\left(\frac{Q}{V} + R\right)t\right] \qquad (2.6.12)$$

If the constituent input from both the rainfall and the traffic is assumed constant (i.e., there is no variation over the duration of the storm), each source would be considered as a single step input into the system. The concentration of constituent in the runoff attributable to the step input, c_S, is given by:

$$c_S = \frac{W}{Q}\left\{1 - \exp\left[-\left(\frac{Q}{V}\right)t\right]\right\} \qquad (2.6.13)$$

that describes the build-up of concentration to an equilibrium level given by:

$$c_S = \frac{W}{Q} \qquad (2.6.14)$$

The lack of volume, or "shallowness" of the highway stream bed, results in the instantaneous and complete mixing of the constituent mass contributed by rainfall and vehicles. Therefore, Equation 2.6.14 best describes the steady state input of material from rainfall and traffic.

Finally, the total response of the storm to an initial accumulation of material on the highway surface and a constant input from rainfall and traffic is the sum of Equations 2.6.12 and 2.6.14 and is expressed mathematically as

$$c = c_F + c_S = \frac{W}{Q} + c_o \exp\left[-\left(\frac{Q}{V} + R\right)t\right] \qquad (2.6.15)$$

Plots of Equations 2.6.12, 2.6.14, and 2.6.15 are presented in Figure 2.6.2. At the start of the storm the amount of dry material that has accumulated on the highway, plus the amount contributed by traffic/rainfall, yields an initial runoff concentration c_0. If the storm continues indefinitely, the initial accumulation of dry material is removed completely by the runoff. Simultaneously, new constituent mass from the traffic and/or rainfall is added to the system at a constant rate. Note that even in the presence of a constant constituent input, the combined response shows the familiar first flush pattern.

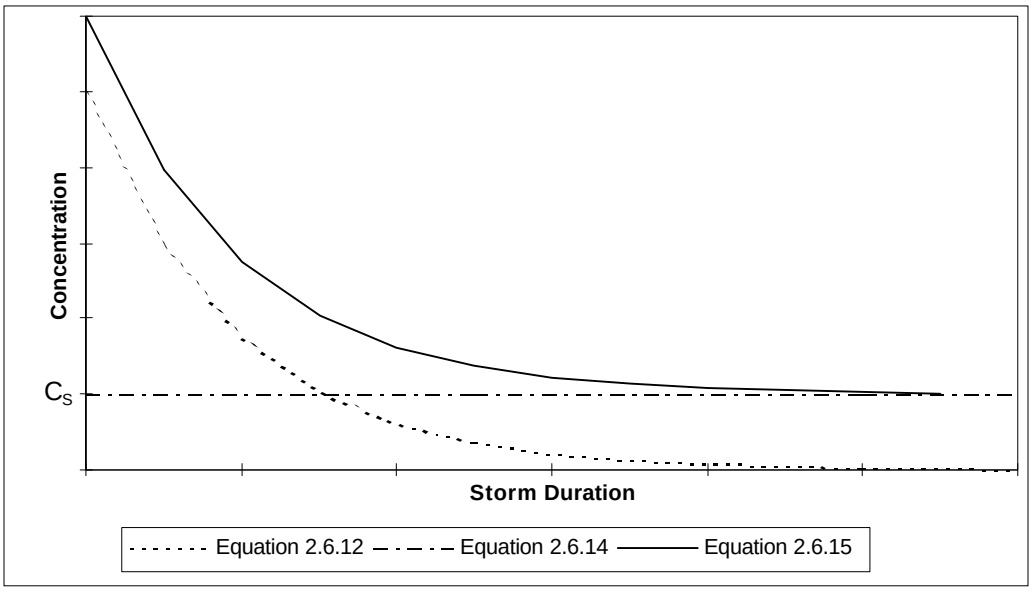

Figure 2.6.2 Theoretical Wash-Off Pattern

The variables that influence dry weather build-up and the traffic/rainfall input rate must be identified to predict the storm load. The response to these variables is easily distinguishable if the storm maintains a steady state condition over a prolonged period. Of course, this is never the case in nature. However, if a designed series of "steady state" storms could be created, it may be possible to identify the causal variables of storm load. The use of a rainfall simulator to create such a storm is the subject of Chapter 3.

2.7 Summary

The cost of storm water control accounts for as much as 20% of the overall cost of highway construction in the Barton Springs segment of the Edwards Aquifer recharge

zone. Because of concern that the current runoff control structures are not constructed in the "best" (either environmentally or cost-effective) manner, TxDOT initiated research that would (1) determine the variables that affect the build-up and wash-off of constituents from highways in the Austin area and (2) develop a predictive model that incorporates the variables which affect runoff quality.

A review of highway runoff literature indicates that (1) the build-up and wash-off of materials from highway pavements is a very complex process, (2) there is considerable disagreement over the importance of the "first-flush" effect, and (3) street sweeping is generally not effective for the removal of the smaller sized particles that are associated with the majority of the constituents. However, constituent runoff patterns would be distinguishable if a steady-state storm event (i.e., constant rainfall and constant traffic input) is sampled at regular intervals throughout the duration of the event.

3.0 Data Collection

3.1 Introduction

The development of the highway runoff predictive model is supported by data collected at two sampling sites along Loop 1 (MoPac Highway) in Austin. The principal sampling site was located near the West 35th Street overpass. A rainfall simulator was erected at this site, and between July 6, 1993 and July 14, 1994, a total of 35 simulated storm events were conducted for the purpose of measuring storm water loading during "controlled" rainfall events. All of the simulated storms were performed over active traffic with the exception of three "no-traffic" storms. In addition, 23 natural storm events were sampled at the West 35th Street site between September 14, 1993 and April 28, 1994.

The second sampling site was located on a MoPac expressway overpass near Convict Hill Road. The major differences at this site are the watershed size (approximately 10% of the West 35th Street site), the low traffic count (average daily traffic volume at the site is approximately 20% of that at the West 35th Street site) and the high guardrails along the overpass that possibly trap contaminants as they move along the highway. Otherwise, the surrounding land use, traffic mix, and prevailing weather conditions are all similar to the West 35th Street site. A site comparison is presented in Table 3.1.1. Twenty natural storm events were sampled at the Convict Hill site between April 29, 1994 and November 5, 1994. The primary use of these data was the verification of the model, that was formulated using the West 35th Street data.

3.2 Rainfall Simulation

Rainfall simulation has been used in highway runoff research since the mid-1960's (Hamlin and Bautista, 1965; Sartor and Boyd, 1972; Wiland and Malina, 1976; Irwin and Losey, 1978). The rainfall simulator is used to produce an artificial rainfall event during that certain parameters thought to affect highway runoff loading are "controlled." The most commonly controlled parameters during a highway rainfall simulation include the storm intensity, storm duration, and the antecedent dry period. The influence of average daily traffic count, surrounding land use, seasonal variations

and street maintenance operations may also be determined with the use of a rainfall simulator. Two different methods have been used to produce the artificial runoff: (1) a sprinkler system set up over the road surface and (2) a pressurized wash.

Table 3.1.1 Highway Characteristics at the MoPac Test Sites

Highway Characteristic	MoPac & West 35th Street	MoPac & Convict Hill
Number of Lanes	3	2
Inside Shoulder Width	2.4 m	3.0 m
Outside Shoulder Width	3.0 m	6.4 m
Length of Watershed	300 m	30 m
Impervious Area	4,358 m^2	511 m^2
Percent Watershed in Active Traffic Lanes	77%	44%
Percent Impervious	100%	100%
Time of Concentration	12 minutes for a storm intensity of 31 mm/hr	NA
Highway Construction	Asphalt with 15 cm Curb	Asphalt with 1 m Retainer Walls
Speed Limit	88 km/hr	88 km/hr
Local Land Use	Residential/Light Commercial	Residential/Undeveloped

The sprinkler system approach attempts to simulate natural rainfall by using a series of spray nozzles set up to sprinkle water onto the highway surface. Experiments are designed to determine the constituent loads that result from different storm patterns. Although rain droplet size and impact energy may vary considerably from actual rainfall, it is important that the simulator be able to reproduce a spatially uniform rainfall intensity (Reed and Kibler, 1989). The section of roadway exposed to the "rain" is typically 40 to 85 square meters in size (Sartor and Boyd, 1972; Reed and Kibler, 1989) and the highway must be closed to traffic during the experiment.

The pressurized wash method is designed to remove all accumulated material from the highway surface. A high-pressure stream of water is used to dislodge material residing on the highway surface and wash it to a sampling station. The wash is accomplished by using a fire hose supplied by a water hydrant or water tank, and no

attempt is made to simulate natural rainfall. Similar to the sprinkler system approach, the highway is closed to traffic during the experiment. The total amount of material residing on the highway surface may be determined using this method; however, no relationship can be established between the quality of the runoff and the temporal variations in rainfall and traffic. This approach is typified by the work of Hamlin and Bautista (1965); Wiland and Malina (1976); and Irwin and Losey (1978).

A "sprinkler" type rainfall simulator was constructed at the MoPac & West 35th Street site to facilitate data collection for this research. The West 35th Street site was selected because of site-specific hydrologic, traffic, and safety characteristics that allowed the design of a rainfall simulator that could be operated over active traffic. The simulator was set up along a 300-meter section of highway that drained to a single curb inlet box. This condition greatly simplified sample collection during the artificial storms. Furthermore, spray from the simulator covered approximately the entire natural watershed for the curb inlet box, which allowed a direct comparison of natural events to simulated events at the site.

The average daily volume of traffic at the West 35th Street site is approximately 60,000 vehicles per day. The high traffic volume allowed for a significant variation in the number of vehicles exposed to the "storm," depending on the time of day the simulator was operated. Traffic variations during daylight hours ranged from 3,000 vehicles/hr (between 10:00 am and 11:00 am) to 6,000 vehicles/hr (between 7:00 am and 8:00 am).

Safety considerations, however, were the most important aspect in the rainfall simulator site selection process. The West 35th Street site proved an excellent choice because of the excellent traction characteristics of the pavement in the wet zone. A high-speed service road also provided a convenient by-pass around the simulator for motorists who did not want to drive through the artificial rain storm.

Finally, the commitment and support of the staff of the TxDOT made it possible to operate the rainfall simulator over high-speed highway traffic. This simulator provided the unique opportunity to study a design storm under actual highway conditions.

The major advantages of using a rainfall simulator under these conditions are:

1. Control of the parameters that affect highway runoff, such as:

- Rainfall intensity
- Rainfall duration
- Antecedent dry period
- Traffic intensity during the storm
- Pavement maintenance operations

2. Execution of a precise water quality sampling scheme based on a pre-known storm event during ideal sampling conditions.
3. The ability to generate a large number of runoff events for statistical analysis.
4. The ability to generate "rainfall" during extended periods of dry weather (a common summertime occurrence in the Austin area).
5 Provide a "steady-state" storm, with respect to rainfall and traffic intensity, in which to measure the response of storm loading to different causal variables.

3.3 Rainfall Simulator Design

The objective of the rainfall simulator design was to produce a system capable of simulating natural rainfall over a section of highway during actual traffic conditions. The system must operate to produce highway runoff that can be collected and evaluated to determine constituent loads that result from various combinations of climatological conditions and vehicle use patterns. Specifically, the rainfall simulator had to meet the following criteria:

1. provide rainfall of varied and controlled intensities;
1. produce a rain that falls uniformly over a 3-lane width of traffic;
1. produce rainfall over the entire length of the highway watershed serviced by a curb inlet drain;
1. provide rainfall from above a 14-foot height in order to clear tractor trailer traffic;
1. operate within the normal 10-foot width of a highway shoulder because no structure could be built over or across the highway;
1. be portable, but structurally stable and secure to safely withstand the wind forces resulting from high-speed traffic turbulence.

Natural rainfall consists of numerous water droplets of varying sizes. These droplets are constantly changing mass as they fall through the atmosphere as a result of evaporation, shear stresses, and collisions with other droplets. Furthermore, the droplets travel with varying downward velocity components as a result of the effects of wind, lift,

and air drag. Light rainfall events will produce small droplets and mist, whereas heavy rainfall events will produce a wide range of droplet sizes including mist. The success of a rainfall simulator design depends on the ability of the simulator spray head to produce a variety of water droplet sizes and distribute them over a large area. A simulator that must deliver rainfall from outside the target sampling area, such as from the shoulder of a highway, can only accomplish this by creating a water droplet size distribution at the spray head with a velocity distribution spread over each droplet size. The simulator must produce droplets of various sizes and throw each droplet size through a wide range of velocities. The velocity of the droplet will determine the distance of travel, and the droplets having the greatest velocity must travel across the entirety of the sampling zone. A large amount of energy is required to propel droplets, as opposed to a stream, a given distance from the spray head. The smaller the droplet, the more energy is required to throw the droplet a given distance. An illustration of this principle is shown in Appendix C.

The spray head is the most critical operating part of the rainfall simulator. The spray head is responsible for the application and even distribution of water over the highway surface. It must be adjustable, light-weight, and capable of continuous operation for the duration of the sampling session. Furthermore, the design of the spray head drives the design of the water supply and distribution lines and the support stands. During the initial part of the research, spray head design concentrated on investigating the applicability of agricultural irrigation equipment. However, modern irrigation spray heads are designed to provide small water droplet size to prevent damage to crops and soils. Conversely, the rainfall simulator is designed to produce large droplets, capable of damaging soils (as in erosion studies) or dislodging materials from the surface of vehicles as required in this study. This fundamental difference played a major role in the final design of the spray head.

Irrigation spray heads generally fall into two categories. The first category is the mist application spray head. These spray heads are most commonly seen on center-pivot irrigation equipment. A spray nozzle directs a stream of water toward a splash plate that diffuses the water in all directions. The design of the splash plate determines the size of the droplet and the pattern of spray. Spray coverage is a full 360 degrees, but a deflector

may be used to limit the direction of the spray pattern. These spray heads are capable of evenly distributing a continuous spray over a 21-meter-diameter circular area. These designs are most likely to have applications in studies simulating drizzles, mists, or heavy fogs, where the application area is under 353 square meters per spray head (177 square meters for non-centered spray heads). The Nelson R30 Series is representative of this type of spray head.

The second category of irrigation spray head is the impact sprinkler. This type of spray head is most commonly seen on golf courses, parks, and other turf areas where a large water droplet size will not cause damage to the soil. Impact sprinklers are capable of throwing large droplets of water over 185 meters. These spray heads use a nozzle similar to that of mist spray heads; however, instead of hitting a 90 degree splash plate, the water stream glances off a spring-loaded or levered splash plate mounted tangent to the stream. The water that hits the splash plate breaks into small droplets or mist. However, if the splash plate has a long lever arm, the majority of the water stream will not collide with the splash plate. The water that does not collide with the splash plate will break-up into large droplets as the unimpeded stream of water travels through the air. The unbroken stream of water results in the great throw distances achieved by the impact sprinkler. The width of continuous coverage of the impact sprinkler is only as large as the dispersion of water stream. Therefore, the impact sprinkler is commonly swivel-mounted in order to obtain 360-degree spray coverage. The Rainbird Model 35A-TNT is representative of the impact sprinkler type of irrigation spray head.

Neither type of spray head is suitable for use in a large-area simulator where the spray head and associated support structures have to be mounted outside of the area of rainfall. The impact sprinkler can spray a great distance, but the width of spray is extremely narrow. The mist spray head is capable of providing a large area of continuous spray, but the water droplet is small and the throw distance is short. A rainfall simulator for an active highway requires a spray head that can throw large drops of water a great distance, yet continuously cover as wide an area as possible. It is therefore necessary to design a spray head that combines the characteristics of both the impact sprinkler and the mist spray head.

An analysis of water droplet formation in the various different irrigation spray heads provides insight into how this objective can be reached. Surface tension is the mechanism that holds the water droplet together and subsequently controls the size range of droplets that can be produced. If surface tension is uncontrollable, the water droplet size produced by a simulator is a function of (1) the type of splash plate used, (2) the angle of approach of the water stream, and (3) water pressure. Any droplet size can be obtained by holding two of the variables constant, and varying the third. A specific splash plate, for example, set at a constant angle can produce a range of droplet sizes from very large (low pressure) to very small (high pressure) by only changing the pressure. Similarly, if pressure and angle of attack are held constant, droplet size can be regulated by changing the type of splash plate (i.e., a rough or rotating splash plate will yield small drops, and a smooth or yielding splash plate will provide large drops). A graphical illustration of these parameters is shown in Figure 3.3.1.

Experiments were conducted at the Center for Research in Water Resources (CRWR) to evaluate the performance of various splash plates. The “best” rainfall, judged by observation, was produced by a large, smooth splash plate mounted tangent to the exiting water stream. This design allows the water stream to spread out across the surface of the plate with a minimum loss of velocity. The water leaves the plate at all edges, giving width to the spray pattern. Additionally, the splash plate is flexible, which allows some droplets to leave the plate sooner and with higher velocity than others. Because droplets of all sizes are being produced on the plate, all droplet sizes are subject to leaving the plate at varying velocities.

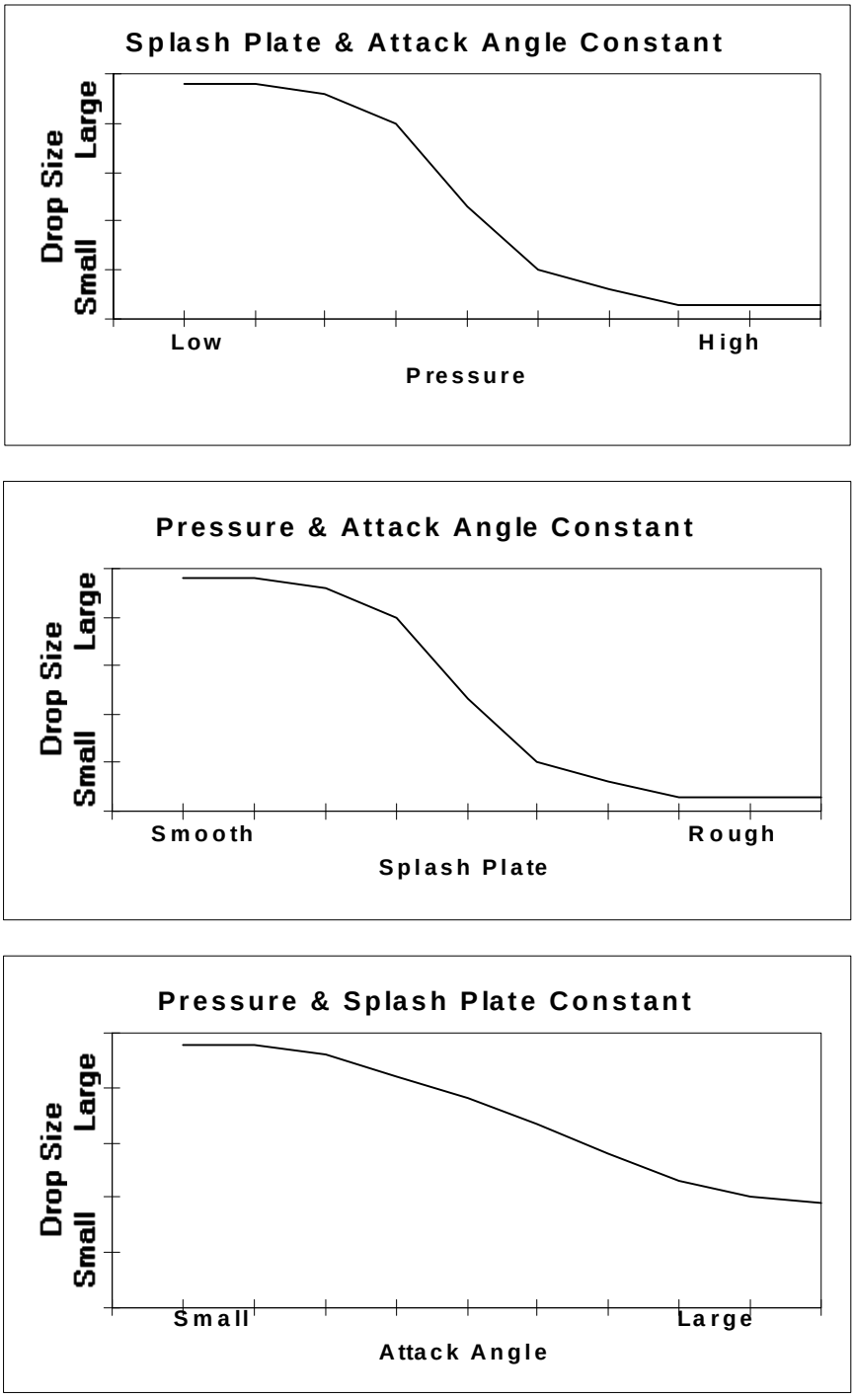

Figure 3.3.1 Relationship Between Nozzle Pressure, Splash Plate Design, Attack Angle, and Droplet Size

Experiments also were conducted to determine the optimal water pressure and nozzle diameter required to drive the water stream across the splash plate. Nozzle diameters up to 16 mm and pressures up to 586 kpa were tested. It was observed that if the water pressure is too high with respect to the nozzle diameter, atomization occurred at the nozzle. If the water pressure is too low, there is not enough energy to break the water stream into smaller drops as it crosses the splash plate. Water pressure in the range of 310 to 450 kpa worked the best with most nozzle diameters. Pressures above 500 kpa will atomize the water stream in the range of nozzle diameters tested at CRWR. Pressures below 175 kpa generally resulted in insufficient throw distance, depending on nozzle diameter. Holding pressure constant at 450 kpa, a 3-meter increase in throw distance was observed for each 0.8 mm increase in nozzle diameter through the range of 3 mm to 6 mm in diameter.

The simulator spray heads must be mounted on the highway shoulder within 2 to 3 meters of the first lane of traffic. The spray heads must also be mounted at a 4.3-meter height so the spray can clear tractor trailer traffic. This arrangement presented the challenge of creating water droplets that will fall both 2 meters and 15 meters from a 4.3-meter elevation. Experiments at CRWR showed that a single nozzle would not satisfactorily perform this task. The simulator spray head was therefore designed with two vertically mounted nozzles. The top nozzle was used to spray water droplets across the center and far lanes of traffic. The lower unit was a smaller diameter nozzle used to cover the near to center lanes. The splash plate for each nozzle was the same size and was set at the same angle of attack. Exit pressure was also the same for both nozzles. The shorter throw distance was achieved by using a smaller orifice, resulting in a smaller flow rate.

The departure angle of the water droplets is also an important consideration. Commercial irrigation equipment manufacturers generally set impact spray heads at a 23-degree angle. However, tests at CRWR during calm conditions indicated that throw distance increased as nozzle angle increased to 45 degrees. The outdoor tests indicated that different nozzle angles could off-set the effects of some wind speeds and directions. The simulator nozzle was therefore swivel mounted to allow for infinite control of nozzle

angle to accommodate various weather conditions. A simple pull-string arrangement allowed the spray head to be set at any angle from the ground.

The nozzle angle may also be used to shorten the throw distance in situations where high rainfall intensities are simulated. Rainfall intensities greater than 75 mm/hr require a nozzle diameter/water pressure combination that produces a throw distance greater than 15 meters (i.e., the width of the highway segment). This situation is remedied by increasing the nozzle angle greater than 45 degrees to obtain the appropriate throw distance.

Figure 3.3.2 shows the assembly of the simulator spray head. The entire head is constructed of PVC in order to reduce weight. No special machining or assembly techniques are required to produce the spray heads, and the nozzles are easily changed for different operating conditions and maintenance.

The spray stand is the structure that supports, and delivers water to, the elevated spray head. The stand has to be lightweight and portable, yet steady and safe when subjected to roadside turbulence and vibrations. A tripod configuration was selected for the stand. Two collapsible swivel legs were forward mounted to support a riser pipe that delivers water to the spray head. The legs can be positioned and locked anywhere along the length of the riser pipe to accommodate for uneven ground. Additionally, the legs swivel in all directions, allowing for various set-up possibilities. Further flexibility is gained from using rubber hose to connect the riser pipe to the distribution piping. Quick-disconnect fittings are used to attach the stand supply hose to the distribution piping. A safety cable is secured to a ground anchor that is placed in the center of the tripod footprint. The entire stand and spray head assembly can be set up and positioned by a single person.

The spray head is the forward-most component of the spray stand, and the legs are as far removed from the traffic lane as possible. The rear-most component of the stand is the bottom of the riser. This configuration insures that all water delivery hardware is as far off the road as possible. The spray stand is illustrated in Figure 3.3.3.

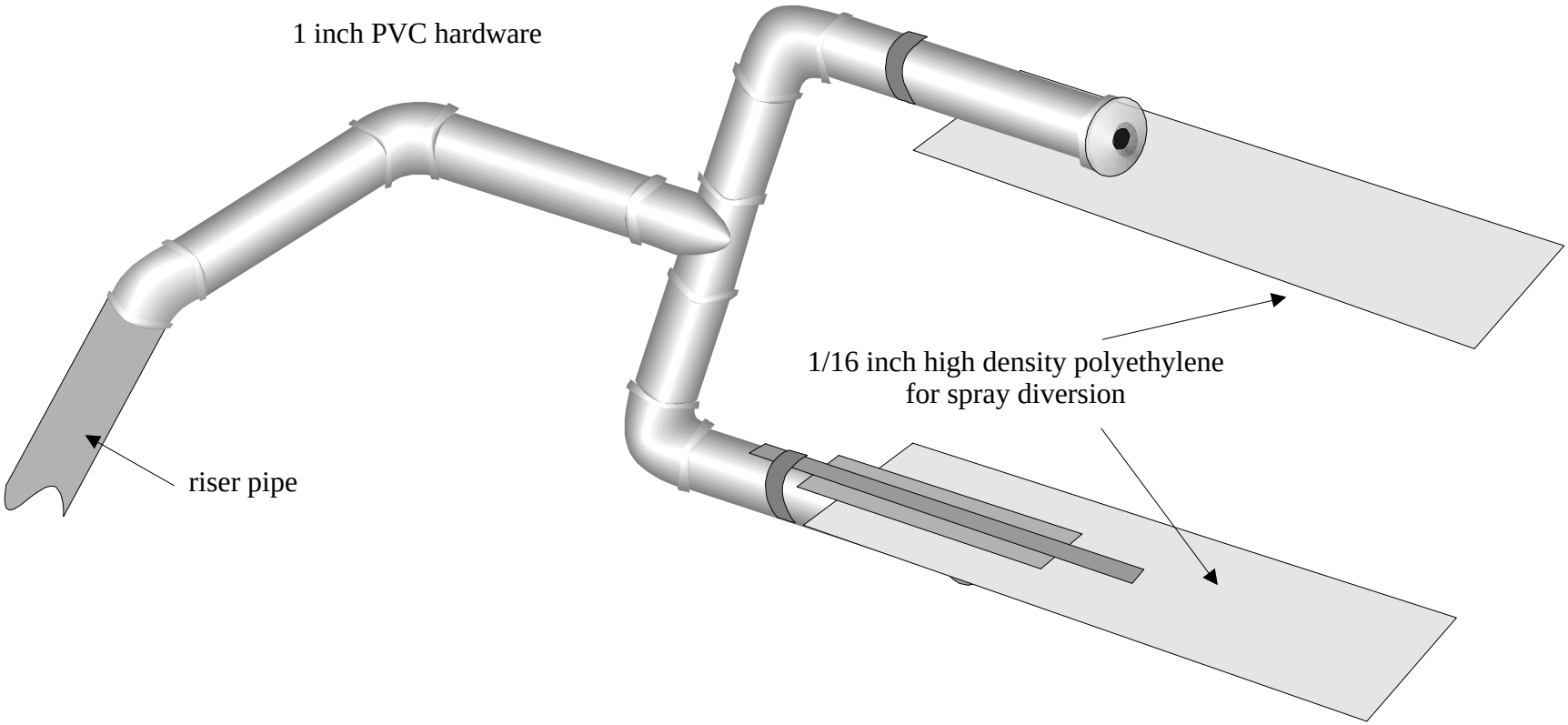

Figure 3.3.2 Spray Head Assembly

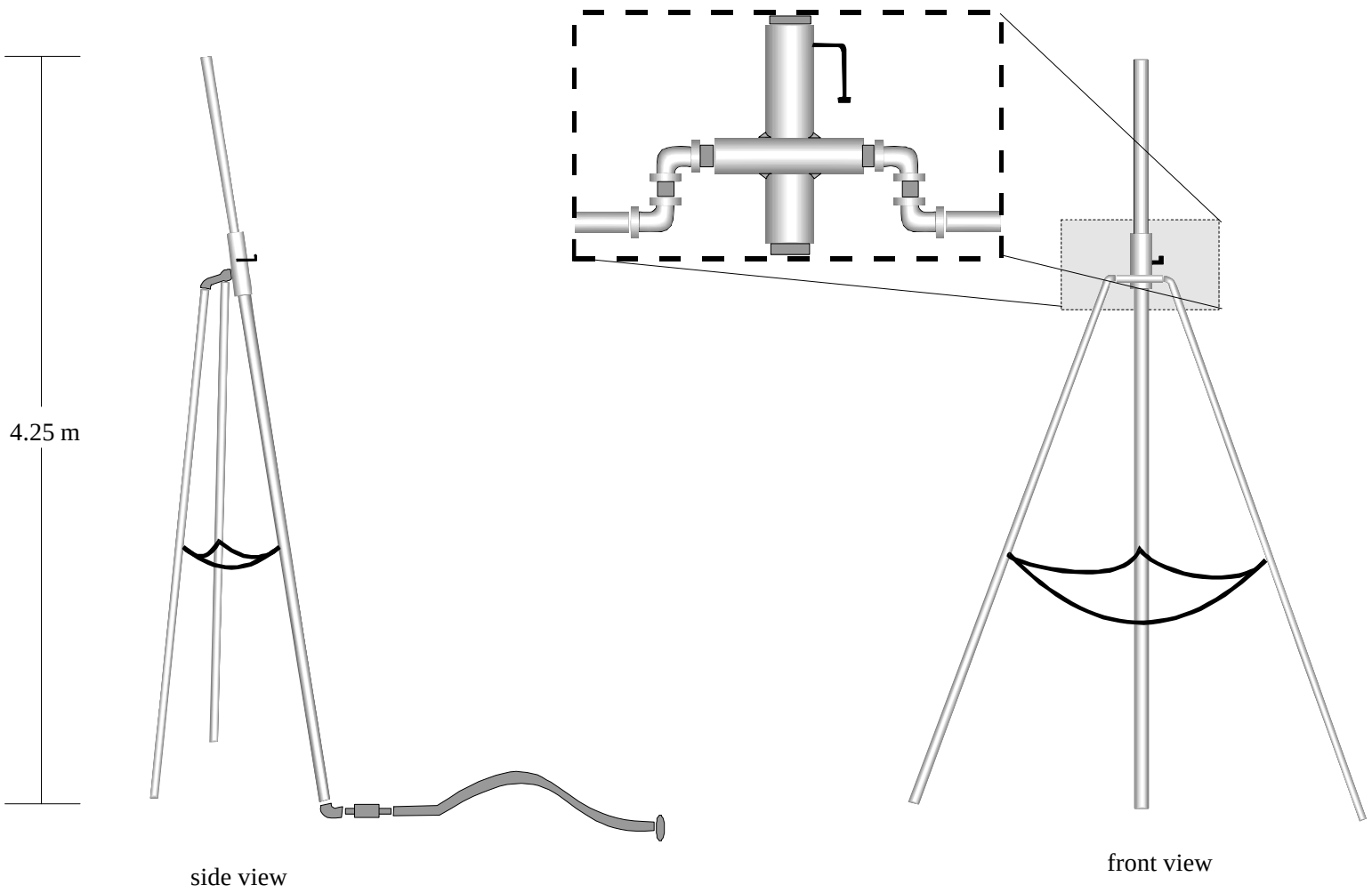

Figure 3.3.3 Spray Stand Assembly

The water supply at the West 35th Street sampling site is a City of Austin fire hydrant. The water must be transported a distance of more than 300 meters to the rainfall simulator. High-pressure aluminum irrigation piping was selected for this task because it is lightweight, sturdy, and easily assembled. The pipe string was assembled by use of a cam lock connection at the end of each joint.

The main design consideration for the delivery and distribution piping was choosing a pipe diameter that would minimize water hammer in the system. Good engineering practice is to keep the water velocity under 1.5 m/sec. The anticipated water flow rate in the system was 56 L/s, based on 67 spray heads (each spray head has a 4-mm diameter nozzle and a 5-mm nozzle) with an operating pressure of 415 kpa. The minimum pipe diameter allowed by this flow rate is calculated as:

$$Diameter = 2\sqrt{\frac{Flow}{(\pi)(Velocity)}} = 2\sqrt{\frac{(56)}{(3.1416)(1.5)(1000)}} = 0.22m \qquad (3.3.1)$$

The supply piping chosen for the initial simulator was 204-mm nominal diameter by 1.6-mm wall thickness. A 6-meter joint length was selected to facilitate handling.

The water supply piping must also distribute water to each spray stand along the sampling zone. If the stands are located every 4.6 meters, 67 stands are required in a 300-meter sampling zone. High-pressure aluminum irrigation piping was again chosen for this task. An outlet was installed every 4.6 meters along the length of the pipe string to facilitate water distribution to the spray stands. Each outlet was threaded and equipped with a quick-disconnect fitting for ease in connection to the stand.

The flow rate through the piping is reduced as water is distributed to the spray stands and is a function of the number of remaining stands (RS) and the flow per stand (FS). A smaller diameter pipe can therefore be employed and not violate the 1.5 m/sec maximum velocity rule. The point where the nominal pipe diameter can be reduced to 153 mm was determined as follows:

$$\begin{aligned} \text{Total Remaining Flow (TRF)} &= \text{RS x FS} \\ &= (\text{RS})(0.8\ \text{L/s}) \end{aligned} \qquad (3.3.2)$$

The nominal diameter of the piping can be reduced to 153 mm at the point where the following number of stands remain in the system:

$$RS = \frac{(Velocity)(Area)}{(13.28)(0.0022)} = \frac{(1.5)(0.018)(1000)}{(0.84)} \cong 32 \qquad (3.3.3)$$

Equation 3.3.3 suggests that the nominal piping diameter can be reduced to 153 mm for the last 152 meters of the sampling zone. Therefore, if the sampling zone is 300 meters long, the first 150 meters should be 204-mm nominal diameter while the last 150 meters can be 153-mm nominal diameter. The 153-mm nominal diameter pipe selected for this section of the system has a wall thickness of 1.5 mm with distribution outlets every 4.6 meters similar to the 204-mm distribution piping. Pipe lengths for the 153-mm nominal diameter pipe was six meters.

The total system assembly is illustrated by the diagram in Figure 3.3.4. The City of Austin provided a 153-mm nominal diameter turbine meter with screen filter to account for water usage. The meter had a maximum delivery of 126 L/s. The meter, screen filter, and a 153-mm nominal diameter resilient wedge gate valve were trailer-mounted to provide a single operating unit that could easily be connected to both the hydrant and the supply piping by flexible hoses. The gate valve provided the main on/off valve for the system. An 204-mm nominal diameter supply line delivers water to the distribution section. The length of the area draining to the sampling point was 225 meters. The initial 150 meters of the distribution piping is 204-mm nominal diameter, and the final 75 meters is 153-mm nominal diameter. Flexible 32-mm nominal diameter hose connected the distribution piping to the main 25.4-mm nominal diameter riser of the spray stand. The spray head was mounted at the top of the spray stand riser. Each spray stand was positioned along the shoulder of the highway to minimize overlapping of spray from each stand.

3.4 Rainfall Simulator Operation

The simulator was engaged by opening the gate valve located on the meter trailer. The use of this valve was preferable to that of the hydrant since the hydrant could be

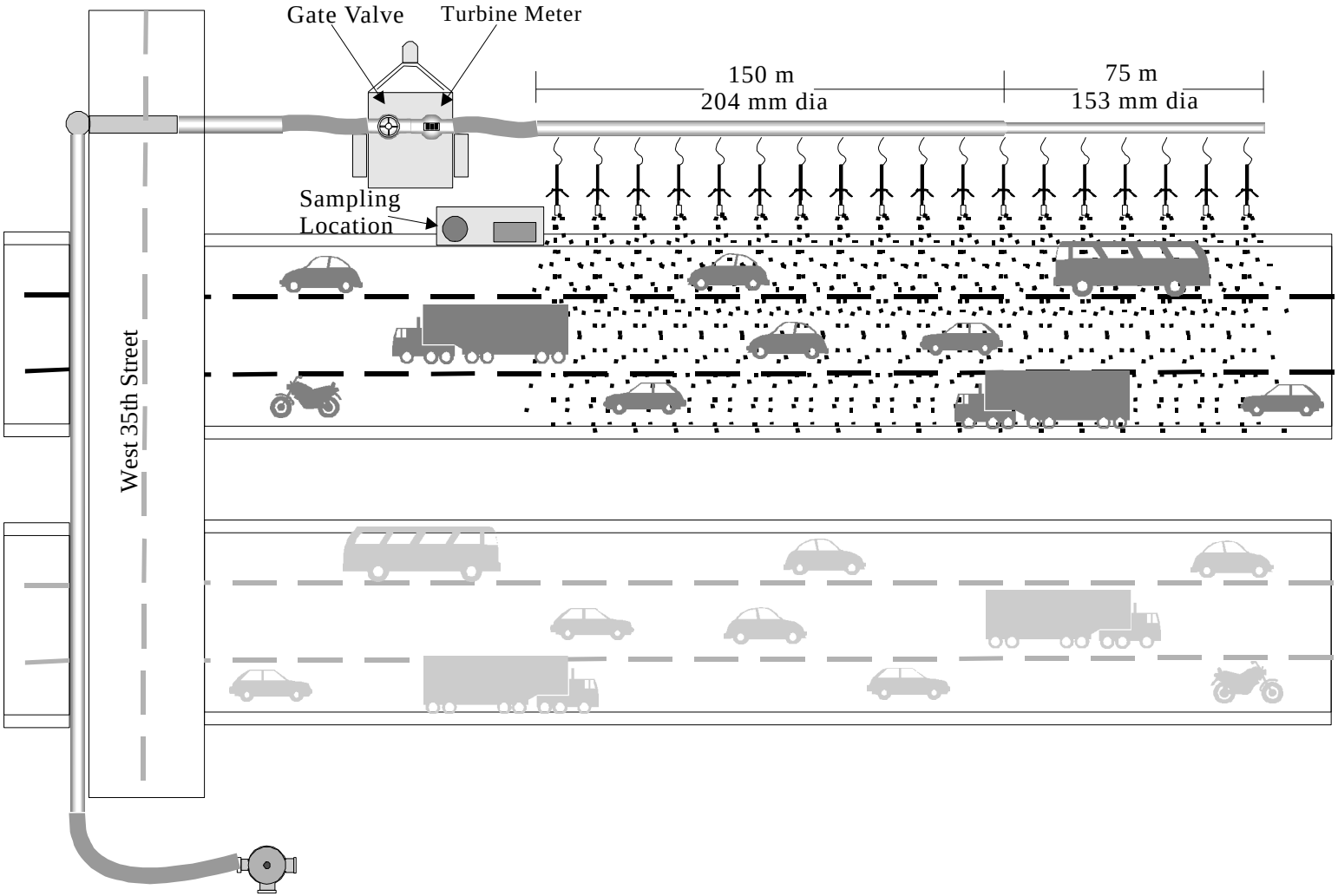

Figure 3.3.4 Total Rainfall Simulator Assembly

damaged as a result of numerous openings and closings. The initial opening of the gate valve was always performed very slowly, allowing the supply piping, distribution piping, and spray stands the opportunity to fill with water and bleed all air before full pressure of the hydrant was applied to the system. Similarly, the valve was always closed slowly to prevent a shock wave that could damage the hydrant.

Water usage by the system is a function or nozzle diameter, water pressure, and number of nozzles. The relationship between nozzle diameter, water pressure, and flow rate is shown in Table 3.4.1. Accordingly, different rainfall intensities are simulated by applying more or less water to the sampling zone, which is regulated by different combinations of nozzle sizes and nozzle pressures. The selection of the correct nozzle size and pressure for a given rainfall intensity was a trial and error process. Table 3.4.2 shows the observed rainfall intensities that resulted from selected nozzle diameters and pressures. The values given in Table 3.4.2 are only used as a guide and assume that there is no loss of water to evaporation or other means, and that all of the water falls evenly over the sampling zone. Following the selection of a nozzle size and pressure combination, the nozzle angle was adjusted to keep the spray within the sampling zone or offset wind effects. The rainfall simulations at the West 35th Street site used 5.2-mm and 4.0-mm diameter nozzles under a pressure of 207 kpa to produce a 28 mm/hr rainfall. The nozzle angle was set at approximately 45 degrees.

Table 3.4.1 Flow Rate (L/s) Given Nozzle Diameter (mm) and Pressure (kpa)

	Nozzle Diameter (mm)					
Pressure (kpa)	3.6	4	4.4	4.8	6.4	9.5
207	0.20	0.24	0.29	0.35	---	1.84
241	0.21	0.26	0.32	0.38	---	1.98
276	0.23	0.28	0.34	0.40	0.73	2.12
310	0.24	0.30	0.36	0.43	0.77	2.25
345	0.25	0.31	0.38	0.45	0.81	2.38
379	---	0.33	0.40	0.47	0.86	2.50
414	---	0.34	0.41	0.49	0.90	2.61

Source: Rainbird Irrigation Equipment (metric conversion made by the author)
Example: A 4-mm diameter nozzle under 207 kpa pressure produces 0.24 L/s flow

Table 3.4.2 Rainfall Intensities Produced by Selected Spray Head Nozzle Sizes and Pressures

Rainfall Intensity (mm/hr)	Diameter of Small Nozzle (mm)	Diameter of Large Nozzle (mm)	Nozzle Pressure (kpa)	Nozzle Flow Rate (L/s)
38	3.6	4.8	207	35
51	3.6	4.8	345	47
64	4.0	5.2	414	56
76	4.0	6.4	310	72
89	4.0	6.4	414	83

Calculations showed that there was only a 14 to 21 kpa pressure loss across the 67 spray stands. There is negligible performance change in the spray head from this small amount of pressure change, so there was no need for more precise control (e.g., placing pressure regulators at the riser pipe of each stand).

The rainfall simulator is shown in Figure 3.4.1a, and the sampling station set-up at the curb-inlet is shown in Figure 3.4.1b. The actual operating parameters of the simulator are listed in Table 3.4.3. A more extensive description of the rainfall simulator is described by Irish (1992).

3.5 Water Quality Sampling

The characterization of a storm water runoff event is entirely dependent upon the design of the sampling program since constituent concentrations and storm water flow rates must be determined from water quality samples that are collected throughout the runoff event. Furthermore, a complete characterization will only be obtained if the sampling interval is short enough, as compared to the total storm duration, to provide an accurate "picture" of the event. This is a difficult task during natural storm events since it is impossible to predict the duration and intensity of the rainfall and subsequently the discharge of the storm. An automatic sampler that is programmed to collect on a predetermined schedule with limited sample jars will inevitably miss the entirety of an event (e.g., either the early part of a light storm or the latter part of a heavy storm will be missed). It is for this reason that the researcher must be at the site with an adequate

(a) View of the rainfall simulator in operation

(b) The storm water sampling station

Figure 3.4.1 The rainfall simulator at MoPac and West 35th Street, Austin, Texas

Table 3.4.3 Rainfall Simulator Actual Operating Parameters

Length of Spray	228.6 m
Maximum Spray Distance	15.2 m
Maximum Spray Height	Approximately 9 m
Maximum Flow @ Pressure	38 L/s @ 206.9 kpa
Maximum Rainfall Intensity	30.5 mm/hr

supply of sampling jars if a true representation is to be obtained of a natural storm. The major advantage of a simulated runoff event is that the researcher knows in advance both the duration of the event and the total volume of runoff that will be produced. With this knowledge, the sampling plan can be designed to precisely capture any desired runoff characteristic.

A selected "grab" sample will yield the instantaneous constituent concentration at a precise moment in the event. The temporal changes in concentration during the event are determined by the comparison of a set of regularly collected grab samples. Furthermore, any number of grab samples may be mixed to yield a single average, or "composite," sample. The intervals at that grab samples are collected may be time-paced, flow-paced, or a combination of both. The time-paced method schedules sample collections at specified time intervals throughout the storm (e.g., every 5 minutes). The flow-paced method collects the sample following the passage of a specified volume of runoff. The decision of that protocol to use depends largely upon the runoff characteristic of interest. Temporal changes in concentration, such as the magnitude and duration of the first flush, can only be determined from a series of grab samples that are collected frequently throughout the storm. The event mean concentration, however, can be determined from a single flow-paced composite sample.

The rainfall simulation sampling protocol was based on the time-paced method. The first sample was collected as soon as runoff was established at the curb inlet box, typically about 3 minutes after the start of the spray. Subsequent samples were collected on 5-minute intervals throughout the remainder of the storm. Observations during the first six storms revealed that the sharpest reduction in constituent concentrations occurred within the first 30 minutes of wash-off. The sampling interval was therefore extended to 10 minutes during the latter half of all subsequent simulations. All samples were collected manually by laboratory technicians on-site during the rainfall simulation. The

storm sampling scheme, shown in relation to the simulated storm hydrograph, is illustrated in Figure 3.5.1. The rainfall simulator was turned off immediately following the collection of the 48 minute sample and the final runoff sample was collected 10 minutes later, or approximately 58 minutes from the start of the spray. Because the time of concentration for the site was approximately 12 to 14 minutes, this sampling scheme yielded two samples from the "rising leg" of the hydrograph, a sample at the beginning and end of the hydrograph "plateau," and a sample from the "falling leg" of the hydrograph.

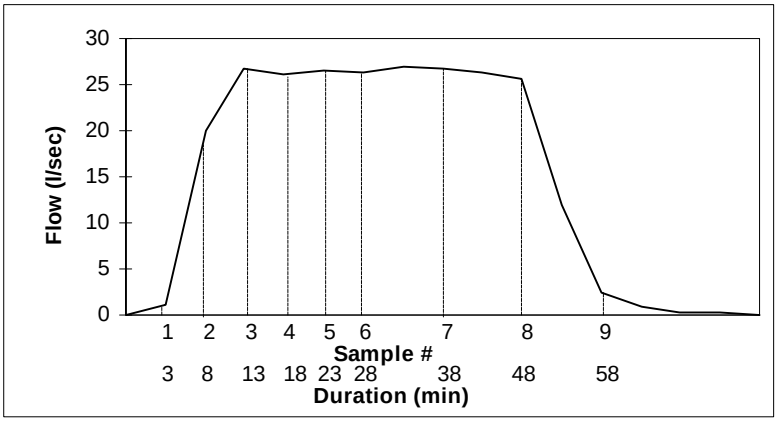

Figure 3.5.1 Simulated Storm Sampling Scheme

The sampling protocol for natural storm events was initially designed to imitate the simulator sampling plan. An automatic sampler was programmed to collect the first grab sample on the detection of runoff along the curb, collect two successive grab samples on a 5-minute interval, and collect a fourth composite sample based on 5-minute intervals over the following 20 minutes. This sampling scheme would yield three grab samples over the first 10 minutes of the storm and a composite sample of the next 20 minutes for a total of 30 minutes of sampling coverage. The plan was based on the observation that once flow was established at the sampling site, the flow normally lasted for at least 30 minutes. This protocol was used to sample all natural storms through November 2, 1993. After this date, the fourth (composite) sample was changed to a flow-weighted composite with collections occurring every 1,900 liters of runoff.

The protocol was changed once more on June 1, 1994 to a schedule which collected four flow-weighted composite samples over the first 10 mm of rainfall during the storm. Each composite consisted of six samples collected every 1900 liters of flow. A full composite therefore represented approximately 2.5 mm of rainfall on the watershed.

Many waste stream constituents are found in the receiving stream prior to the waste outfall, because they either occur naturally in the surface water or they have originated from other waste discharges further upstream. In either case, a blank sample is usually collected to determine the upstream concentration of constituents, or "background," that exists prior to the influence of the subject waste source.

Highway runoff can only occur during and after a rain storm (or snow melt, which was not considered by this study); therefore, the background concentration is the constituent concentration in the rain water. Constituents such as nitrate, phosphate, and metals in rainfall are common in highway runoff. Therefore, an attempt was made to collect a rainfall sample during each natural runoff event. The concentrations of constituents measured in the rainfall sample were subtracted from the concentrations measured in the samples collected at the curb inlet box to determine the true contribution of the highway. Unfortunately, a full sample of rain water could not be collected for each runoff event. At least 10 to 13 mm of total rainfall was required to collect a full sample using the rainfall/atmospheric dust collectors available to this study. Runoff at the West 35th Street site was observed following 0.25 mm of rainfall in a 15-minute period. The median concentration measured of all rainfall samples collected was used as the rainfall blank values. These values are reported in Table 3.5.1.

Highway runoff constituents are also found in the City of Austin tap water that is used for rainfall simulations. Nitrates, phosphates, carbon, and iron are common in the city water. A blank sample was collected near the beginning and end of each simulation. The two samples were averaged to determine a value for background concentrations during each rainfall simulation. These values are reported in Table 3.5.1

Table 3.5.1 Median Background Constituents

Constituent	Austin Tap Water (mg/L except pH)	Natural Rainfall (mg/L except pH)
pH	9.5	NA
TSS	ND	ND
VSS	ND	ND
BOD_5	2 (0.3)	2 (1.1)
COD	5 (0.5)	15 (0.8)
Total Carbon	10 (0.4)	7 (0.8)
Dis. Total Carbon	11 (0.4)	7 (0.8)
Nitrate	0.15 (0.5)	0.47 (0.8)
Total Phosphorus	0.3 (0.4)	0.05 (0.9)
Oil and Grease	0.2 (1.1)	ND
Copper	0.006 (1.3)	0.007 (0.9)
Iron	0.067 (1.0)	0.080 (0.9)
Lead	< 0.042 (1.6)	0.011 (1.1)
Zinc	0.025 (2.8)	0.022 (0.9)

Number in parenthesis is the coefficient of variation;
ND (Non-Detectable); NA (Not Available)

3.6 Runoff Constituents

The primary measure of the quantity of a constituent contained in storm water is *concentration*. Concentration, C, is defined as the amount of mass of constituent contained in a unit volume of runoff. Mathematically,

$$C = \frac{\text{Mass of Pollutant}}{\text{Volume of Fluid}} \quad \frac{[M]}{[L^3]} \tag{3.6.1}$$

Concentration is reported for most constituents in either milligrams per liter (mg/L) or micrograms per liter (mg/L). The exceptions are bacteria counts ("colony-forming units" per 100 mL, CFU/100 mL), turbidity ("nephelometric turbidity units," NTU), and conductivity (microsiemens per cm, µS/cm).

The water quality samples collected during the simulated and natural storm events were analyzed for constituents listed in Table 3.6.1. The laboratory methodology is presented in Appendix A. Microbiology work was not performed on the simulated samples since the Austin tap water contained chloramine for disinfection purposes. Dissolved oxygen measurements also were suspended during simulated storms since the value was near 100% saturation for all measurements.

Table 3.6.1 Highway Runoff Constituents

Field Measurements	pH, Dissolved Oxygen, Conductivity, Water Temperature
Laboratory Analysis	
Bacteriological	Total Coliforms, Fecal Coliforms, Fecal Streptococci
Solids	Total Suspended Solids, Volatile Suspended Solids, Turbidity
Oxygen Demand / Organics	Biochemical Oxygen Demand, Chemical Oxygen Demand, Total Carbon, Dissolved Total Carbon, Oil and Grease
Nutrients	Nitrate, Total Phosphorus
Metals	Cadmium, Chromium, Copper, Iron, Lead, Nickel, Zinc

Dissolved oxygen, conductivity, water temperature, and pH were measured for natural storms only when a technician was on site at the start of the storm. Natural storm event samples were collected using an ISCO Model 3700 Portable Sampler and ISCO Model 3230 flow meter. Simulation grab samples were collected manually on-site during the simulation. All field measurements were made using the Ciba Corning Analytical Checkmate Modular Testing System.

3.7 Flow Measurement

The primary measure of storm water discharge is *flow*. The flow rate, Q, is defined as the volume of runoff per unit time. The units reported in this research are liters per second (L/s). Mathematically, the flow rate is:

$$Q = \frac{\text{Volume of Runoff}}{\text{Time}} \quad \frac{[L^3]}{[T]} \tag{3.7.1}$$

It is important to measure the total storm discharge since both a pollutant mass balance and flow balance must be performed to predict the final concentration of a constituent in the receiving stream (Thomann and Mueller, 1987). During the storm, the

rate at that constituent mass is discharged is termed the *load*, W, and is expressed mathematically as:

$$W = \text{(Concentration)(Flow)} \quad \left[\frac{M}{T}\right] \tag{3.7.2}$$

Load commonly is expressed in units of kilograms per day (kg/d). However, there are many variations adapted to describe a particular process, and units of mass per time-related property (i.e., rainfall or runoff volume) are not unusual. Highway runoff loading often is expressed as mass/time/length of road, mass/time/area of road, or mass/area of road/millimeters of runoff (Barrett et al., 1993). Load is reported in this research as grams per square meter of highway surface (g/m^2).

Instantaneous flow rates were recorded every 5 minutes using an ISCO Model 3230 flow meter with plotter. This flow meter is a "bubbler" type. The meter determines the depth of water in a channel by measuring the amount of air pressure required to force an air bubble from a submerged tube. As the depth of water increases, the pressure required to emit a bubble increases. The meter has an accuracy of ± 1.5 mm in the range of water levels possible in highway curbs and gutters. The flow meter will convert the level measurements to flow with a user-defined equation or interpolate a flow value from a known rating curve.

Installation of a weir or flume along the curb of the highway at the West 35th Street site was not practical. The height of the curb is too low, and the device would extend onto the highway shoulder, causing a hazard to traffic. Any attempt to measure the flow of water inside the curb inlet box would require the installation of a weir or flume and a stilling basin for accurate measurements. This equipment would restrict the drainage capacity of the inlet box, causing a hazard of roadway flooding during heavy flows. Measuring the water level in the discharge pipe of the inlet box is also impossible because of the steep angle of descent of the pipe. Furthermore, flow measurements inside the curb inlet box are complicated because the curb inlet box at this location also functions as a junction box (i.e., flows from other watersheds move through the box during natural rain events). The only practical way to measure the storm water discharge rate at this site was to measure the level of water along the highway curb. These measurements can subsequently be converted to flow rates using either Manning's

equation (Urbonas and Roesner, 1992) or the stage-discharge relationship of the gutter. The stage-discharge relationship, or rating curve, for the gutter at the West 35th Street site was developed using the metering equipment of the rainfall simulator and is presented in Figure 3.7.1. This curve provided the basis for flow measurement at the West 35th Street site.

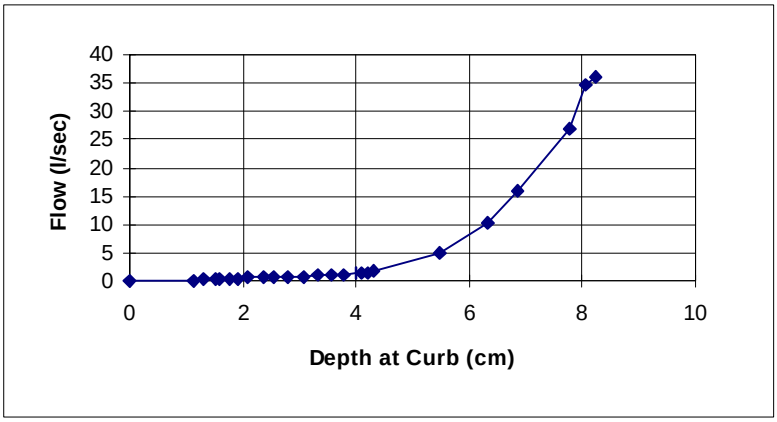

Figure 3.7.1 Rating Curve for Highway Curb at MoPac & 35 Street

Flow measurement at the Convict Hill site presented a different challenge. The highway runoff flowed off the Convict Hill overpass to ground below via a down-spout. A weir or flume could not be installed along the curb for the same reasons as at West 35th Street, and there was no practical way to rate the curb. A catch box with a weir was installed at the bottom of the down-spout to measure descharge. The depth of water in the box was measured with an ISCO Model 3230 flow meter, and the flow conversion was made using a weir formula.

3.8 Event Mean Concentration

The event mean concentration (EMC) is commonly used to describe storm water runoff events. The EMC is defined as the total constituent mass discharged during an event divided by the total volume of discharge during the event (Huber, 1992). Mathematically,

$$EMC = \frac{M}{V} = \frac{\int C(t)Q(t)dt}{\int Q(t)dt} \qquad (3.8.1)$$

The EMC is a flow-weighted average of the constituent concentration and is reported in units of mg/L. The total mass loading of a constituent during the storm may be obtained by multiplying the EMC by the total volume of storm runoff.

The EMC is the concentration of a constituent in a single composite sample collected on a flow-paced interval throughout the storm. However, if only concentration data are available for sequential grab samples collected at discrete time intervals, the hydrograph (plot of flow vs. time) and the pollutograph (plot of constituent concentration vs. time) of the storm must be known in order to calculate the EMC. Furthermore, the concentration measured at a specific time, *T*, is the average concentration in the sample collected during the interval that begins one-half way between *T* and the time of the previous sample, and that ends one-half way between *T* and the time of the next sample. The mass load is obtained by multiplying this "average" concentration by the total flow accumulated during the interval and the length of the interval. This procedure is described mathematically by the trapezoidal rule and the calculation proceeds as follows:

1) $$EMC = \frac{M}{V} = \frac{\sum_i C_i Q_i \Delta t_i}{\sum_i Q_i \Delta t_i} \qquad (3.8.2)$$

2) $$M = \int C(t)Q(t)dt = \sum_i C_i Q_i \Delta t_i \qquad (3.8.3)$$

3) $$V = \int Q(t)dt = \sum_i Q_i \Delta t_i \qquad (3.8.4)$$

4) The concentration, C(i), at time t(i), is equal to the average concentration for a period Δ T(i) beginning at time t(i) - 0.5[t(i) - t(i-1)] and ending at time t(i) + 0.5[t(i+1) - t(i)].

5) Q(i) is equal to the total volume of flow during period Δ T(i) divided by the duration of period Δ T(i).

3.9 Rainfall Measurement

Rainfall was measured at each site using an ISCO Model 674 rain gage equipped with a "tipping bucket" that measures rainfall in 0.25 mm increments. A pulse signal is sent to the ISCO flow recorder on each tip of the bucket. The rainfall hyetograph was

recorded in 5-minute intervals throughout the duration of a storm. Rainfall measurements are reported in millimeters.

3.10 Miscellaneous Measurements

The traffic count during both wet and dry periods was measured using a StreeterAmet traffic data system installed at the MoPac test site by TxDOT. Wind speed (m/s) and direction were measured during rainfall simulations with a Kahlsico hand-held anemometer at the test site. Air temperature (^{0}C) was obtained from the National Weather Service Office, Austin, TX. Simulator duration time (minutes) and sampling intervals were measured with a stop watch.

3.11 Detection Limit Data

Concentrations of highway runoff constituents are often near the detection limit of analytical equipment. For example, metal concentrations typically are in the micrograms-per-liter range. For cases where the concentration of constituents are below the detection limit of the analytical methodology or equipment in use, the constituent concentration is reported as below the "limit of detection" (LOD) or "non-detectable" (ND). Specifically, the LOD for a particular method is defined in 40 CFR Part 136 as the "...lowest concentration of the analyte that can be measured and reported with a 99% confidence that the analyte concentration is greater than zero."

Concentrations less than the LOD are reported in a variety of ways, such as "non-detectable," "0," or "less than values." In this report, the notation used is the LOD proceeded by a "<" sign. Although the true concentration of the constituent is unknown, it is recognized that the concentration is greater than zero but less than the LOD.

The are several common methods of treating ND values (Gilbert, 1987). The method selected for this research is to replace ND with a value of one half the LOD. This substitution yields an unbiased estimate of the true population mean as long as the analytical procedure does not yield a value of less than zero. However, estimate of the variance is biased. The expected value, or mean, of a ND observation is an appropriate substitution in most cases, but it cannot be made universally.

The application of the term ND requires care and consideration of the type of sample and the constituent in question. A sample of tap water or rainfall provides the background concentration that exists before the influence of the highway and is considered to be the blank. The highway contribution is established by subtracting the background concentration measured in the blank sample from the instantaneous concentration measured in the runoff samples. An approximation of the true mean of the background concentration is appropriate for this calculation. Therefore, ND values are replaced by a value of one half the LOD. However, in the case of oil and grease, which are not expected to be in the blank sample, a reported ND value is assigned a zero since oil and grease are not be expected to be in either the City of Austin drinking water or in the natural rainfall.

A value of ND may also be reported for a runoff sample. The runoff sample can be a single sample collected at a particular instant during the event, or a composite of collections from several intervals during the event. Since all of the constituents listed in Table 3.6.1 are expected to be in the highway runoff, any ND value in a runoff sample is replaced by one half of the LOD value, and the EMC for the event will be calculated using this value. However, if a large number of ND values are reported for a pollutant during a single event, the value of the EMC could be less than the value of the LOD. The most extreme case is a ND value reported for all samples collected during the runoff event in which the expected value for the constituent is one half the LOD.

3.12 Summary

A rainfall simulator was constructed to aid in the collection of highway runoff data. The simulator covered nearly 4,400 m^2, which was the entirety of the watershed that drained to a single curb inlet, and was operated over active highway traffic. The advantages of the simulator were (1) the control of parameters that affect highway runoff, (2) the execution of a precise water quality sampling scheme during ideal sampling conditions, (3) the generation of storm events during extended periods of dry weather, (4) the generation of a large number of runoff events for statistical analysis, and (5) the production of a steady-state storm event.

The highway runoff constituents measured during this research included TSS, VSS, turbidity, BOD_5, COD, TOC, dissolved TOC, oil and grease, nitrate, total phosphorus, cadmium, chromium, copper, iron, lead, nickel, zinc, pH, dissolved oxygen, conductivity, water temperature, total coliforms, fecal coliforms, and fecal streptococci. The sampling protocol for simulated storm events was based on time-paced grab samples. Natural event sampling protocol was based on flow-weighted composite samples. Blank samples of Austin tap water and rainfall were collected to provide background concentrations. Runoff volume was measured using rating curves established for the street curbs at the sampling site.

4.0 Data Summary

4.1 Introduction

A total of 35 simulated rainfall events were sampled at the West 35th Street site between July 6, 1993 and July 14, 1994. A total of 23 natural storm events were sampled at the West 35th Street site between September 14, 1993 and April 28, 1994, and 20 events were sampled at the Convict Hill site between April 29, 1994 and December 9, 1994. An analysis of the data is presented in this chapter and includes the characteristics of each sampled storm event, an analysis of the underlying distribution of the data, the computation of descriptive statistics, analysis of constituent wash-off patterns, and an analysis of daily and seasonal trends.

Total suspended solids (TSS), nitrate, and oil and grease were selected for detailed analysis because (1) there is local concern regarding the input quantities of these constituents into the Edwards Aquifer and (2) these constituents best represent the wash-off patterns of all constituents in highway runoff. The characteristics of other highway runoff constituents are presented in the appendices noted throughout the chapter.

4.2 Storm Event Characteristics

Thirty-two rainfall simulations were conducted over active traffic during the study period and the characteristics of each event are presented in Table 4.2.1. Samples of runoff were collected over a 60 minute time period, and variations in the event duration were a result of equipment failure and other unforeseen circumstances. The variations in the measured flow are a result of adverse wind conditions that carried the spray outside of the sampling zone. Traffic volume during the simulated storm event ranged from 1,358 to 3,733 vehicles and varied with the time of day the simulation was conducted. The temperature during the simulated events varied with the season.

The duration of the antecedent dry period varied as a result of the simulator spray schedule. The Austin area experienced no rainfall from June 23, 1993 through August 31, 1993, which allowed for several simulations to be preceded by a 14-day dry

Table 4.2.1 Characteristics of Simulated Storm Events (Traffic Sessions)

Date	Event Duration (min)	Event Flow (l/m^2)	Vehicles During the Event	Temp. (^0C)	Antecedent Dry Period (hrs)	Antecedent Traffic Count	Preceding Storm Flow (l/m^2)
7/6/93	60	19.9	3,132	30	241	548,020	58.5
7/12/93	50	14.2	3,637	30	141	328,670	20.9
7/20/93	35	11.3	1,673	30	192	473,380	14.9
7/27/93	50	15.6	2,521	31	166	405,540	11.8
8/10/93	65	19.9	3,361	31	335	811,060	16.3
8/24/93	25	3.4	1,358	32	335	811,060	20.9
9/23/93	60	15.5	3,610	31	268	578,260	22.6
10/7/93	60	15.8	3,733	26	267	644,990	1.8
11/4/93	60	18.3	3,092	21	25	68,060	9.3
11/17/93	60	18.5	3,618	12	25	66,120	3.3
12/1/93	60	17.9	3,406	12	334	734,000	19.5
12/10/93	45	5.4	2,709	12	214	547,260	18.8
12/16/93	60	13.6	3,989	12	83	230,750	4.2
1/4/94	60	16.0	2,689	11	310	610,250	16.4
1/11/94	60	18.1	2,910	17	21	50,710	0.5
1/13/94	60	18.1	2,879	14	4	16,090	3.9
2/3/94	60	16.7	2,956	7	132	282,170	0.3
2/17/94	60	16.1	3,139	14	160	365,750	10.3
2/24/94	60	17.5	2,995	10	47	85,410	22.9
3/1/94	60	14.1	3,282	12	6	32,860	12.6
3/10/94	60	16.9	3,352	9	26	77,920	36.2
3/17/94	60	14.8	3,352	19	37	78,240	13.9
4/8/94	60	16.2	3,337	19	65	168,396	10.4
4/13/94	60	15.7	3,116	19	42	112,264	1.8
4/20/94	60	16.2	3,116	22	17	42,099	2.9
5/12/94	60	16.1	3,116	27	233	561,320	9.0
5/26/94	60	22.0	3,116	26	213	505,188	0.3
5/31/94	60	16.3	3,282	28	35	112,264	26.3
6/8/94	60	20.5	3,238	31	118	280,660	18.6
6/16/94	60	19.2	3,433	29	18	84,198	10.3
7/1/94	60	18.7	3,190	30	118	304,420	48.6
7/14/94	60	17.8	3,050	31	310	733,620	20.8

period. At least one simulated storm event was produced having an antecedent dry period of each daily interval between 1 and 14 days. The total natural rainfall during the period of operation of the simulator was 444 mm, that is approximately one-half the average annual rainfall of 856 mm.

Three simulated storm events were conducted under "no-traffic" conditions, and the characteristics of these events are presented in Table 4.2.2. The no-traffic experiments were conducted by closing the sampling site to traffic and operating the rainfall simulator in the same manner as during a traffic event. The no-traffic events occurred on early Sunday morning's, as soon after sunrise as possible, to minimize disruption of highway use.

Table 4.2.2 Characteristics of Simulated Storm Events (No-Traffic Sessions)

Date	Event Duration (min)	Event Flow (l/m^2)	Temp. (^0C)	Antecedent Dry Period (hrs)	Antecedent Traffic Count	Preceding Storm Flow (l/m^2)
9/12/93	60	21.5	28	283	668,550	19.8
2/6/94	60	22.5	17	68	167,090	18.8
6/26/94	60	22.4	31	53	140,330	1.0

A primary reason for using a rainfall simulator in highway runoff research is the control of all, or at least most, of the parameters that influence constituent loads in highway runoff. However, there are many factors beyond the control of the experiment that cause variation among the parameters that are suppose to be under "control." For example, the total volume of water sprayed during the simulated event was held constant for all simulated storm events; however, there was considerable variation in the volume of runoff recorded between simulated events because the spray was affected by "wind drift" and "traffic drag-out" differently during each simulation. The best the experimenter can do is repeat enough runs so that the variation in the "uncontrolled" parameters exhibit a normal distribution. The total volume of runoff, the total volume of traffic during the storm, and the total volume of flow during the preceding storm were all uncontrolled variables during the rainfall simulations. However, enough simulated storm events were conducted so that the probability of occurrence of each uncontrolled

parameter is normally distributed. The normal distribution of uncontrolled parameters is illustrated in Figure 4.2.1. The units of the abscissa are the same units indicated in Table 4.2.1 and the frequency of occurrence is shown on the ordinate.

There are certain variables that affect the loading of constituents in highway runoff that the rainfall simulator was able to control. One of these is the duration of the antecedent dry period (ADP), which is controlled by the choice of the time and day that the simulated event is conducted. The volume of traffic during the antecedent dry period (ATC) was controlled by the ADP because of the nature of the traffic pattern. The experiments were designed to obtain a number of repetitions for each ADP between 1 and 14 days in length. Therefore, the frequency distribution for these variables is more rectangular than the distribution of the uncontrolled variables.

The frequency distributions for ADP and ATC are shown in Figure 4.2.2. The units of the abscissa are the same units indicated in Table 4.2.2, and the frequency of occurrence is shown on the ordinate.

Twenty-three natural storm events were sampled using automatic samplers at the same site as the simulated storm events (West 35th Street) between September 14, 1993 and April 28, 1994. The characteristics of these natural storm events are reported in Table 4.2.3. The second column of Table 4.2.3 titled “Event Duration (min)” reflects the total time interval that samples were collected during the storm and not necessarily the total duration of the storm. Sampling intervals during the natural storm events at the West 35th Street site ranged from 25 minutes to 830 minutes (13.8 hrs). The third column titled “Event Rainfall (mm)” is the volume of rainfall recorded during the sampling interval. Sampled rainfall volumes ranged from 0.25 mm to 19.28 mm. The fourth column titled “Vehicles During the Event” is the total number of vehicles recorded during the sampling interval. The average temperature recorded during the storm event by the National Weather Service Office, Austin, is reported in degrees Celsius. The duration of the antecedent dry period (hrs), the traffic count during the antecedent dry period, and the total volume of storm flow during the preceding storm event (L/m^2) also are reported in Table 4.2.3.

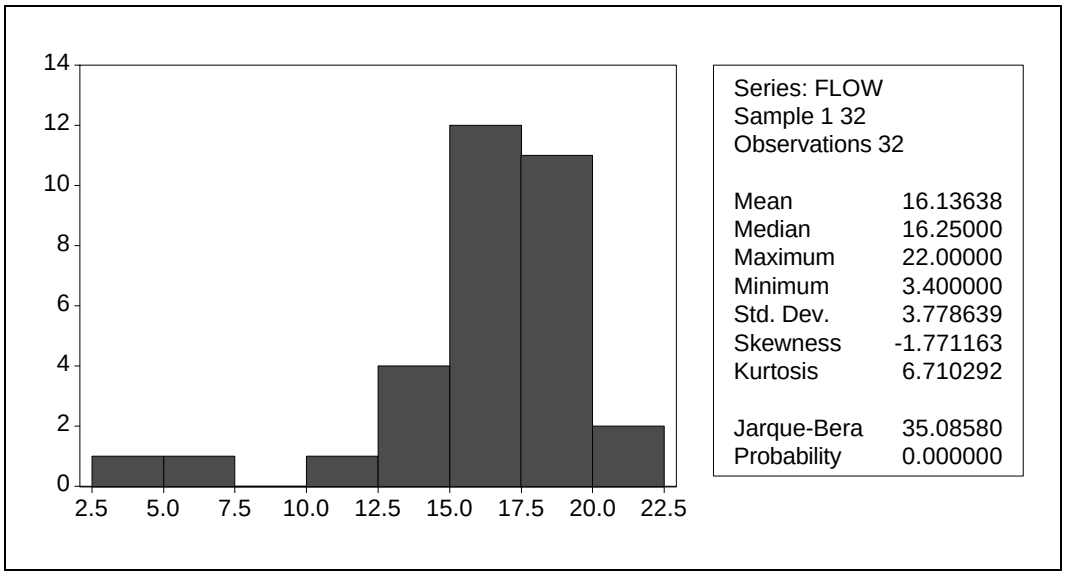

(a) Storm Event Runoff (L/m^2)

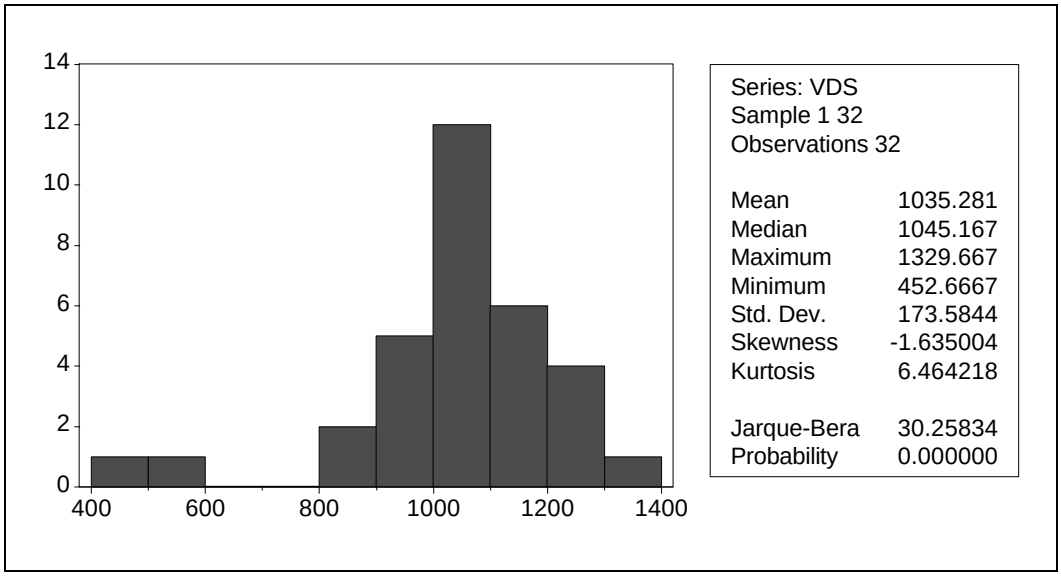

(b) Number of Vehicles during the Storm Event

Figure 4.2.1 Distribution of Uncontrolled Variables during Rainfall Simulations

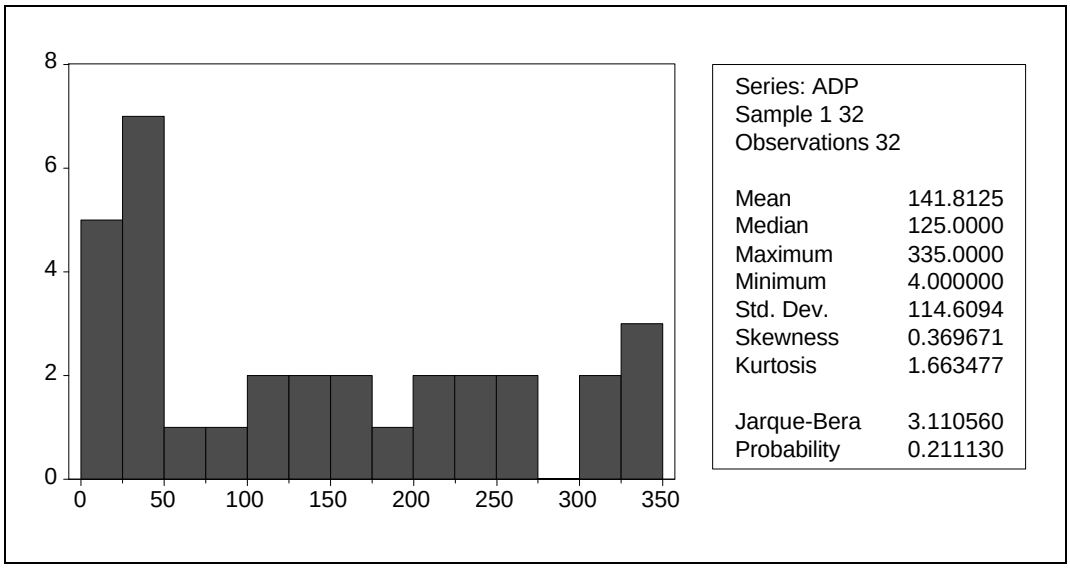

(a) Duration of the Antecedent Dry Period (hrs)

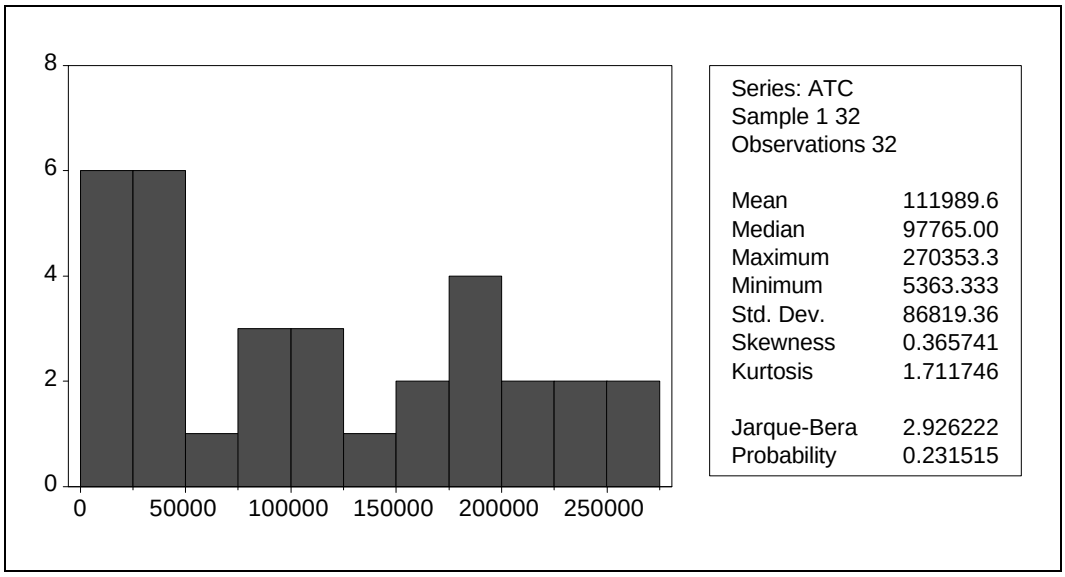

(b) Traffic Count during the Antecedent Dry Period

Figure 4.2.2 Distribution of Controlled Variables during Rainfall Simulations

Table 4.2.3 Characteristics of Sampled Natural Storm Events (West 35th St. Site)

Date	Event Duration (min)	Event Rainfall (mm)	Vehicles During the Event	Temp. (^{0}C)	Antecedent Dry Period (hrs)	Antecedent Traffic Count	Preceding Storm Flow (l/m^2)
9/14/93	45	0.25	110	26	42	124,660	22.6
10/13/93	60	1.52	120	19	120	270,580	0.3
10/20/93	40	11.68	162	18	159	398,750	0.8
10/20/93	45	1.27	1,470	20	9	18,740	7.6
10/20/93	60	1.52	1,695	20	3	9,950	0.3
10/29/93	175	6.86	9,940	13	192	480,710	0.5
11/2/93	50	1.52	720	12	99	221,630	6.6
12/22/93	135	1.40	9,140	5	93	214,730	0.2
1/13/94	55	2.31	210	9	33	75,150	19.5
1/20/94	620	2.31	22,190	9	157	375,890	19.1
1/22/94	190	1.32	6,205	8	20	43,530	11.4
2/21/94	800	19.28	13,610	19	27	63,800	1.2
2/28/94	830	10.13	25,510	14	97	226,110	18.5
3/9/94	25	8.13	190	7	172	437,490	14.3
3/13/94	595	7.62	31,230	16	44	115,570	17.9
3/15/94	85	8.38	1,430	17	50	93,620	9.0
3/27/94	30	1.02	95	9	60	149,670	1.1
4/5/94	30	12.19	1,975	19	223	500,200	2.3
4/11/94	205	1.78	10,460	22	69	173,320	17.2
4/15/94	25	4.32	2,425	23	50	146,180	16.7
4/19/94	25	3.05	2,400	23	95	231,740	3.3
4/28/94	50	1.52	3,620	28	188	483,980	17.4
4/28/94	170	9.91	7,190	19	9	31,220	1.0

The distribution of the sampled rainfall volumes and the duration of the antecedent dry periods are shown in Figure 4.2.3. The distribution of the rainfall exhibits normality, as evidenced by a 94% confidence level using the Jarque-Bera test (refer to Section 4.3 for details of the Jarque-Bera test). The distribution of the duration of the antecedent dry period is expected to be exponential (Chow et. al., 1988). However, the distributions of the recorded duration of the antecedent dry periods for the sampled natural events at the West 35th Street site are rectangular, similar to what would be expected if the duration of dry period had been controlled. This is a result of the rainfall simulations, which were conducted during the dry period between natural storms.

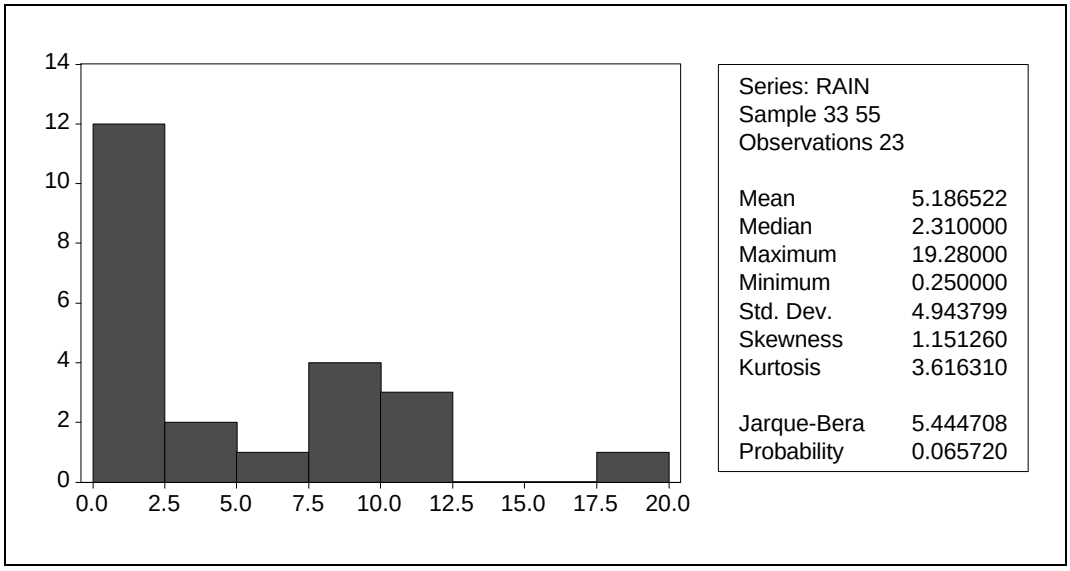

(a) Event Rainfall (mm)

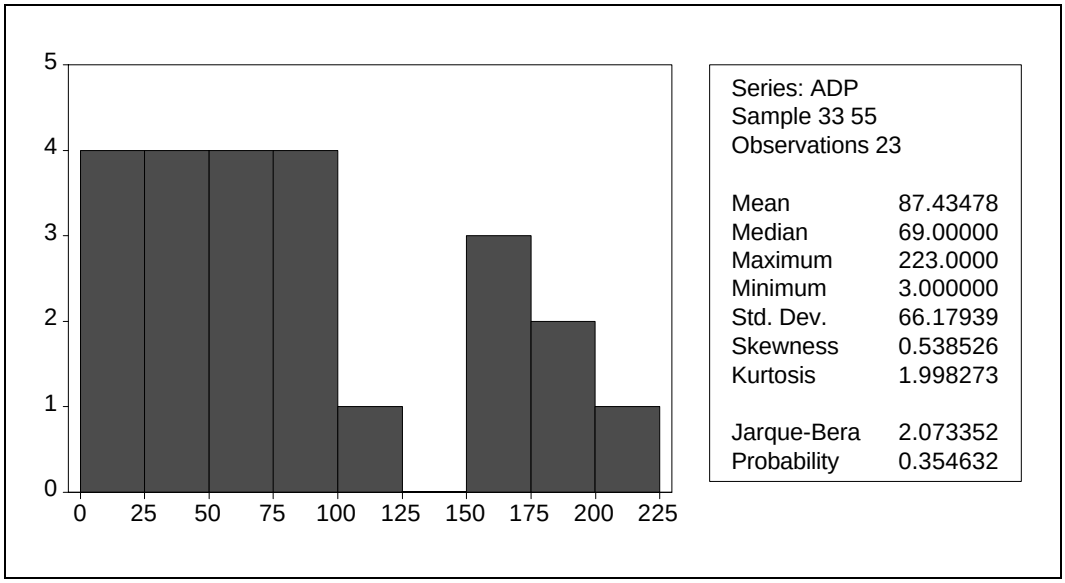

(b) Antecedent Dry Period (hrs)

Figure 4.2.3 Distribution of Natural Rainfall Event Variables

Twenty natural storm events were sampled at the Convict Hill site between April 29, 1994 and December 9, 1994. The characteristics of these storms are reported in Table 4.2.4. Similar to the characteristics reported in Table 4.2.3, the event duration, event rainfall, vehicles during the storm, and average temperature reported in Table 4.2.4 each represent observations during the sampling interval of the storm.

The relationship between rainfall volume and runoff volume is presented in Figure 4.2.4 for the West 35th Street watershed and the Convict Hill watershed. The reported rainfall volume and runoff volume are for the entirety of the storm event, not the

Table 4.2.4 Characteristics of Sampled Natural Storm Events (Convict Hill)

Date	Event Duration (min)	Event Rainfall (mm)	Vehicles During the Event	Temp (^{0}C)	Antecedent Dry Period (hrs.)	Antecedent Traffic Count	Preceding Storm Flow (l/m^2)
4/29/94	27	2.29	5	24	12	3,528	4.6
5/2/94	228	2.79	1388	17	6	1,764	1.5
5/13/94	40	11.68	382	21	261	76,734	3.8
5/14/94	10	6.35	39	23	30	8,820	28.7
5/16/94	112	1.78	109	23	24	7,056	19.3
6/10/94	20	4.32	115	29	152	44,688	3.6
6/19/94	12	5.84	39	28	24	7,056	5.1
6/21/94	16	4.06	24	28	43	12,642	6.9
8/8/94	15	4.57	39	31	48	14,112	0.5
8/9/94	75	9.14	102	26	6	1,764	6.1
8/16/94	52	7.62	357	28	175	51,450	78.2
8/22/94	94	6.86	514	27	19	5,586	1.5
9/7/94	27	4.32	173	29	166	48,804	2.0
9/8/94	7	6.86	2	24	12	3,528	4.3
9/9/94	37	11.94	354	24	16	4,704	44.4
10/7/94	133	9.40	452	24	75	22,050	0.5
10/14/94	195	6.10	500	18	155	45,570	140.2
10/25/94	68	14.22	11	18	159	46,746	22.1
10/27/94	503	5.33	2975	12	43	12,642	41.1
11/5/94	34	12.45	6	19	193	56,742	5.3
11/15/94	308	3.81	1956	14	240	70,560	24.6
12/2/94	48	7.62	362	13	333	97,902	1.5
12/9/94	139	2.29	109	10	150	44,100	7.4

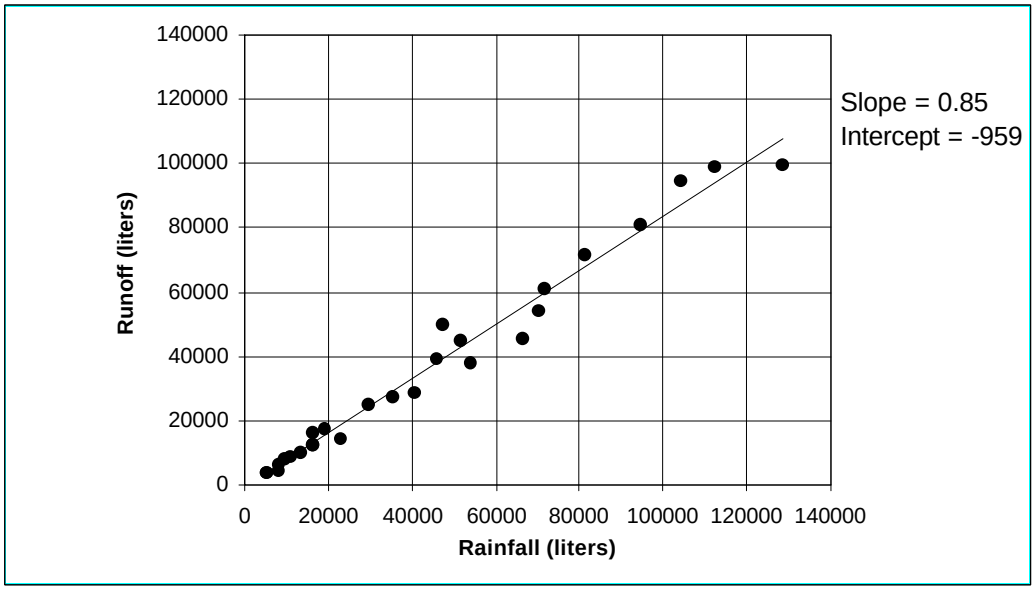

(a) West 35th Street Sampling Site

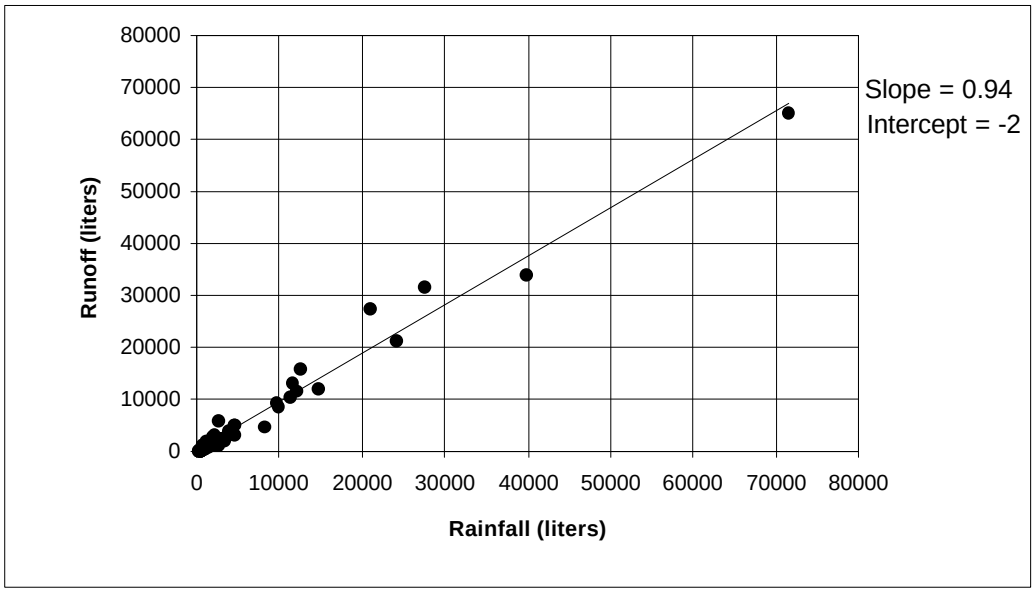

(b) Convict Hill Sampling Site

Figure 4.2.4 Rainfall / Runoff Relationship

water quality sampling interval. The runoff coefficient is 0.85 at the West 35th Street site and 0.94 at the Convict Hill Site. This difference is possibly a result of the West 35th Street watershed being ten times longer than the Convict Hill watershed (Table 3.1.1).

4.3 Distribution of Highway Runoff EMCs

The lognormal distribution is the most commonly used probability density model for environmental contaminant data (Gilbert, 1987). The event mean concentrations (EMCs) of constituents in urban runoff, and highway runoff in particular, have been described by the lognormal distribution (USEPA, 1983; Driscoll et. al., 1990). The shape of the underlying distribution must be known in order to select the statistics that will best estimate the parameters of the population. Methods that are used to evaluate distributional shape include (1) probability plotting, (2) examination of the coefficient of variation, (3) skewness, (4) kurtosis, and (5) normality testing with the Jarque-Bera statistic.

Probability plotting is commonly used to determine the shape of an underlying distribution. Probability plotting methods exist for normal, lognormal, Weibull, gamma, and exponential distributions (Gilbert, 1987). Driscoll et al. (1990) extensively used log probability plots to demonstrate the lognormality of the EMCs of highway runoff constituents. Probability plotting can provide a quick determination of whether the data are likely to have come from a specific type of distribution; however, the principal application of the method is the determination of the mean and variance of the distribution once the shape is known.

Normal and lognormal probability plots were constructed for all highway runoff constituents in this study. The results indicate that each constituent is best represented by a skewed distribution. It is risky, however, to rely on the "straightness" of the plotted points to determine the normality or non-normality of the distribution. Although a probability plot can detect a skewed distribution, the plot cannot evaluate the amount of skewness, a factor that is imperative in the selection of descriptive statistics. Therefore, probability plots have limited value for the determination of distributional shape. The normal and lognormal probability plots for the TSS data collected at the West 35th Street site are presented in Figures 4.3.1.

The properties of skewness and kurtosis each measure an aspect of non-normality. Skewness (S) is the standardized third cumulant defined as:

$$S = \frac{\frac{1}{N}\sum_{n=1}^{N}(y_n - \bar{y})^3}{s^3} \qquad (4.3.1)$$

where: N = sample size;

y = value of the observation;

$\bar{y}$ = sample mean;

σ = standard deviation of the sample.

If the distribution is skewed to the left, then S is negative and if the distribution is skewed to the right, then S is positive. For a symmetrical distribution, S is equal to zero.

Kurtosis (K) is the standardized fourth cumulant defined as:

$$K = \frac{\frac{1}{N}\sum_{n=1}^{N}(y_n - \bar{y})^4}{s^4} - 3 \qquad (4.3.2)$$

For a normal distribution, K is equal to zero. If K is positive, the distribution is said to be leptokurtic and typically has less pronounced "shoulders" and heavier "tails" than the normal distribution. If K is negative, the distribution is said to be platykurtic and typically has squarer shoulders and lighter tails than the normal distribution (Box and Tiao, 1973).

Histograms of the event mean concentrations for TSS, nitrate, and oil and grease are presented in Figures 4.3.2, 4.3.3, and 4.3.4 respectively. The skewness and kurtosis are given in each figure. These plots were produced using MicroTSP Econometric Views software (Quantitative Micro Software, Irvine, CA). The equation used by this software to calculate kurtosis does not subtract three from the standardized fourth cumulant as shown in Equation 4.3.2. Therefore, the kurtosis of a normal distribution is equal to three

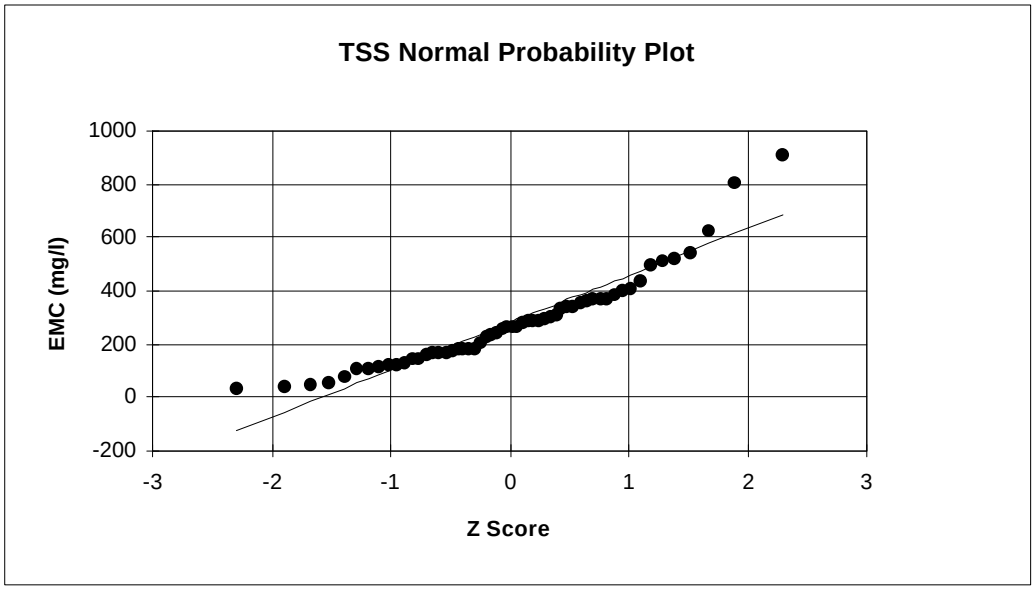

(a)

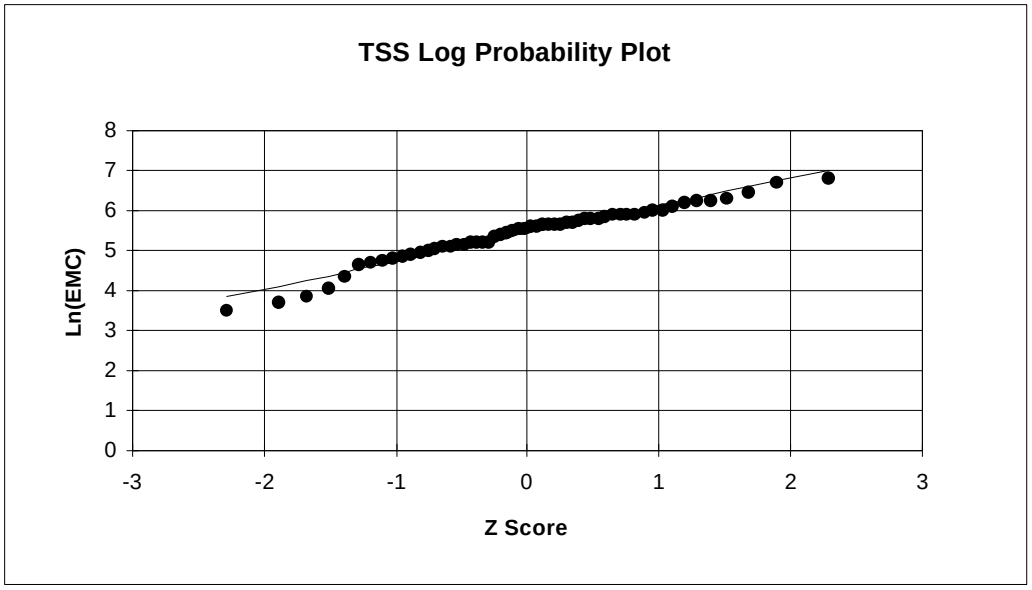

(b)

Figure 4.3.1 Normal and Lognormal Probability Plots for the TSS Data

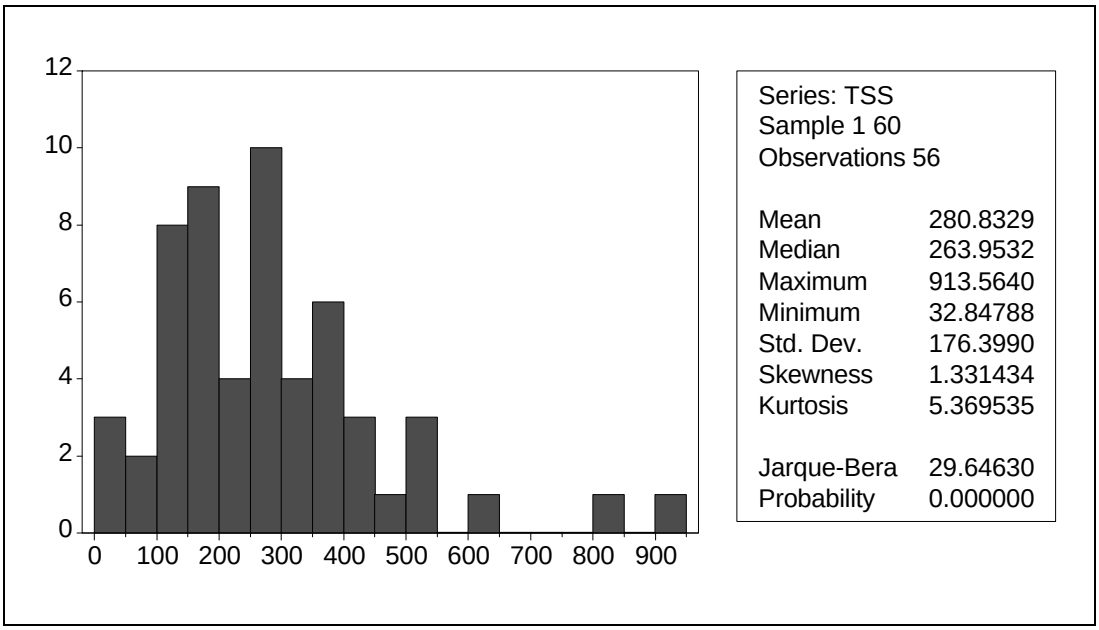

Figure 4.3.2 Histogram of TSS Observations

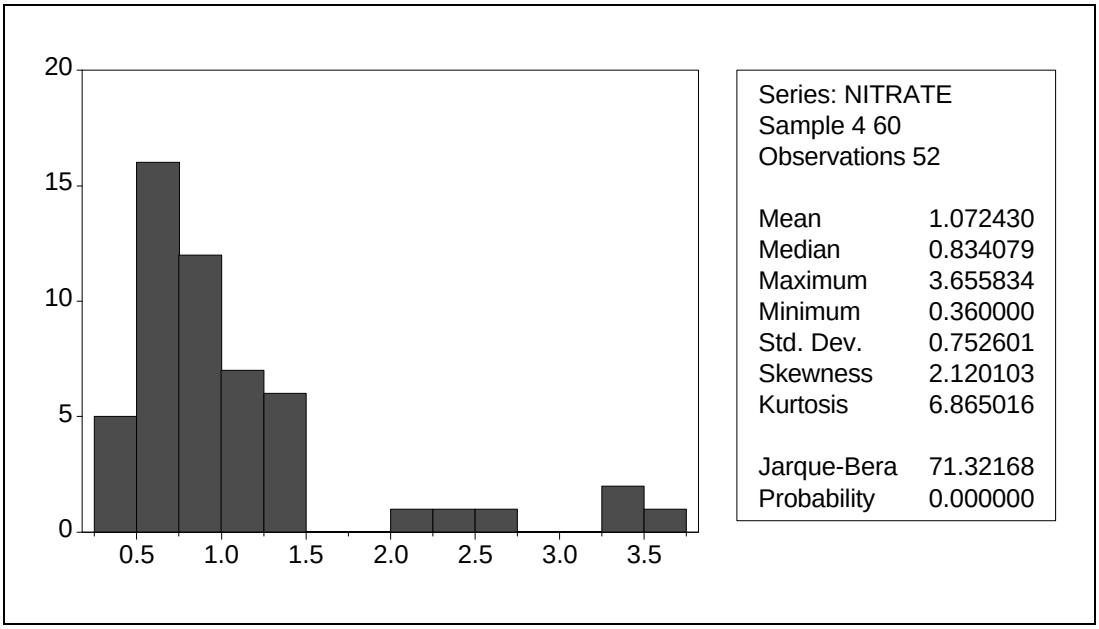

Figure 4.3.3 Histogram of Nitrate Observations

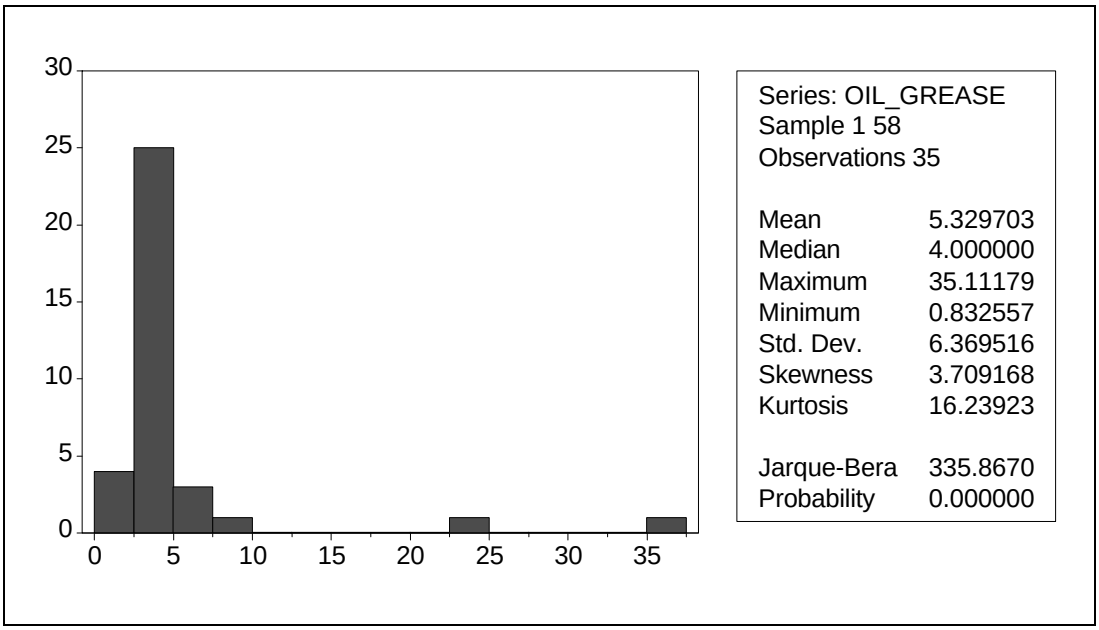

Figure 4.3.4 Histogram of Oil and Grease Observations

in these results. The skewness and kurtosis results presented in Figures 4.3.2, 4.3.3, and 4.3.4 indicate that there is positive skew, or lognormality, in the underlying distributions of highway constituent EMCs.

The Jarque-Bera statistic tests whether a series is normally distributed (Quantitative Micro Software, 1994). The Jarque-Bera statistic is distributed chi-squared (χ^2) with two degrees of freedom under the null hypothesis of normality. The critical value of χ^2 is 5.99 at a 0.95 confidence level. The Jarque-Bera statistic, *J*, is calculated as:

$$J = \frac{N}{6}[S^2 + 0.25(K)^2] \qquad (4.3.3)$$

The value of the Jarque-Bera statistic and associated probability is included in the histograms presented in Figures 4.3.2, 4.3.3, and 4.3.4. The results of the Jarque-Bera test indicate that the skew in the underlying distributions of the highway constituent EMCs is not statistically distinguishable from a normal distribution.

The amount of skew in the distribution is an important measure in the selection of descriptive statistics. The arithmetic mean, median, and variance of a sample is

statistically an unbiased estimator of the true population parameters regardless of the shape of the underlying distribution; however, it is the minimum variance unbiased (MVU) estimator only if the underlying distribution is normal. The MVU estimators can be derived for a lognormal distribution and are presented in Gilbert (1987). Since the normal distribution is a special case of the skewed distribution (i.e., skewness = 0), the normal MVU estimators will provide better estimates if the distribution has little or no skew, whereas the lognormal MVU estimators will be a better estimate if there is a large amount of skew in the distribution. The relative amount of variation in the distribution determines that estimators are the best to use. The normal estimators are preferred if the coefficient of variation is believed to be less than 1.2 (Koch and Link, 1980). All of the data collected during both simulated and natural events had coefficients of variation less than 1.2, which suggests the use of the normal estimators. This result is consistent with the result of the Jarque-Bera test.

The probability plots for all highway runoff constituents are presented in Appendix D, and the histograms for all highway runoff constituents are presented in Appendix E. The units of the abscissa are mg/L and the frequency of occurrence is shown on the ordinate.

4.4 Descriptive Statistics

The event mean concentration for each storm event sampled is shown in Tables 4.4.1 through 4.4.4. The median values of the event mean concentrations (EMC) measured during all sampled storm events are presented in Table 4.4.5. The values reported for all natural storm events are the EMCs observed during the event and have not been corrected for any of the constituents in the rain water. The EMCs for simulated storm events have been corrected for the background constituents in Austin tap water.

The relative variation observed in EMCs among different storm events is given by the coefficient of variation (i.e., the standard deviation divided by the mean) enclosed by

Table 4.4.1 Event Mean Concentrations for Simulated Rainfall Events with Traffic

DATE	Flow (liters)	TSS (mg/L)	VSS (mg/L)	BOD (mg/L)	COD (mg/L)	TC (mg/L)	DTC (mg/L)	N (mg/L)	TP (mg/L)	O&G (mg/L)	Cu (mg/L)	Fe (mg/L)	Pb (mg/L)	Zn (mg/L)
7/6/93	86773	522	54	4.1	92	44	18	N/A	0.34	2.5	0.020	4.2	N/A	0.84
7/12/93	61839	352	45	5.3	101	63	23	N/A	0.39	3.8	0.007	5.4	N/A	0.26
7/20/93	49054	291	23	9.2	139	88	46	N/A	0.54	4.7	0.010	4.0	N/A	0.25
7/27/93	67801	298	23	8.4	72	48	24	0.73	0.28	4.7	0.010	3.2	N/A	0.08
8/10/93	86797	260	24	N/A	122	64	28	0.75	0.38	4.9	0.010	2.8	N/A	0.14
8/24/93	14858	622	55	27.7	182	113	74	1.38	0.84	4.0	0.009	6.7	N/A	0.51
9/23/93	67372	264	38	12.5	100	60	32	N/A	0.41	4.0	0.069	4.2	N/A	0.27
10/7/93	68843	509	41	8.2	126	74	26	1.24	0.51	2.3	0.040	5.5	N/A	0.49
11/4/93	79702	499	54	9.5	83	62	21	0.57	0.37	4.2	0.009	6.6	0.036	0.05
11/17/93	80837	264	29	3.8	86	42	16	0.55	0.12	2.5	0.018	4.5	0.065	0.05
12/1/93	78187	337	38	4.9	120	28	21	0.81	0.42	2.6	0.027	3.9	0.040	0.21
12/10/93	23719	364	40	5.4	118	55	24	1.24	0.35	3.4	0.015	4.7	0.110	0.23
12/16/93	59355	335	25	5.2	109	60	20	0.88	0.30	5.4	0.029	5.3	0.058	0.14
1/4/94	69708	400	59	5.4	39	102	25	0.79	0.20	3.7	0.029	7.6	0.181	0.05
1/11/94	79077	170	33	2.4	68	37	16	0.68	0.23	3.0	0.033	3.6	0.021	0.03
1/13/94	78793	337	41	2.2	93	54	18	0.64	0.35	3.9	0.021	4.9	0.048	0.17
2/3/94	72964	371	45	4.5	76	54	17	0.69	0.21	3.0	0.024	5.1	0.153	0.21
2/17/94	70200	441	61	4.7	111	76	18	0.61	0.33	4.5	0.029	7.8	0.183	0.29
2/24/94	76389	299	22	3.7	64	46	17	N/A	0.25	2.9	0.025	4.9	0.106	0.19
3/1/94	61626	225	17	3.2	81	61	16	N/A	0.28	4.0	0.021	5.1	0.116	0.17
3/10/94	73683	280	32	3.6	70	42	14	0.55	0.21	3.0	0.015	4.1	0.082	0.12
3/17/94	64314	409	42	3.7	49	62	12	0.55	0.33	N/A	0.022	5.7	0.092	0.15
4/8/94	70692	165	25	4.1	68	38	15	0.78	0.09	N/A	0.033	3.2	0.084	0.12
4/13/94	68251	237	17	5.6	84	40	16	0.64	0.24	N/A	0.023	2.9	0.063	0.15
4/20/94	70749	208	22	3.0	54	25	9	0.58	0.16	N/A	0.018	2.2	0.057	0.11

Table 4.4.1 Event Mean Concentrations for Simulated Rainfall Events with Traffic (Continued)

DATE	Flow (liters)	TSS (mg/L)	VSS (mg/L)	BOD (mg/L)	COD (mg/L)	TC (mg/L)	DTC (mg/L)	N (mg/L)	TP (mg/L)	O&G (mg/L)	Cu (mg/L)	Fe (mg/L)	Pb (mg/L)	Zn (mg/L)
5/12/94	70162	N/A	N/A	3.6	54	30	13	0.71	0.25	N/A	0.022	2.2	0.011	0.08
5/26/94	95733	143	14	5.4	91	37	24	1.08	0.23	N/A	0.019	2.8	0.024	0.13
5/31/94	70938	242	37	3.0	85	47	13	0.90	0.32	N/A	0.023	6.3	0.120	0.17
6/8/94	89222	166	23	3.9	68	59	13	0.80	0.16	N/A	0.027	4.1	0.086	0.19
6/16/94	83619	183	19	2.7	67	33	15	0.65	0.16	N/A	0.023	3.5	0.084	0.14
7/1/94	81575	180	34	6.2	92	44	18	1.03	0.14	1.0	N/A	N/A	N/A	N/A
7/14/94	77771	182	32	6.2	87	33	19	0.99	0.27	3.2	0.011	3.1	0.014	0.16

Table 4.4.2 Event Mean Concentrations for Simulated Events without Traffic

Date	Flow (liters)	TSS (mg/L)	VSS (mg/L)	BOD (mg/L)	COD (mg/L)	TC (mg/L)	DTC (mg/L)	N (mg/L)	TP (mg/L)	O&G (mg/L)	Cu (mg/L)	Fe (mg/L)	Pb (mg/L)	Zn (mg/L)
9/12/93	93689	26	2	2.1	19	14	14	0.73	0.08	0.0	0.009	0.9	0.141	0.027
2/6/94	98023	67	6	2.1	24	15	13	0.55	0.07	0.4	0.009	1.5	0.023	0.050
6/26/94	97720	81	7	2.1	30	14	12	0.56	0.08	0.0	0.009	1.2	0.022	0.060

Table 4.4.3 Event Mean Concentrations for Natural Rainfall Events at the West 35th Street Sampling Site

DATE	Flow	TSS	VSS	BOD	COD	TC	DTC	N	TP	O&G	Cu	Fe	Pb	Zn
	(liters)	(mg/L)	(mg/L)	(mg/L)	(mg/L)	(mg/L)	(mg/L)	(mg/L)	(mg/L)	(mg/L)	(mg/L)	(mg/L)	(mg/L)	(mg/L)
9/14/93	450	58	26	19	248	N/A	N/A	2.74	0.61	4.2	0.04	0.3	0.02	N/A
10/13/93	1832	106	26	25	190	84	72	3.26	0.61	3.2	0.04	1.2	0.44	0.28
10/20/93	10243	385	36	12	42	32	15	0.52	0.30	0.8	0.05	2.0	0.12	0.18
10/20/93	1264	157	42	28	195	79	33	1.11	0.50	4.3	0.08	5.6	0.24	0.36
10/20/93	1601	116	47	28	185	68	31	1.07	0.47	4.7	0.08	4.4	0.23	0.34
10/29/93	26957	147	33	18	126	53	33	0.84	0.33	9.6	0.06	2.5	0.09	0.24
11/2/93	5620	175	44	21	209	82	45	2.11	0.39	5.0	0.07	2.7	0.19	0.29
12/22/93	6271	48	8	0	149	66	38	1.32	0.30	5.9	0.06	3.5	0.13	0.22
1/13/94	10408	123	24	6	142	35	33	1.41	0.15	4.1	0.01	0.7	0.03	0.06
1/20/94	10444	286	81	40	336	145	80	3.44	1.04	35.1	0.05	5.7	0.04	0.36
1/22/94	5988	79	40	43	264	128	85	2.36	0.51	24.0	0.04	5.3	0.05	0.30
2/21/94	87156	370	40	5	88	16	11	0.37	0.33	N/A	0.12	3.1	0.12	0.23
2/28/94	45877	N/A	N/A	N/A	N/A	39	10	0.43	N/A	N/A	0.04	7.7	0.27	0.59
3/9/94	65514	N/A	N/A	7	64	33	13	0.49	0.27	N/A	N/A	4.7	0.15	0.31
3/13/94	31975	40	20	9	75	26	19	1.08	0.12	N/A	N/A	N/A	N/A	N/A
3/15/94	36692	313	37	9	79	46	14	0.41	0.30	N/A	0.02	4.4	0.10	0.21
3/27/94	1964	131	57	15	90	N/A	N/A	1.03	N/A	N/A	N/A	N/A	N/A	N/A
4/5/94	41803	808	86	23	135	79	20	0.73	0.70	N/A	0.05	9.7	0.23	0.26
4/11/94	7627	540	114	23	292	153	53	0.96	0.73	N/A	0.07	7.8	0.21	0.51
4/15/94	13203	914	130	22	203	80	20	0.00	0.93	N/A	0.05	7.5	0.18	0.40
4/19/94	12084	N/A	N/A	N/A	217	61	28	1.39	0.76	N/A	N/A	N/A	N/A	N/A
4/28/94	3471	126	44	56	452	123	89	3.66	1.09	N/A	N/A	N/A	N/A	N/A
4/28/94	31525	266	49	10	80	39	18	0.62	0.39	N/A	0.02	2.0	0.06	0.16

Table 4.4.4

Event Mean Concentrations for Natural Rainfall Events at the Convict Hill Sampling Site

Date	Flow (liters)	TSS mg/L	VSS mg/L	BOD mg/L	COD mg/L	TC mg/L	DTC mg/L	N mg/L	TP mg/L	O&G mg/L	Cu mg/L	Fe mg/L	Pb mg/L	Zn mg/L
4/29/94	1420	239	39	10	72	49	28	1.47	0.062	NA	0.015	NA	NA	0.063
5/2/94	1420	86	23	6	78	41	23	0.89	0.109	NA	0.020	2.9	NA	0.081
5/13/94	3975	403	42	5	92	39	17	0.71	0.260	NA	0.010	8.9	0.141	0.174
5/14/94	1325	348	20	7	NA	29	11	0.78	0.358	1.5	0.009	4.0	0.090	0.099
5/16/94	1514	6	6	7	46	24	21	0.75	0.078	2.0	0.002	1.0	0.033	0.053
6/10/94	1514	512	50	24	174	89	43	NA	0.380	NA	0.032	11.8	0.223	0.310
6/19/94	1514	4	0	5	75	20	20	0.60	NA	1.9	0.011	4.5	0.100	0.292
6/21/94	2271	40	12	6	68	31	22	1.61	0.112	2.4	0.001	0.5	0.171	0.033
8/8/94	2271	176	68	13	114	NA	NA	NA	0.200	8.1	0.003	2.2	0.021	0.042
8/9/94	3407	42	14	3	32	11	5	0.21	0.048	1.6	0.001	0.9	0.007	0.010
8/16/94	3407	80	8	10	39	23	21	1.80	NA	1.7	0.001	1.1	0.007	0.028
8/22/94	3407	40	12	3	15	14	11	0.43	0.060	0.8	0.002	0.8	0.012	0.017
9/7/94	1703	292	44	16	49	22	19	1.02	0.080	1.8	0.009	1.8	0.017	0.079
9/8/94	3407	0	0	5	17	5	5	0.53	0.025	0.4	0.003	0.3	0.016	0.022
9/9/94	6814	3	2	3	10	5	5	0.40	0.025	1.3	0.008	0.5	0.007	0.028
10/7/94	5110	68	7	8	49	21	16	0.60	0.077	0.9	0.003	0.8	0.011	0.019
10/14/94	4826	24	16	6	43	32	14	0.78	0.030	2.4	0.003	0.9	0.021	0.055
10/25/94	6814	146	15	4	19	18	8	NA	0.041	0.9	0.003	0.7	0.009	0.016
10/27/94	5962	68	16	4	40	24	10	NA	0.113	1.8	0.007	2.5	0.014	0.215
11/5/94	6814	192	24	3	29	19	8	NA	0.078	0.9	0.007	1.5	0.013	0.045
11/15/94	1136	12	4	5	33	20	17	NA	0.060	1.7	0.006	1.2	0.014	0.081
12/2/94	3407	156	28	5	39	21	5	0.39	0.070	7.6	0.007	1.4	0.007	0.052
12/9/94	1420	136	28	3	29	13	12	0.55	0.005	NA	NA	NA	NA	NA

Table 4.4.5

Median Event Mean Concentrations (mg/L)

	West 35th St. Traffic Simulation*	West 35th St. No-Traffic Simulation*	West 35th St. Natural Event	Convict Hill Natural Event
TSS	291 (0.4)	67 (0.5)	157 (0.9)	83 (1.1)
VSS	33 (0.4)	6 (0.5)	42 (0.6)	16 (0.9)
BOD_5	4.7 (0.8)	2.1 (0.0)	15.3 (0.7)	5.4 (0.8)
COD	86 (0.3)	24 (0.2)	142 (0.6)	44 (1.0)
Total Carbon	51 (0.4)	14 (0.02)	57 (0.6)	22 (0.7)
Dis. Total Carbon	18 (0.6)	13 (0.1)	28 (0.7)	16 (0.6)
Nitrate	0.74 (0.3)	0.56 (0.2)	1.00 (0.8)	0.73 (0.6)
Total Phosphorus	0.28 (0.5)	0.08 (0.1)	0.41 (0.5)	0.08 (1.0)
Oil & Grease	3.7 (0.3)	0.4 (1.7)	5 (1.2)	2 (1.0)
Copper	0.022 (0.5)	0.009 (0.03)	0.049 (0.6)	0.006 (1.0)
Iron	4.2 (0.3)	1.2 (0.2)	3.5 (0.8)	1.4 (1.2)
Lead	0.082 (0.6)	0.023 (1.1)	0.123 (0.8)	0.016 (1.3)
Zinc	0.16 (0.8)	0.050 (0.4)	0.263 (0.7)	0.053 (1.1)

* West 35th St. simulation data has been corrected for the background in Austin tap water; Number in parenthesis is the coefficient of variation.

parentheses. The relative variation for most constituents is less during the simulated events than during natural events. This phenomenon is a result of the "steady-state" nature (e.g., a constant rainfall, runoff, and traffic rate) of the simulated rain storm. The similar event duration and sampling protocols among the simulated storms also contributed to the lower variations observed in the simulated EMCs.

The EMCs for natural storm events are higher than the simulated storm event EMC values for every constituent except TSS. These results are attributed to a lack of adequate sampling coverage over the entire duration of most of the natural storm events. The automatic sampler was programmed with a predetermined sampling sequence to sample the duration of the expected storm. However, if the rainfall intensity is higher than anticipated, only the first part of the storm is sampled. Concentrations of constituents were observed to be higher in the earlier stages of the runoff event, and in particular during the rising leg of the hydrograph, for all of the constituents under study. The values for natural storm EMCs would have been smaller had the entirety of each natural storm been sampled. Likewise, sample collection during the simulated events always lasted the entirety of the simulated storm event.

The higher concentrations of TSS observed during the simulated events are explained by the intensity of the simulated rainfall. The simulated storms were, on average, a higher intensity rainfall than the natural storms. The higher flow rates associated with the simulated events moved more of the heavier dirt particles than the smaller natural storms.

4.5 Constituent Wash-Off Patterns

The wash-off patterns observed during the simulated storm events for TSS, nitrate, and oil and grease are shown graphically in Figures 4.5.1a-c, 4.5.2a-c, and 4.5.3a-c, respectively. Part A of these figures shows the variation in the concentration of the constituents during the simulated storm events. A period of high concentration is evident at the beginning of the storm for each constituent. The period of high concentration, however, occurs simultaneously with the rising leg of the hydrograph and ends at the time of concentration for the watershed. It is difficult to ascertain from the graph if the high concentration in the beginning of the storm results from a large amount of material being washed from the highway early in the storm event (e.g., a true first flush) or from the smaller volume of water on the watershed at the start of the storm.

The loads for TSS, nitrate, and oil and grease observed during the simulated events are shown in Figures 4.5.1b, 4.5.2b, and 4.5.3b, respectively. These plots indicate that load increases linearly with increased flow volume for each constituent as long as there is traffic to provide an input of constituent mass. The cumulative load curve becomes relatively flat for the no-traffic simulations, which is a result of the lack of constituent mass in the runoff. The single exception is nitrate. The cumulative load curve for nitrate continues to increase even under no-traffic conditions. This phenomenon is explained by (1) the mobility of nitrate, because of its anionic form (NO_3), does not require the energy associated with vehicles (i.e., the forces resulting from tires and vehicle-induced winds) to mobilize in the runoff and (2) the amount of nitrates in the tap water used for the rainfall simulations.

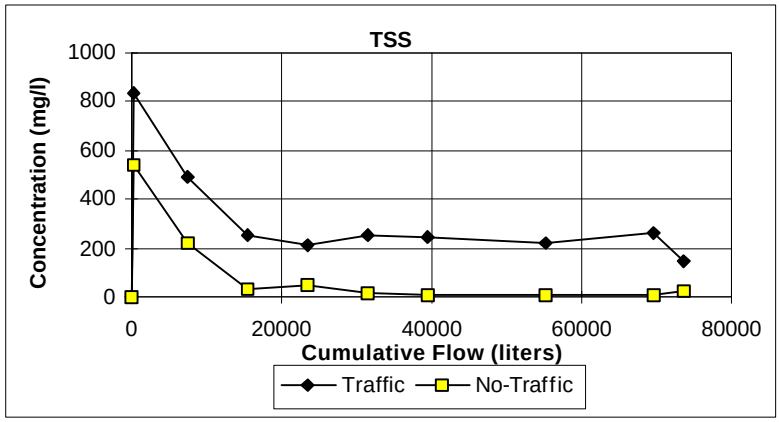

(a) Median TSS Concentration During a Simulated Storm Event

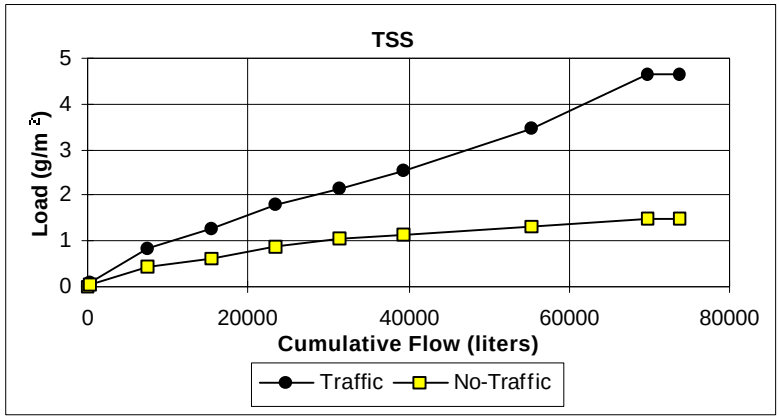

(b) Median TSS Load During a Simulated Storm Event

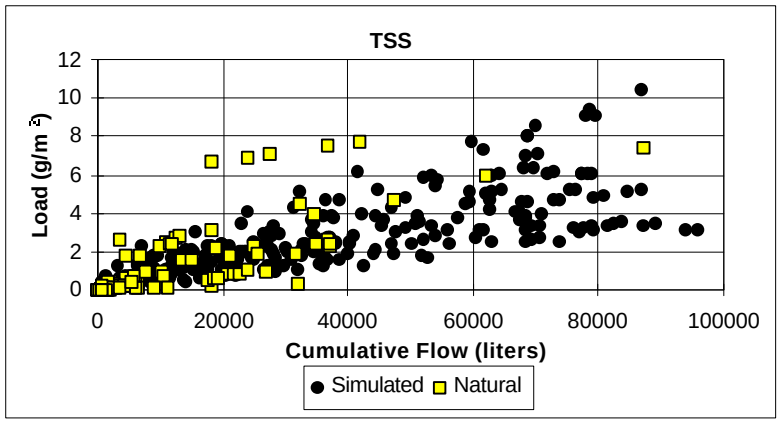

(c) TSS Load During Natural and Simulated Storm Events

Figure 4.5.1

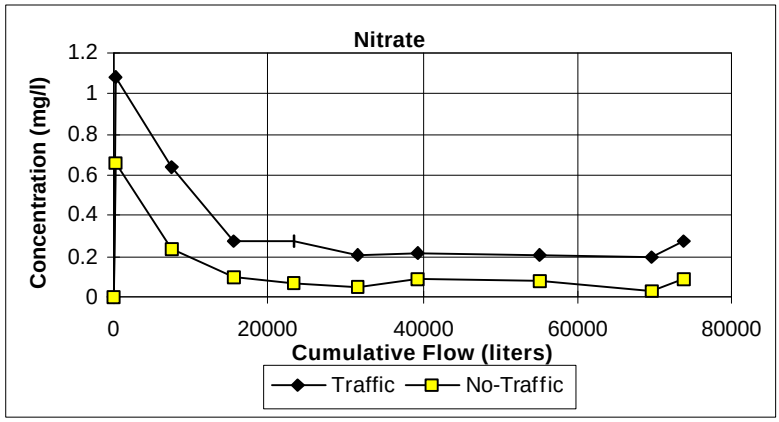

(a) Median Nitrate Concentration During a Simulated Storm Event

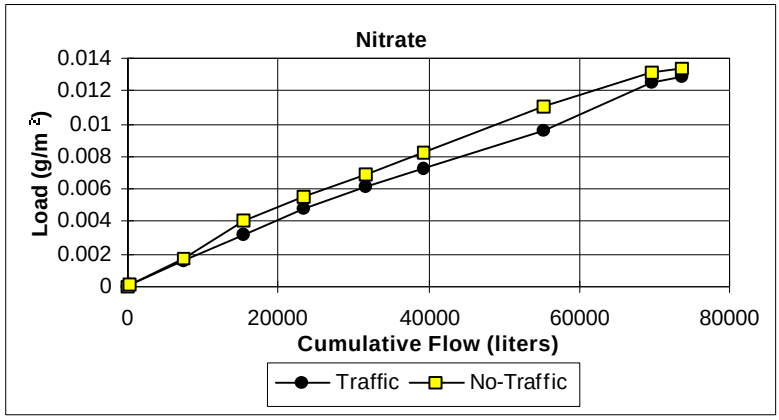

(b) Median Nitrate Load During a Simulated Storm Event

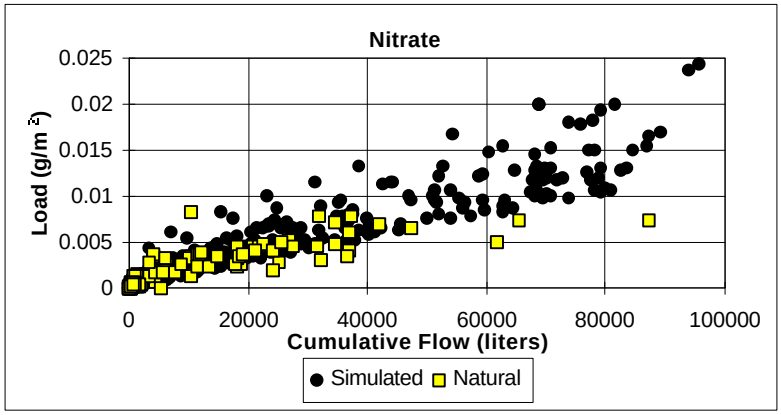

(c) Nitrate Load During Natural and Simulated Storm Events

Figure 4.5.2

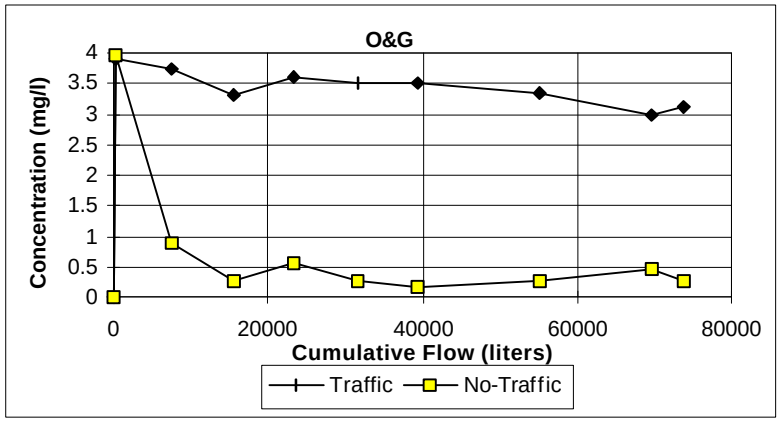

(a) Median Oil and Grease Concentration During a Simulated Storm Event

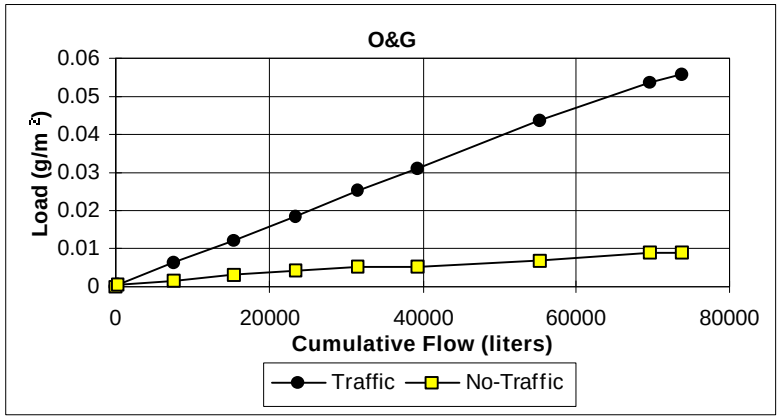

(b) Median Oil and Grease Load During a Simulated Storm Event

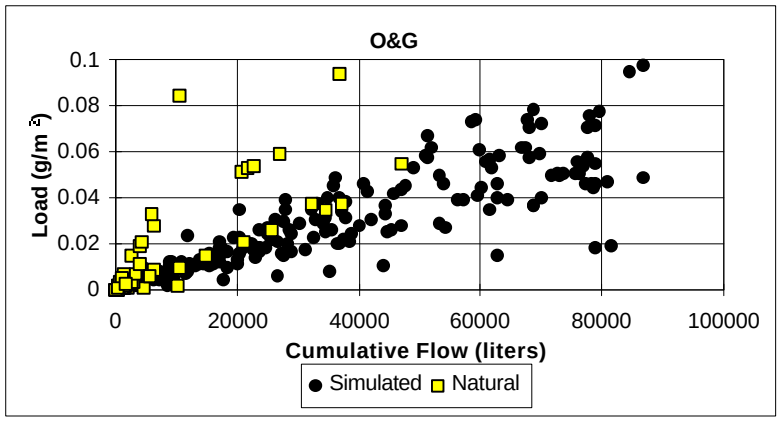

(c) Oil and Grease Load During Natural and Simulated Storm Events

Figure 4.5.3

A plot of the total observed load in relation to the total volume of flow is shown in Figures 4.5.1c, 4.5.2c, and 4.5.3c for TSS, nitrate, and oil and grease, respectively. Observations for both natural events and simulated events are plotted. No statistical difference was found between the data observed for simulated events and the natural events; this is visually evident from the graphs.

The wash-off patterns for all highway runoff constituents are presented in Appendix F.

4.6 First Flush

The "first flush" of constituents in highway runoff is examined in Figures 4.6.1a-c and 4.6.2a-c. The percent of the total storm load in relation to the percent of the total storm flow is shown in Figure 4.6.1a-c. First flush of constituent mass is not strongly pronounced on pavements with high speed traffic. The percentage of total mass discharged is only slightly higher than the percentage of the total runoff volume discharged. The results of Figure 4.6.1a-c are shown numerically in Table 4.6.1.

The fraction of percent mass discharged to percent runoff discharged is plotted in relation to storm volume in Figure 4.6.2a-c. A value of one indicates the percentage of the total storm load that has passed is equal to the percentage of the total volume of storm flow that has passed. The value of this fraction rapidly approaches one and becomes approximately equal to one shortly after the half-way point in the storm.

4.7 Daily and Seasonal Variations

There is no evidence that any constituents exhibited daily or seasonal trends. A time-series plot of the TSS and nitrate data collected during the period July 1993 through July 1994 is presented in Figure 4.7.1. The variation during the day for TSS and nitrate for the same time period is plotted in Figure 4.7.2.

4.8 Street Sweeping Variations

Street sweeping operations were suspended at the West 35th Street sampling site during the first 7 months of the study period, and resumed during the last months of the

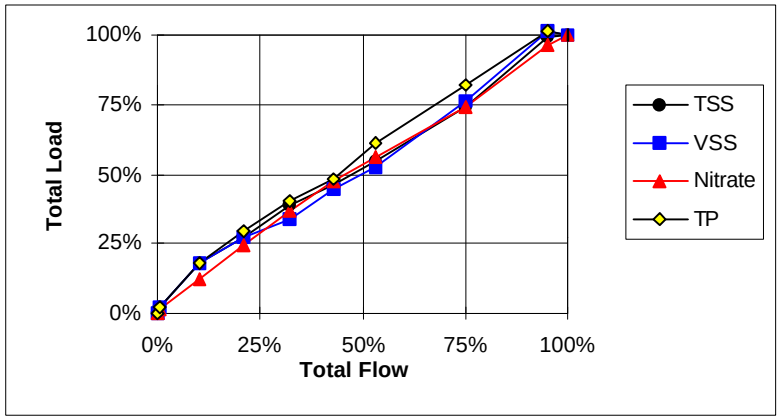

(a) Load vs. Flow for Solids and Nutrients

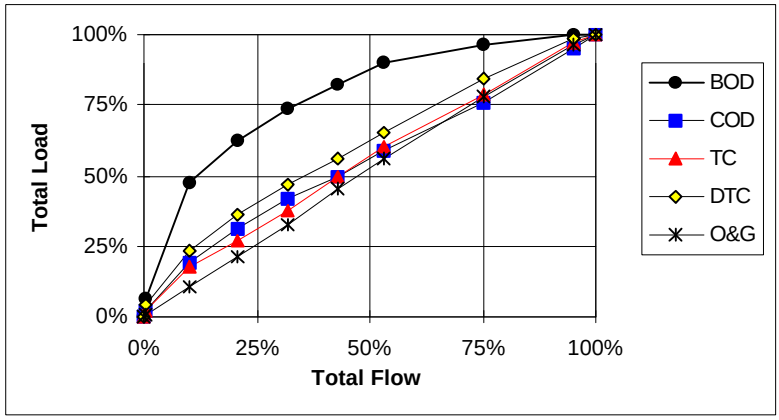

(b) Load vs. Flow for Organics and Oil and Grease

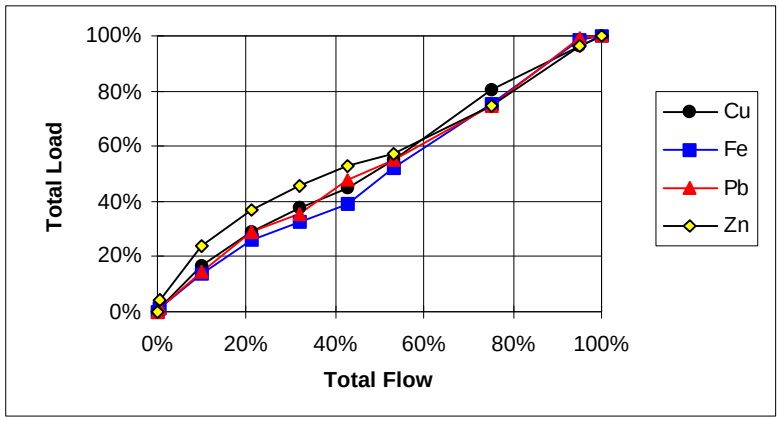

(c) Load vs. Flow for Metals

Figure 4.6.1

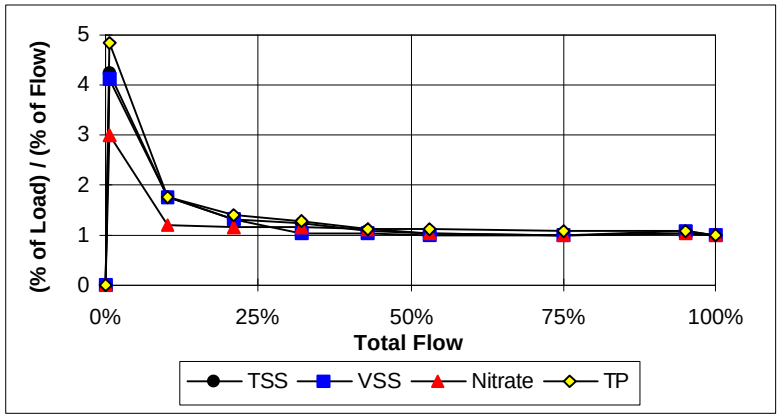

(a) Percent Load vs. Flow for Solids and Nutrients

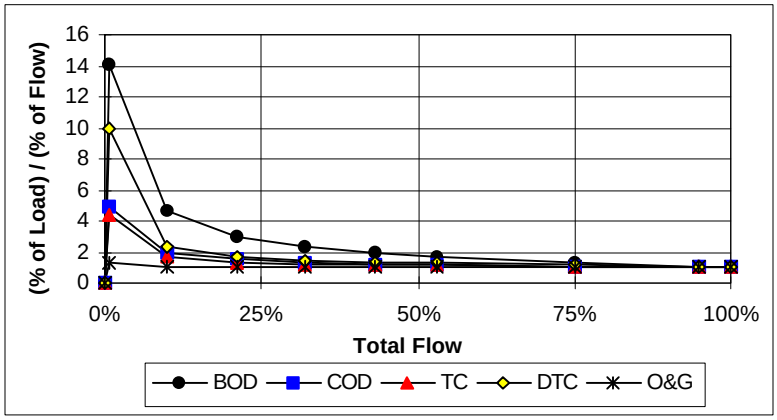

(b) Percent Load vs. Flow for Organics and Oil and Grease

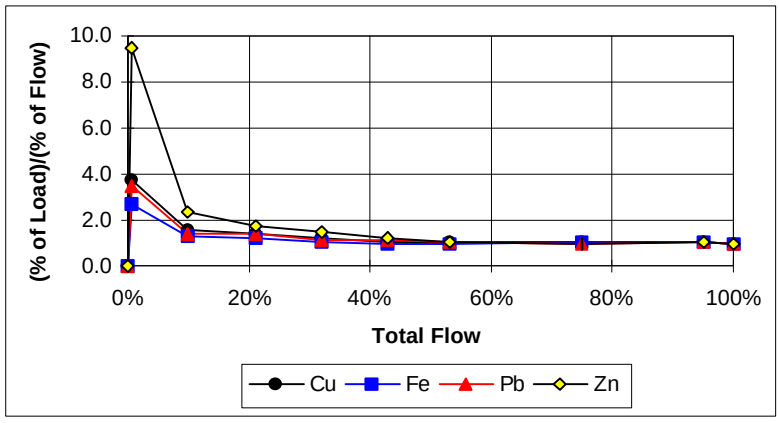

(c) Percent Load vs. Flow for Metals

Figure 4.6.2

Table 4.6.1 First Flush of Highway Runoff Constituents (percentage of constituent load versus percentage of total runoff*)

	Traffic Conditions			No-Traffic Conditions		
	Total Storm Runoff = 21 mm			Total Storm Runoff = 28 mm		
% of Runoff	21%	53%	75%	19%	53%	75%
Volume of Runoff	(4.3 mm)	(11.2 mm)	(15.7 mm)	(5.3 mm)	(15.0 mm)	(21.1 mm)
TSS	27%	55%	74%	42%	75%	87%
VSS	28%	52%	76%	44%	65%	73%
BOD_5	63%	90%	97%	100%	100%	100%
COD	32%	59%	76%	51%	93%	95%
Total Carbon	27%	60%	79%	45%	72%	90%
Dis. Total Carbon	36%	66%	85%	31%	59%	79%
Nitrate	25%	56%	74%	31%	62%	83%
Phosphorus	29%	61%	82%	63%	82%	94%
Oil and Grease	21%	56%	78%	33%	60%	73%
Copper	29%	55%	80%	70%	74%	74%
Iron	26%	52%	75%	80%	96%	98%
Lead	29%	55%	75%	84%	96%	96%
Zinc	37%	57%	75%	56%	85%	93%

* Based on the median of all loads and flows recorded during the simulated storm events.

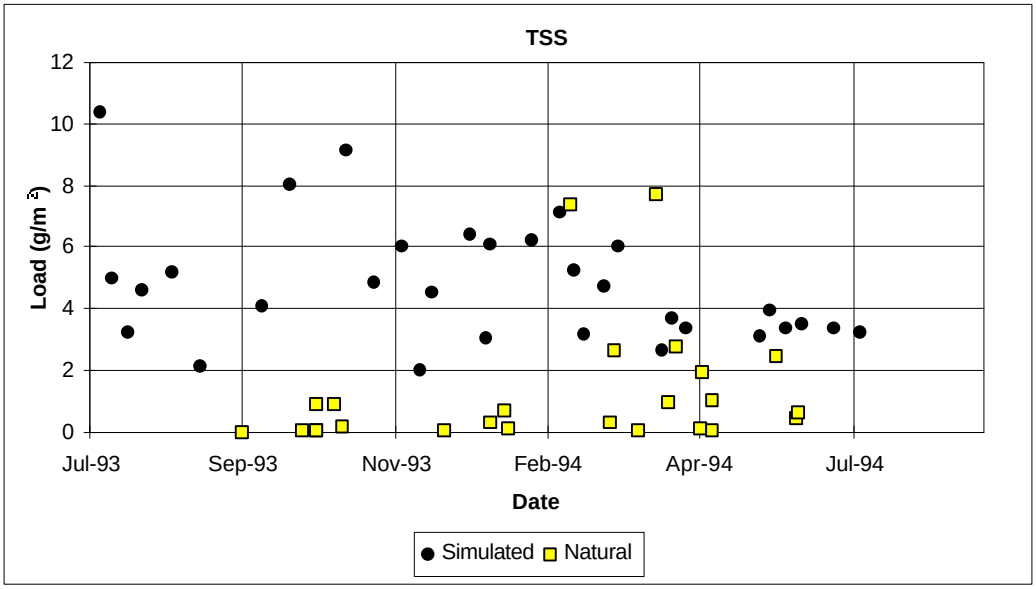

(a) Seasonal Variation (July 1993 - July 1994), TSS

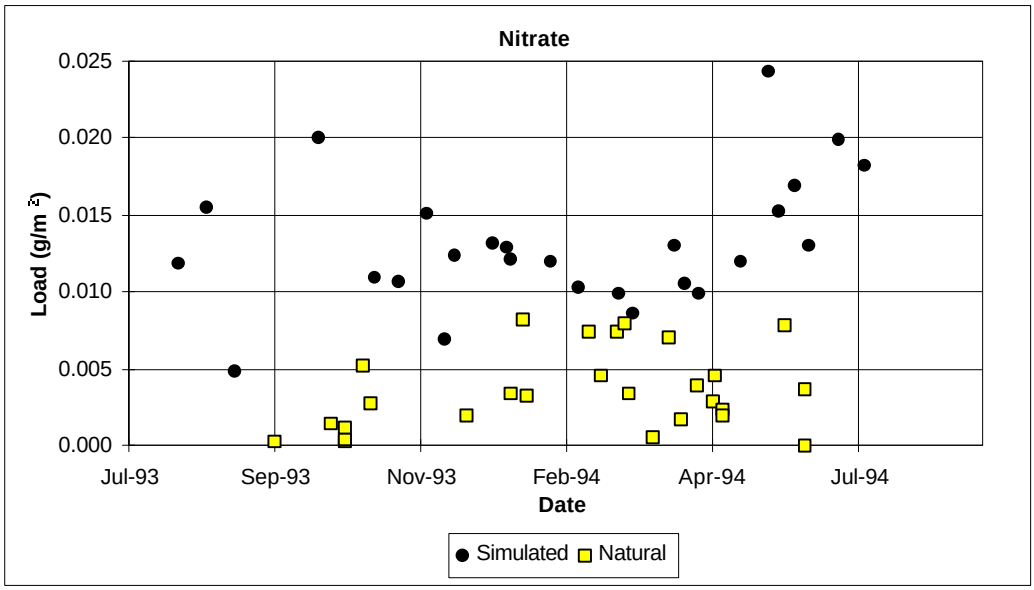

(b) Seasonal Variation (July 1993 - July 1994), Nitrate

Figure 4.7.1

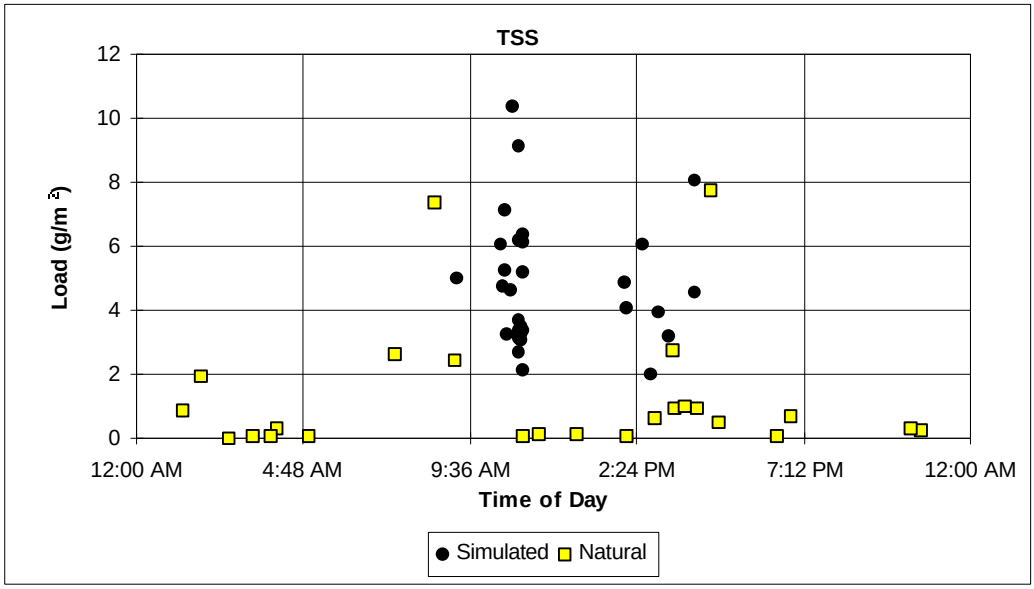

(a) Hourly Variation (July 1993 - July 1994), TSS

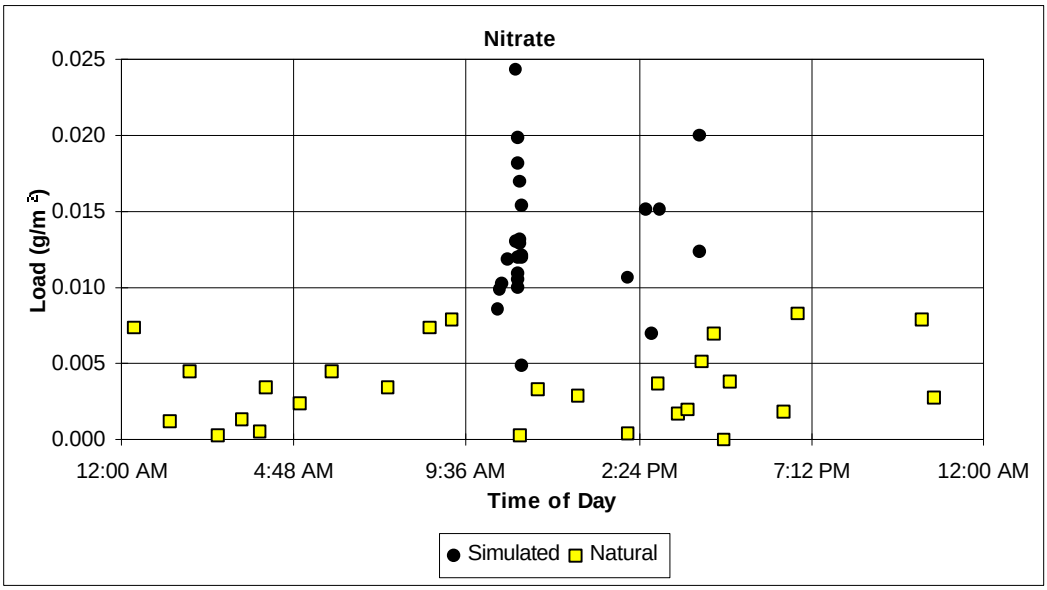

(b) Hourly Variation (July 1993 - July 1994), Nitrate

Figure 4.7.2

study at a sweeping frequency of once every 2 weeks. There were a total of 18 simulated storm events and 11 natural events sampled during the no-sweep period. Fourteen simulated events and 12 natural events were sampled during the sweeping period. Two of the three no-traffic simulated events were conducted during the no-sweeping period.

Using the simulated data only, the median load for the no-sweep period was compared to the median load for the sweeping period for each constituent. Statistical difference between the two groups was determined using a *t*-test. The only constituents that showed a significant difference between the sweeping periods were the solids. The storm water loading of both TSS and VSS was reduced as a result of sweeping once every 2 weeks. The computed values the *t*-statistic are shown in Table 4.8.1. A negative sign in front of the *t*-statistic in Table 4.8.1 indicates that the median load of the constituent increased during the sweeping period. However, no constituent showed a significant increase during the sweeping period.

Table 4.8.1 Computed Street Sweeping *t*-Statistics

Constituent	Computed *t*-Statistic
TSS	3.53[(a)]
VSS	2.19[(b)]
BOD_5	0.01
COD	1.14
Total Carbon	1.57
Dissolved Total Carbon	1.58
Nitrate	-1.29
Total Phosphorus	1.80
Oil and Grease	-0.91
Copper	0.43
Iron	-0.79
Lead	-1.40
Zinc	1.80

(a) $|t| > t_{0.01,¥} = 2.326$; (b) $|t| > t_{0.05,\infty} = 1.960$

4.9 Summary

A total of 35 simulated rainfall events and 23 natural storm events were sampled at the West 35th Street sampling site. The distribution of EMCs at this site were positively skewed; however, the degree of skewness was not enough to justify the use of lognormal estimators to calculate the sample parameters.

Constituent wash-off patterns during the simulated events were similar to those predicted by the wash-off theory presented in Chapter 2. A first flush of constituent mass was evident during all simulated events; however, it was much more pronounced during the no-traffic simulations because of the absence of the traffic input.

A street sweeping frequency of once every 2 weeks was found to significantly reduce the loading of solids (TSS and VSS) in the highway runoff. Street sweeping did not significantly change the loading of other constituents.

5.0 Model Development

5.1 Introduction

Predictive modeling of storm water quality is used to provide insight and analysis into the control of storm water constituents. Storm water models range from simple screening equations that can be solved on a hand-held calculator to complex simulation methods that require considerable computer time to complete. The three most common types of storm water predictive models include regression models, statistical techniques, and deterministic simulation models.

The regression model is a mathematical equation that defines the line of average relationship between a dependent variable and one or more independent, or causal, variables. Storm water regression models commonly identify constituent concentration or load as variables that are dependent upon runoff volume, rainfall intensity, traffic intensity, antecedent dry period, surrounding land use, etc. The mathematical approach used to formulate the regression model is the method of least squares. The method of least squares minimizes the sum of the squared differences, or residuals, between the values predicted by the regression equation and the observations. If correctly specified, the method least squares will provide the best linear and unbiased estimate of the population parameters.

Regression equations are easy to use and provide a quick method for screening storm water quality. The storm water regression model can be formulated to predict total storm load and inner-event loads. Regression models especially are well suited for predicting the cumulative constituent load that results from a continuous series of storm events. Regression models have been criticized as poor predictors when applied beyond the original data set or region from that they were created (Driscoll et al., 1990); however, this statement is universally true of all water quality modeling methods. Site-specific quality data is critical for the calibration and verification of urban runoff quality simulation models (Huber, 1986).

The National Urban Runoff Program (NURP) employed a statistical method for storm water quality modeling (Driscoll et al., 1990). The NURP statistical method is based on the assumption that rainfall, runoff volumes, and runoff event mean

concentrations (EMC) are all independent, random variables that vary between storm events. The NURP study concluded that EMCs are random variables that are best described by a lognormal distribution (USEPA, 1983). Rainfall data historically have been considered to be represented by a gamma distribution (Chow et al., 1988).

The storm event is assumed to be independent of previous events if the time span between event midpoints is greater than some minimum time period. This minimum inter-event time (MIT) is typically in the range of 3 to 24 hours. The MIT is selected by making use of the assumption that MITs are exponentially distributed (Chow et al., 1988) and therefore have a coefficient of variation (COV) equal to one. Trial values of the MIT are chosen until the COV of the time between event midpoints in equal to one (Driscoll et. al., 1990).

Runoff volumes are calculated using rainfall and runoff statistics. The mean runoff volume is computed by multiplying the mean volume of a rainfall event by the ratio of average runoff to rainfall. The mean constituent load is determined by multiplying the mean EMC by the mean runoff volume (Eq. 3.8.2). All variation in the constituent loads is assumed to be attributable to the variation in the runoff volume.

The NURP statistical method is relatively easy to apply and can provide a quick screening like regression equations. The method has also been successfully applied as part of the NURP program. A shortcoming to the method is that temporal changes in concentration or load cannot be predicted during the storm. Therefore, the method has limited use in the evaluation of highway runoff control structures.

Physically based deterministic simulation models represent the most complex tools available for storm water analysis. Modern computers allow these models to time-step through the build-up and wash-off of highway constituents, as well as the change in runoff quantity and quality throughout a drainage system, including storage and treatment facilities. Most simulation models are capable of performing both single and continuous event simulations. Build-up and wash-off functions are used to determine the amount of material removed from the highway surface, and either the nonlinear reservoir method or kinematic wave method is used to route the runoff throughout the remainder of the drainage system. Several of the more common simulation models include:

1. Storm Water Management Model (SWMM)

2. FHWA Urban Highway Storm Drainage Model
3. Storage, Treatment, Overflow, Runoff Model (STORM)
4. Hydrological Simulation Program - FORTRAN (HSPF)

These models are considered “operational” water quality models and each one has (1) a user's manual and documentation, (2) is in use by someone other than the model developer, and (3) has continued support (Huber, 1986).

Simulation models typically consider constituent build-up as a function of the length of the antecedent dry period and consider constituent wash-off as a function of the storm duration. Linear equations are sometimes used to describe specific regions of correlation, but intuition suggests that neither build-up nor wash-off should be entirely linear. The most common curve forms used to describe constituent build-up are power, exponential, and Michaelis-Menton expressions. Wash-off curves are generally a variation of the first-order decay formulation (Huber, 1986). However, a special case of the regression equation known as a rating curve is also used to describe wash-off. The rating curve expresses the relationship between load or concentration and flow rate. Rating curves are almost always power functions, although other forms are sometimes used (Huber, 1986). Runoff flow routing downstream of the highway pavement is accomplished using the nonlinear reservoir method or the kinematic wave method.

Simulation models have been designed to model extensive storm water collection and transfer systems. The models are best applied to urban storm sewer designs that include extensive pipelines, channels, storage elements, treatment elements, etc. Simulation models produce the most varied output of any of the modeling methods and provide the detailed analysis required for the extensive evaluation of comprehensive storm water controls.

5.2 Selection of an Appropriate Modeling Technique

The selection of a storm water quality modeling technique must consider the objective of the task at hand. The objective of this research is the development of a model that predicts the amount of material that is washed from the highway surface during either a design storm event or a design series of storm events. The model output is the predicted constituent load at the edge of the pavement, at any point during the storm. All three of the previously mentioned modeling techniques can accomplish this goal; however, there are several important factors that must be considered in model selection.

The model should be applicable to both single-event and continuous-event design scenarios. The model should be capable of producing a single storm event loadograph for the evaluation of the effectiveness of storm water controls. However, receiving waters respond relatively slowly to constituent inputs. The total load input over an extended period of time (i.e., weeks to years) is required to estimate response of receiving waters. All three modeling techniques are capable of single-event and continuous-event modeling.

The modeling technique also must be capable of estimating the cumulative amount of load produced at any specific instance during the storm. The ability to predict cumulative edge-of-pavement loads throughout the storm is an important aspect if the model is to be used to evaluate control structure efficiency. The amount of constituent mass captured by a fixed-capacity control structure will be the amount of mass that has washed from the highway at the time the structure is filled. Subsequently, the amount of constituent mass released to the receiving stream will be that portion that is washed from the highway after the structure is full. As shown by the data presented in Chapter 4, the amount of constituent that is washed from the highway surface varies throughout the duration of the storm (Figures 4.6.1 and 4.6.2). The concentration of the constituent will be greater early in the storm than later due of the effect of “first-flush.” The model must therefore predict the fraction of constituent mass captured by the control structure and the mass of constituent released by the control structure based on load rate variations during the storm. Both regression models and physically-based deterministic simulation models can accomplish this task. However, this condition eliminates the NURP statistical technique from consideration.

A final consideration is the amount of information that the model uses to determine constituent loading. The more commonly used simulation models (e.g., SWMM) determine constituent build-up in terms of elapsed time since the last cleaning (either by rain or sweeping). Although the available build-up functions include linear, power, exponential, and Michaelis-Menton, the only information utilized by the model is the duration of the dry period. The best fit of an exponential function to the TSS data collected during sampling at the 35th Street site is presented in Figure 5.2.1. The correlation coefficient (R^2 = 0.0013) in Figure 5.2.1 suggests that there are other variables that influence the build-up of TSS. If the dry period duration was calculated from a continuous rainfall record, other known variables would include the intensity of the preceding storm. This new information will indicate the extent of the previous wash-off and subsequently the amount of residual material remaining on the highway from the previous storm event. The improved explanatory power that results from using both dry period duration and previous storm intensity to predict TSS loading at the West 35th street site is illustrated in Figure 5.2.2

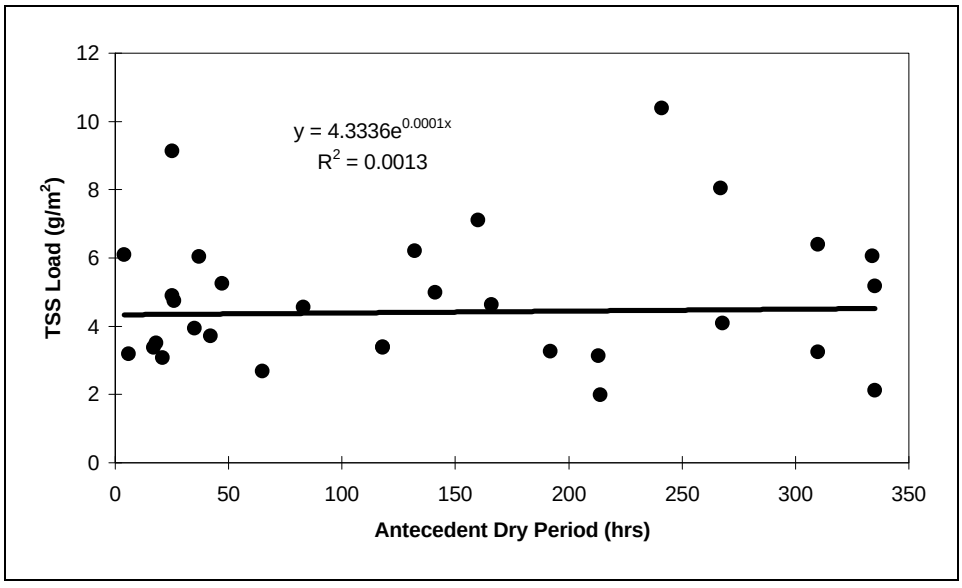

Figure 5.2.1 Exponential Function Fit to the Data Collected at the West 35th St. Sampling Site

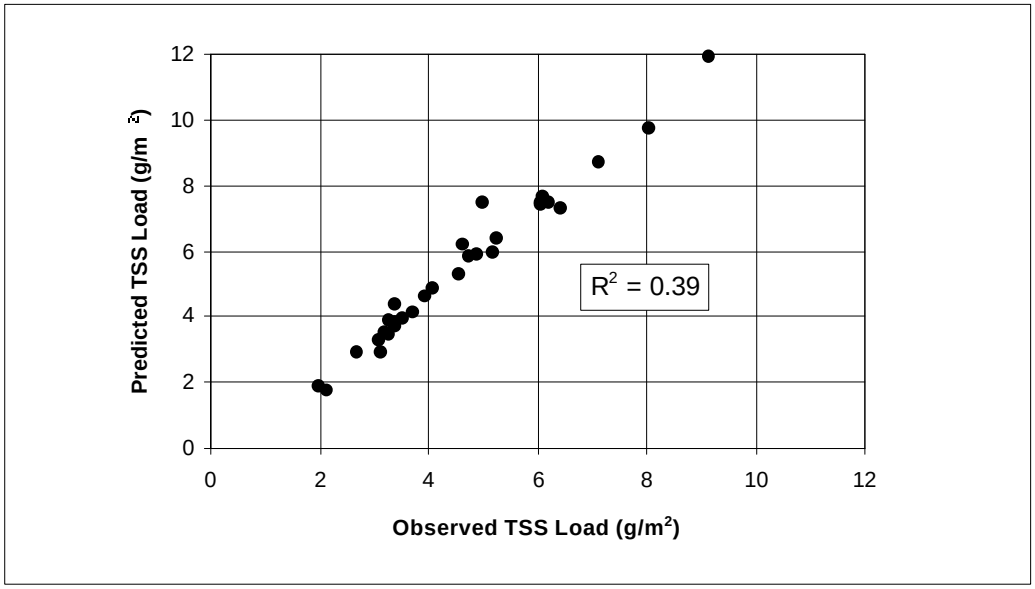

Figure 5.2.2 Observed TSS Load vs. Predicted TSS Load using Duration of the Antecedent Dry Period and the Intensity of the Preceding Storm as Causal Variables

Regression analysis can determine the relationship between numerous causal variables and the constituent load. Regression analysis will also indicate the statistical significance of each causal variable as it relates to a specific constituent, which in turn may suggest possible mitigation procedures or model applicability scenarios. Furthermore, the formulated regression equation may be used as input to a physically based deterministic simulation that might model a much broader system.

In summary, regression analysis was chosen as the modeling technique best-suited for edge-of-the-pavement load calculations because of the following:

- Regression equations can be used to calculate both single-event and continuous storm loading patterns.
- Regression models make use of multiple causal variables (e.g., runoff intensity, traffic volume, duration of the dry period, etc.).
- The regression analysis will evaluate the statistical significance of all causal variables in relation to a specific constituent. This information can suggest mitigation procedures or model applicability situations.
- The regression model can be attached as the input to a larger model simulating a much broader system.

5.3 Identification of Relevant Model Variables

The most important step in the development of an empirical model is the identification of the relevant explanatory variables. The term "relevant" has two distinct meanings in regression analysis: scientific relevance and statistical relevance (Johnson et al., 1987). Scientific relevance is based on the underlying theory guiding the process. Variables are included in the model because scientific theory suggests inclusion. Statistical relevance is based on hypothesis tests that suggest whether a coefficient is "statistically" different from zero. This section describes the process that is used to identify the set of relevant highway storm water quality causal variables. Note that it may not be necessary, nor desirable, to use all of the relevant variables in the final storm water model. The process of selecting the "model variables" from the identified set of "relevant variables" is discussed Section 5.7.

The mass of constituent that is washed from the highway surface during a storm event is related positively to the total volume of runoff (Eq. 3.7.2). Scientific theory suggests that a regression of constituent load against storm runoff will result in the sign of the runoff coefficient being positive. Furthermore, the computed *t*-ratio for the runoff coefficient should be greater than the critical *t*-ratio at the 0.95 level, which suggests statistically a 95% confidence level in any decision to reject the null hypothesis that the runoff coefficient is actually equal to zero. It is possible for scientific theory to suggest variable relevancy yet be contradicted by statistics, which is the case when the exclusion of a relevant variable from the model has led to a bias in the statistical analysis. Likewise, statistical relevance can be established between variables that are correlated only by happenstance. These inconsistencies make it difficult to distinguish between the truly relevant explanatory variables and those with only circumstantial correlation. There are certain traits, however, that are exhibited by all relevant explanatory variables. These traits include:

(1) some underlying scientific theory explains the response of the dependent variable to a change in the independent variable;

(2) the variable, when included with all of the other independent variables, must add some explanatory information to the model (i.e., the variable cannot be perfectly collinear with any other variable);

(3) the variable is known with certainty or at least capable of being measured with a high degree of accuracy.

The process of identifying relevant variables must be based on scientific theory, otherwise there is no way to distinguish between true causation and circumstantial correlation. A detailed discussion of correlation and causation is reserved for Section 5.5. It should be noted here that a high degree of correlation between two variables in no way implies causation. There is a high degree of correlation, for example, between the yearly number of publications by Professor Sydney Chapman and the yearly means of sunspot relative numbers for the years 1910 through 1967 (Campbell, 1968). This correlation is curious, especially considering that Dr. Chapman worked in fields of research related to solar changes, but there is absolutely no evidence of causation. The correlation coefficient is only a measure of the degree of covariation between Dr. Chapman's productivity and the sunspot cycle and nothing more. The correlation coefficient, or the more commonly used square of the correlation coefficient (R^2), is a measure of the "explanatory" power of the regression equation only if the variables that are selected for use in the regression are derived from some guiding theory that bestows the equation with causality.

A variable that is "relevant" also must add explanatory information that is independent of the information collectively added by all other relevant variables in the model. The "independence" of the explanatory variable must be considered in the selection process because many variables in the storm water runoff process tend to move together. The size of a storm event, for example, may be expressed in terms of rainfall volume, runoff volume, duration of the storm, or the number of vehicles that traveled through the storm. The lack of independent movement among the explanatory variables is a condition known as multicollinearity.

Multicollinearity affects every storm water runoff data set. A precise estimate of the effect of single variable is difficult since all of the variables move together. This results in is high values for the variance of the estimated coefficients which increases the standard error of the regression and reduces the *t*-ratio. A small *t*-ratio is not necessarily a problem as long as the analyst is not mislead by a small *t*-ratio that is the result of the presence of multicollinearity. However, multicollinearity causes the statistical

significance of the computed variable coefficient to vary depending on what other variables happen to be present in the equation. This situation is interpreted as "instability" in the regression coefficients. Scientific theory provides only general guidelines for the selection of specific empirical variables (e.g., a general mass balance says that the amount of material contained in the output of a storm water system is determined by the amount of material input into the system, plus or minus any decay or production of the material within the system; the mass balance does not indicate what the specific inputs might be for a particular system); therefore, it is customary when working with highway runoff data to experiment with alternative specifications of the same basic equation. A number of formulations of the runoff model are developed that differ only by the specific causal variables used, such as storm duration, rainfall volume, runoff volume, traffic during the storm, duration of the antecedent dry period, traffic during the dry period, etc. A correlation among the variables in the sample exists; therefore, the coefficients of some variables will be significant in some formulations and not significant in others. The coefficients will appear to be "unstable" under these conditions.

Multicollinearity does not effect the predictive performance of a regression equation (Anselmi, 1987). The reason is that multicollinearity only obscures the individual effects of each explanatory variable on the dependent variable. The regression results will remain valid in terms of the effects on the dependent variable by the collective action of the explanatory variables as long as the conditions that originally caused the multicollinearity remain constant.

A perfect correlation between variables is seldom the case in storm water data sets, if for no other reason than measurement error. However, perfect correlation may occur, if the regression model is used to predict storm loading. For example, if the predictive model uses both rainfall volume and runoff volume as explanatory variables, and rainfall totals are the only data available, the user of the model would have to estimate runoff as a function of rainfall. Runoff volume, in this case, would be perfectly correlated to rainfall volume and would therefore not add any new information to the model.

A trait of a relevant variable is measurability. The regression equation assumes that there is measurement error associated with the value of the dependent variable. This

error is one of the primary reasons for the existence of a disturbance term associated with each regression equation (refer to Appendix G). However, the regression assumes that there is no measurement error in the independent variables. Any measurement error on the right-hand side of the equation will invalidate the regression. Therefore, any variable selected for use as an independent variable in the model should be one that is known or can be measured with certainty. For example, consider the variables total rainfall and total runoff. If there is no variation in the rainfall over the highway watershed, which is a reasonable assumption for short highway watersheds between curb inlets, the total rainfall can be measured more accurately than the total runoff from the watershed. All other factors equal, total rainfall would make a better explanatory variable than total runoff.

In summary, ordinary least squares regression will determine the correlation between any two variables, but sound scientific principles determine if the response of one variable is truly attributable to a change in another. Once a variable is determined to have scientific significance, other factors such as multicollinearity and measurability should be considered in order to establish the relevancy of the variable. The final variables used in the model are selected using statistical procedures outlined in Section 5.7.

The causal variables that influence constituent loading in highway storm water runoff were determined to originate during three different time periods: (1) the current storm, (2) the antecedent dry period, and (3) the preceding storm. Mathematically, the general population regression equation is given as:

$$\begin{aligned} Y = \beta_0 &+ (\beta_{s1} X_{s1} + \beta_{s2} X_{s2} + \ldots + \beta_{si} X_{si}) \\ &+ (\beta_{a1} X_{a1} + \beta_{a2} X_{a2} + \ldots + \beta_{ai} X_{ai}) \\ &+ (\beta_{p1} X_{p1} + \beta_{p2} X_{p2} + \ldots + \beta_{pi} X_{pi}) \\ &+ U_i \end{aligned} \qquad (5.3.1)$$

where the subscripts *s*, *a*, and *p* refer to variables from the storm, the antecedent dry period, and the preceding storm respectively, and *U* is the uncertainty term. Table 5.3.1 lists the relevant variables identified during this study.

Table 5.3.1 Relevant Model Variables

Variable	Example of Effect
Date of the Storm	Seasonal trends
Time of Day of the Storm	Atmospheric conditions may change during periods of industrial activity
Storm Duration	Potential for further constituent input
Total Rainfall or Total Runoff	Directly related to constituent loading
Intensity of Runoff	Higher kinetic energy in runoff may flush more material
Traffic Count during the Storm	Traffic is the source of certain constituents
Traffic Mix during the Storm	Construction vehicles, diesel-powered vehicles, and others may be "dirtier" than the normal population of vehicles
Traffic Speed during the Storm	Scour from tires and vehicle-induced wind forces increase with speed
Surrounding Land Use	Industrial areas are "dirtier" than rural areas
Curb / Guardrail Height	Taller guardrails trap constituents along the highway
Duration of Antecedent Dry Period	Provides the opportunity for the build-up of constituents
Antecedent Traffic Count	Increased opportunity for dry vehicle contributions
Weather Conditions	Heavy winds during the dry period could remove constituents from the highway surface
Maintenance Activities	Grass cutting, bridge sanding, and guardrail maintenance add dirt and debris to the highway surface
Street Sweeping	Potential to remove constituents from highway surface
Previous Storm Characteristics	The degree of removal during the previous storm event will affect the amount of material available for the current storm event.

5.4 Worksheet Development

The worksheet is a systematic way to organize and record the values of all variables used in the regression analysis. The columns of the worksheet identify the variables that are used in the analysis, and the rows contain the respective values of the variables for each observation. This task was accomplished with an *Excel* spreadsheet, that is compatible with the MicroTSP Econometric software used for the regression analysis.

The values of all variables for each observation were recorded as cumulative values from the beginning of the storm event so that each observation could be considered the end of the current runoff. Therefore, the 450 observations recorded during the 35 simulated rainfall events and 23 natural storm events each represent an individual runoff event. The advantages to organizing the data in this manner are (1) an increase in the available number of storm events for the regression analysis and (2) the regression equation formulated from the data set will be able to predict inner-event loading patterns. The disadvantage, however, is the introduction of autocorrelation, into the data set. Autocorrelation results when the value of a variable is dependent on the preceding value of the variable. A data set can be transformed, however, to account for the autocorrelation prior to the formulation of the regression equation. The method used to transform the data in this research is presented in Appendix G.

The constituent loads are adjusted for background concentrations of the constituent prior to the formulation of the regression equation. Background concentrations for the rainfall simulations are the constituent concentrations measured in the tap water, and background concentrations for the natural storm events are the constituent concentrations measured in the rainfall. In the worksheet, only the observations recorded during the rainfall simulations were adjusted for background concentrations of the constituents. The difference between the constituent concentration measured in the tap water and the average concentration measured for the constituent in the natural rainfall was added/subtracted to the constituent concentration measured in the simulated runoff sample. This method essentially "normalized" the simulated runoff samples to match the natural runoff samples.

Scaling of the variables is also identified in the worksheet. The objective of the regression analysis is to formulate a predictive equation that is applicable to highway watersheds other than the West 35th Street site. Constituent loads recorded in the worksheet are in units of grams per square meter of highway surface (g/m^2) to account for differences in watershed areas. Likewise, runoff discharge rates were recorded in liters per minute per square meter of highway surface ($l/m^2/min$). Vehicle counts during the wet and dry periods were recorded as the average count per lane of traffic in order to be compatible with watersheds with a different number of traffic lanes.

5.5 Covariance, Correlation, and Causation

Covariance is the measure of linear dependence between two variables. The covariance is given by:

$$Cov(x, y) = \frac{\sum (x_i - \bar{x})(y_i - \bar{y})}{n-1} \qquad (5.5.1)$$

where: x_i = ith observation of variable x;

y_i = ith observation of variable y;

$\bar{x}$ = mean of x;

$\bar{y}$ = mean of y;

n = number of observations.

A large value of covariance indicates a strong linear relationship between two variables and is equal to zero if the two variables are independent. The covariance also could equal zero if the two variables are related by a non-linear function such as a quadratic or exponential. The covariance, however, has little application to highway storm water quality because the covariance is dependent on the scales chosen for the two variables. This makes it impossible to know whether the value of the covariance is truly large or small.

The problem is solved by converting the covariance to a scaleless covariance by dividing by the standard deviations of the two variables. The scaleless covariance is called the correlation coefficient, r, and is shown mathematically as:

$$r(x, y) = \frac{\frac{\sum (x_i - \bar{x})(y_i - \bar{y})}{n-1}}{S_x S_y} \qquad (5.5.2)$$

where: S_x = standard deviation of x;

S_y = standard deviation of y.

The value of the correlation coefficient ranges from -1 to +1, and values that approach -1 or +1 indicate a strong correlation between x and y. If the sign of the correlation coefficient is positive, the value of x increases with an increase in y, and if the sign is negative, the value of x decreases with an increase in y.

The coefficient of multiple determination, or R^2, is the square of the correlation coefficient and is often used in regression analysis to measure the percent of variation in the dependent variable associated with, or explained by, variation in the independent variable. The degree of correlation between two variables in no way implies causation. However, the correlation coefficient can be used to measure the degree of causation if there is reason to believe the two variables are related in the system under study. Furthermore, R^2 is only a measure of the linear association between two variables. Two variables may be related according to a nonlinear function and have a low value of R^2.

The correlation coefficients between suspected causal variables and highway runoff constituents are presented in Table 5.5.1.

Table 5.5.1 Correlation Coefficients Between Suspected Causal Variables and Constituent Load (g/m^2)

	TSS	VSS	BOD_5	COD	Total Carbon	Dis. Total Carbon	NO_3	TP	Oil & Grease	Cu	Fe	Pb	Zn
Duration	0.07	0.05	0.24	0.30	0.07	0.12	0.11	0.31	0.42	0.49	0.12	0.17	0.32
Flow	0.91	0.92	0.76	0.87	0.87	0.96	0.94	0.82	0.86	0.59	0.91	0.51	0.67
Intensity	0.79	0.79	0.61	0.67	0.72	0.77	0.77	0.64	0.60	0.38	0.74	0.37	0.54
VDS	0.15	0.13	0.39	0.43	0.18	0.27	0.25	0.40	0.56	0.40	0.23	0.23	0.40
Air Temp.	-0.04	0.04	0.14	0.09	-0.07	0.06	0.10	0.14	-0.01	-0.01	0.03	-0.09	0.06
ADP	0.14	0.21	0.28	0.16	0.16	0.27	0.31	0.21	0.09	0.06	0.12	0.05	0.22
ATC	0.11	0.18	0.28	0.18	0.13	0.25	0.31	0.21	0.09	0.05	0.09	0.03	0.23
ADP Temp.	-0.18	-0.12	0.02	-0.03	-0.19	-0.05	0.01	0.00	-0.12	-0.06	-0.12	-0.17	-0.04
P-Duration	0.14	0.16	0.05	-0.16	0.27	0.05	-0.05	-0.10	0.04	0.01	0.17	0.12	-0.12
P-Flow	0.11	0.10	0.19	0.16	0.10	0.16	0.22	0.21	0.07	-0.04	0.13	0.05	0.20
P-Intensity	0.03	0.03	0.18	0.29	-0.08	0.15	0.27	0.32	0.04	-0.02	0.04	-0.02	0.32
P-VDS	0.06	0.12	-0.01	-0.17	0.20	0.01	-0.09	-0.16	-0.01	0.03	0.12	0.10	-0.12
P-Temp.	-0.30	-0.29	-0.05	-0.07	-0.34	-0.15	-0.07	-0.05	-0.19	-0.12	-0.27	-0.28	-0.12

Duration of storm is in units of minutes; Flow = L/m^2; Intensity = volume of runoff / duration;
VDS = Vehicle count during the storm; ADP = Duration of the antecedent dry period;
ATC = Vehicle count during the antecedent dry period; Temperature in ^oC;
P prefix indicates previous storm characteristic.

5.6 Model Misspecification

There are four assumptions regarding the residuals that must be made for ordinary least squares (OLS) regression to be valid. The implications of these assumptions and the remedies used to satisfy misspecifications are discussed in Appendix G. A fifth assumption, which of multicollinearity, is made when formulating a multiple regression model. The effects of multicollinearity have been described in Section 5.3.

5.7 Variables Included in the Model

Theoretically, all of the variables identified in Table 5.3.1 influence the constituent load in highway runoff and should be included in any empirical model used to predict the constituent loading in highway runoff. Unfortunately, it is not possible to include all of the identified variables in the model, nor is it particularly desirable. Some of the variables, such as surrounding land use, traffic speed, and traffic mix cannot be used in the model because their values are fixed in the data set. There are other variables that influence constituent loading in highway runoff that have not been identified because of a lack of knowledge of the build-up/wash-off process. Furthermore, the inclusion of all relevant variables in the model, or model overfitting, can be harmful because the prediction error of the model is proportional to the number of parameters in the model (Berthouex and Brown, 1994). The goal is to determine an adequate model with the fewest possible terms. Unfortunately, the method of selecting the final model is strictly trial and error and dependent on the subjectivity of the analyst.

A three-phase approach was used to search for the simplest, "adequate" model. The first phase begins with an overfit of the model. The regression equation is formulated using every known causal variable and each coefficient is examined for statistical relevance (a computed *t*-ratio greater than the critical *t*-ratio for rejecting the null hypothesis at the 0.95 level) and scientific relevance (the coefficient has the expected sign) to determine that variables are candidates for discard. The variables that fail both tests are eliminated one at a time, the regression equation is reformulated, and the new coefficients are examined for relevance. The procedure is repeated until there are no longer any variables that are statistically insignificant *and* display the wrong sign.

The second phase of the search involves making a judgment on the variables that show statistical significance and not scientific significance, or vise versa. If the variable is statistically significant and scientifically relevant, but does not have the expected sign, it is allowed to remain in the model since the probable cause of the sign change is multicollinearity with an included or excluded variable. The decision is not as straightforward if the variable is scientifically relevant and has the expected sign, but is not statistically significant. In most cases, the variable is eliminated from the model.

However, there are some circumstances in which the variable should be allowed to remain in the model. Multicollinearity may have reduced the value of the computed *t*-ratio below the critical *t*-ratio, which could lead to the wrong conclusion.

The final phase of the search involves a reconsideration of the discarded variables since scientific theory suggests that all of the variables should be included in the model. It is possible for a variable that was discarded early in the process to become statistically relevant in a new model formulation with a fewer number of variables. All discarded variables, therefore, should be individually reinserted into the trimmed model and tested for relevance.

The model development included the testing of different functional forms of the major independent variables. For example, it is not scientifically appealing to use the duration of the antecedent dry period in a linear form. Intuitively, the build-up of material on the highway surface is not linear throughout the range of possible dry period durations, but becomes asymptotic at some level. In this case, it is more appealing to specify the reciprocal of the dry period duration in the model.

During model development, the linear, reciprocal, and quadratic forms of the major independent variables were specified in model. The log-log [i.e., $\text{Ln}(y) = C + \beta\text{Ln}(x)$] and linear-log [i.e., $y = C + \beta\text{Ln}(x)$] model forms also were specified. Interestingly, a linear-linear specification showed the greatest explanatory power for all constituents in the West 35th Street data.

It is tempting to rank the independent variables in order of their relative importance during the selection process. Methods used to rank variables include comparing the magnitudes of the variable coefficients, comparing simple correlation coefficients, and comparing *t*-ratios. None of these methods, however, are particularly attractive.

The absolute values of the coefficients should not be used to make statements about the relative importance of the variables in the equation. The magnitude of the coefficient is meaningless since the variables are scaled in different units. Simple correlation coefficients, such as those in Table 5.5.1, also should not be used to rank the importance of variables. Correlation coefficients are computed without regard for the effect on the dependent variable of the other relevant variables in the equation.

A third basis for assigning importance to model variables is ranking by the magnitude of the respective *t*-ratio. The *t*-ratio cannot be used to rank variables. If a variable has a *t*-ratio that is twice the size of the *t*-ratio of another variable, it does not follow that the variable is twice as important. All it suggests is that the relative variance of one estimated coefficient is smaller than the relative variance of the other. If the computed t-ratio exceeds the critical t-ratio for the confidence level of the test, all that can be stated is that the null hypothesis can be rejected.

The methods of beta coefficients and elasticities offer the best possibilities for ranking model variables. A description of these methods may be found in most texts on regression analysis including Johnson et al. (1987). However, there are no compelling reasons to rank the variables of the highway constituent runoff model.

5.8 Summary

The regression model was found to have the most applicability for predicting edge-of-pavement constituent loads in highway runoff. Regression equations can (1) be formulated that calculate both single-event and continuous storm loading patterns, (2) make use of multiple causal variables, (3) provide information that can suggest mitigation procedures or model applicability situations, and (4) be attached as the input to a larger model simulating a much broader system.

The model was developed using a three-stage approach to examine the applicability of suspected causal variables. The goal was to formulate the model with the fewest explanatory variables in order to reduce prediction error. Because the explanatory variables selected for use in the model are based on both scientific and statistical relevance, the calculated correlation coefficient is an effective measure of the explanatory power of the equation. The linear forms of the explanatory variables were found to have greater explanatory power than other functional forms such as reciprocal and quadratic.

6.0 Model Results

6.1 Introduction

The results of the regression equations that were formulated using the data collected at the West 35th Street sampling site are presented in this chapter. Although data were collected during both simulated and natural rainfall events, no statistical difference was detected among the data generated with the rainfall simulator and those collected during the natural storm events. Therefore, no attempt was made to segregate simulated from natural data during model formulation. The regression equations were formulated using the combined data for storm events sampled at the West 35th Street site.

A statistical difference was detected among the street sweeping data. Street sweeping was not conducted at the West 35th Street during the first 7 months of the study period, but resumed during the last 5 months of the study at a sweeping frequency of once every 2 weeks. No significant correlation was detected among the constituent loads and the amount of time since the street sweeping activity. However, a statistical difference was detected among the data collected for each period. Therefore, two sets of regression equations were formulated. The first set applies to highway pavements where no street sweeping activity occurred and the other to highway pavements that are swept on a frequency of approximately once every 2 weeks. Examples of each equation are given in the chapter. The results of all regression analysis are presented in Tables 6.2.1, 6.2.2, and 6.2.3, and in Figures 6.2.1 through 6.2.4. Additional data also are presented in Appendix I.

6.2 Results of the Regression Analysis

The numerical results of the regression formulation are presented in Tables 6.2.1 and 6.2.2. The first column lists the constituents that were modeled. The second column, *N*, is the size of the sample used to formulate the regression. The differences in sample size among the constituents is mostly a result of missing data. The maximum sample size possible is 422, which is the result of the 423 observations recorded less 1 observation

Table 6.2.1 Summary of Model Coefficients (Non-Metals)

Constituent (g/m^2)	N	S (g/m^2)	R^2	C	Duration (min)	Flow (L/m^2)	Intensity (L/m^2min)	VDS	ADP (hrs)	ATC	PDUR (min)	PFLOW (L/m^2)	PINT (L/m^2min)
TSS	402	0.5482	0.93	0.2556*		0.3068	2.0181		0.0037				-2.9865
				(0.2721)		(0.0140)	(0.8077)		(0.0007)				(0.6989)
VSS	401	0.0630	0.93	-0.0186*		0.0348	0.1649		0.0005			0.0069	-0.6721
				(0.0322)		(0.0016)	(0.0932)		(0.0001)			(0.0013)	(0.1336)
COD	420	0.1169	0.95	-0.0613*	0.0007	0.0773	0.7785		-0.0041	6.0E-6			
				(0.0343)	(7.8E-5)	(0.0025)	(0.1156)		(0.0009)	(1.2E-6)			
Phosphorus	411	0.0005	0.90	-0.0005	3.3E-6	0.0002	0.0032			5.1E-9			
				(0.0002)	(3.6E-7)	(1.1E-5)	(0.0005)			(8.0E-10)			
Nitrate	351	0.0010	0.95	-0.0015		0.0006	0.0086			1.2E-8			
				(0.0004)		(2.8E-5)	(0.0016)			(1.6E-9)			
Total Carbon	404	0.0766	0.94	-0.0657*	-0.0011	0.0411	0.7307	1.1E-4		6.7E-7			
				(0.0322)	(1.6E-4)	(0.0015)	(0.0965)	(1.7E-5)		(1.3E-7)			
Dis. TC	402	0.0265	0.91	-0.0306		0.0073	0.3585	2.2E-5		1.3E-7			0.1983
				(0.0108)		(0.0005)	(0.0324)	(2.8E-6)		(5.5E-8)			(0.0585)
BOD_5	398	0.0145	0.86	-0.0081*		0.0035	0.0619	1.1E-5		1.5E-7			
				(0.0046)		(0.0004)	(0.0228)	(1.6E-6)		(2.3E-8)			
Oil and Grease	263	0.0054	0.94	-0.0004*		0.0030		1.0E-5					
				(0.0020)		(8.9E-5)		(5.8E-7)					

N = # of observations.; S = std. error of regression (g/m^2); R^2 = correlation coefficient adjusted for degrees of freedom; C = intercept;
Duration = duration of storm event (min); Flow = total volume of runoff per unit area of watershed (L/m^2);
Intensity = Flow divided by Duration (L/m^2/min); VDS = single-lane vehicle count during storm; ADP = duration of antecedent dry period (hrs);
ATC = single-lane vehicle count during ADP; PDUR = duration of the previous storm event (min);
PFLOW = total volume of runoff per unit area of watershed during the previous storm event (L/m^2); PINT = PFLOW divided by PDUR (L/m^2/min);
An asterisk indicates the coefficient is not statistically different from zero; Numbers in parenthesis are the standard error of estimate of the coefficients;
Example: TSS (g/m^2) = 0.2556 + 0.3068(*Flow*) + 2.0181(*Intensity*) + 0.0037(*ADP*) - 2.9865 (*PINT*)
This table is applicable only to highway pavements with no street sweeping activity. Refer to Table 6.2.3 for street sweeping adjustments.

Table 6.2.2 Summary of Model Coefficients (Metals)

Constituent (g/m^2)	N	S (g/m^2)	R^2	C	Duration (min)	Flow (L/m^2)	Intensity (L/m^2min)	VDS	ADP (hrs)	ATC	PDUR (min)	PFLOW (L/m^2)	PINT (L/m^2min)
Iron	399	0.0084	0.92	-0.0028*		0.0042	0.0282		2.3E-5				
				(0.0028)		(0.0002)	(0.0082)		(1.0E-5)				
Zinc	399	0.0007	0.92	0.0002*	2.5E-6	0.0001				4.9E-9	-3.2E-6	0.0003	-0.0241
				(0.0002)	(4.2E-7)	(7.9E-6)				(1.1E-9)	(3.0E-7)	(1.5E-5)	(0.0016)
Lead	319	0.0004	0.68	0.0008		6.5E-5	-0.0020	8.0E-8					-0.0023
				(0.0002)		(8.9E-6)	(0.0006)	(2.4E-8)					(0.0008)
Copper	398	8.1E-5	0.90	1.9E-5*	3.8E-6	2.4E-5		-2.4E-7					
				(2.0E-5)	(1.5E-7)	(9.6E-7)		(1.6E-8)					

N = # of observations.; S = std. error of regression (g/m^2); R^2 = correlation coefficient adjusted for degrees of freedom; C = intercept;
Duration = duration of storm event (min); Flow = total volume of runoff per unit area of watershed (L/m^2);
Intensity = Flow divided by Duration (L/m^2/min); VDS = single-lane vehicle count during storm; ADP = duration of antecedent dry period (hrs);
ATC = single-lane vehicle count during ADP; PDUR = duration of the previous storm event (min);
PFLOW = total volume of runoff per unit area of watershed during the previous storm event (L/m^2); PINT = PFLOW divided by PDUR (L/m^2/min);
An asterisk indicates the coefficient is not statistically different from zero; Numbers in parenthesis are the standard error of estimate of the coefficients;
Example: Iron (g/m^2) = -0.0028 + 0.0042(*Flow*) + 0.0282(*Intensity*) + 0.000023(*ADP*)
This table is applicable only to highway pavements with no street sweeping activity. Refer to Table 6.2.3 for street sweeping adjustments.

lost due to the first-order autocorrelation adjustment. The third column, *S*, is the standard error of the regression. Ninety-five percent of the regression predictions fall within plus or minus two standard errors of the regression. The fourth column is the coefficient of multiple determination, R^2, adjusted for degrees of freedom.

The following terms/acronyms are used in Table 6.2.1 to identify the variables used in the regression equations:

C	=	the constant (*y*-intercept) term in the equation;
Duration	=	total duration of storm in minutes;
Flow	=	the total volume of flow per unit area of watershed during the storm (L/m^2);
Intensity	=	Flow divided by Duration ($L/m^2/min$);
VDS	=	average number of vehicles traveling through the storm in a single lane;
ADP	=	total duration of the antecedent dry period in hours;
ATC	=	average number of vehicles using the highway during the ADP in a single lane;
PDUR	=	the total duration of the preceding storm in minutes;
PFLOW	=	the total volume of flow per unit area of watershed (L/m^2) the preceding storm event;
PINT	=	PFLOW divided by PDUR ($L/m^2/min$)

Columns 5 through 14 of Tables 6.2.1 and 6.2.2 list the coefficients of the independent variables of the equation. The number in parentheses is the standard error of the coefficient. A coefficient marked with an asterisk indicates that the coefficient is not statistically different than zero as determined by the *t*-statistic (i.e., one cannot be 95% confident the coefficient is not zero since ± 2 standard errors include zero). The only coefficients included in the final regression equation that failed the *t*-test are those of the *y*-intercept term C. The combination of high adjusted R^2 values with the statistically significant coefficients indicate that the equations are a "good fit" of the West 35th Street data (further evidence of a good model fit is the normality of the residuals exhibited in Appendix H).

The constituents listed in both Tables 6.2.1 and 6.2.2 are listed in ascending order according to the importance of the traffic count during the storm (VDS) in the regression equation. For example, the first constituent listed in Table 6.2.1, TSS, has the regression

equation comprised of the fewest number of explanatory variables of that VDS is not included. The last constituent listed, oil and grease, has the regression equation comprised of the fewest number of explanatory variables of that VDS is included. Traffic count during the antecedent dry period was considered to be less important than traffic during the storm in this order system.

The interpretation of Tables 6.2.1 and 6.2.2 is presented below using TSS for an example. The predictive equation for the edge-of-pavement loading for TSS is determined using the coefficients shown in line 1 of Table 6.2.1, columns 5 through 14. The predictive equation for TSS is therefore:

$$TSS(\text{g/m}^2) = 0.2556 + 0.3068(Flow) + 2.0181(Intensity) + 0.0037(ADP) - 2.9865(PINT) \quad (6.2.1)$$

The positive (+) sign preceding the coefficients of *Flow*, *Intensity*, and *ADP* indicates that an increase in the value of any of these variables will result in an increase in the load of TSS. Likewise, the greater the intensity of the preceding storm event (*PINT*), the less the TSS load (i.e., there is less material remaining on the highway following a larger storm event). The values given in parenthesis under each coefficient in Table 6.2.1 are the standard errors of the coefficients. There is a 95% probability that the true value of the variable coefficient is within +/- 2 standard errors (the given coefficients are not necessarily the "true" values since there is uncertainty, or a lack of knowledge, regarding the underlying build-up and wash-off processes of TSS in nature). For example, there is a 95% probability that the true value of the coefficient for *ADP* is between 0.0023 and 0.0051. Note that if there is no storm event at all (i.e., *Flow*, *Intensity*, *ADP*, and *PINT* are all equal to zero), the load of TSS is not equal to zero, but rather 0.2556 g/m^2. However, the standard error for the constant term, *C*, is 0.2721, and there is a 95% chance that the true value of the constant term is between -0.2886 and 0.7998. Since this range includes the value of zero, the equation actually states that there is a 95% probability that the true load of TSS is zero if there is no storm at all.

The TSS equation was formulated from a data set consisting of 402 observations (shown in column 2 of Table 6.2.1). This information is helpful in determining the degrees of freedom of the regression analysis (i.e., the number of linear independent pieces of information in *n* observations). For example, the TSS regression has 397

degrees of freedom, which is the result of 402 (number of observations) less 5 (the number of estimated parameters, or the coefficients of the three explanatory variables plus the constant term).

The standard error of the TSS regression is 0.5482 (shown in column 3 of Table 6.2.1). This number is an estimate of the uncertainty (i.e., lack of knowledge) that exists within the West 35th Street TSS data. During the fit of the West 35th Street TSS data, 95% of the equation predictions were within +/- 1.0964 g/m^2 (i.e. two standard errors) of the observed value. Note that this is not the same as the standard error of the forecast, which is almost always larger than the standard error of the regression.

The adjusted R^2 of the TSS regression is 0.93 (shown in column 4, Table 6.2.1). This number indicates that 93% of the variation in the TSS loading observed at the West 35th Street sampling site is explained by the variables *Flow*, *Intensity*, *ADP*, and *PINT*.

Table 6.2.3 gives the set of "street sweeping shifts" determined from the analysis of the West 35th Street data. These coefficient shifts should be added to the coefficient values given in Tables 6.2.1 and 6.2.2 if the regression equations are to be used for highway pavements where street sweeping is performed approximately once every 2 weeks. The following equations demonstrate the use of the street sweeping shifts for iron:

The predictive model for iron from Table 6.2.2 (i.e., used if there is no sweeping):

$Iron(g/m^2) = -0.0028 + 0.0042(Flow) + 0.0282(Intensity) + 0.000023(ADP)$

The predictive model for iron if there is once every two week sweeping:

$Iron(g/m^2) = -0.0028 + (0.0042-0.0006)(Flow) + 0.0282(Intensity) + 0.000023(ADP)$

Table 6.2.3 Street Sweeping Shifts (once every 2 weeks sweeping schedule)

Constituent (g/m^2)	C	Duration (min)	Flow (L/m^2)	Intensity (L/m^2min)	VDS	ADP (hrs)	ATC	PDUR (min)	PFLOW (L/m^2)	PINT (L/m^2min)
TSS	-0.8225		-0.1484	2.6652						
	(0.3031)		(0.0190)	(1.0463)						
VSS	-0.0574		-0.0142	0.2724		-0.0003			-0.0034	0.1236
	(0.0413)		(0.0022)	(0.1231)		(0.0002)			(0.0018)	(0.2120)
BOD_5			-0.0014	0.0728	-7.6E-6					
			(0.0006)	(0.0278)	(0.0000)					
COD			-0.0181							
			(0.0023)							
Total Carbon		0.0011		-0.6375	-0.0001					
		(0.0002)		(0.0877)	(1.9E-5)					
Dis. Total Carbon				-0.2597	-1.5E-5		3.3E-7			-0.1916
				(0.0302)	(2.9E-6)		(8.9E-8)			(0.0737)
Nitrate	0.0017		0.0002	-0.0096						
	(0.0005)		(3.7E-5)	(0.0020)						
Phosphorus			-8.0E-5							
			(1.1E-5)							
Oil and Grease			-0.0009							
			(0.0002)							
Copper		-3.5E-6			2.2E-7					
		(2.1E-7)			(1.9E-8)					
Iron			-0.0006							
			(0.0002)							
Lead	-0.0010			0.0031						0.0028
	(0.0002)			(0.0006)						(0.0012)
Zinc								2.7E-6	-0.0003	0.0233
								(3.7E-7)	(2.1E-5)	(0.0024)

Shifts should *only* be used with coefficients in Tables 6.2.1 and 6.2.2. Refer to Tables 6.2.1 and 6.2.2 for acronym descriptions.
Example: Iron (g/m^2) = -0.0028 + (0.0042 - 0.0006)(*Flow*) + 0.0282(*Intensity*) + 0.000023(*ADP*)

The values shown in parentheses in Table 6.2.3 are the standard errors of the estimates of the sweeping shifts. All of the shifts in Table 6.2.3 have been determined to be statistically different from zero by using the *t*-test.

As shown in Table 4.8.1, not all constituent loads were reduced during the period of street sweeping. The street sweeping shifts reflect these results. The highway runoff model was used to calculate the expected storm water loading for each constituent during a design storm under two assumptions: (1) a street sweeping program with a once every 2 weeks schedule was currently being conducted and (2) no street sweeping program was being conducted. The results are presented in Table 6.2.4. The parameters of the design storm are footnoted in Table 6.2.4.

The results of the regression analysis are shown graphically in Figures 6.2.1 through 6.2.4 for TSS, COD, nitrate, and zinc, respectively. Similar figures are presented

Table 6.2.4 Expected Loads based on MoPac Street Sweeping Program

Constituent	Expected Load with Street Sweeping (g/m^2)	Expected Load without Street Sweeping (g/m^2)
TSS	3.2	5.8
VSS	0.4	0.6
BOD_5	0.09	0.10
COD	1.3	1.6
Total Carbon	0.7	1.0
Dissolved Total Carbon	0.19	0.29
Nitrate	0.014	0.012
Total Phosphorus	0.003	0.005
Oil and Grease	0.07	0.07
Copper	0.0004	0.0004
Iron	0.07	0.08
Lead	0.0014	0.0007
Zinc	0.003	0.001

Storm duration = 60 minutes; Rainfall intensity = 25.4 mm/hr (1 in/hr);
Vehicles during the storm = 3,136; Antecedent dry period = 7 days;
Traffic count during dry period = 131,396; Previous storm duration = 60 minutes
Previous storm intensity = 25.4 mm/hr (1 in/hr); Watershed size = 4358 m^2 (46,910 ft^2)
Traffic lanes = 3

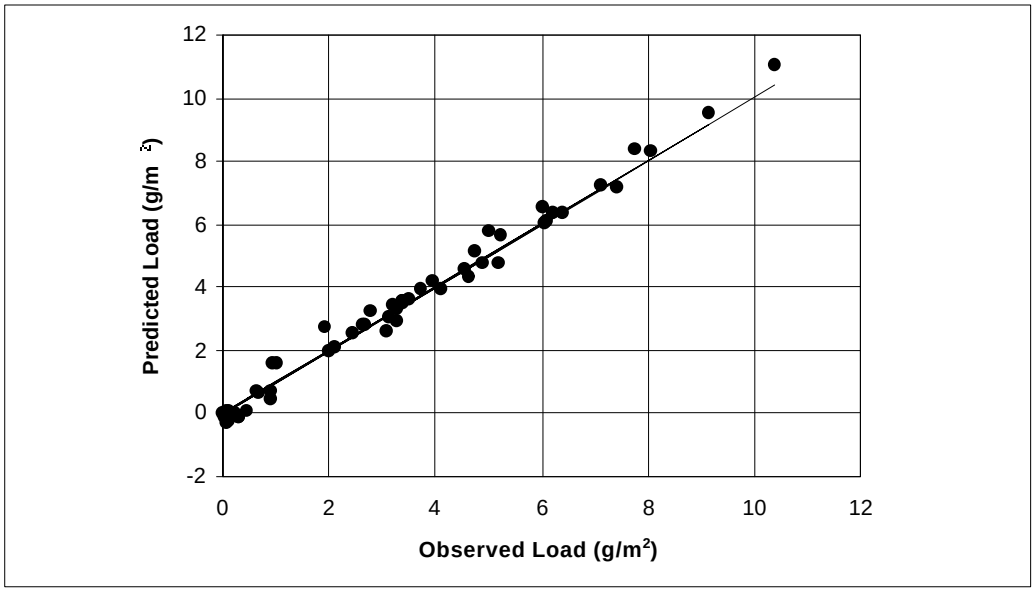

(a) Fit of Data from West 35th Street Site

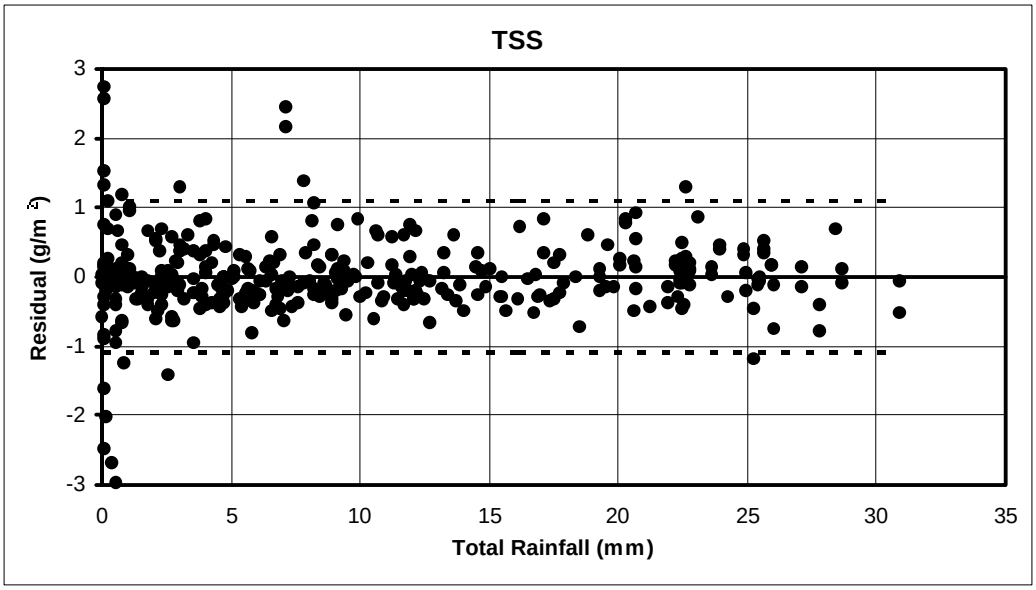

(b) Model Residuals vs. Total Rainfall (Dashed Lines Indicate ± 2 Std. Error)

Figure 6.2.1 TSS Model Results

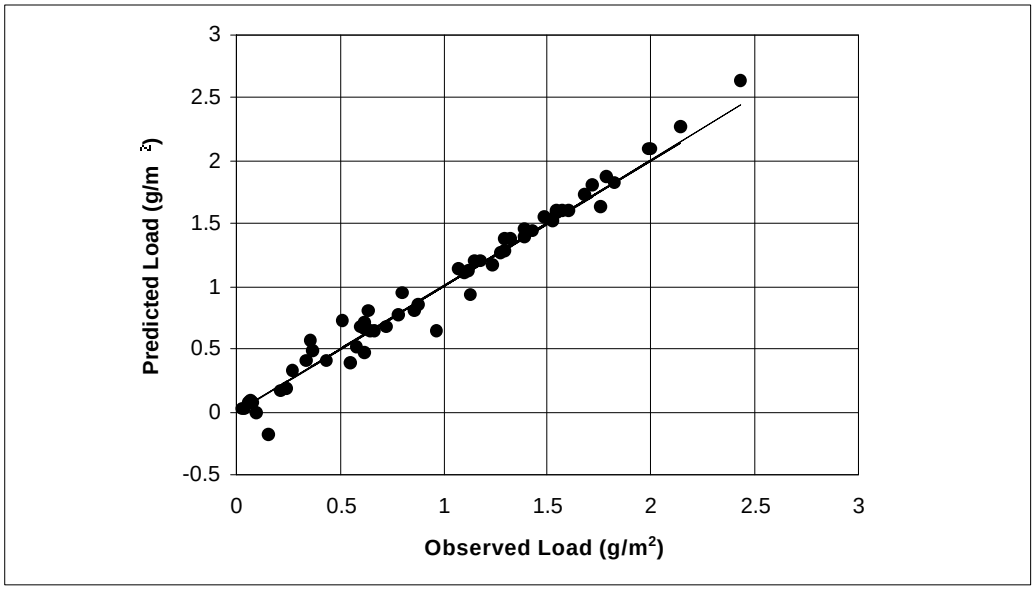

(a) Fit of Data from West 35th Street Site

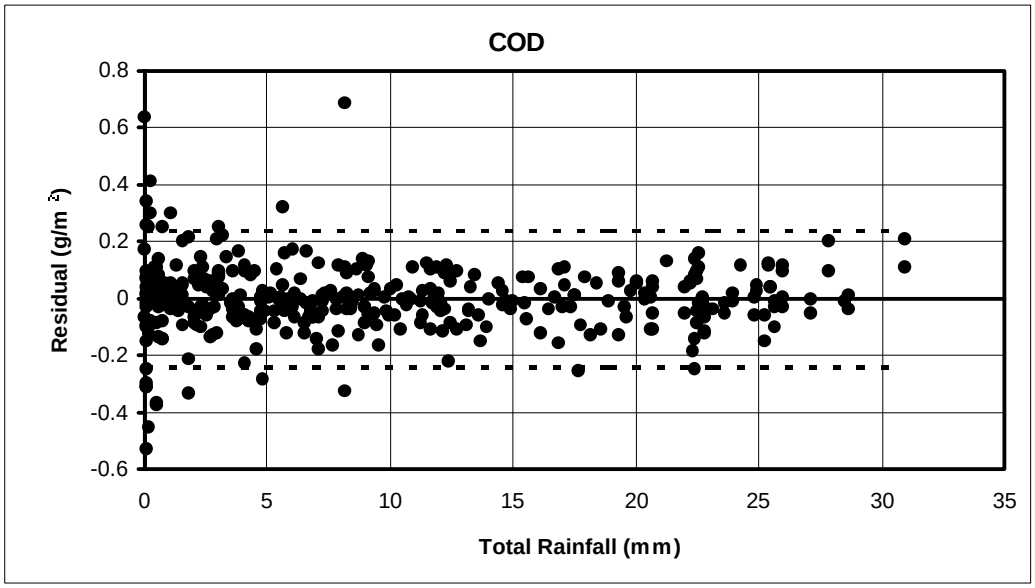

(b) Model Residuals vs. Total Rainfall (Dashed Lines Indicate ± 2 Std. Error)

Figure 6.2.2 COD Model Results

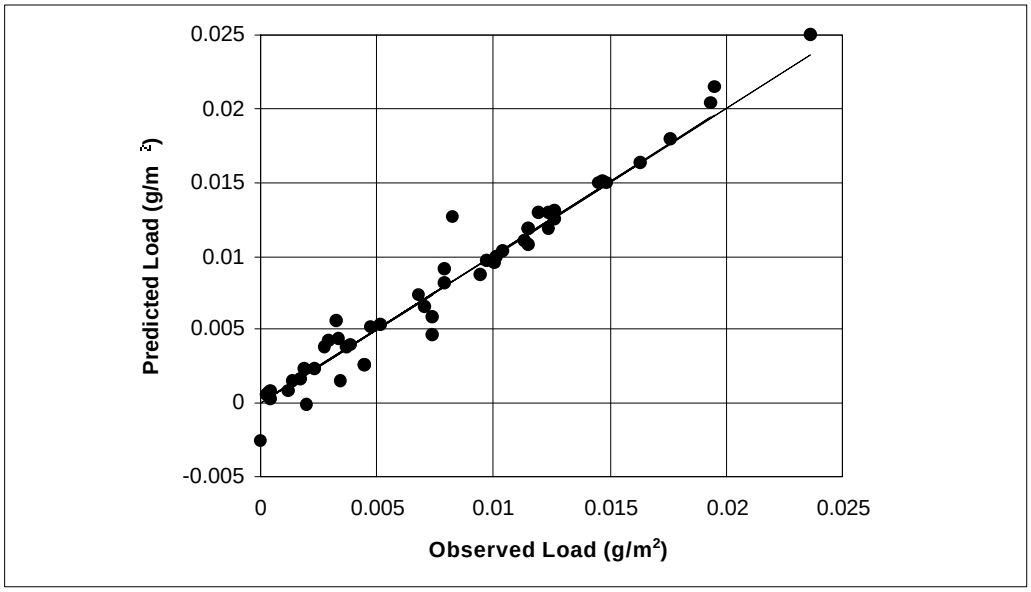

(a) Fit of Data from West 35th Street Site

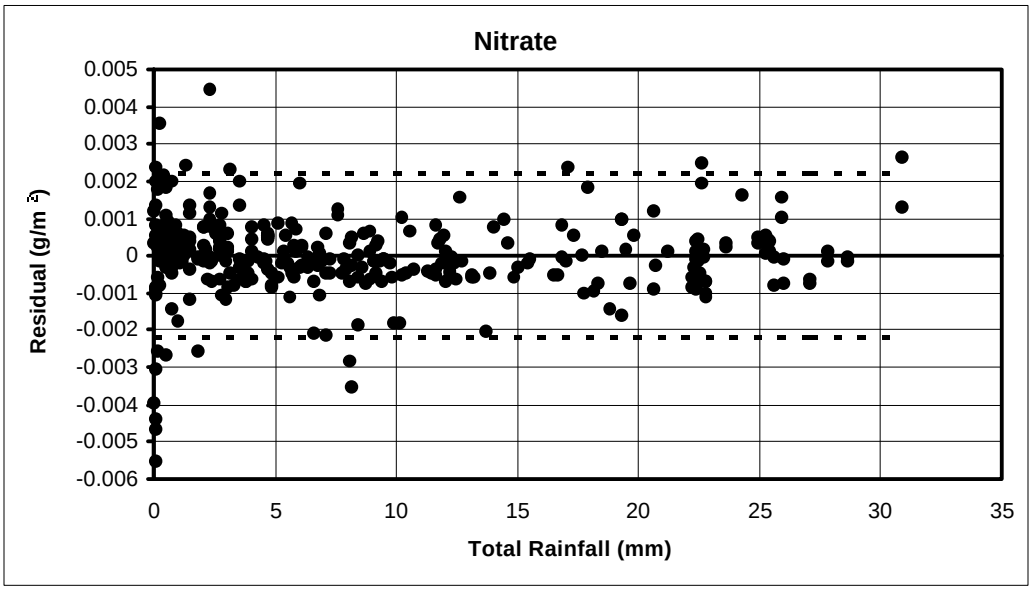

b) Model Residuals vs. Total Rainfall (Dashed Lines Indicate ± 2 Std. Error)

Figure 6.2.3 Nitrate Model Results

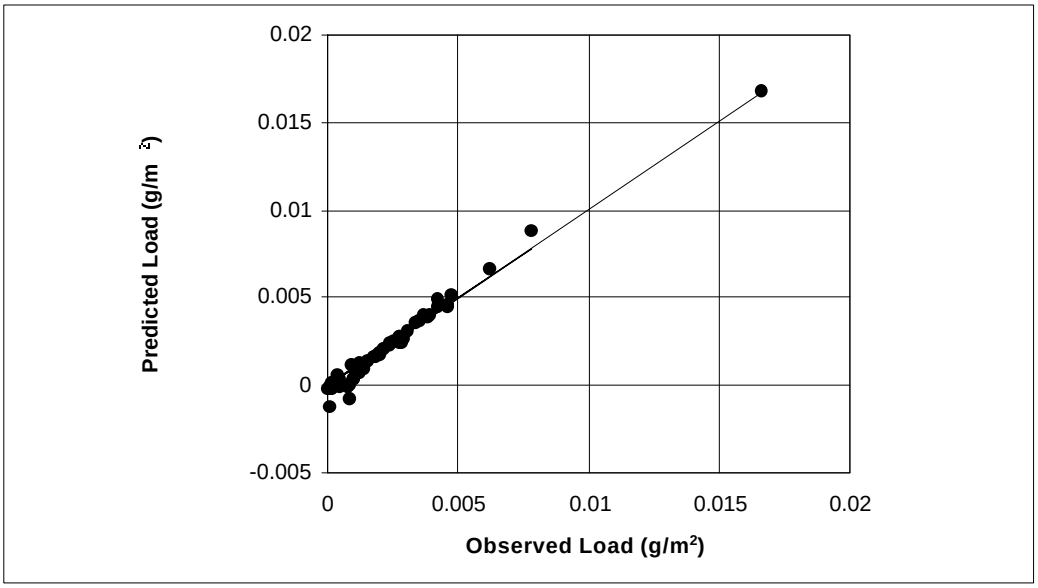

(a) Fit of Data from West 35th Street Site

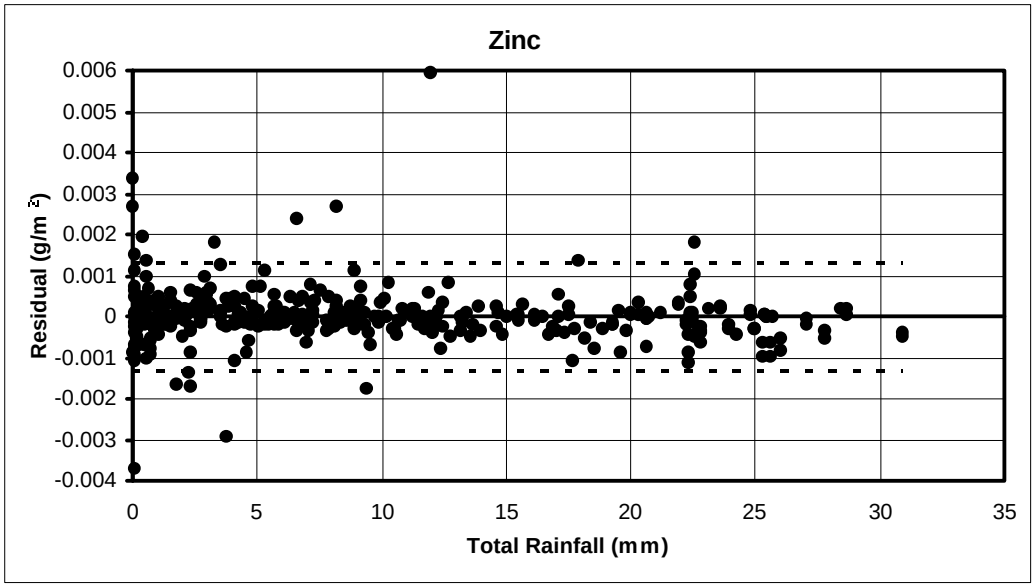

(b) Model Residuals vs. Total Rainfall (Dashed Lines Indicate ± 2 Std. Error)

Figure 6.2.4 Zinc Model Results

for all other highway runoff constituents in Appendix I. Part A of Figures 6.2.1 through 6.2.4 shows a plot of the observed total load versus the predicted total load for each storm recorded at the West 35th Street site. The solid line represents a perfect prediction, and the distance the predicted point is away from the line is a measure of the prediction error. Part B of each figure shows a plot of all of the residuals from the fit of the West 35th Street site data versus the total rainfall amount at the time of the observation. The dashed lines represent ± 2 standard errors of the regression.

Note in Part B of Figures 6.2.1 through 6.2.4 that the variation of the residuals is similar for storms of all magnitudes and that there is a normal distribution of residuals about the zero axis. This is graphic evidence that two fundamental ordinary least squares assumptions are satisfied: (1) homoscedasticity (at least with respect to runoff magnitude), and (2) a normal distribution of residuals (refer to Appendix G).

6.3 Model Verification with Data from the Convict Hill Site

The 20 storms that comprise the Convict Hill data were the only storm events available with which to verify the model. Unfortunately, there are many inaccuracies in the measurement of the explanatory variables at the Convict Hill site (relative to the West 35th Street site). Hourly traffic counts, for example, are measured at the site by TxDOT one day a year, and therefore, the number of vehicles that use the highway during both wet and dry periods must be estimated from these annual traffic counts (at West 35th Street, hourly traffic counts are recorded year around). The weekend traffic count, which is known to be much less than the weekday count, is complicated because the annual traffic count is conducted on a weekday. The Convict Hill site also has experienced a traffic growth rate of approximately 10% per year since 1993 because of increased residential development, which further complicates the traffic estimate. The predictive ability of each model that has traffic as an explanatory variable is adversely effected by the inaccuracy of the traffic counts.

The estimate of storm water discharge also is subject to errors. The Convict Hill sampling site is an overpass from that storm water drains via a downspout. Storm flow is directed from the downspout to a box that has a V-notch weir for one side. The water level is measured in the box using a bubbler flow meter and converted to flow using a

weir formula. The box has been known to overflow on several occasions, resulting in the loss of accurate flow data. Any inaccuracy in the flow measurements will adversely affect the predictive ability of all constituent models.

The model predictions for the Convict Hill storms are illustrated in Figures 6.3.1 through 6.3.4. The results from the fit of the West 35th Street data are shaded in the background to give a "feel" for the prediction error for storms occurring at the Convict Hill site.

The over-prediction tendency exhibited by the models at the Convict Hill site also can be attributed to the large area of pavement in the Convict Hill watershed that is not exposed to traffic (the loading differences observed for highway pavements under traffic and no-traffic conditions is shown in Figures 4.5.1, 4.5.2, and 4.5.3). Approximately 44% of the Convict Hill site watershed is exposed to traffic, compared to 77% at the West 35th Street site.

6.4 Interpretation of the Regression Results

The identification of the causal variables that influence constituent loading is among the more important findings of this study. There are two major applications of this knowledge. First, recognition of the specific variables that influence a given constituent load may suggest constituent-specific mitigation procedures, and second, the applicability of the model is directly reflected in the causal variables.

Because the dependent variable in the regression is expressed as load (g/m^2), the total volume of flow during the storm event will appear in every constituent model. Similarly, the intensity of the runoff and the duration of the runoff also will frequently appear in the models. The variables flow, intensity, and storm duration, therefore, offer little diagnostic information in the interpretation of the model specification. The appearance of the other variables in the model, such as VDS, ADP, and the previous storm event are the variables that "control" the constituent loading. The examination of the controlling variables in each model adds insight into the applicability of the model

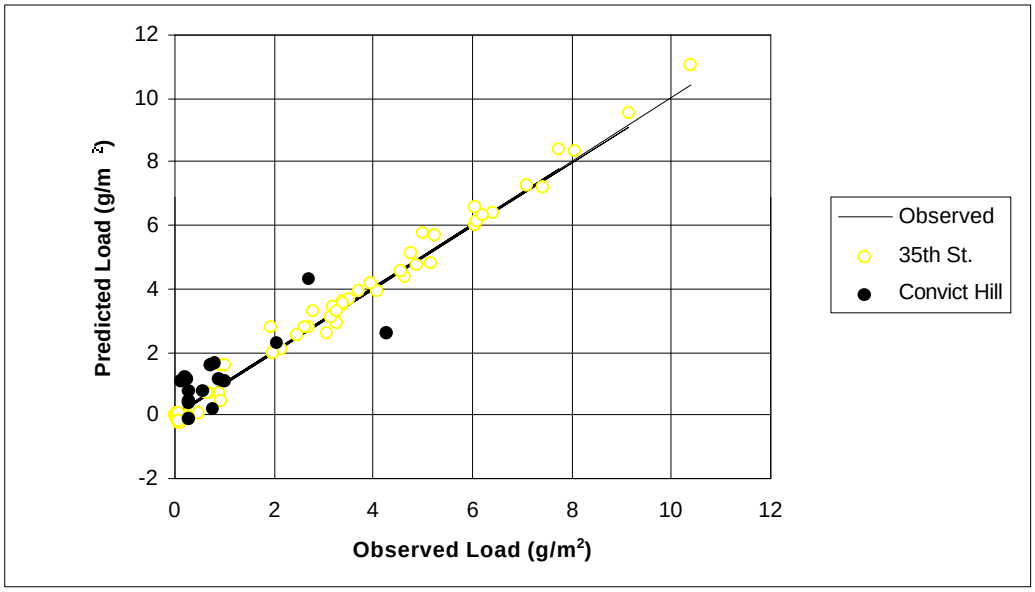

(a) Model Predictions at the Convict Hill Site

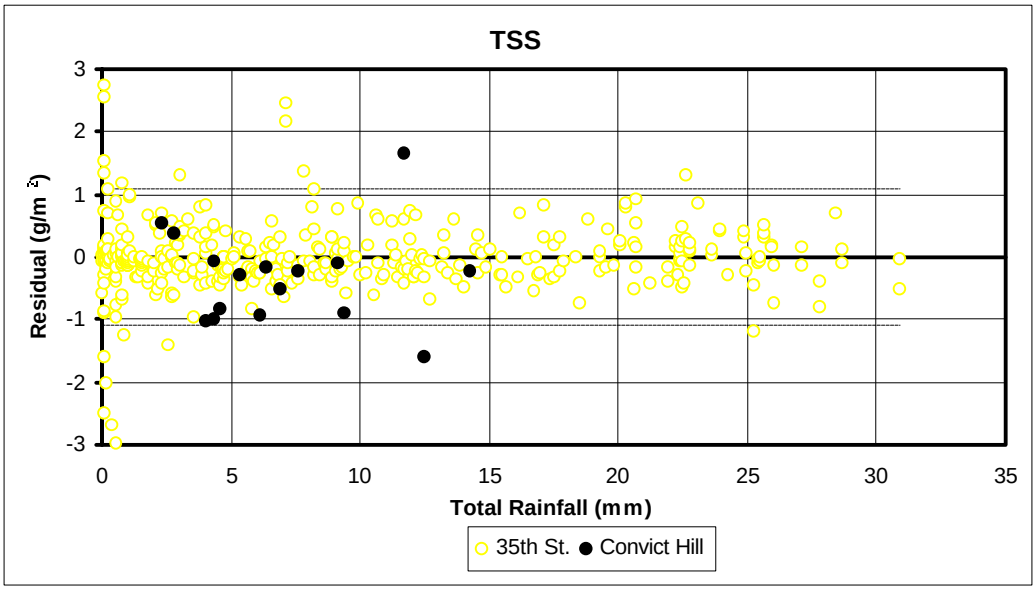

(b) Prediction Error vs. Total Rainfall

Figure 6.3.1 TSS Model Predictions

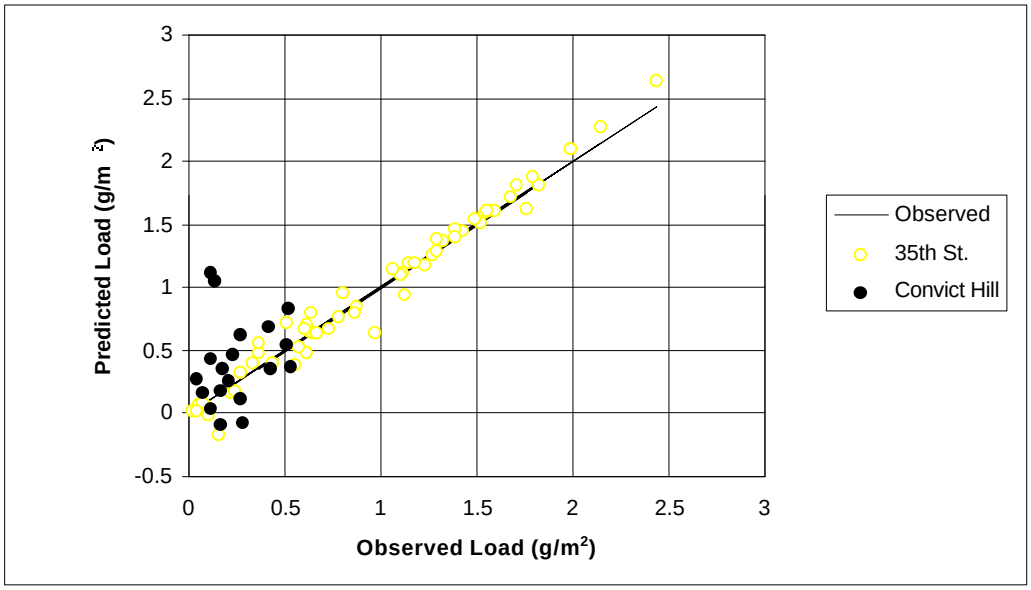

(a) Model Predictions at the Convict Hill Site

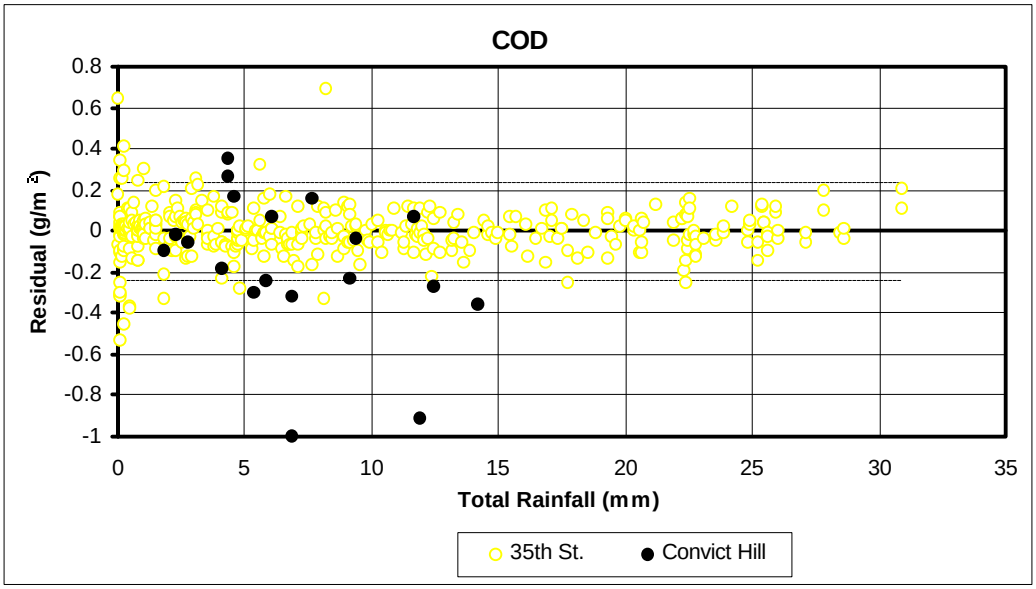

(b) Prediction Error vs. Total Rainfall

Figure 6.3.2 COD Model Predictions

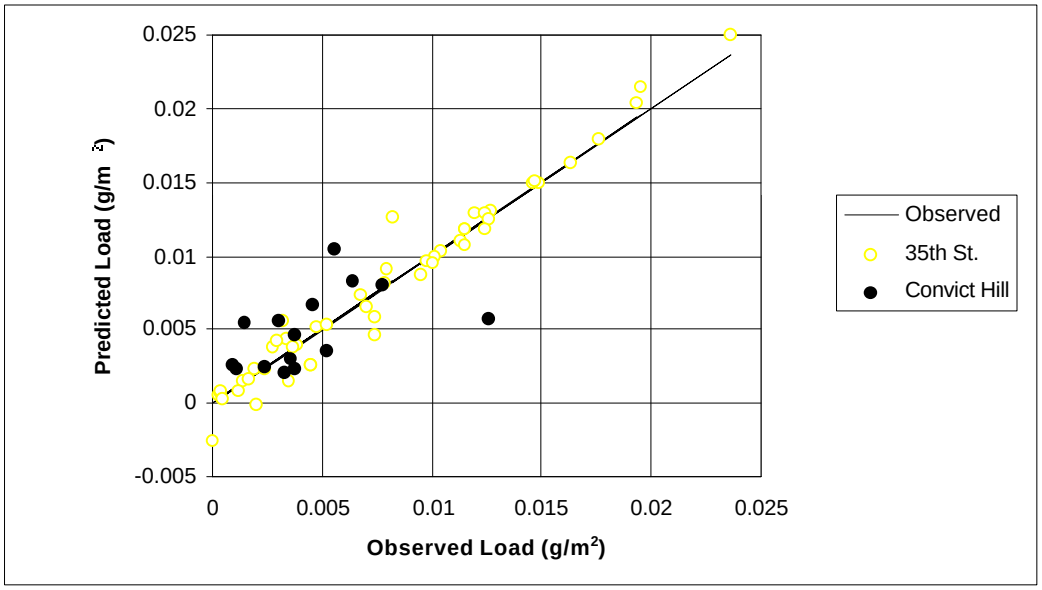

(a) Model Predictions at the Convict Hill Site

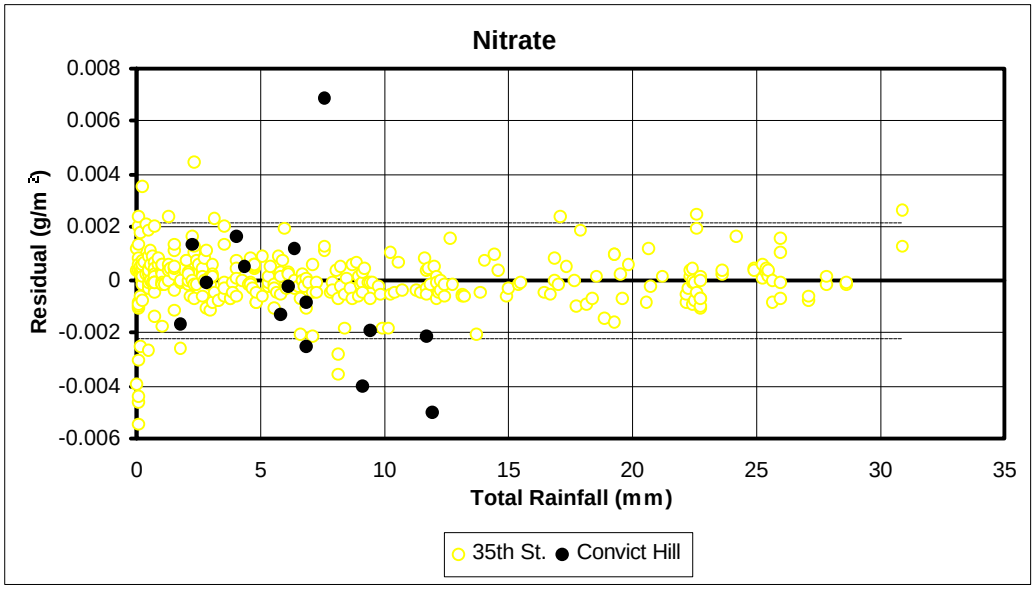

(b) Prediction Error vs. Total Rainfall

Figure 6.3.3 Nitrate Model Predictions

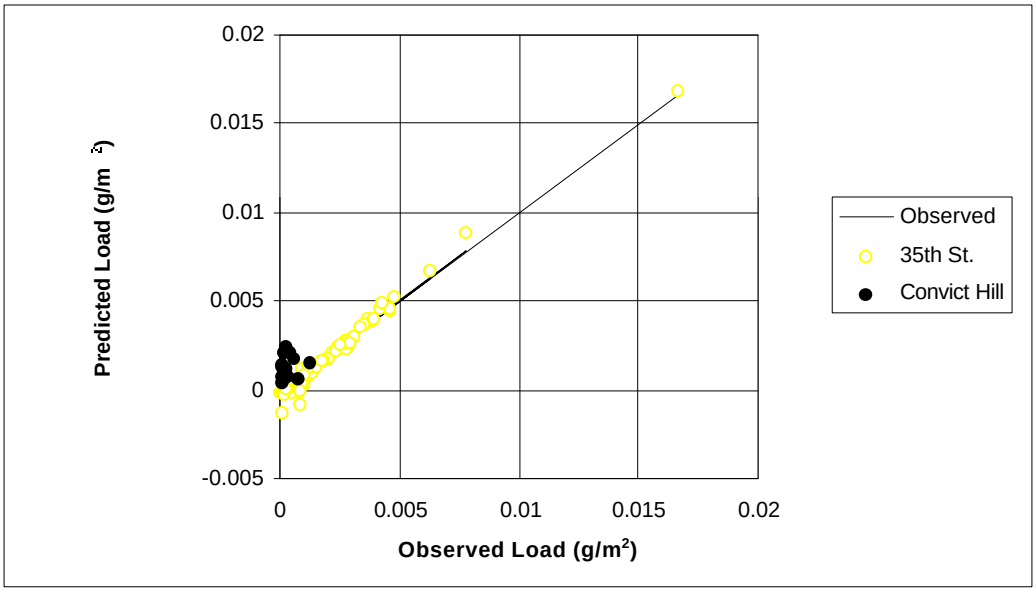

(a) Model Predictions at the Convict Hill Site

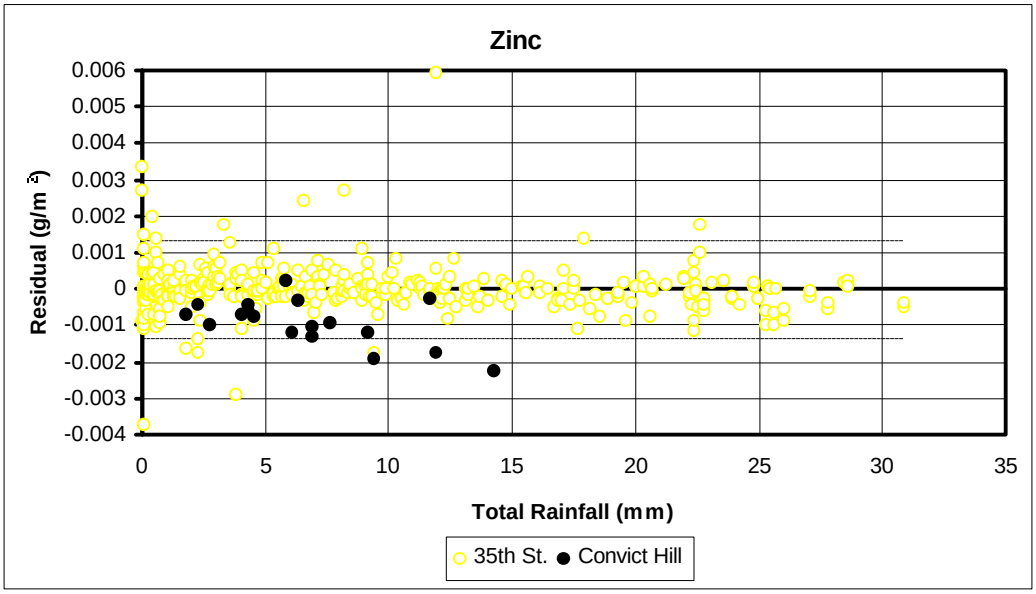

(b) Prediction Error vs. Total Rainfall

Figure 6.3.4 Zinc Model Predictions

and the mitigation of constituent loading. The following sub-sections examine the role of the controlling variables for each constituent group.

6.4.1 Solids

The regression results for TSS and VSS indicate that conditions during the antecedent dry period, such as dustfall and street maintenance activities (e.g., grass cutting, guardrail repair, bridge sanding, street sweeping, etc.), and the intensity of flow during the preceding storm event are the most significant variables that influence the storm loading of TSS and VSS. The absence of traffic as an influential variable does not suggest that there is no traffic contribution of solids during the storm, but simply that dustfall, street maintenance activities, and other dry period conditions overwhelm the contribution from vehicles (Figures 4.5.1 and F-2 illustrate that traffic does have some positive influence on the storm loads of TSS and VSS).

An examination of the signs of the coefficients in the solids models indicates that the storm water loading of TSS and VSS will increase with an increase in the duration of the antecedent dry period and will decrease with an increase in the intensity of the previous storm event. The (+) sign on the coefficient of the variable PFLOW in the VSS model is most likely a result of multicollinearity with PINT. This formulation is consistent with the theory that longer ADPs will result in a greater build-up of materials on the highway and that a more intense storm event will more completely cleanse the highway surface. More importantly, however, is that these formulations suggest the applicability of the solids models. For example, the duration of the antecedent dry period is a strong controlling variable (i.e., ADP is “strong” because there is only one other competing controlling variable in the model formulation); therefore, the solids model is applicable only to highways located in regions where the antecedent dry period conditions are similar to that at the West 35th Street site. For example, ADP conditions throughout the Barton Springs segment of the Edwards Aquifer recharge zone are generally similar to that at the 35th Street sampling site. For this reason, the model would be expected to give reasonable results throughout the region. However, the model would be expected to under-predict if applied in an area where the ADP is dominated by heavier dustfalls than those experienced at the West 35th Street site (e.g., summertime

conditions in west Texas). Furthermore, the model will prove inaccurate if extreme ADP conditions (e.g., such as the tracking of mud onto the highway by construction vehicles, wintertime bridge sanding, etc.) are suddenly experienced in an area where the solids models are known (or at least thought) to provide reasonable results.

The formulation of the solids models also suggests constituent-specific mitigation procedures. For example, the formulation suggests that efforts to clean the highway during the dry period will reduce the storm water loading of TSS and VSS during subsequent rainfalls. The reduction in solids was confirmed by comparing the average loading of TSS and VSS in the no-sweeping data to that of the sweeping data. A *t*-test confirms a 99% probability that the TSS loads are reduced during street sweeping and a 95% probability that the VSS loads are reduced (Section 4.8).

Street sweeping should be conducted following any activity that deposits a large amount of dirt and debris onto the highway surface (this is currently a normal procedure for TxDOT). However, it also might be beneficial to sweep following a large storm event (e.g., rainfall intensities > 25.4 mm/hr). A prominent silt line was observed following both simulated and heavy natural rainfall events. The silt line was formed along the high-water mark approximately 2 to 2.5 m from the curb. The silt line is a concentration of dirt and debris that is readily accessible to street sweeping equipment.

In summary, the evaluation of the dry-period conditions are important in determining the applicability of the solids models. Reasonable results cannot be expected in regions where the dustfall is considerably different than in the Austin area or where other extreme ADP conditions exist, such as bridge sanding, the tracking of mud by construction vehicles, etc. Differences in rainfall patterns that might cause an unusual difference in the preceding storm event intensity should also be considered; however, these effects are much more subtle and not expected to have a major impact on the applicability of the model. Efforts to reduce the loading of solids in storm water runoff should be focused on (1) the removal of solids from the highway during the dry period or (2) the elimination of dry period conditions that cause dirt and debris to be deposited on the highway surface.

6.4.2 Oxygen Demand / Organics

The storm water loading patterns of the group of constituents consisting of BOD_5, COD, total carbon, dissolved total carbon, and oil and grease, are dominated by traffic. Traffic volume during both wet and dry periods influences the loading of BOD_5, total carbon, and dissolved total carbon. Traffic during the dry period alone is important in the COD model, whereas traffic during the wet period alone in important to the oil and grease model. The signs of all traffic variable coefficients in this group are positive, which is consistent with the theory that traffic is a contributor of constituents to runoff.

Traffic variations will control model applicability for this group. The model will yield the best results when used on a highway with traffic patterns similar to those at the West 35th Street site (i.e., three-lane traffic counts near 50,000 vehicles per day). The model is expected to over-predict in situations where the traffic count is significantly less, and under-predict in situations where the traffic count is significantly more. Furthermore, the models for this group are not expected to provide reasonable results for highways with extremely low vehicle counts (i.e., less than 2,500 vehicle per day).

The model formulation suggests that the storm water loading of these constituents will increase as the average daily traffic use of the highway increases, which is an expected result of local population growth. Since traffic is the principal source of these constituents, source reduction (i.e., a reduction of the traffic) is not considered a viable alternative. Mitigation procedures should therefore focus on the collection and treatment of the highway runoff.

6.4.3 Nutrients

The storm water loadings of nitrate and total phosphorus are dependent on the average traffic count during the dry period. However, the antecedent traffic count, which is a measure of the duration of the antecedent dry period, is only a marginally better predictor for this group than the duration of the antecedent dry period measured in hours. Therefore, the overall conditions during the dry period may actually be the controlling variable for this group.

Rainfall, however, is the most distinguishable source of nutrients in the storm water runoff. The analysis of rainfall samples determined that there are high

concentrations (relative to the storm water runoff concentrations) of nitrate and total phosphorus in the Austin area rainfall. The median rainfall concentration for nitrate was as high as the contribution from the highway (i.e., rainfall samples contained a median concentration of nitrate of 0.47 mg/L, whereas the median EMC of nitrate in the storm water runoff was 1.00 mg/L). The median rainfall concentration of total phosphorus was approximately 25% of the total median concentration observed in the highway runoff. Nutrient levels in the rainfall will depend on atmospheric conditions both before and during the rainfall event.

Mitigation procedures should be similar to those of the organics group since source control is not a viable alternative. Similarly, the model is expected to give reasonable results only in regions where the nutrient content of the rainfall is similar to the Austin area.

6.4.4 Metals

The models for copper and lead are similar to the models formulated for the organics group in that they are highly influenced by the volume of traffic during the storm. Efforts to manage copper and lead loadings should therefore be directed toward storm water controls that collect and treat the storm water. Model applicability will be similar to that of the organics group.

The iron model is similar to TSS in that the controlling variables are conditions during the dry period. Iron loading is not influenced significantly by either wet-weather or dry-weather traffic volume. The model formulation suggests that iron should be managed similar to the solids group of constituents. Unfortunately, no significant difference was detected between the average load of iron observed during the street sweeping period compared to the average load during the no-sweeping period. Model applicability, however, should follow criteria similar to those for the solids group.

The model for zinc is influenced by the traffic count during the dry period and the runoff characteristics of the preceding storm. The model suggests that dry-period traffic is a source since traffic volume during the antecedent dry period was found to be a better predictor than the duration of the antecedent dry period measured in hours. This finding is consistent with past observations that tire wear is a significant contributor of zinc in

highway runoff (Gupta, et al., 1981). Mitigation of the storm water loading of zinc is therefore limited to the control options available to copper, lead, and the organics group.

6.5 Summary

The model is applicable only to high-speed highway pavements. In general, the model will be most accurate for highway segments that are similar to the West 35th Street sampling site. The principal similarities include (1) a curbed highway segment that drains to a single outlet, (2) three active lanes of traffic, (3) average daily traffic counts greater than 50,000 vehicles/day, (4) paved shoulder widths less than 10 feet wide, (5) a relatively long watershed (i.e., greater than 700 feet) and (6) surrounding land use that is light commercial or residential. Model inaccuracies can be expected if there are extreme deviations in pavement use, average daily traffic counts, or dry period conditions. Specifically, model results can be expected to vary under the following conditions:

- The model will over-predict for watersheds where the paved shoulders (or other non-traffic-baring pavement areas) account for more than approximately 35% of the watershed.
- The model is applicable to highway segments with any number of active traffic lanes; the model will not be accurate where average daily traffic counts are extremely low (i.e., less than approximately 2500 vehicles/day)
- The model will under-predict where dry-period conditions are extreme, such as heavy mud tracking by construction vehicles, unusually heavy dustfalls (either natural or the result of local industry), or extreme highway maintenance activities such as bridge sanding.

GLOSSARY

$\bar{y}$	Arithemetic mean of the transformed data set
$\bar{x}$	Arithmetic mean of the sample data
η	Coefficient of variation
S_y	Standard deviation of the log transformed data
μ_y	True mean of the transformed random variable y=ln(x)
μ	True population mean
σ	True population standard deviation
σ^2	True population variance
σ_y^2	True variance of the transformed random variable y=ln(x)
$\hat{M}$	Unbiased estimator of the true lognormal population median
S_y^2	Variance of the log transformed data
S^2	Variance of the sample data
$\hat{\mu}$	Minimum variance unbiased (MVU) estimator of a lognormal population mean
σ_y	True standard deviation of the transformed random variable y=ln(x)
ADP	Antecedent Dry Period
ADT	Average Daily Traffic
C	Concentration (mg/L)
COV	Coefficient of Variation
CRWR	Center for Research in Water Resources
EMC	Event Mean Concentration (mg/L)
HMT	Hazardous Material Trap
K	Kurtosis
L	Length (meters, kilometers, etc.)
L^2	Area (square meters, etc.)

L^3	Volume (cubic meters, liters, etc.)
LOD	Limit of Detection
M	Mass (grams, milligrams, etc.)
m	Rank of an ordered set of data
MIT	minimum inter-event time
n	Sample size
ND	Non-Detectable
NURP	USEPA Nationwide Urban Runoff Program
Q	Flow (liters/sec, etc.)
S	Standard deviation of the sample data or Skewness
T	Time (seconds, minutes, hours, etc.)
TWC	Texas Water Commission (now integrated into the Texas Natural Resource Conservation Commission)
TxDOT	Texas Department of Transportation
USEPA	U. S. Environmental Protection Agency
VDS	Vehicles During the Storm
VIDS	Vehicle Intensity During the Storm (vehicles/hr)
W	Load (kg/d, kg/hr/m^2, kg/mm rainfall/km, etc.)
x	Sample measurement
y	Sample measurement, or ln(x)
Z	Standard Normal Deviate

BIBLIOGRAPHY

American Public Health Association, 1992, *Standard Methods for the Examination of Water and Wastewater*, A. E. Greenberg, L. S. Clesceri, A. D. Eaton, eds.

Anselmi, Lt. Col. M.S., 1987, "Multicollinearity: Guidelines on its Detection and Treatment," Air Force Center for Studies and Analysis.

Asplund, R.L., Ferguson, J.F., and Mar, B.W., 1980, *Characterization of Highway Runoff in Washington State*, Washington State Department of Transportation, Report No. WA-RD-39.6.

Asplund, R.L., Ferguson, J.F., and Mar, B.W., 1982, "Total Suspended Solids in Highway Runoff in Washington State," *Journal of Environmental Engineering Division of ASCE*, Vol. 108, pp. 391-404.

Austin Geological Society, 1987, *Hydrology of the Edwards Aquifer, Northern Balcones and Washita Prairie Segments, Guide Book 11*, Austin, TX.

Aye, R.C., 1979, *Criteria and Requirements for Statewide Highway Runoff Monitoring Sites*, Washington State Department of Transportation Report No. WA-RD-39.5.

Barnes, J.W., 1994, *Statistical Analysis for Engineers and Scientists, A Computer-Based Approach*, McGraw-Hill, Inc.

Barrett, M.E., Zuber, R.D., Collins, E.R., III, Malina, J.F., Jr., Charbeneau, R.J., and Ward, G.H., 1993, *A Review and Evaluation of Literature Pertaining to the Quantity and Control of Pollution from Highway Runoff and Construction*, Technical Report CRWR 239, Center for Research in Water Resources, The University of Texas at Austin, Austin TX.

Berthouex, P.M., and Brown, L.C., 1994, *Statistics for Environmental Engineers*, CRC Press, Inc.

Box, G.E.P., and Tiao, G.C., 1973, *Bayesian Inference in Statistical Analysis*, John Wiley and Sons, Inc.

Campbell, W.H., 1968, "Correlation of Sunspot Numbers with the Quantity of S. Chapman Publications," *Transactions, American Geophysical Union*, Vol. 49, No. 4, Dec. 1968, p 609 - 610.

Chang, G.C., Parrish, J.H., and Soeur, C., 1990, *The First Flush of Runoff and its Effects on Control Structure Design*, City of Austin Environmental and Conservation Services Department, Austin, TX.

Chow, V.T., Maidment, D.R., and Hays, L.W., 1988, *Applied Hydrology*, McGraw-Hill, New York, NY.

Chui, T.W.D., Mar, B.W., and Horner, R.R., 1981, *Highway Runoff in Washington State: Model Validation and Statistical Analysis*, Washington State Department of Transportation, Report No. WA-RD-39.12.

Chui, T.W.D., Mar, B.W., and Horner, R.R., 1982, "Pollutant Loading Model for Highway Runoff," *Journal of Environmental Engineering Division of ASCE*, Vol. 108, pp. 1193-1210.

Driscoll, E.D., Shelley, P.E., and Strecker, E.W., 1990, *Pollutant Loadings and Impacts from Highway Stormwater Runoff, Volume III: Analytical Investigation and Research Report*, FHWA-RD-88-008.

Edwards Aquifer Underground Water District, 1981, *Water, Water Conservation, and the Edwards Aquifer*.

Envirex, Inc., 1981a, *Constituents of Highway Runoff, Volume I: Characteristics of Runoff from Operating Highways, Research Report*, Federal Highway Administration, PB81-241929.

Envirex, Inc., 1981b, *Constituents of Highway Runoff, Volume VI: Executive Summary*, Federal Highway Administration, PB81-241945.

Federal Register, July 1, 1988, "Secondary Treatment Regulation," 40 CFR Part 133.

Gilbert, R.O., 1987, *Statistical Methods for Environmental Pollution Monitoring*, Van Nostrand Reinhold, New York, NY.

Guadalupe-Blanco River Authority, 1988, *The Edwards Aquifer - Underground River of Texas*.

Gupta, M. K., Agnew, R.W., and Kobriger, N.P., 1981, *Constituents of Highway Runoff, Vol. I, State-of-the-Art Report*, Federal Highway Administration, FHWA/RD-81/042.

Hamlin, H. and Bautista, J., 1965, "On-the-Spot Tests Check Gutter Capacity," *The American City*, April.

Harrison, R.M. and Wilson, S.J.W., 1985, "The Chemical Composition of Highway Drainage Waters II: Major Ions and Selected Trace Metals," *The Science of the Total Environment*, Vol 43, pp. 63-77.

Hewitt, C.H. and Rashed, M.B., 1992, "Removal Rates of Selected Pollutants in the Runoff Waters from a Major Rural Highway," *Water Research*, Vol. 26, No. 3, pp. 311-319.

Hines, W.H. and Montgomery, D.C., 1990, *Probability and Statistics in Engineering and Management Science*, 3rd ed., John Wiley & Sons, Inc.

Hirsch, R.M., Helsel, D.R., Cohn, T.A., and Gilroy, E.J., 1992, "Statistical Analysis of Hydrologic Data," *Handbook of Hydrology*, David Maidment, ed., McGraw-Hill, Inc.

Hoffman, E.J., Latimer, J.S., Hunt, C.D., Mills, G.L., and Quinn, J.G., 1985, "Stormwater Runoff from Highways," *Water, Air, and Soil Pollution*, Vol. 25, No. 4.

Horner, R.R., Burges, S.J., Ferguson, J.F., Mar, B.W., and Welch, E.B., 1979, *Highway Runoff Monitoring: The Initial Year*, WA-RD-39.3, Washington State Department of Transportation, Olympia, WA.

Horner, R.R., and Mar, B.W., 1983, "Guide for Water Quality Impact Assessment of Highway Operations and Maintenance," *Transportation Research Record*, 948, pp. 31-40.

Howell, R.B., 1978, *Water Pollution Aspects of Particles that Collect on Highway Surfaces*, California Department of Transportation, Sacramento, CA, FHWA-CA-78-22.

Huber, W.C., 1992, "Contaminant Transport in Surface Water," *Handbook of Hydrology*, David R. Maidment, ed., McGraw-Hill.

Huber, W.C., 1986, "Deterministic Modeling of Urban Runoff Quality," NATO ASI Series, Vol. G10, *Urban Runoff Quality*, eds. H. C. Torno, J. Marsalek, and M. Desbordes, Springer-Verlag, Berlin.

Hvitved-Jacobson, T., and Yousef, Y.A., 1991, "Highway Runoff Quality, Environmental Impacts and Control," *Highway Pollution*, R. S. Hamilton and R. M. Harrison, Eds., Elsevier, New York, NY.

Irish, Jr., L.B., 1992, "Water Quantity and Quality Impacts Assessment of Highway Construction in the Austin, Texas Area: Rainfall Simulator Design," A Departmental Report in Partial Fulfillment of the Requirements for a Masters of Science in Environmental Health Engineering, Department of Civil Engineering, The University of Texas at Austin, Austin, TX.

Irwin, G.A., and Losey, G.T., 1978, *Water-Quality Assessment of Runoff from a Rural Highway Bridge near Tallahassee, Florida*, U. S. Geological Survey, FL-ER-4-79.

James, W., and Boregowda, S., 1986, "Continuous Mass-Balance of Pollutant Build-Up Processes," NATO ASI Series, Vol. G10, *Urban Runoff Quality*, eds. H. C. Torno, J. Marsalek, and M. Desbordes, Springer-Verlag, Berlin.

Johnson, Jr., A.C., Johnson, M.B., and Buse, R.C., 1987, *Econometrics: Basic and Applied*, Macmillian, Inc.

Kent, E.J., Yu, S.L., and Wyant, D.C., 1982, "Drainage Control Through Vegetation and Soil Management," *Transportation Research Record*, 896, pp. 39-46.

Kerri, K.D., Racin, J.A., and Howell, R.B., 1985, "Forecasting Pollutant Loads from Highway Runoff," *Transportation Research Record*, 1017, pp. 39-46.

Koch, Jr., G.S., and Link, R.F., 1980, *Statistical Analyses of Geological Data*, vols. I, and II, Dover, New York, NY.

Larkin, T.J., and Bomar, G.W., 1983, *Climatic Atlas of Texas*, Texas Department of Water Resources, LP-192.

Laxen, D.P.H., and Harrison, R. M., 1977, "The Highway as a Source of Water Pollution: An Appraisal of the Heavy Metal Lead," *Water Research*, Vol. 11, pp. 1-11.

Lord, B.N., 1987, "Nonpoint Source Pollution from Highway Stormwater Runoff," *The Science of the Total Environment*, Vol. 59, pp. 437-446.

Makridakis, S., and Wheelwright, S.C., 1978, *Forecasting: Methods and Applications*, John Wiley & Sons, Inc.

Mar, B.W. et al., 1982, *Washington State Highway Runoff Water Quality Study 1977-1982*, WA-RD-39.16, Washington State Department of Transportation, Olympia, WA.

McKenzie, D. J., and Irwin, G.A., 1983, *Water Quality Assessment of Stormwater Runoff from a Heavily Used Urban Highway Bridge in Miami, Florida*, USGS Water Resources Investigations 83-4153 (FHWA/FL/BMR-84-270).

Metcalf & Eddy, Inc., 1991, *Wastewater Engineering: Treatment, Disposal, and Reuse*, 3rd. Ed., Rev. by George Tchobanoglous and Frank Burton, McGraw-Hill, New York, NY.

Moe, R.D., Bullin, J.A., and Polasek, J.C., 1978, *Characteristics of Highway Runoff in Texas*, FHWA-RD-78-197, Federal Highway Administration, Washington, D.C.

Moe, R.D., Bullin, J.A., and Lougheed, Jr., M.J., 1982, *Atmospheric Particulate Analysis and Impact of Highway Runoff on Water Quality in Texas*, FHWA/TX-82/30+191-1F, Texas State Department of Highways and Public Transportation, Austin, TX.

Montgomery, D.C., 1991, *Design and Analysis of Experiments*, 3rd. ed., John Wiley & Sons, Inc.

Pitt, R., 1979, *Demonstration of Nonpoint Pollution Abatement Through Improved Street Cleaning Practices*, U. S. Environmental Protection Agency, EPA-600/2-79-161.

Quantitative Micro Software, 1994, *Eviews User's Guide*, QMS, Irvine CA.

Reed, J.R., and Kibler, D.F., 1989, "Artificial Rainfall for Pavement Studies," *Proceedings of the International Conference on Channel Flow and Catchment Runoff; Centennial of Manning's Formula and Kuichling's Rational Formula*, University of Virginia.

Sartor, J.D., and Boyd, G.B., 1972, *Water Pollution Aspects of Street Surface Contaminants*, USEPA Report EPA-R2-72-081.

Shelley, P.E., and Gaboury, D.R., 1986, "Pollution from Highway Runoff - Preliminary Results," *Proceedings of Stormwater and Water Quality Model, Users Group Meetings, March 25-26, 1986*, Orlando, Florida, EPA/600/9-86/023.

Stotz, G., 1987, "Investigations of the Properties of the Surface Water Runoff from Federal Highways in the FRG," *The Science of the Total Environment*, Vol. 59, pp. 329-337.

Svensson, G., 1987, *Modeling of Solids and Heavy Metal Transport from Small Urban Watersheds*, Ph.D. thesis, Chalmers University of Technology, Department of Sanitary Engineering, Gothenburg, Sweden

Thomann, R.V., and Mueller, J.A., 1987, *Principles of Surface Water Quality Modeling and Control*, HarperCollins Publishers, Inc., New York, NY, 644 pp.

Tietenberg, T., 1992, *Environmental and Natural Resource Economics*, 3rd ed., HarperCollins Publishers, Inc., New York, NY.

Urbonus, B.R., and Roesner, L.A., 1992, "Hydrologic Design for Urban Drainage and Flood Control," *Handbook of Hydrology*, David R. Maidment, ed., McGraw-Hill, New York, NY.

U.S. Environmental Protection Agency, 1979, *Methods for Chemical Analysis of Water and Wastes*, Cincinnati, OH.

U.S. Environmental Protection Agency, 1981, *Process Design Manual for Land Treatment of Municipal Wastewater*, Cincinnati, OH.

U.S. Environmental Protection Agency, 1983, *Results of the Nationwide Urban Runoff Program, Volume I - Final Report*, Water Planning Division, WH-554, Washigton, D.C.

U.S. Public Health Service, 1963, *Public Health Service Drinking Water Standards - 1962*, Publication No. 956

Wagner, K.J., and Mitchell, D.F., 1987, *Size Fractionation of Pollutants as a Lake Management Tool*, Annual Meeting for North American Lake Management Society, Orlando, FL.

Wanielista, M.P., Yousef, Y.A., and Taylor, J.S., 1981, *Stormwater to Improve Lake Water Quality*, EPA R-80-55800.

Welborn, C.T., and Veenhuis, J.E., 1987, *Effects of Runoff Controls on the Quantity and Quality of Urban Runoff at Two Locations in Austin, Texas*, U.S. Geological Survey, Water-Resources Investigations Report 87-4004.

Wiland, B., and Malina, J.F., Jr., 1976, *Oil, Grease, and other Pollutants in Highway Runoff*, FHWA TX 77-16-1F, Center for Highway Research, The University of Texas at Austin, Austin, TX.

Yousef, Y.A., Wanielista, M.P., Harper, H.H., and Hvitved-Jacobson, T., 1986, *Effectiveness of Retention/Detention Ponds for Control of Contaminants in Highway Runoff*, Final Report submitted to FDOT, FL, ER-34-86.

APPENDICES

Appendix A
Laboratory Analysis

Water quality samples were analyzed at the laboratory operated by The Center for Research in Water Resources at The University of Texas at Austin. The methods used to determine pollutant concentrations are summarized in Table A-1 for each constituent.

Table A-1 Laboratory Methods

Constituent	Method Description	Method Number
Total Coliforms	Membrane Filter Technique: Delayed-Incubation Total Coliform Procedure	SM 9222(C)
Fecal Coliforms	Fecal Coliform Membrane Filter Procedure	SM 9222(D)
Fecal Streptococcus	Membrane Filter Technique	SM 9230(C)
Total Suspended Solids	TSS Dried at 103 - 105^{O}C	SM 2540(D)
Volatile Suspended Solids	Fixed and Volatile Solids Ignited at 500^{O}C	SM 2540(E)
Turbidity	Nephelometric Method	SM 2130(B)
5-Day Biochemical Oxygen Demand	5-Day BOD Test	SM 5210(B)
Chemical Oxygen Demand	Closed Reflux, Colorimetric Method	SM 5220(D)

Table A-1 (Continued) Laboratory Methods

Constituent	Method Description	Method Number
Total Organic Carbon	Combustion-Infrared Method	SM 5310(B)
Nitrogen (Nitrate)	Nitrate Electrode Method	SM 4500-NO_3^- (D)
Phosphate	Colorimetric, Ascorbic Acid, Two Reagents	EPA 365.3
Cadmium	Inductively Coupled Plasma Method	SM 3500-Cd (D)
Chromium	Inductively Coupled Plasma Method	SM 3500-Cr (D)
Copper	Inductively Coupled Plasma Method	SM 3500-Cu (D)
Iron	Inductively Coupled Plasma Method	SM 3500-Fe (D)
Mercury	Inductively Coupled Plasma Method	SM 3500-Hg (D)
Lead	Inductively Coupled Plasma Method	SM 3500-Pb (D)
Nickel	Inductively Coupled Plasma Method	SM 3500-Ni (D)
Zinc	Inductively Coupled Plasma Method	SM 3500-Zn (D)
Oil and Grease	Spectrophotometric, Infrared	EPA 413.2

Procedure numbers with "SM" prefix are from *Standard Methods for the Examination of Water and Wastewater*, (American Public Health Association, 1992).
Procedure numbers with "EPA" prefix are from *Methods for Chemical Analysis of Water and Wastes*, (USGS, 1979).

Appendix B
Precipitation Characteristics for Austin, Texas

Table B-1
Average Precipitation in the Austin, Texas Area Compared to Natural and Simulated Rainfall Observed During the Study Period

Month	Average Precipitation (1951-1980)[a] mm	Precipitation (1993-1994)[b] mm	Simulated Rainfall (1993-1994) mm
July	44	Trace	122
August	57	19	61
September	102	9	61
October	83	61	30
November	57	25	61
December	51	29	91
January	44	36	91
February	64	54	122
March	44	43	91
April	89	43	91
May	108	93	91
June	76	19	61
Total	819	431	973

a) Larkin and Bomar, 1983
b) National Weather Service, Austin Texas

Table B-2

Rainfall Frequency for Austin, Texas (rainfall given in mm)

Duration (hrs) -------- Freq. (yrs)	1/12 -----	1/4 -----	1/2 -----	1 -----	2 ------	3 ------	6 ------	12 ------	24 ------
1			33	41	48	53	61	71	81
2	13	28	41	51	58	66	79	89	104
5			51	64	79	86	104	122	140
10			58	74	91	102	122	145	170
25			69	86	109	119	147	173	201
50			79	99	122	135	163	196	226
100	22	48	86	107	135	152	183	221	254

Appendix C
Water Droplet Trajectory

The amount of energy required to throw a water droplet a given distance is illustrated by comparing the throw distance of a droplet to that of a stream with the same nozzle exit velocity. It is a common simplification to model water streams as a continuous, frictionless stream traveling through the air. The trajectory of the water stream is that of a parabola if air drag is neglected. Figure C.1 depicts the trajectory of a water stream leaving a 4.8-mm-diameter straight nozzle under 276 millipascal pressure. The flow rate is 0.4 L/sec and the exit velocity (V_e) is 23 m/sec. The nozzle is mounted at an elevation of 4.3 m and has a 30^0 departure angle. The height (z) of travel of the stream can be calculated as:

$$z = \frac{V_z^2}{2g} = \frac{[(\sin 30^o)(23m/\sec)]^2}{2(9.8m/\sec^2)} = 6.7m \qquad \text{(Eq. C.1)}$$

The time (T) to reach this height is found using the equation:

$$z = 6.7m = V_z T + 0.5gT^2 = \sin 30^0 (23m/\sec)T + 0.5(9.8m/\sec^2)T^2 \qquad \text{(Eq. C.2)}$$

When solving Equation C.2 using the quadratic equation, T is found to be 0.48 seconds. Using this value of T, the horizontal distance traveled is determined as:

$$x = V_x T = \cos 30^0 (23m/\sec)(0.48\sec) = 9.6m \qquad \text{(Eq. C.3)}$$

The ultimate distance of travel of the water stream can now be found using an approach similar to the above or by defining the equation for the parabola as shown in Figure C.1.

The flight of water droplets is extremely difficult to model. Evaporation, drag forces, and lift forces all affect the trajectory of the droplet. The following analysis makes use of Newton's second law to illustrate the effect of air drag on the travel of a water droplet from an elevated spray stand. The same initial velocity (23 m/sec) is used as in the water stream example. However, to simplify the calculation, the assumption is made that the trajectory is relatively flat and the water droplet leaves the spray head at a zero degree angle (i.e., flat) with respect to the x-axis. The coefficient of drag (C_d) is considered to be 0.03, and if there is little spin of the drop, the coefficient of lift can be

considered zero. Assuming no loss of mass (i.e., evaporation) from the droplet during flight, the following equation can be developed for time of flight (sec) to a particular distance:

$$t = \frac{1}{\beta}[\exp(\frac{\rho C_D S x}{2m} - 1)] \qquad \text{(Eq. C.5)}$$

where:

β = $\frac{\rho C_D S V_x}{2m}$ (sec)

V_x = Velocity (m/sec)

ρ = density of air (mg/l)

m = mass of droplet (g)

S = effective area of droplet (m^2)

x = distance along x axis of flight (m)

The *y*-coordinate, which represents the drop in flight of the droplet, is determined by:

$$y = \frac{-gt^2}{2} = \frac{-(23m/\sec^2)t^2}{2} = -11.5t^2 \text{ (m)} \qquad \text{(Eq. C.7)}$$

Figure C.2 shows the flight paths of 4 different droplet sizes from a 4.3-meter elevated spray head as calculated from the above equations. Comparing Figures C.1 and C.2 illustrates the additional energy required to produce rainfall versus a water stream. The throw distances shown in Figure C.2 are very close to those observed during experiments with the rainfall simulator.

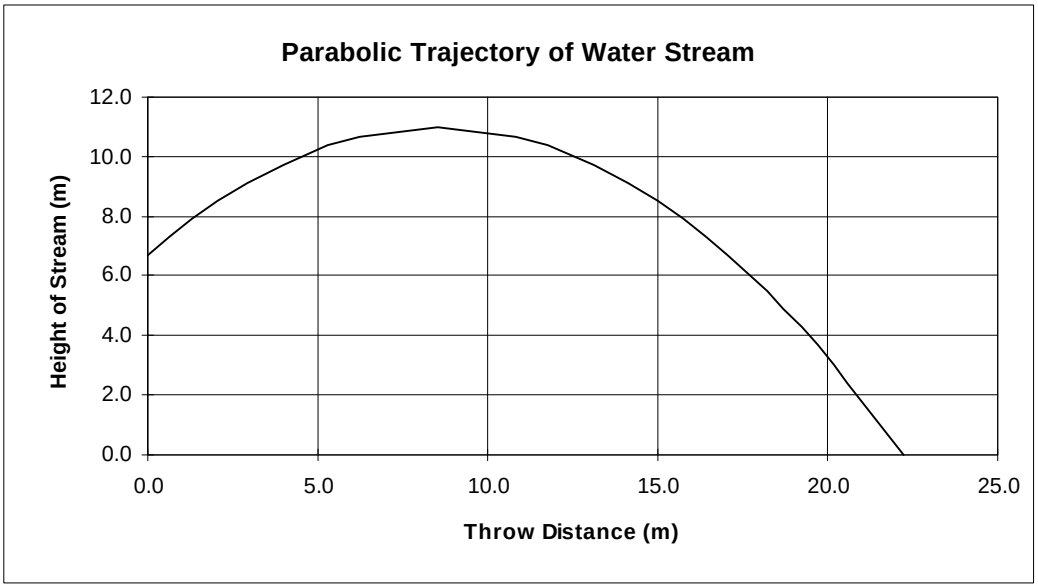

Figure C.1 Trajectory of Water Stream from a nozzle elevation of 4.3m (nozzle angle = 30^0)

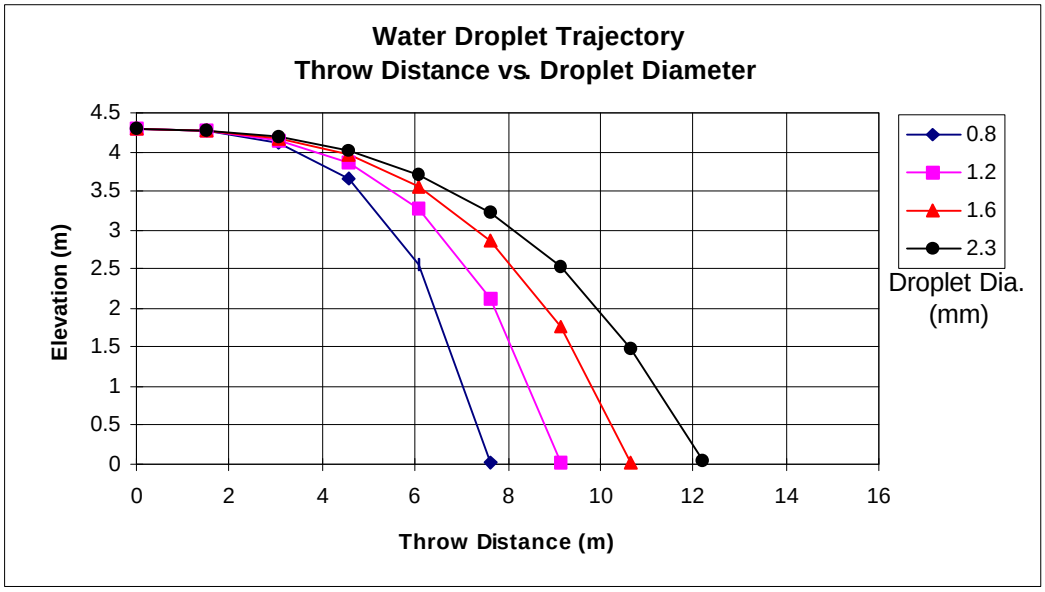

Figure C.2 Water Droplet Trajectory (nozzle angle = 0^0)

Appendix D
Probability Plots

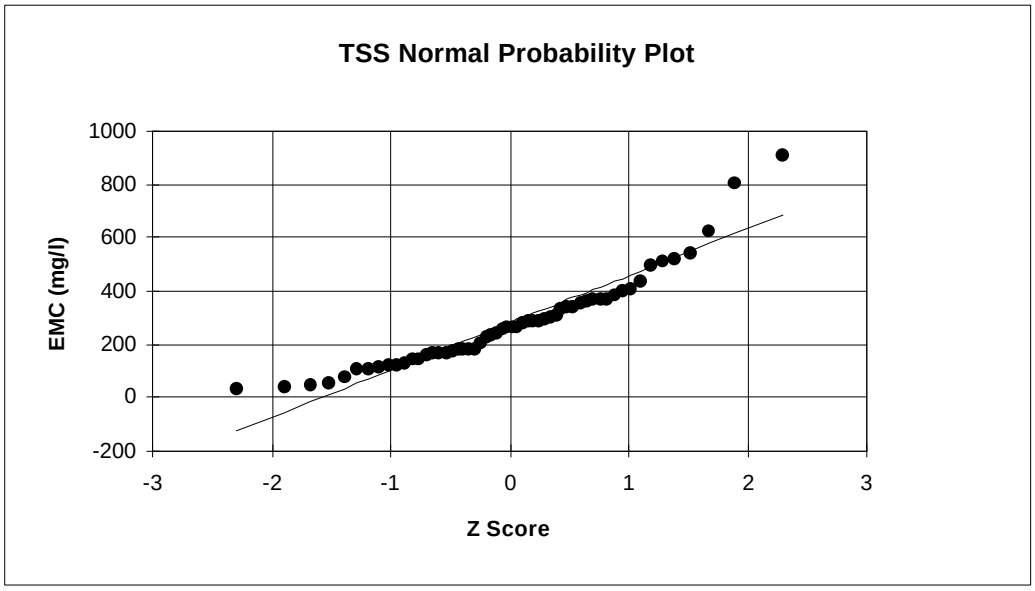

(a)

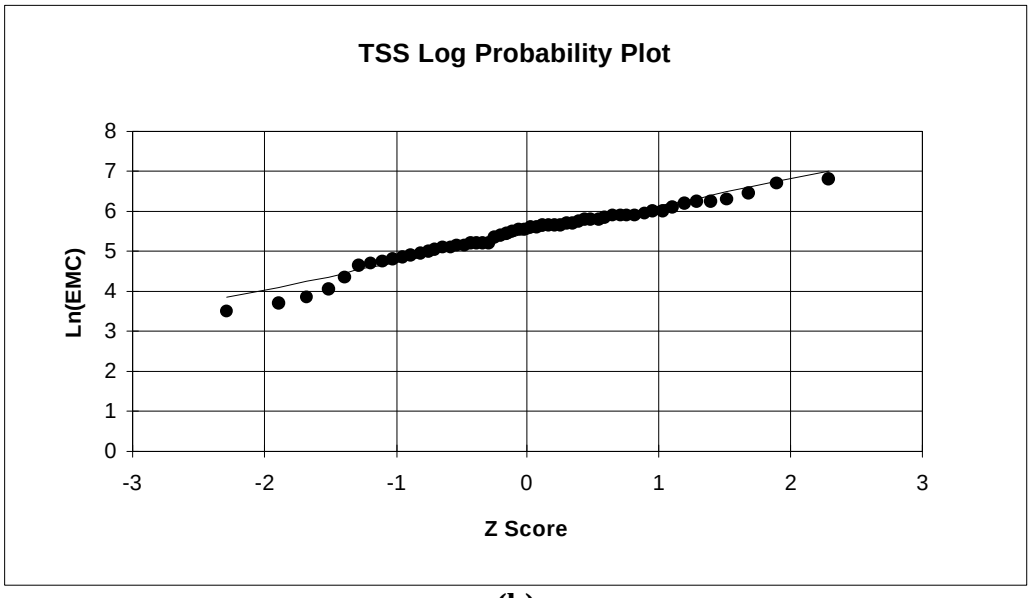

(b)

Figure D-1

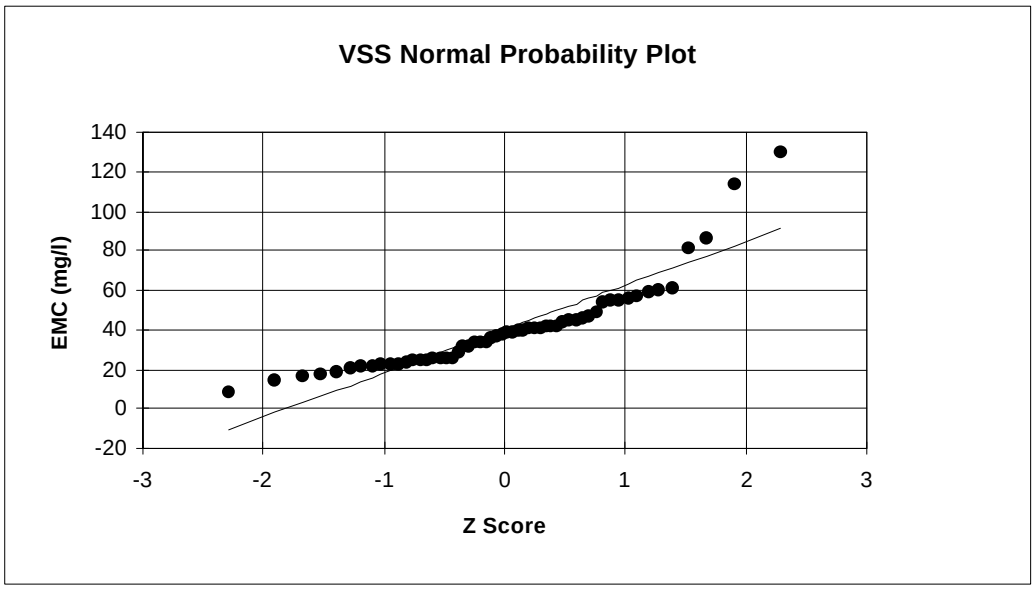
VSS Normal Probability Plot
EMC (mg/l)
140
120
100
80
60
40
20
0
-20
-3
-2
-1
0
1
2
3
Z Score

(a)

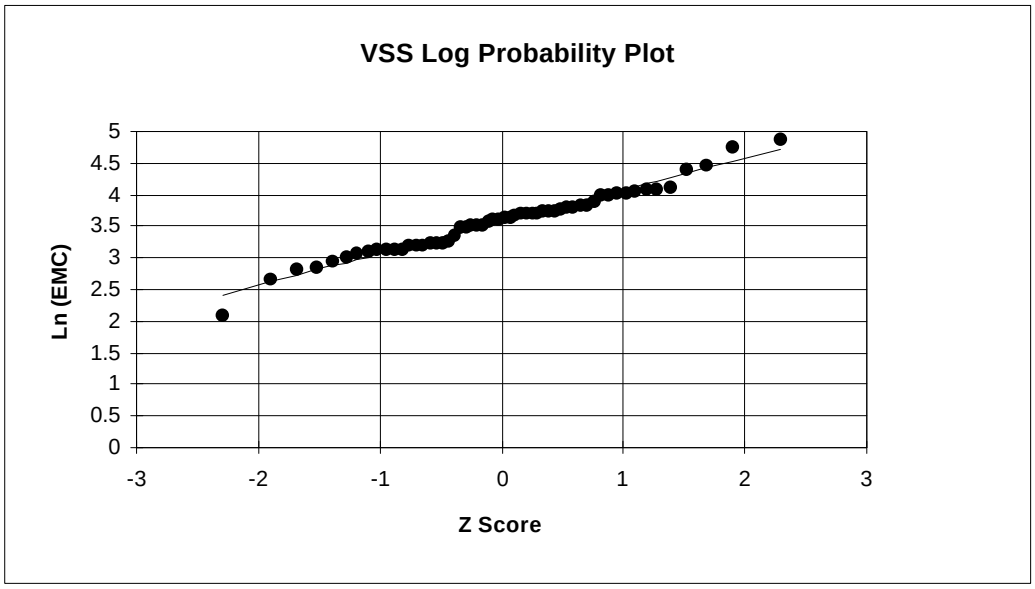
VSS Log Probability Plot
Ln (EMC)
5
4.5
4
3.5
3
2.5
2
1.5
1
0.5
0
-3
-2
-1
0
1
2
3
Z Score

(b)

Figure D-2

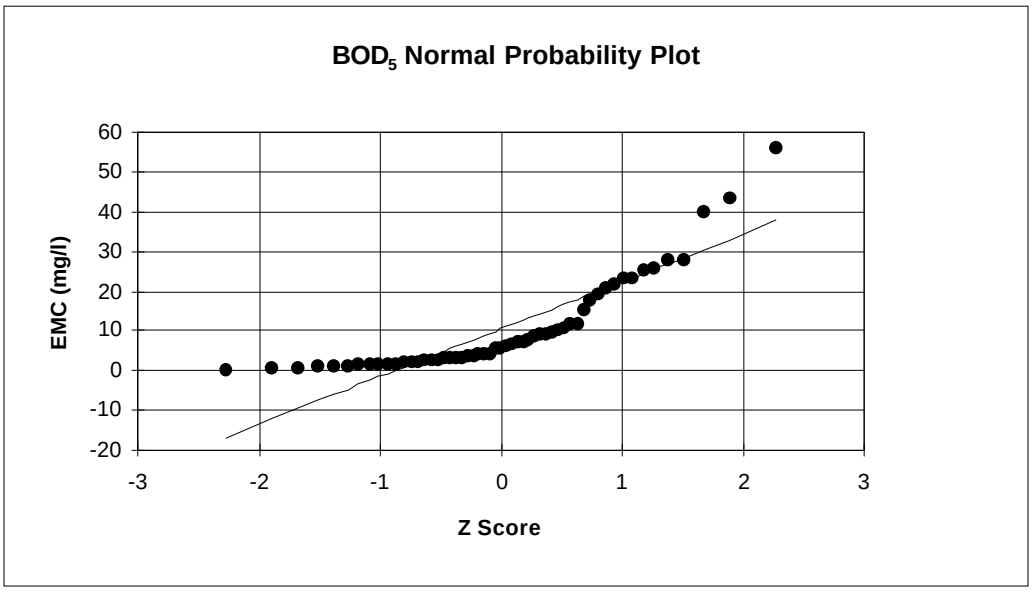
BOD5 Normal Probability Plot
EMC (mg/l)
60
50
40
30
20
10
0
-10
-20
-3
-2
-1
0
1
2
3
Z Score

(a)

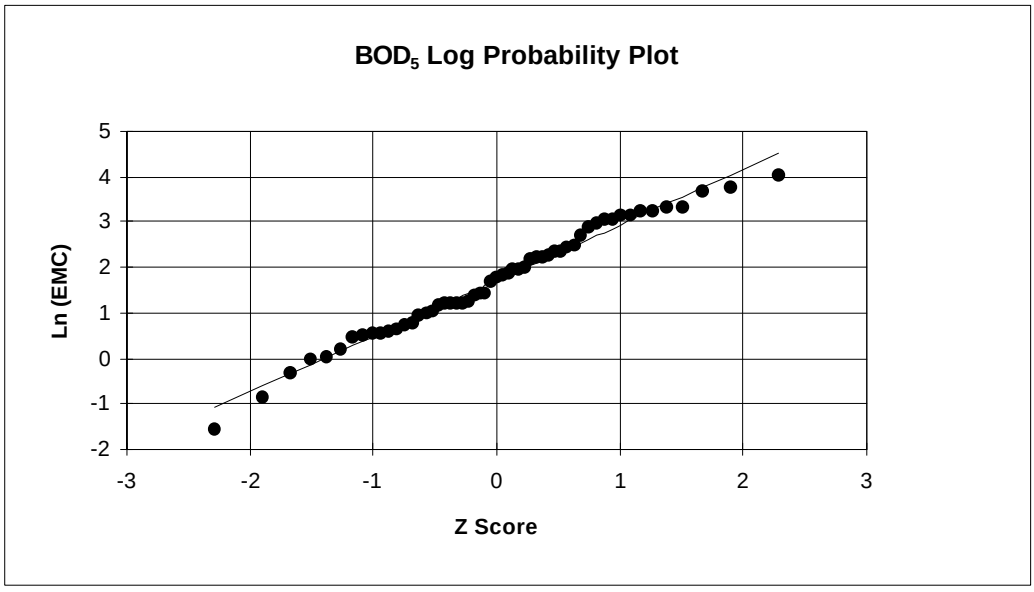
BOD5 Log Probability Plot
Ln (EMC)
5
4
3
2
1
0
-1
-2
-3
-2
-1
0
1
2
3
Z Score

(b)

Figure D-3

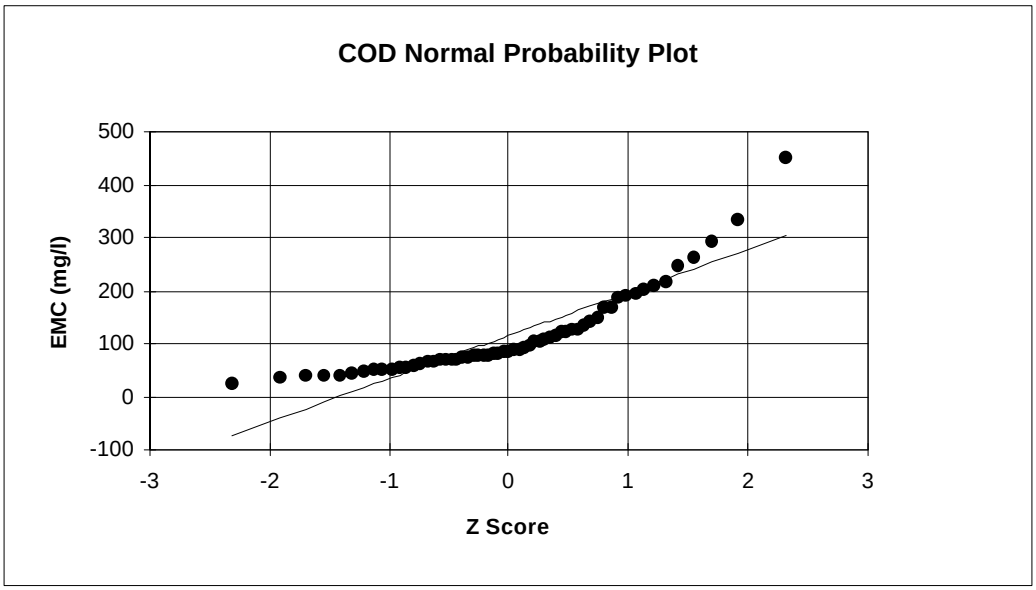
COD Normal Probability Plot
EMC (mg/l)
500
400
300
200
100
0
-100
-3
-2
-1
0
1
2
3
Z Score

(a)

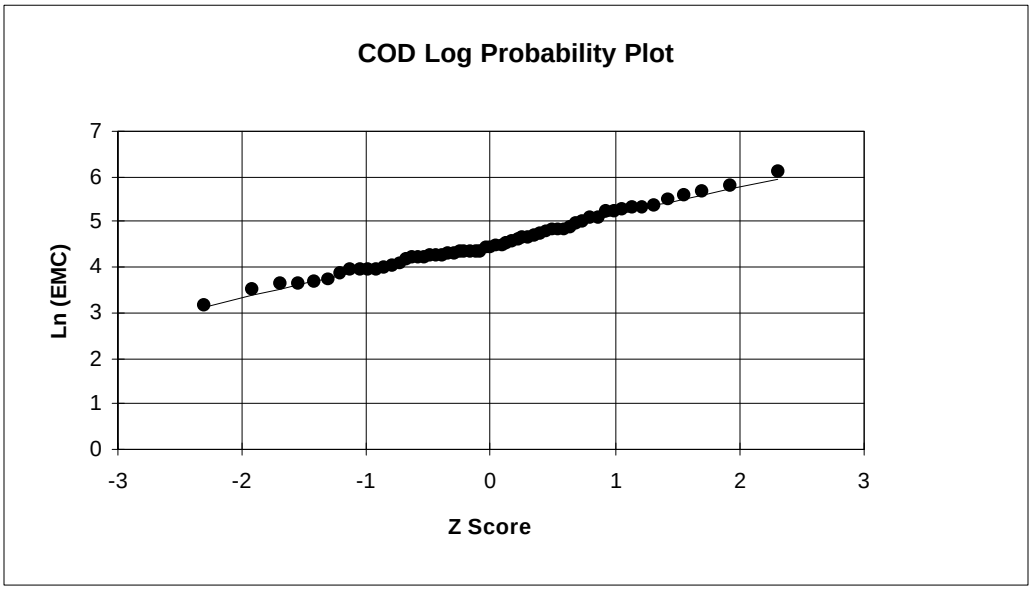
COD Log Probability Plot
Ln (EMC)
7
6
5
4
3
2
1
0
-3
-2
-1
0
1
2
3
Z Score

(b)

Figure D-4

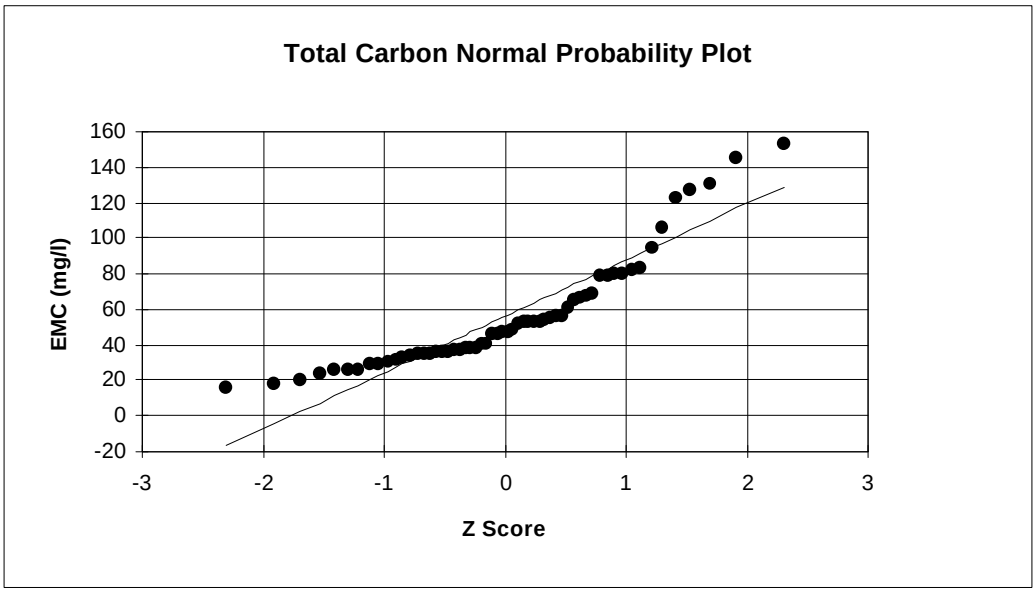
Total Carbon Normal Probability Plot
EMC (mg/l)
160
140
120
100
80
60
40
20
0
-20
-3
-2
-1
0
1
2
3
Z Score

(a)

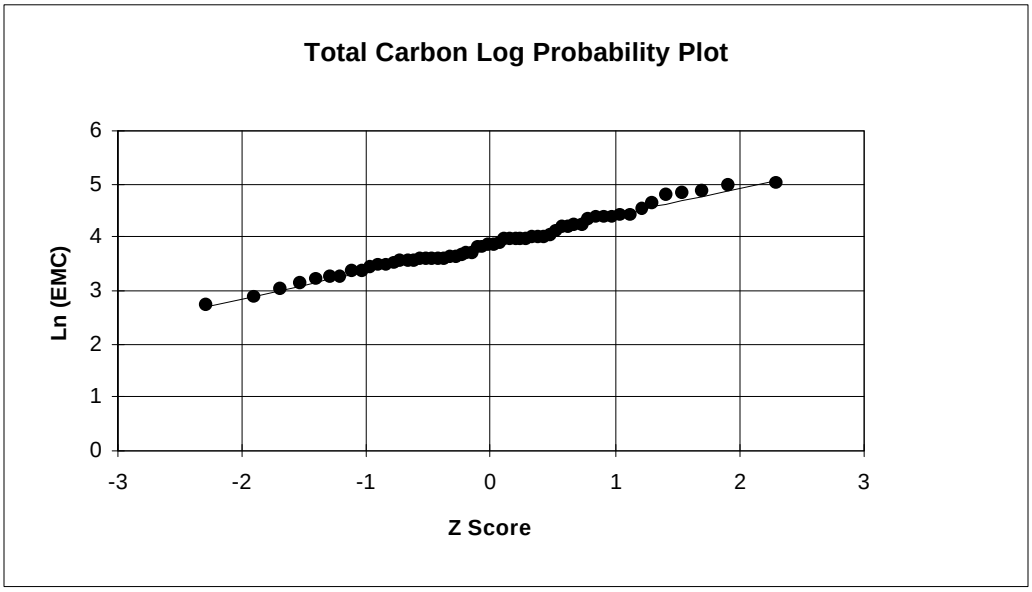
Total Carbon Log Probability Plot
Ln (EMC)
6
5
4
3
2
1
0
-3
-2
-1
0
1
2
3
Z Score

(b)

Figure D-5

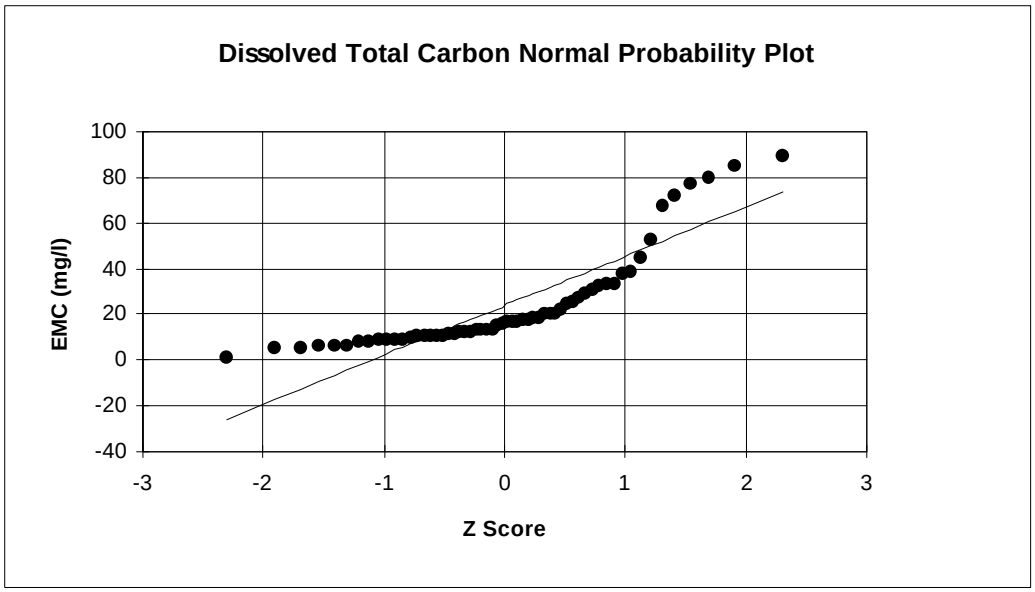
Dissolved Total Carbon Normal Probability Plot
EMC (mg/l)
100
80
60
40
20
0
-20
-40
-3
-2
-1
0
1
2
3
Z Score

(a)

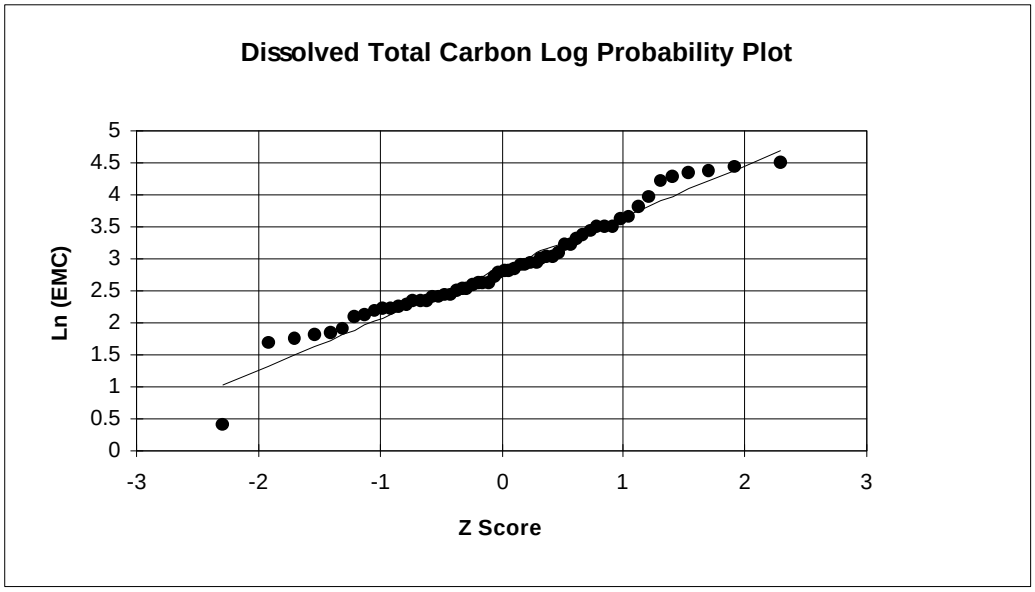
Dissolved Total Carbon Log Probability Plot
Ln (EMC)
5
4.5
4
3.5
3
2.5
2
1.5
1
0.5
0
-3
-2
-1
0
1
2
3
Z Score

(b)

Figure D-6

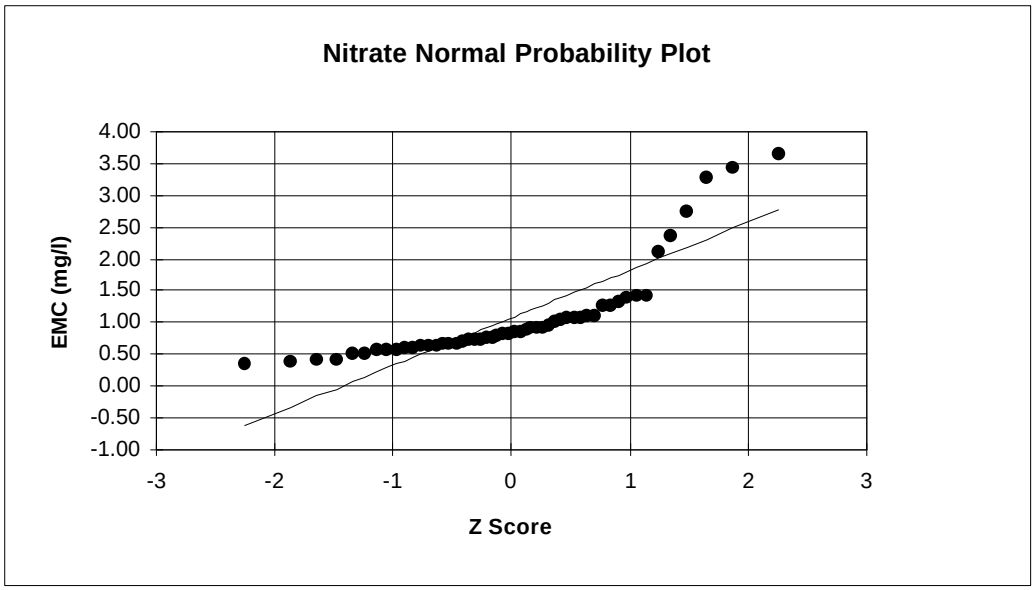
Nitrate Normal Probability Plot
EMC (mg/l)
4.00
3.50
3.00
2.50
2.00
1.50
1.00
0.50
0.00
-0.50
-1.00
-3
-2
-1
0
1
2
3
Z Score

(a)

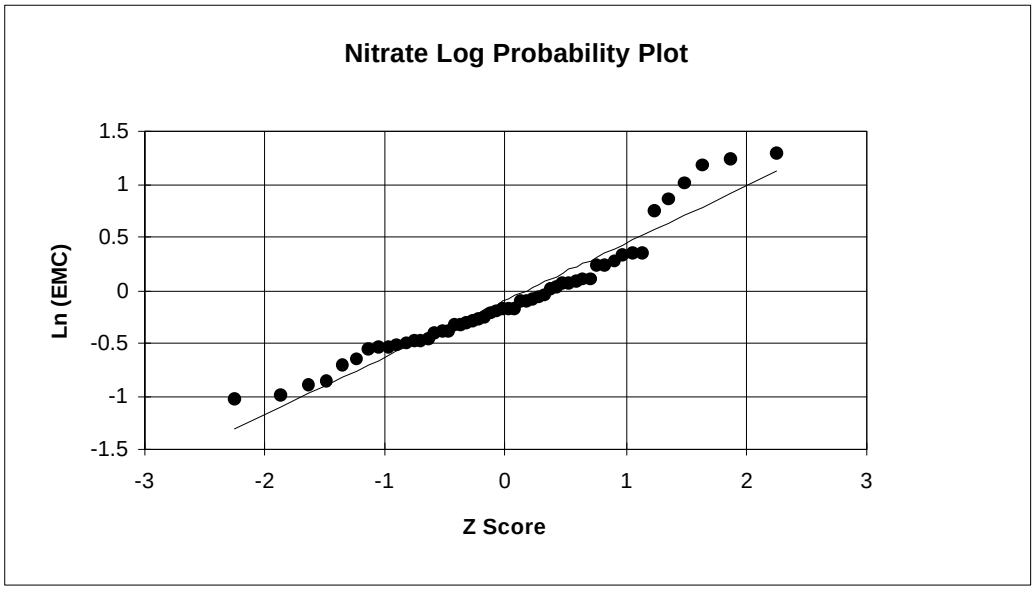
Nitrate Log Probability Plot
Ln (EMC)
1.5
1
0.5
0
-0.5
-1
-1.5
-3
-2
-1
0
1
2
3
Z Score

(b)

Figure D-7

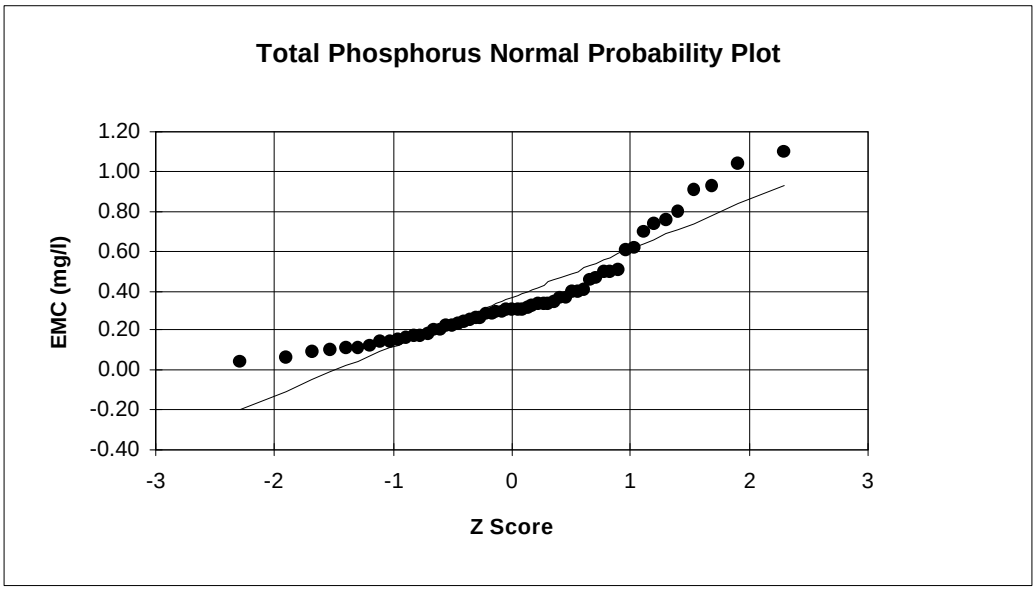
Total Phosphorus Normal Probability Plot
EMC (mg/l)
1.20
1.00
0.80
0.60
0.40
0.20
0.00
-0.20
-0.40
-3
-2
-1
0
1
2
3
Z Score

(a)

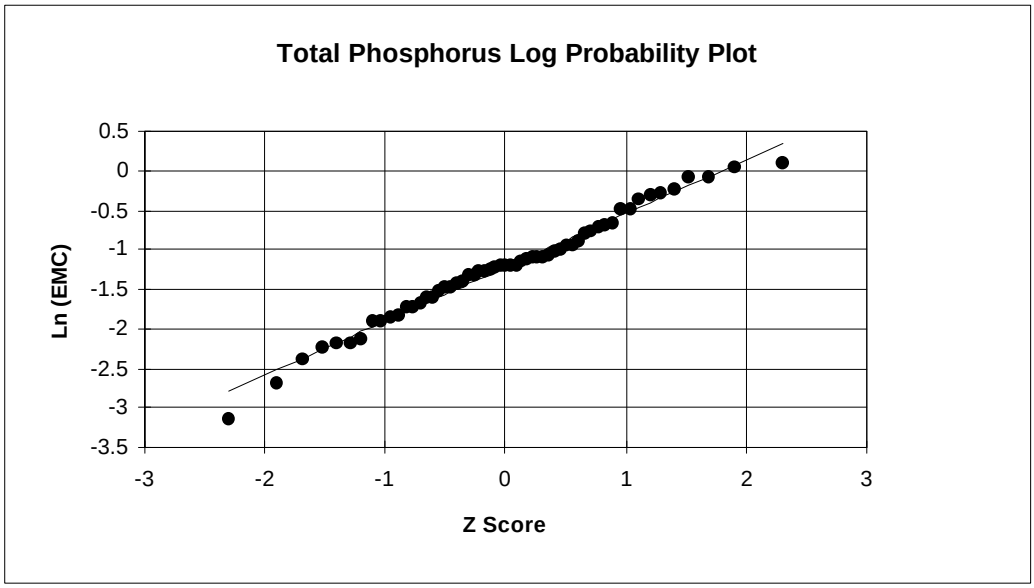
Total Phosphorus Log Probability Plot
Ln (EMC)
0.5
0
-0.5
-1
-1.5
-2
-2.5
-3
-3.5
-3
-2
-1
0
1
2
3
Z Score

(b)

Figure D-8

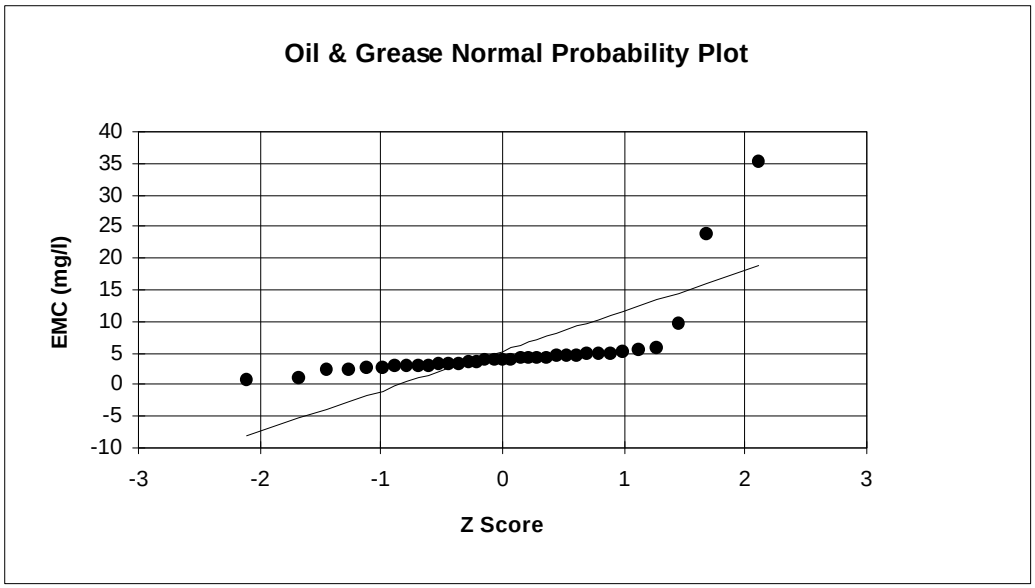
Oil & Grease Normal Probability Plot
EMC (mg/l)
40
35
30
25
20
15
10
5
0
-5
-10
-3
-2
-1
0
1
2
3
Z Score

(a)

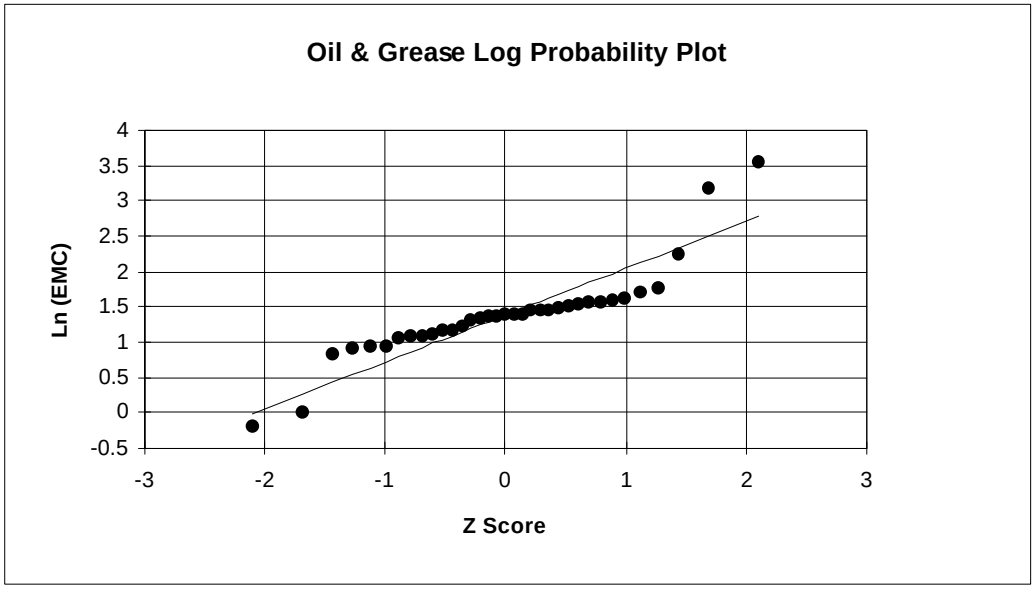
Oil & Grease Log Probability Plot
Ln (EMC)
4
3.5
3
2.5
2
1.5
1
0.5
0
-0.5
-3
-2
-1
0
1
2
3
Z Score

(b)

Figure D-9

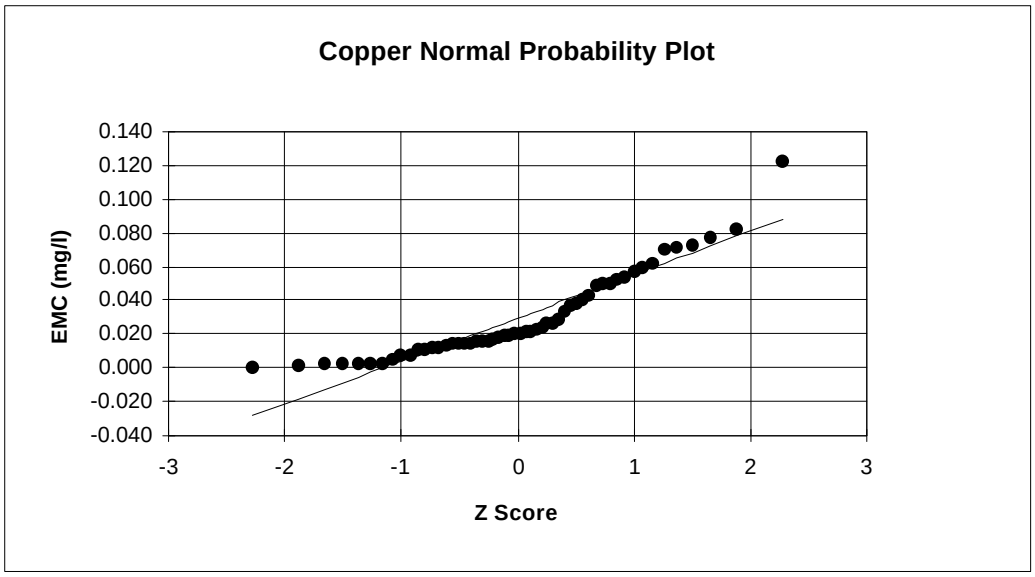

(a)

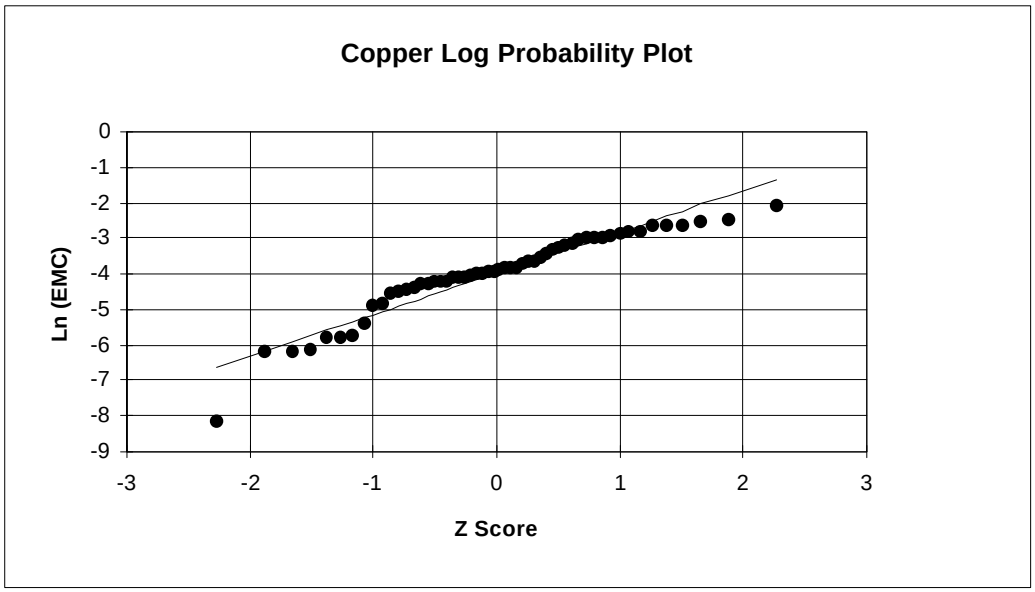

(b)

Figure D-10

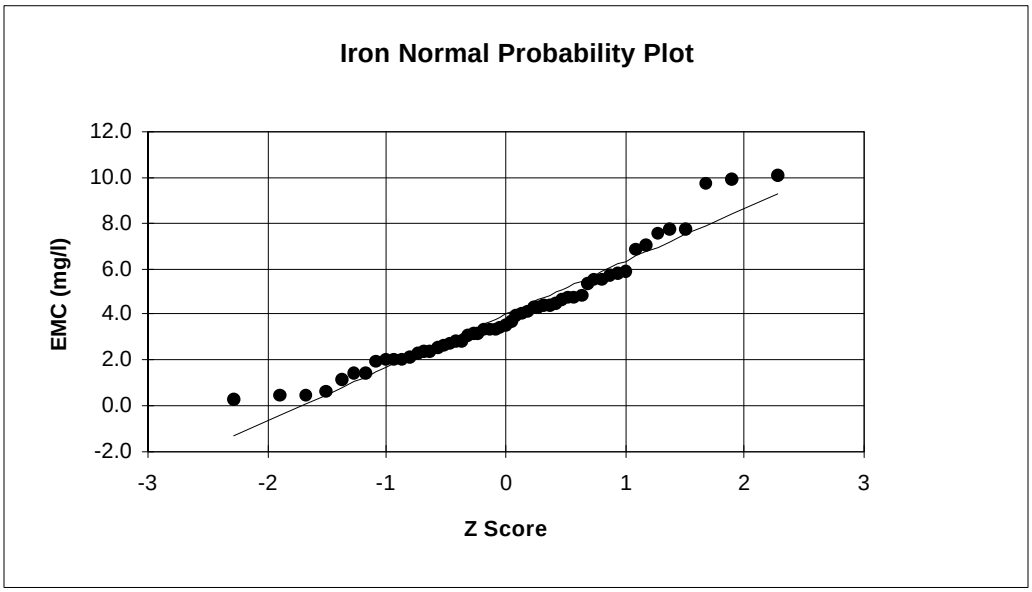

(a)

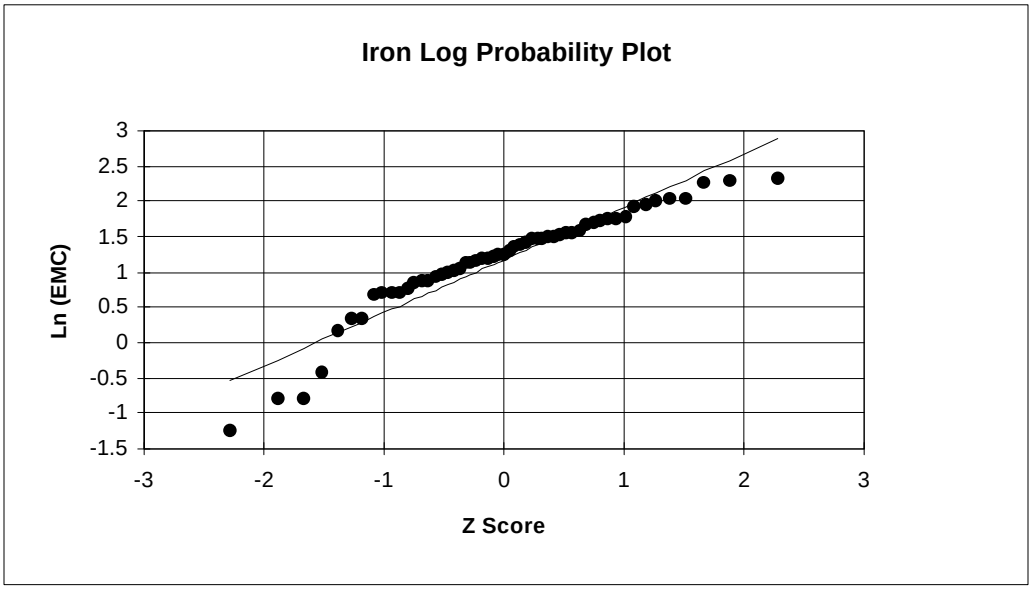

(b)

Figure D-11

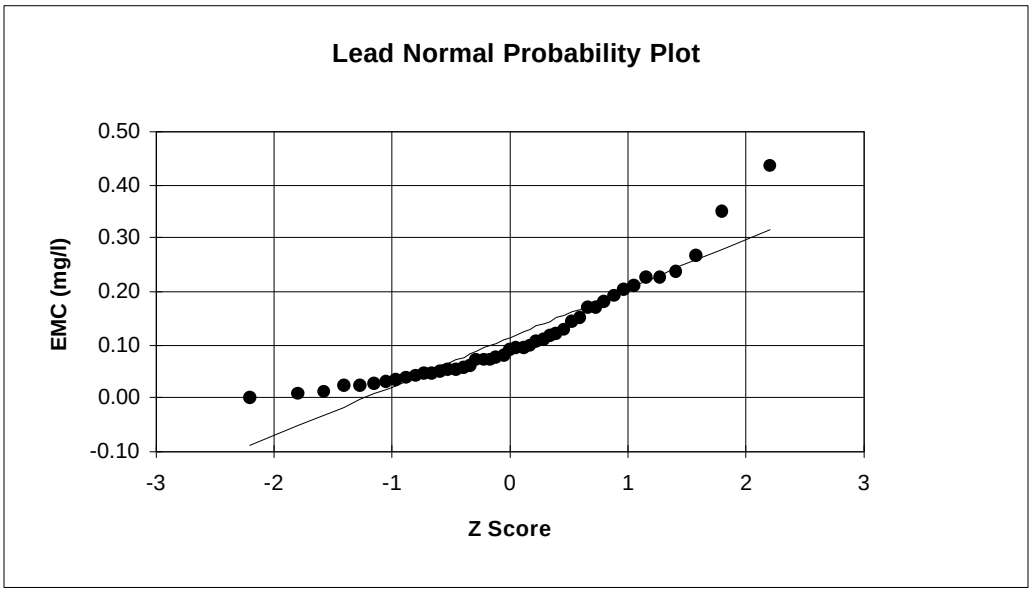

(a)

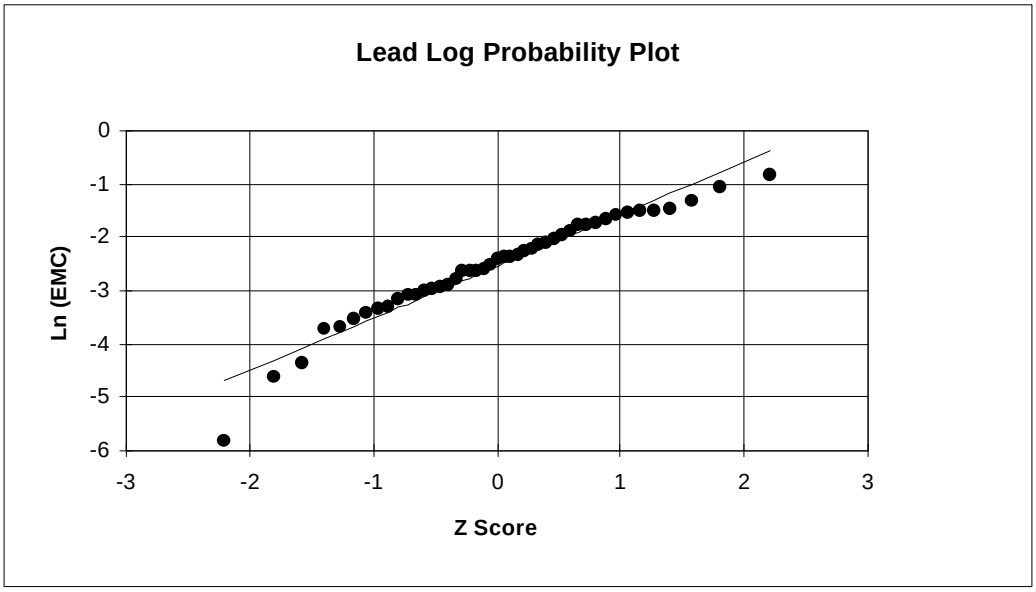

(b)

Figure D-12

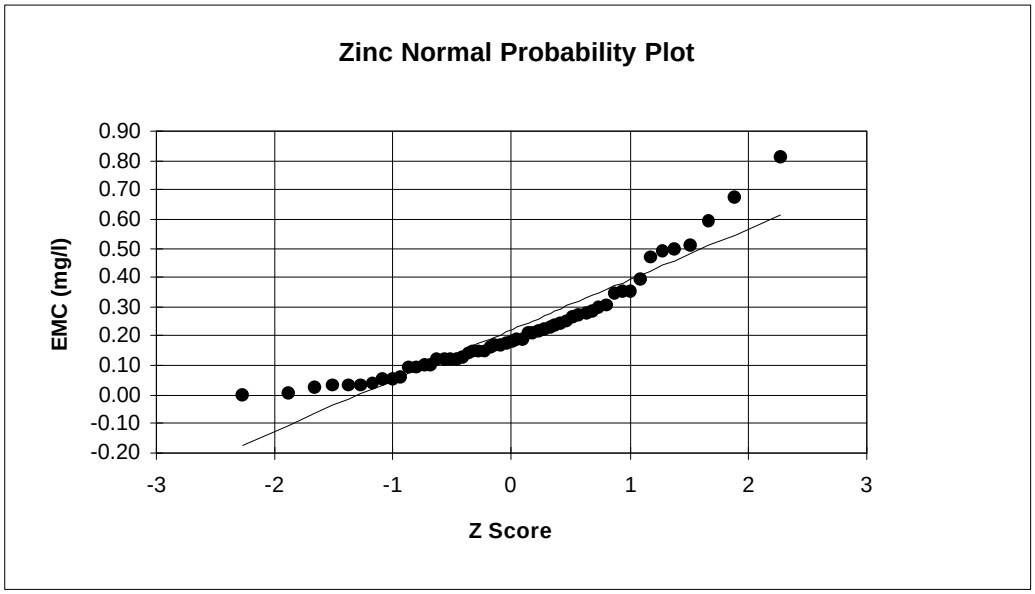

(a)

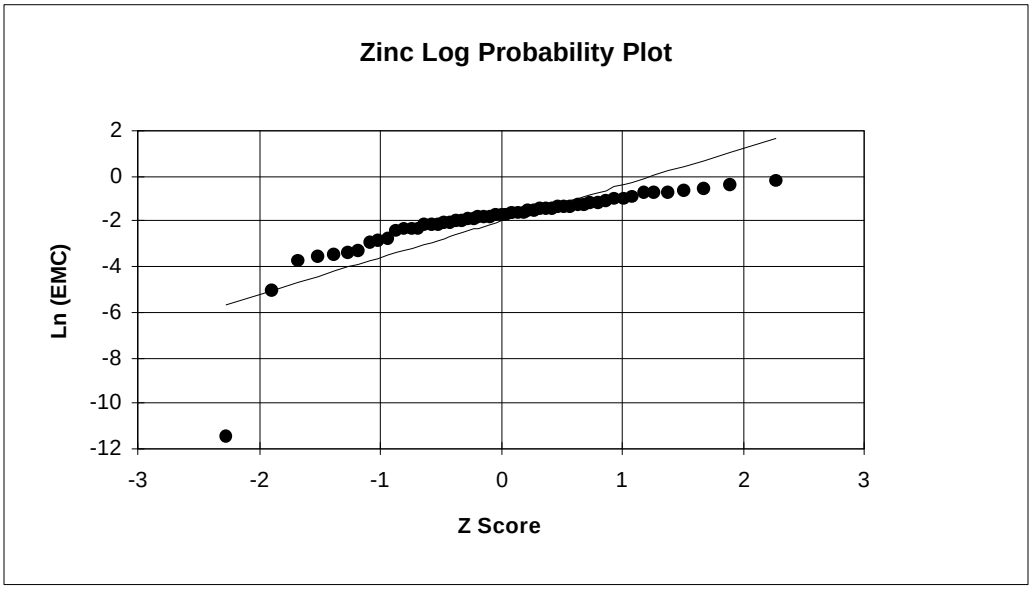

(b)

Figure D-13

Appendix E
Histograms of Constituent Event Mean Concentrations

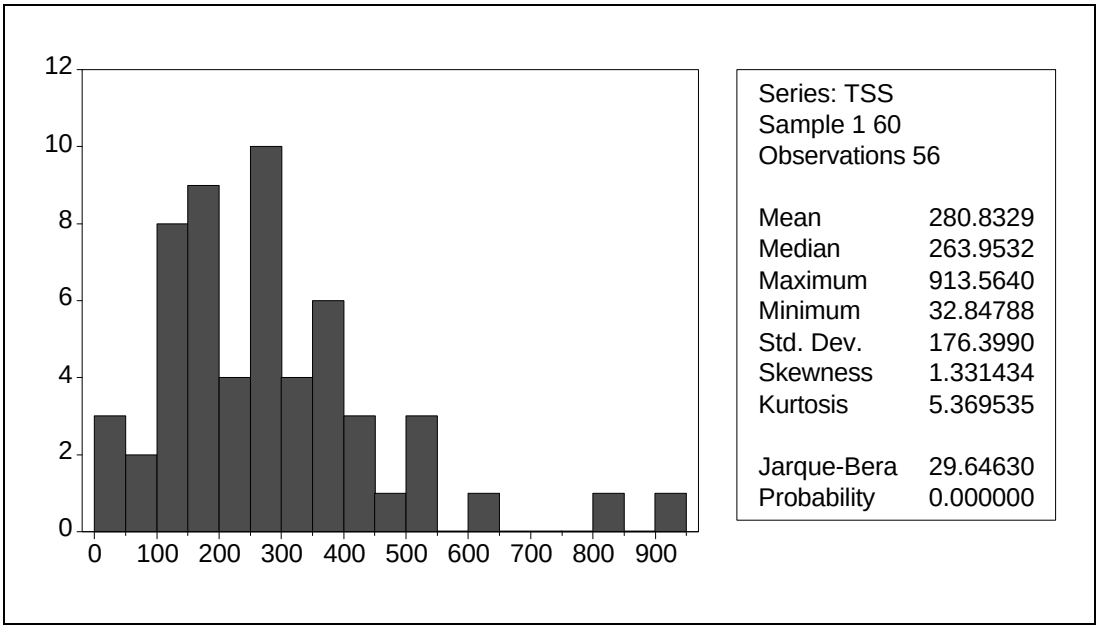

Figure E-1 Histogram of TSS Observations

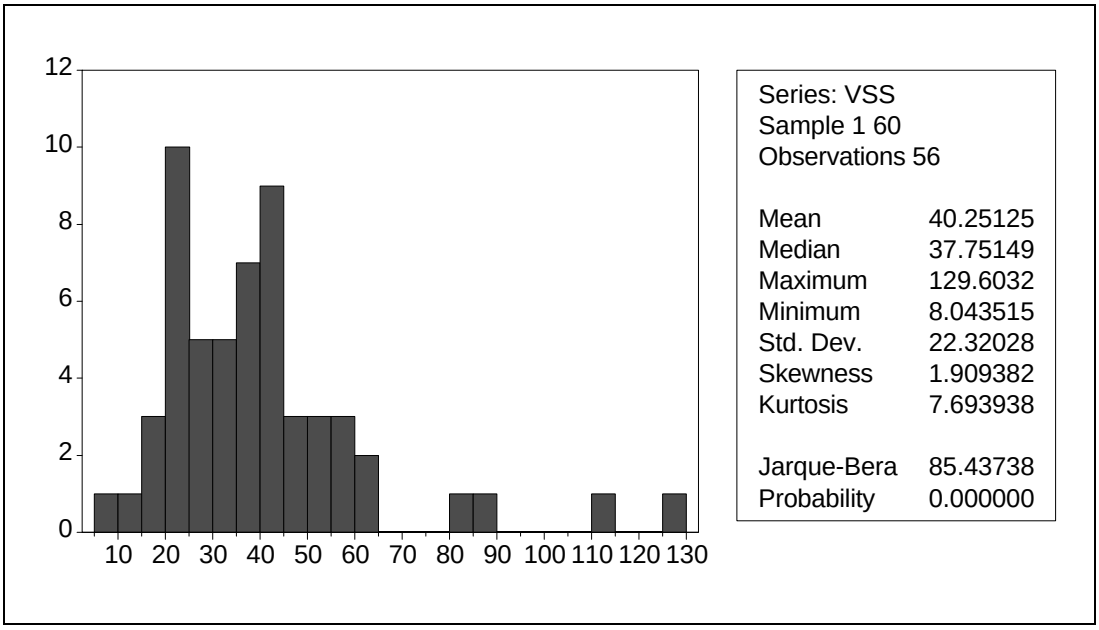

Figure E-2 Histogram of VSS Observations

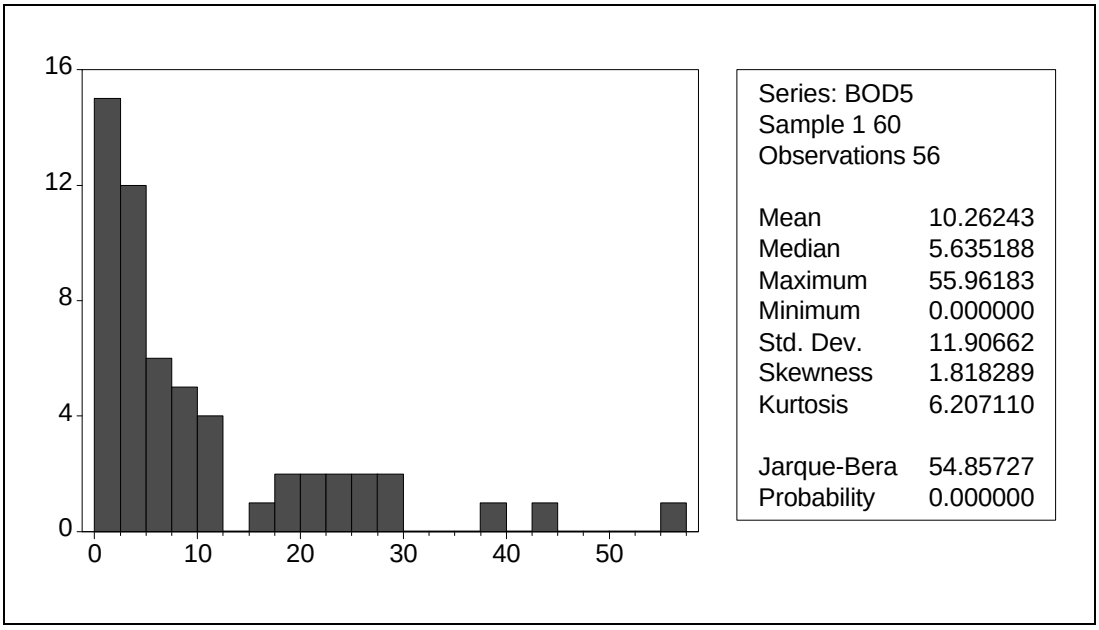

Figure E-3 Histogram of BOD_5 Observations

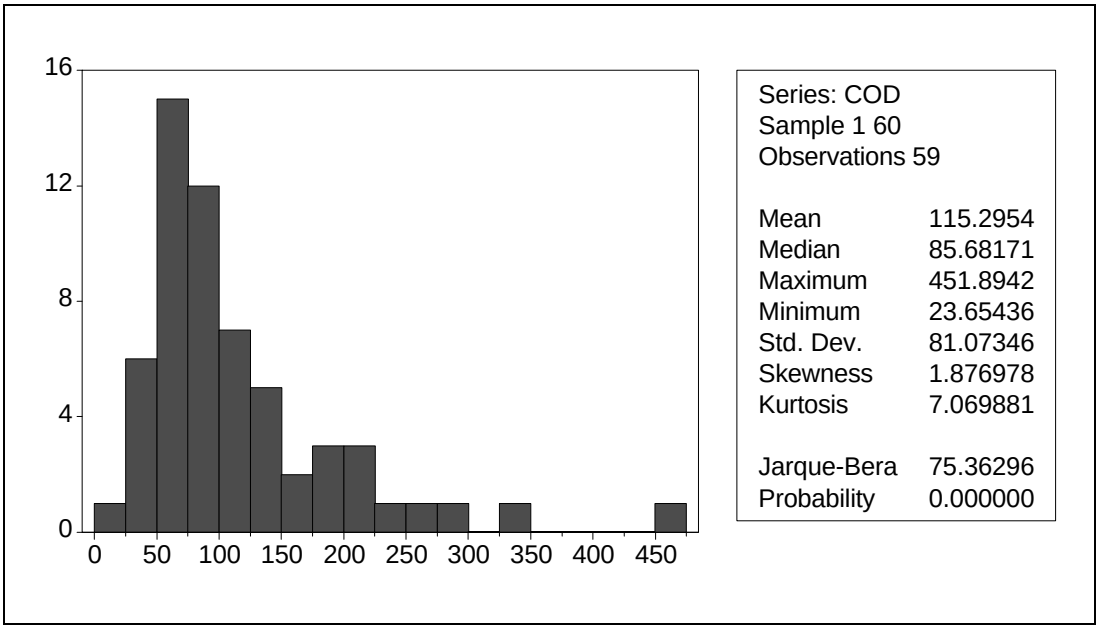

Figure E-4 Histogram of COD Observations

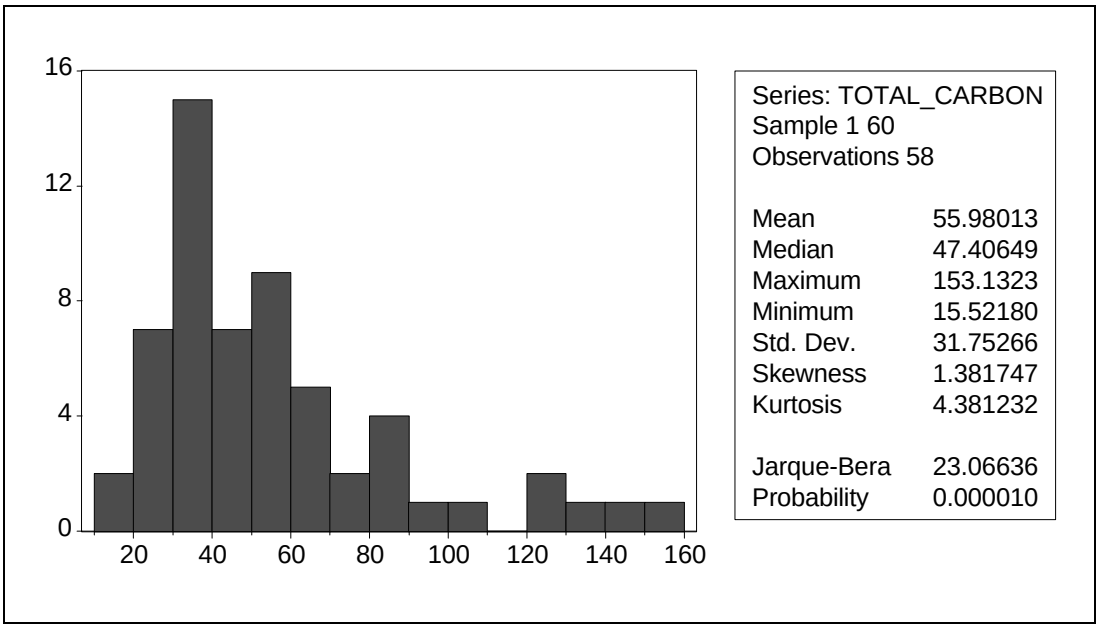

Figure E-5 Histogram of Total Carbon Observations

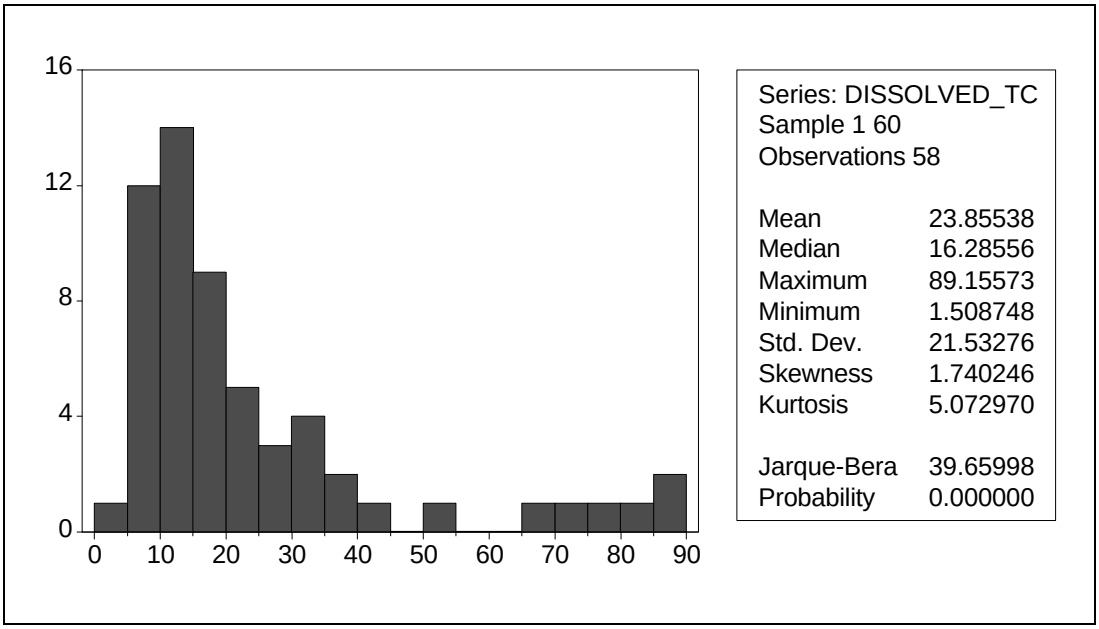

Figure E-6 Histogram of Dissolved Total Carbon Observations

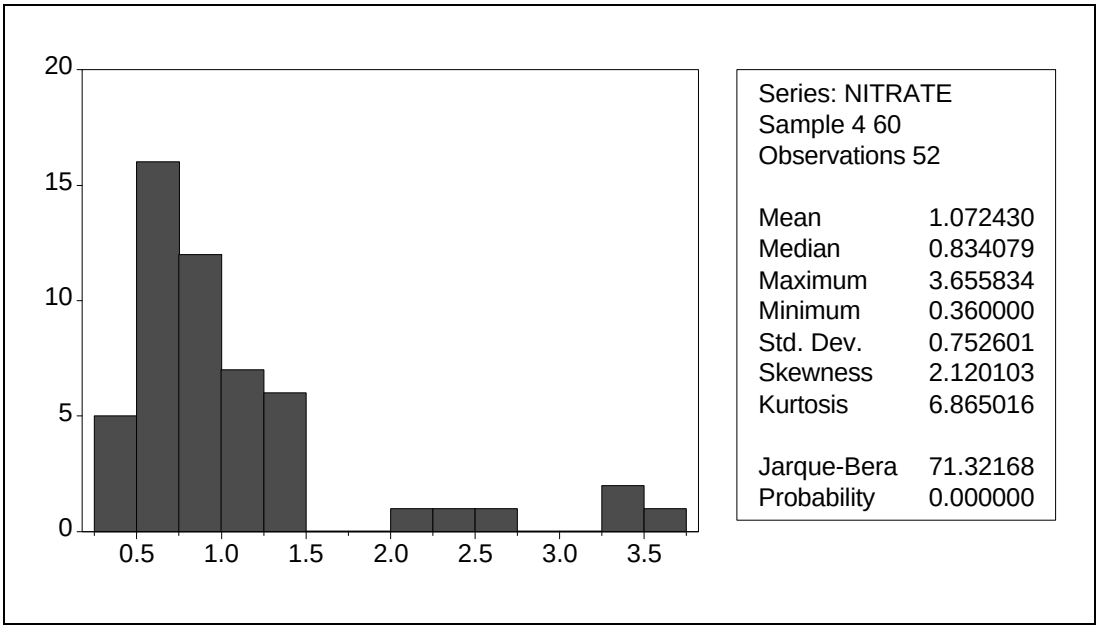

Figure E-7 Histogram of Nitrate Observations

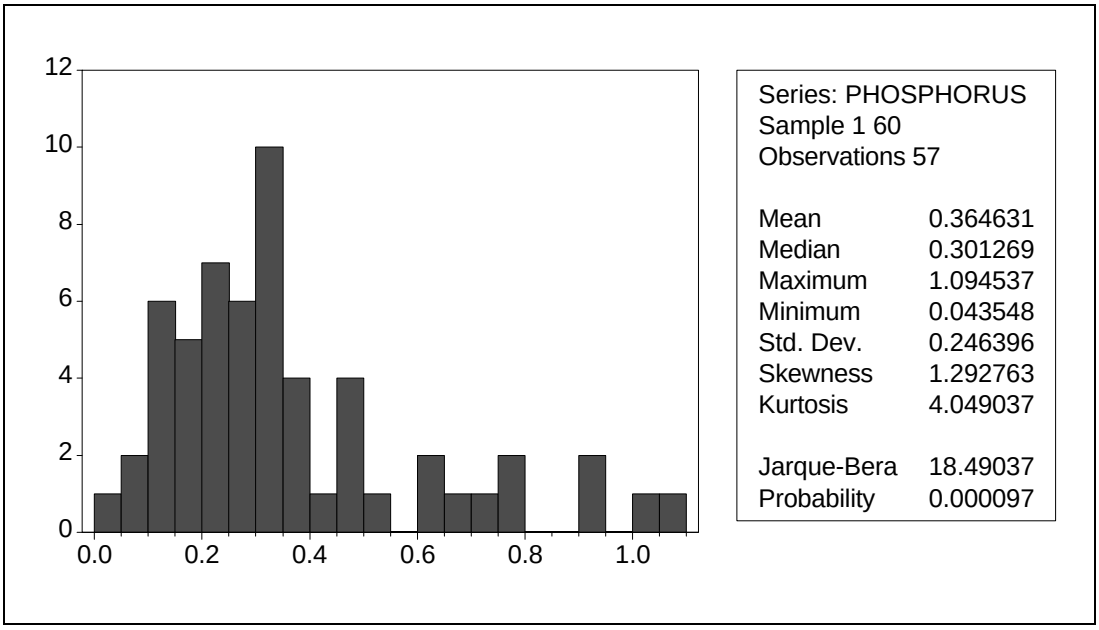

Figure E-8 Histogram of Total Phosphorus Observations

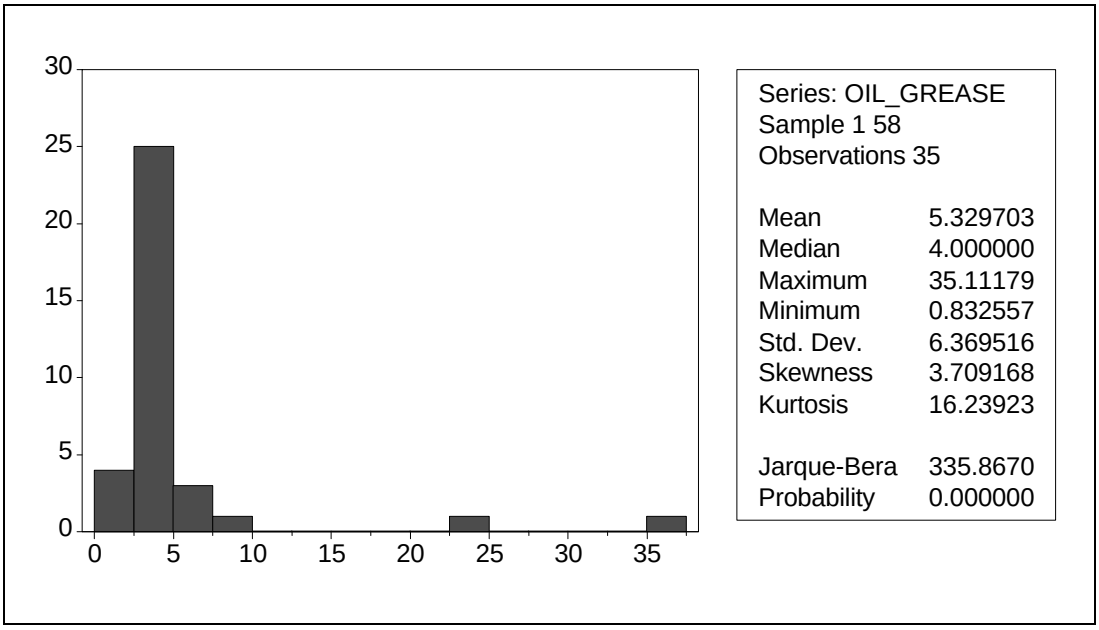

Figure E-9 Histogram of Oil and Grease Observations

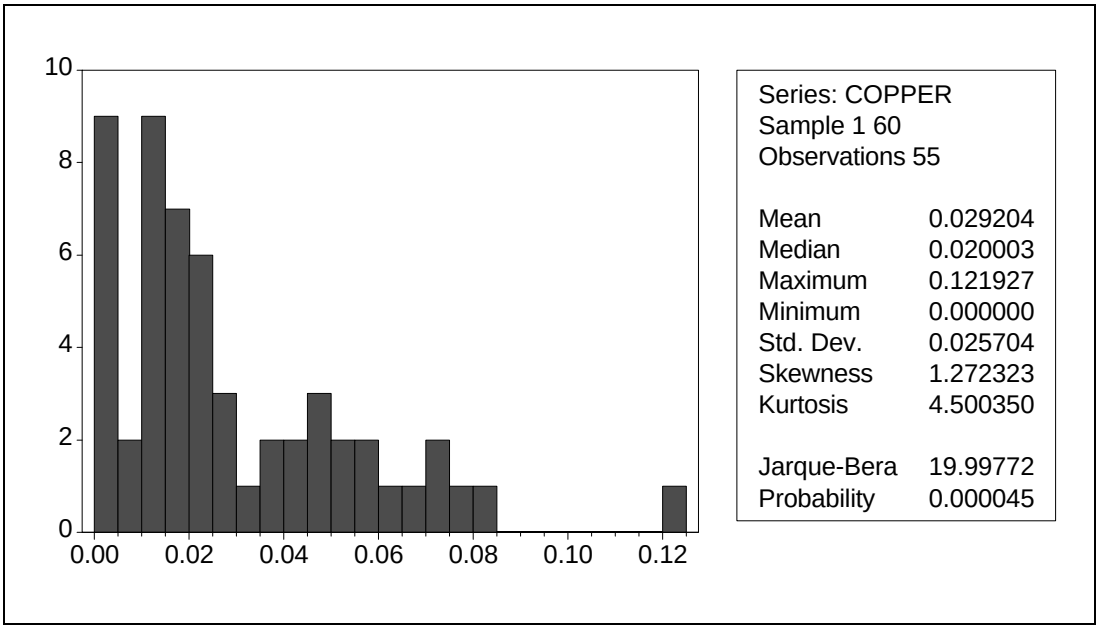

Figure E-10 Histogram of Copper Observations

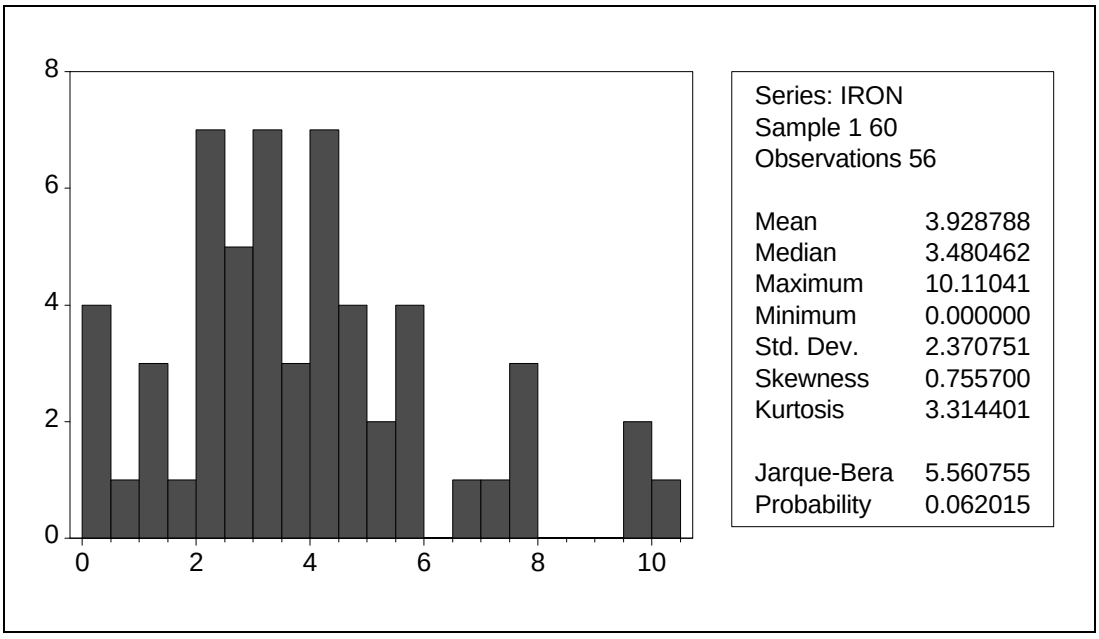

Figure E-11 Histogram of Iron Observation

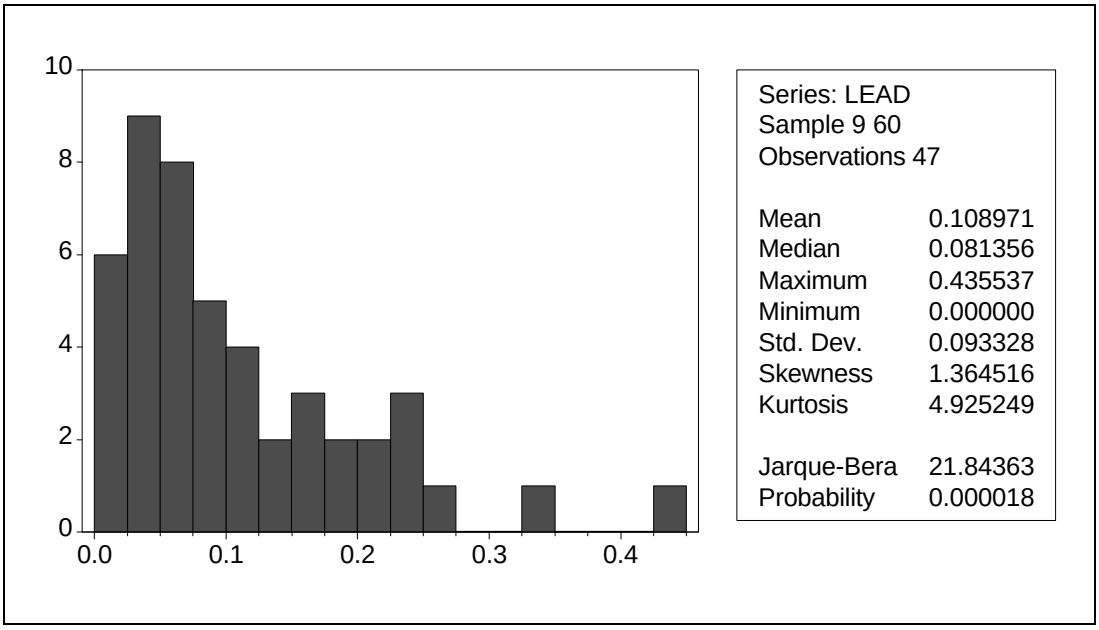

Figure E-12 Histogram of Lead Observations

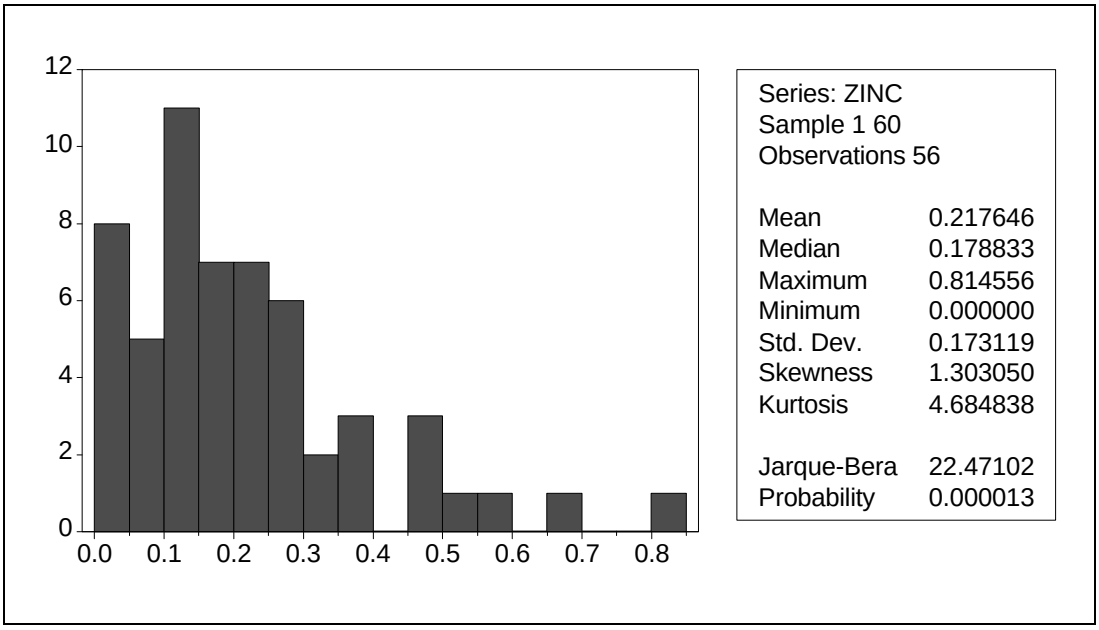

Figure E-13 Histogram of Zinc Observations

Appendix F
Constituent Wash-Off Patterns

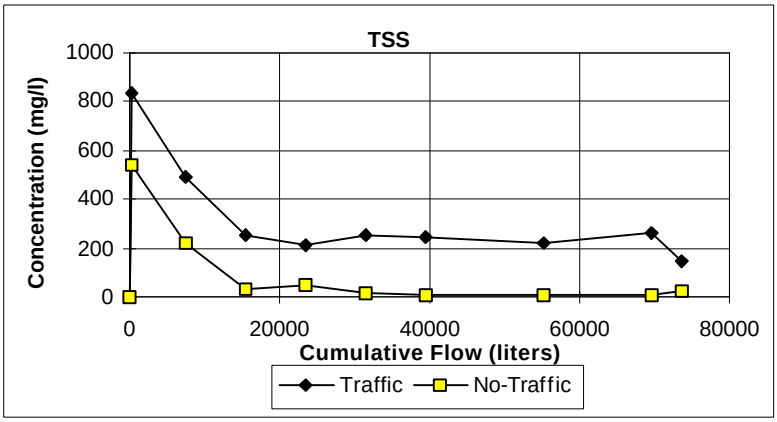

(a) Median TSS Concentration During a Simulated Storm Event

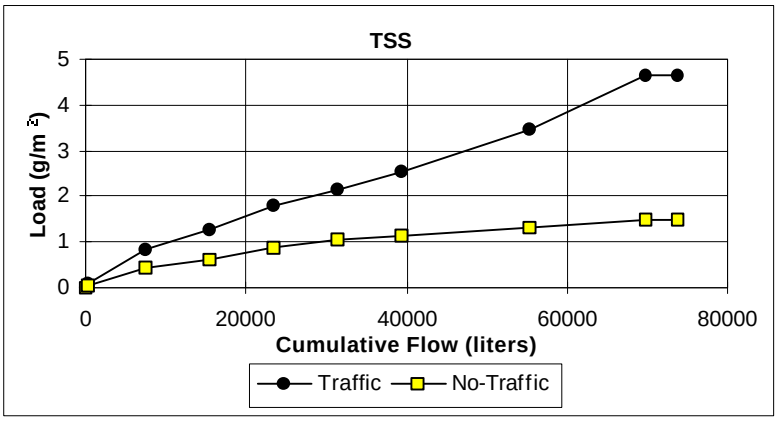

(b) Median TSS Load During a Simulated Storm Event

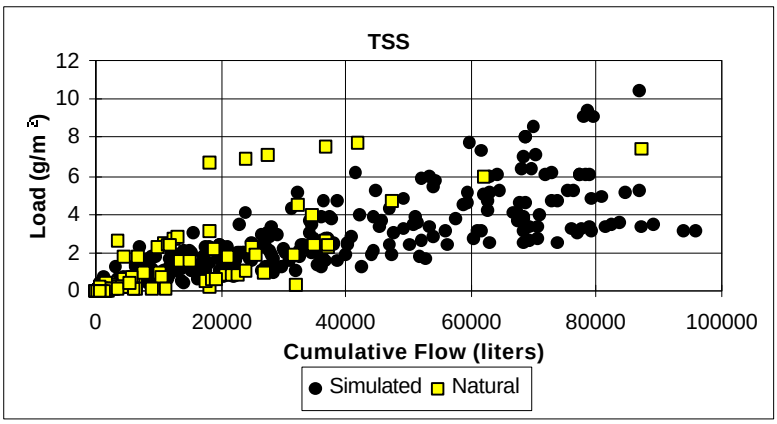

(c) TSS Load During Natural and Simulated Storm Events

Figure F-1

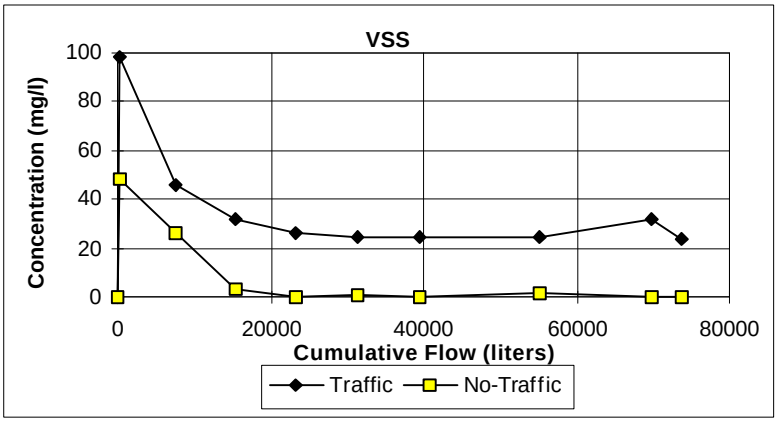

(a) Median VSS Concentration During a Simulated Storm Event

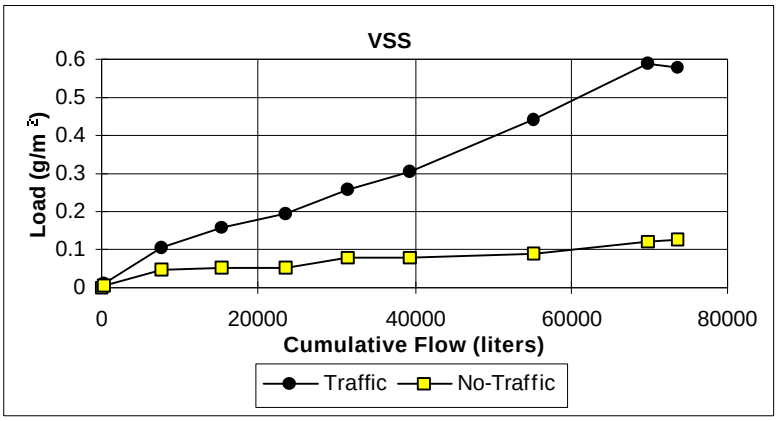

(b) Median VSS Load During a Simulated Storm Event

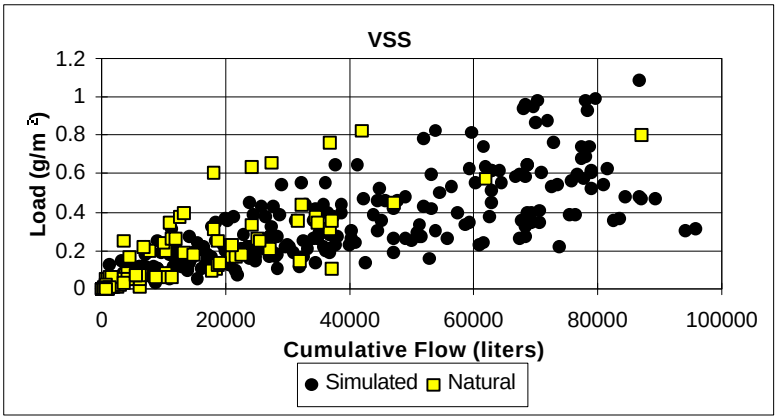

(c) VSS Load During Natural and Simulated Storm Events

Figure F-2

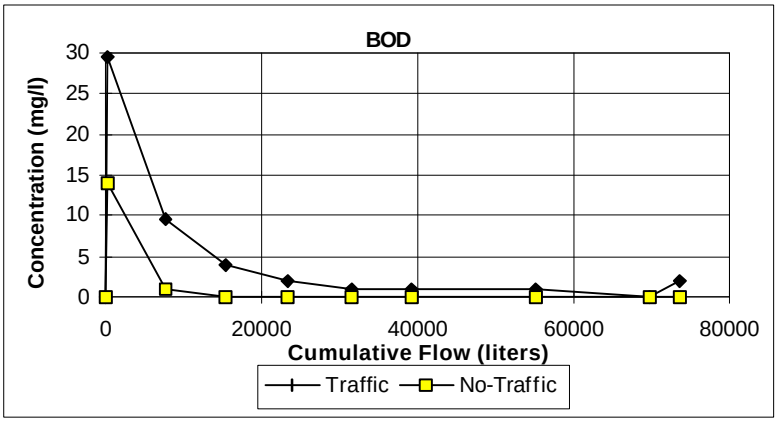

(a) Median BOD_5 Concentration During a Simulated Storm Event

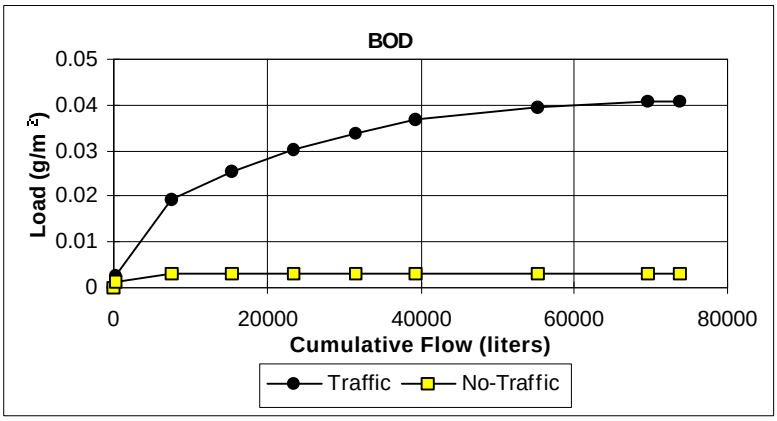

(b) Median BOD_5 Load During a Simulated Storm Event

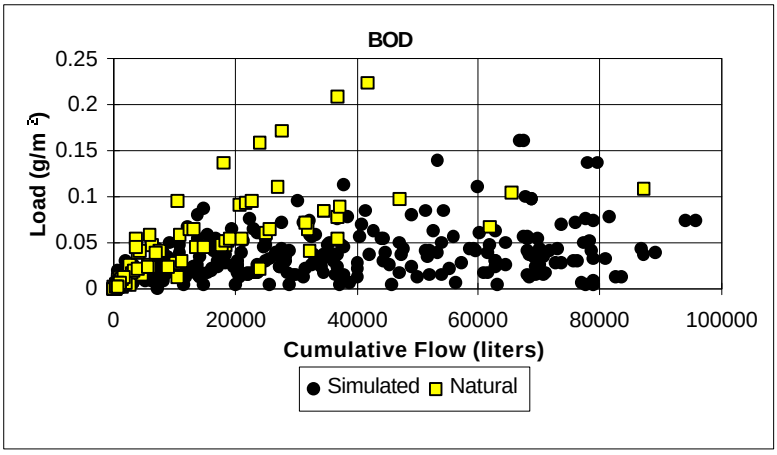

(c) BOD_5 Load During Natural and Simulated Storm Events

Figure F-3

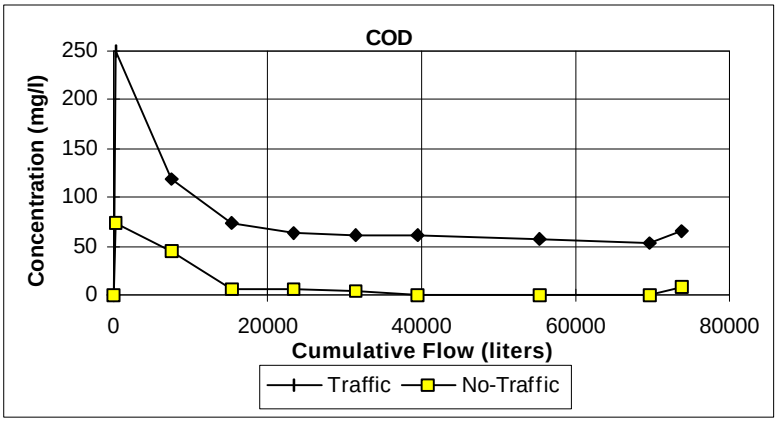

(a) Median COD Concentration During a Simulated Storm Event

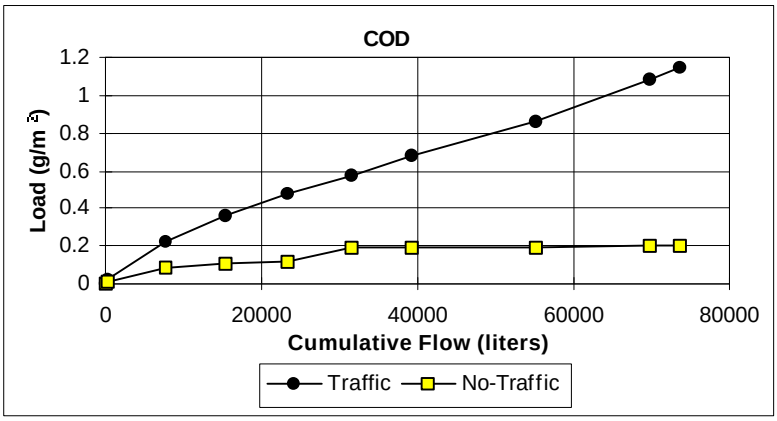

(b) Median COD Load During a Simulated Storm Event

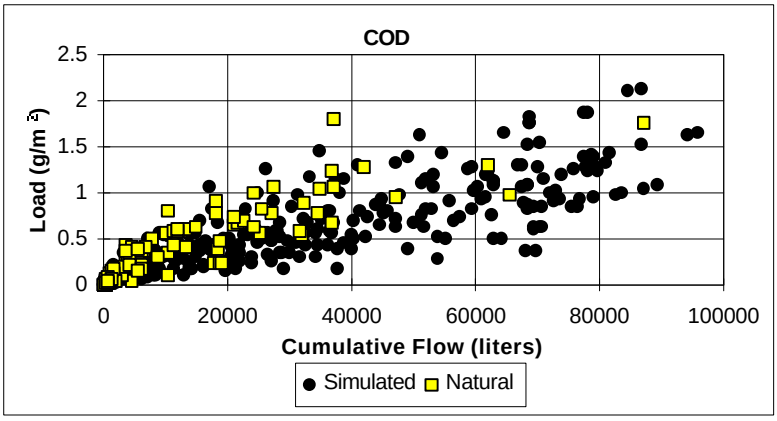

(c) COD Load During Natural and Simulated Storm Events

Figure F-4

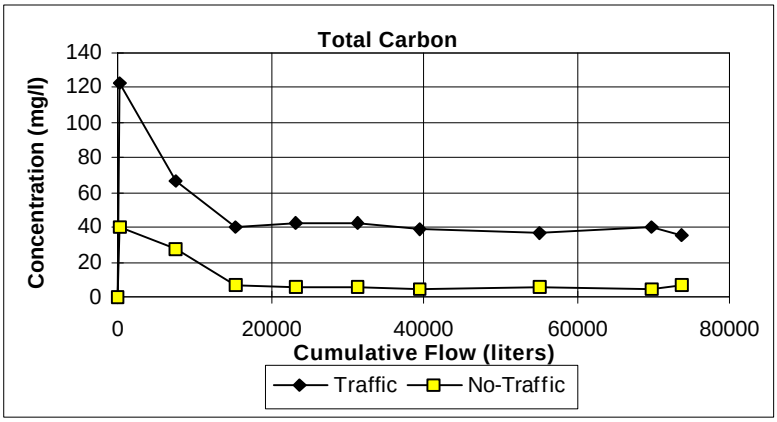

(a) Median Total Carbon Concentration During a Simulated Storm Event

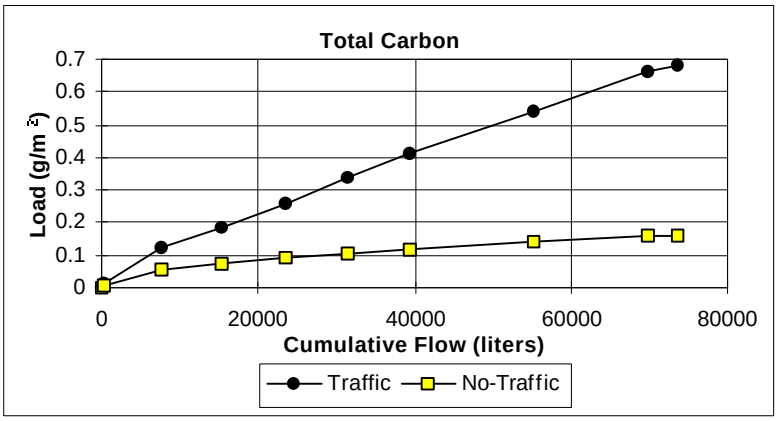

(b) Median Total Carbon Load During a Simulated Storm Event

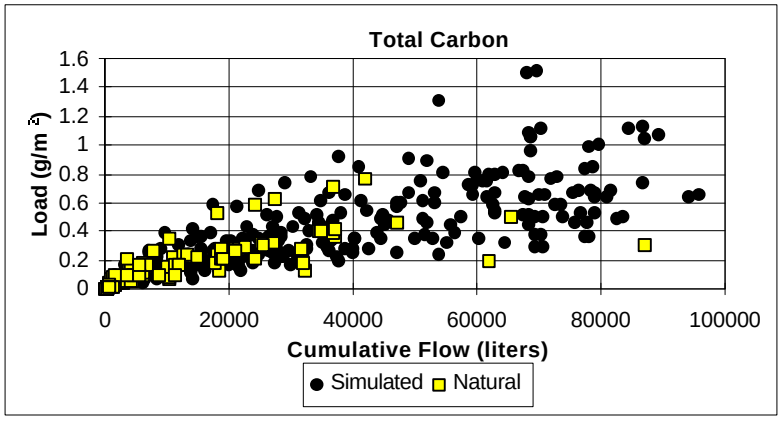

(c) Total Carbon Load During Natural and Simulated Storm Events

Figure F-5

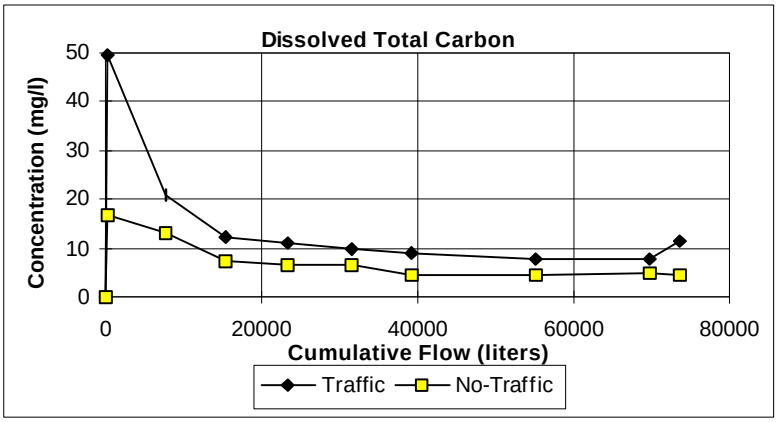

(a) Median Dissolved TC Concentration During a Simulated Storm Event

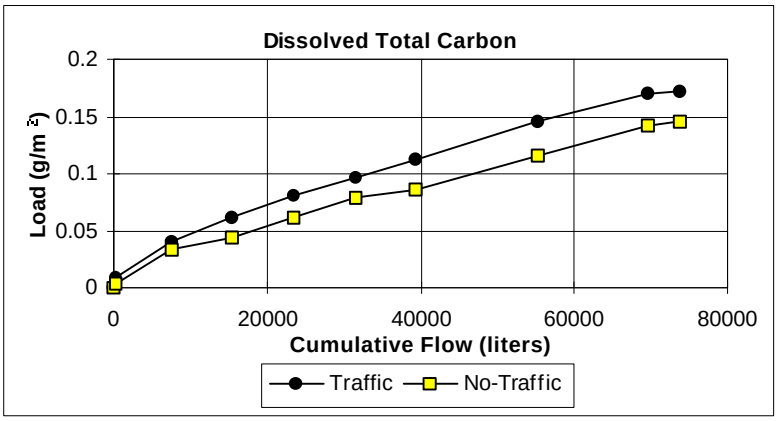

(b) Median Dissolved TC Load During a Simulated Storm Event

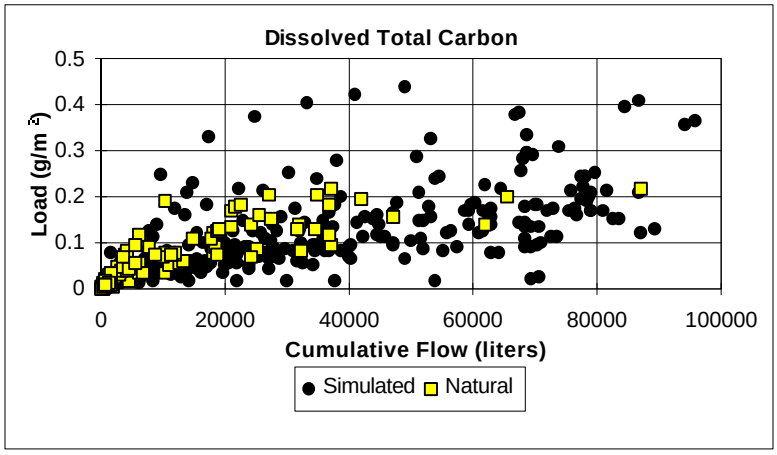

(c) Dissolved TC Load During Natural and Simulated Storm Events

Figure F-6

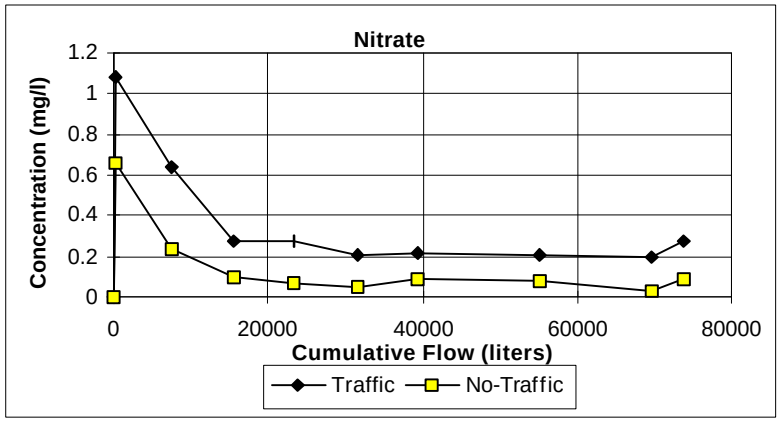

(a) Median Nitrate Concentration During a Simulated Storm Event

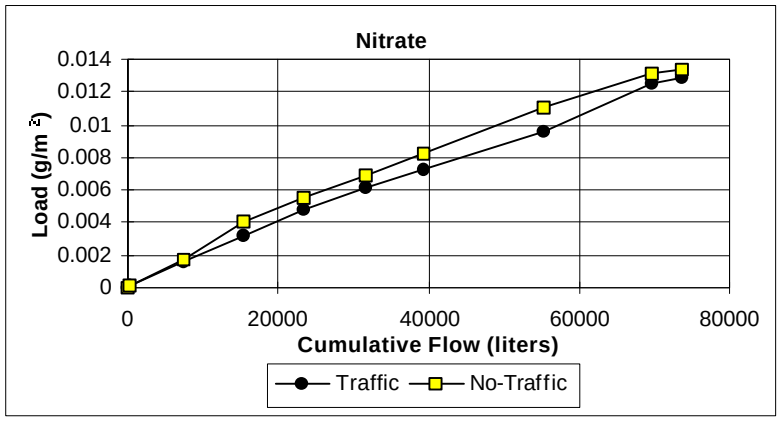

(b) Median Nitrate Load During a Simulated Storm Event

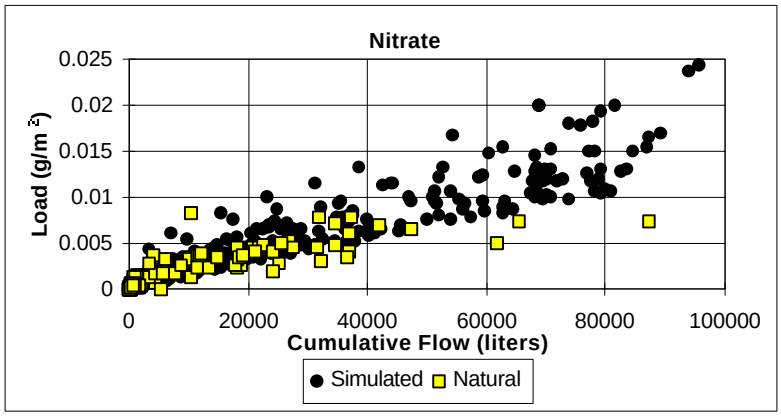

(c) Nitrate Load During Natural and Simulated Storm Events

Figure F-7

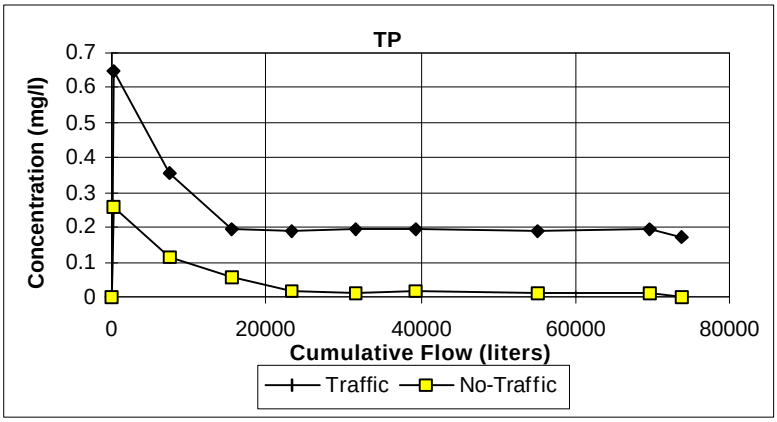

(a) Median Phosphorus Concentration During a Simulated Storm Event

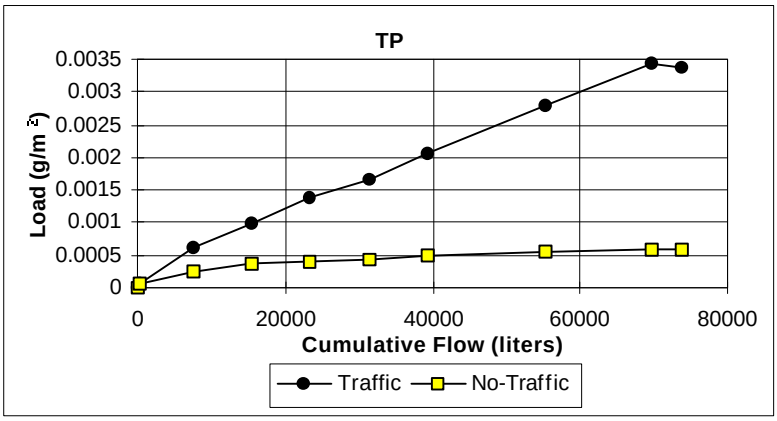

(b) Median Phosphorus Load During a Simulated Storm Event

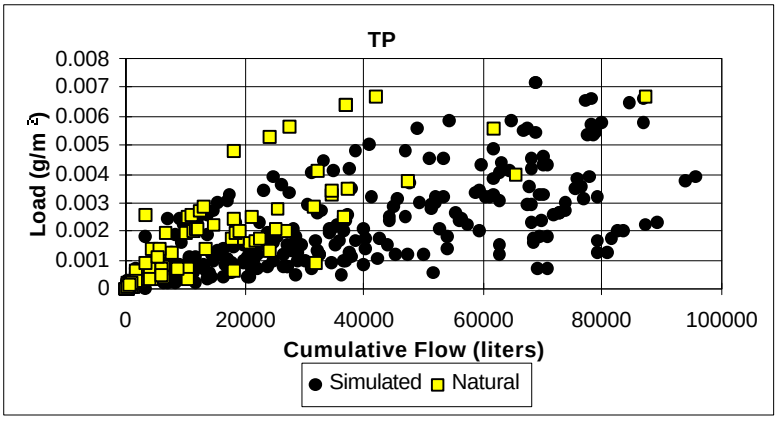

(c) Phosphorus Load During Natural and Simulated Storm Events

Figure F-8

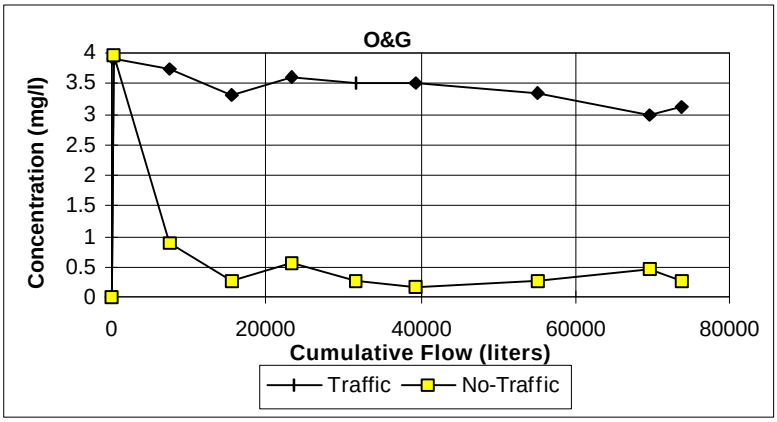

(a) Median Oil and Grease Concentration During a Simulated Storm Event

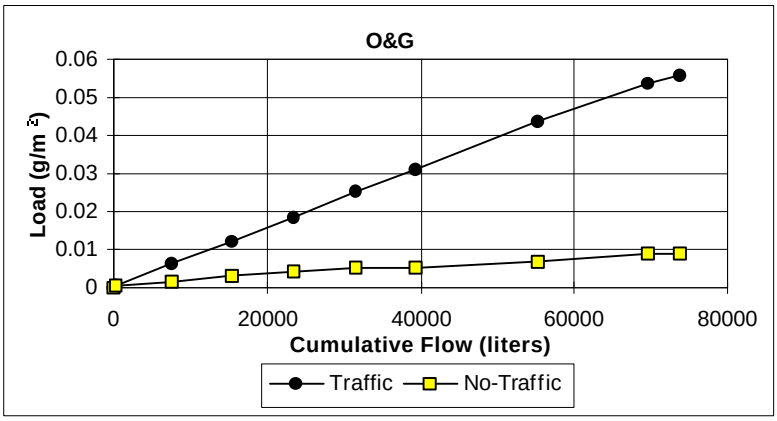

(b) Median Oil and Grease Load During a Simulated Storm Event

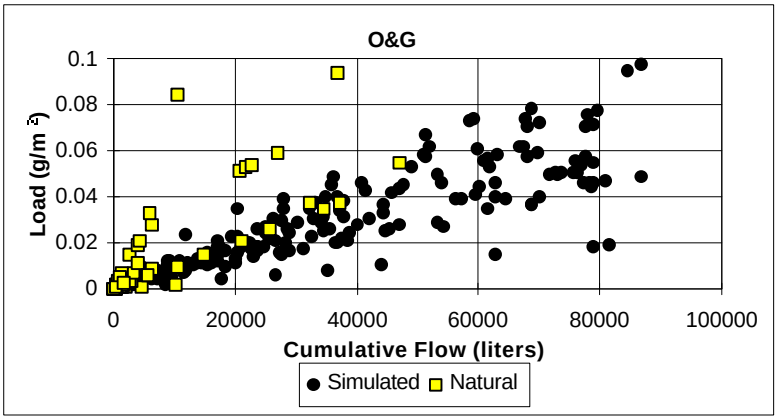

(c) Oil and Grease Load During Natural and Simulated Storm Events

Figure F-9

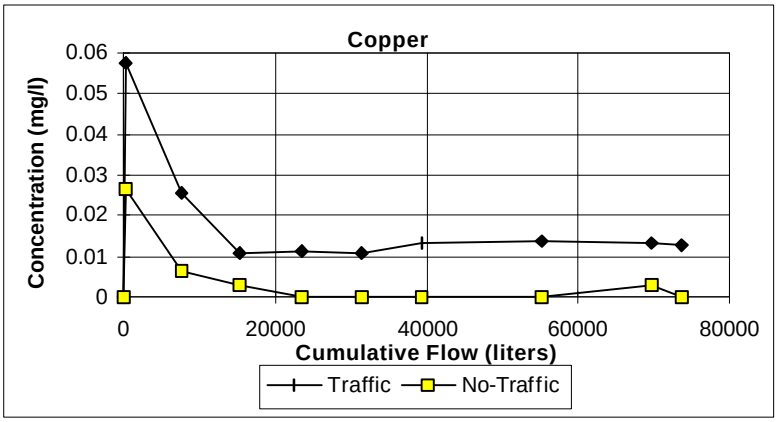

(a) Median Copper Concentration During a Simulated Storm Event

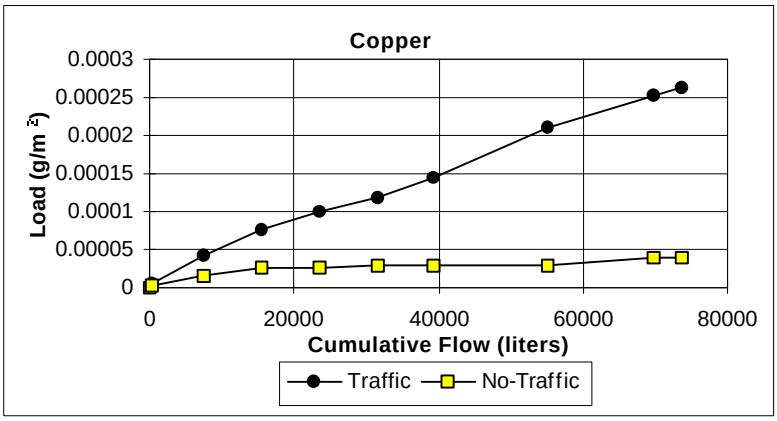

(b) Median Copper Load During a Simulated Storm Event

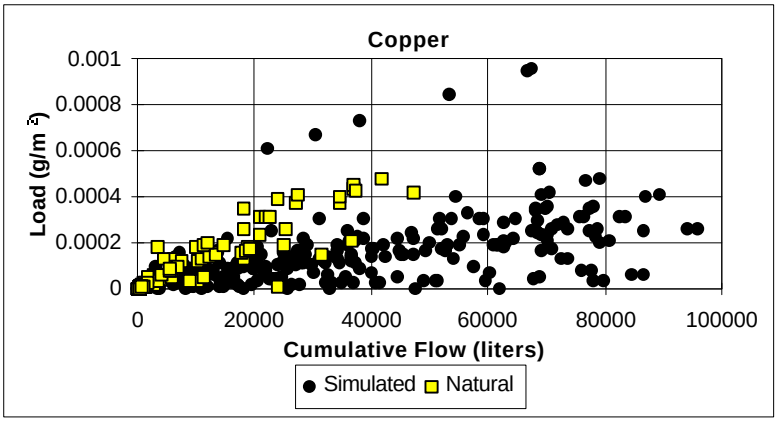

(c) Copper Load During Natural and Simulated Storm Events

Figure F-10

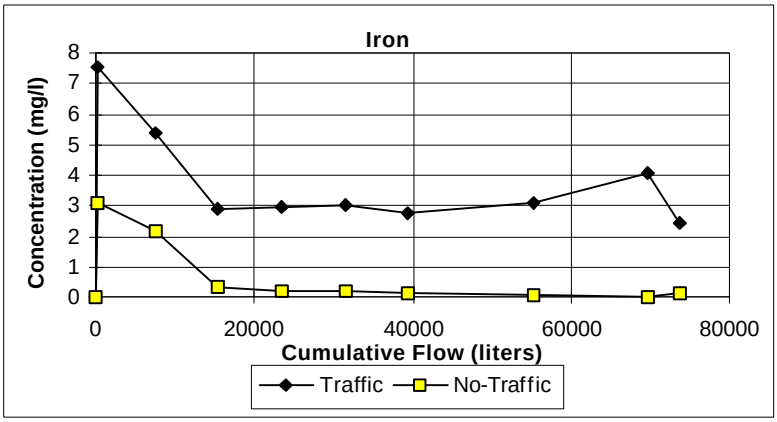

(a) Median Iron Concentration During a Simulated Storm Event

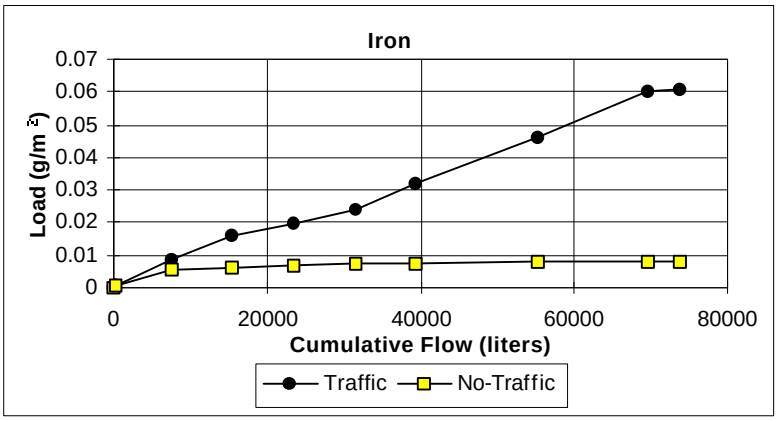

(b) Median Iron Load During a Simulated Storm Event

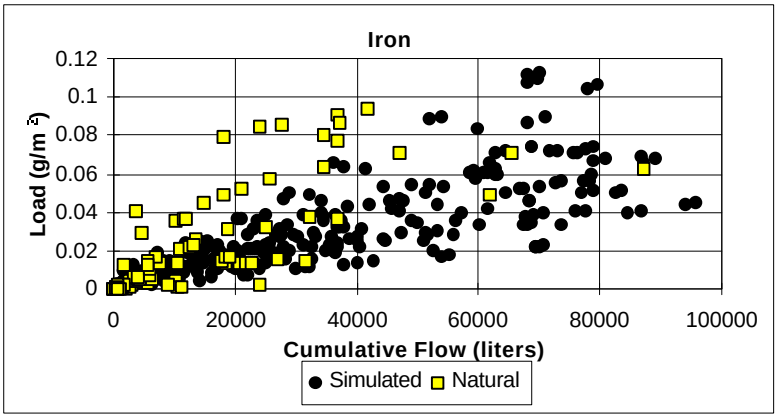

(c) Iron Load During Natural and Simulated Storm Events

Figure F-11

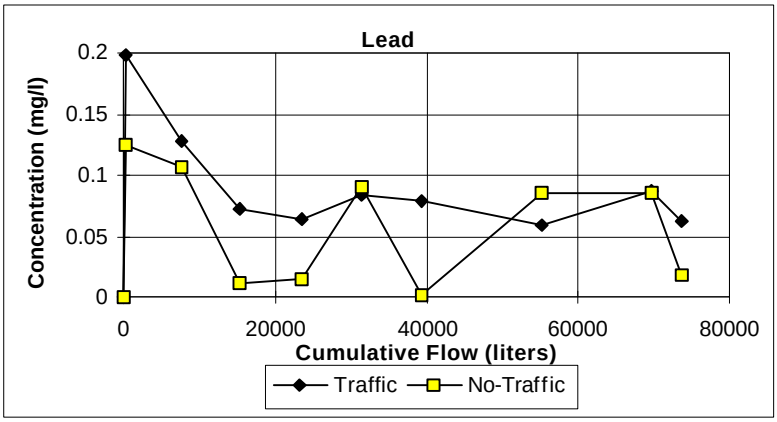

(a) Median Lead Concentration During a Simulated Storm Event

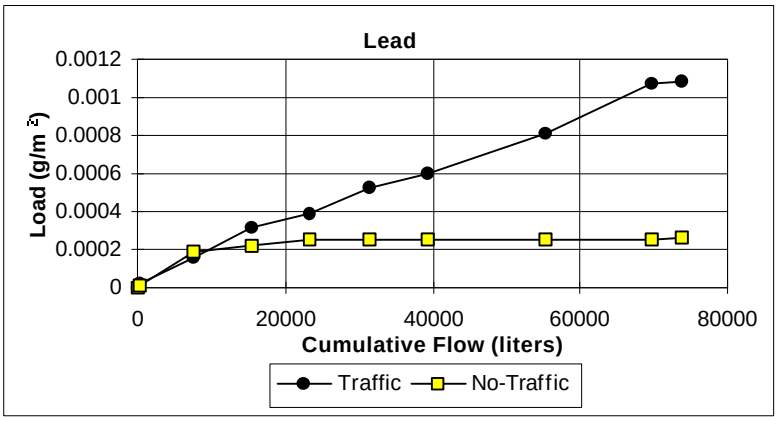

(b) Median Lead Load During a Simulated Storm Event

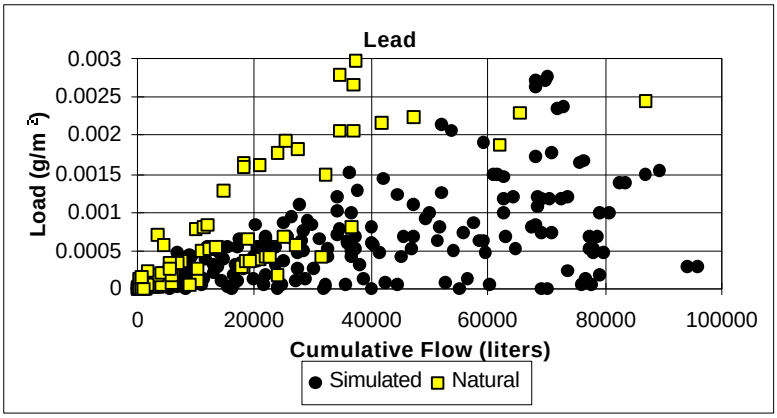

(c) Lead Load During Natural and Simulated Storm Events

Figure F-12

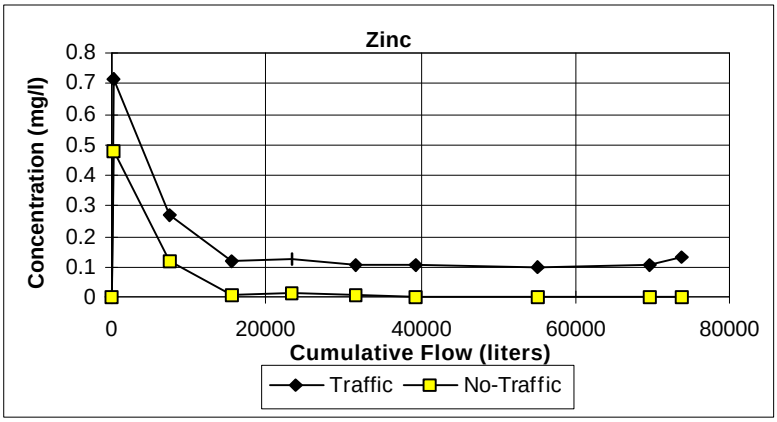

(a) Median Zinc Concentration During a Simulated Storm Event

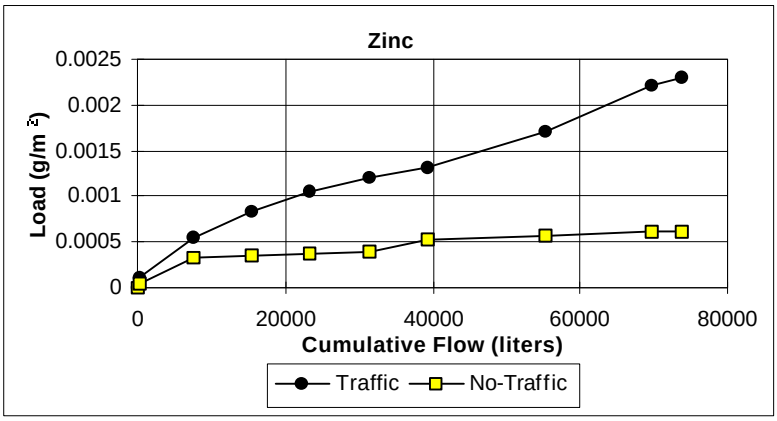

(b) Median Zinc Load During a Simulated Storm Event

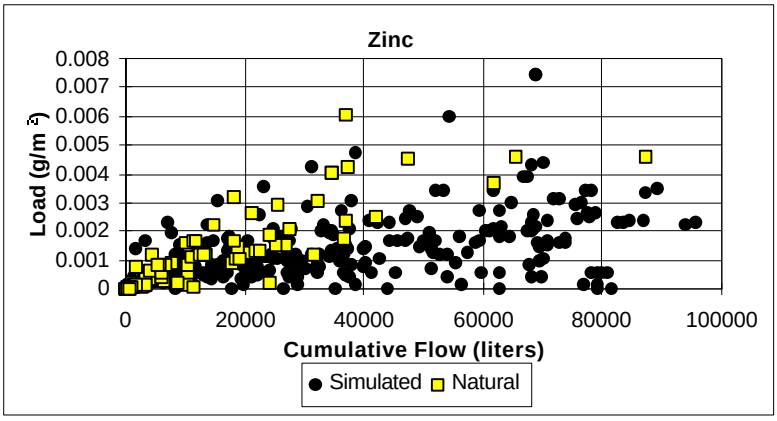

(c) Zinc Load During Natural and Simulated Storm Events

Figure F-13

Appendix G
The Method of Generalized Least Squares:
Corrections for Heteroscedasticity and Autocorrelation

Introduction

Least squares regression is a method used to determine the line of average relationship between a single dependent variable and one or more explanatory, or independent, variables. Consider the simple relationship between COD load, the dependent variable, and total volume of storm flow, the independent variable, illustrated in Figure G-1. Although COD load increases in direct proportion to an increase in total storm flow, there is substantial variation in the value of COD load for individual values of storm flow. The best the regression model can do is estimate the expected, or average, COD load for a given storm size. The regression model assumes that the "disturbances," or the variations from the expected value, are "well behaved," meaning that their expected value is zero, their variance is constant, and they are not correlated with each other. The problems that arise when the disturbances are not well behaved are the subject of this appendix.

Rationale for the Disturbance Term

The regression line illustrated in Figure G-1 is described by the linear function:

$$COD = 0.548 + 0.0002(Flow) \qquad \text{(G-1)}$$

Equation G-1 is not mathematically correct because not all (probably not any) of the values of COD are truly equal to the right-hand side of the equation. To achieve the identity, G-1 must be reformulated to include a disturbance term *e* defined as the difference between the observed value of COD and the equation value of COD for a specific value of flow.

$$COD_i = 0.548 + 0.0002(Flow_i) + e_i \qquad \text{(G-2)}$$

Given a set of observations, each disturbance term *e* is measurable and is referred to as the "residual." The values of the residuals can be either positive, negative, or zero and are collectively described by a normal probability distribution. The variance of this distribution determines the standard error of regression, which is a measure of the "goodness of fit" of the regression equation.

Adding a disturbance term to equation G-1 may seem like an arbitrary mathematical fix, but there are several important reasons for the existence of disturbance in the data set. First, not all of the relevant variables may have been included in the regression. In the previous example, only about 69% of the variation in COD is explained by total storm flow. There also are other variables that act in conjunction with flow to influence COD loads, such as traffic volume, traffic mix, antecedent dry period, etc.

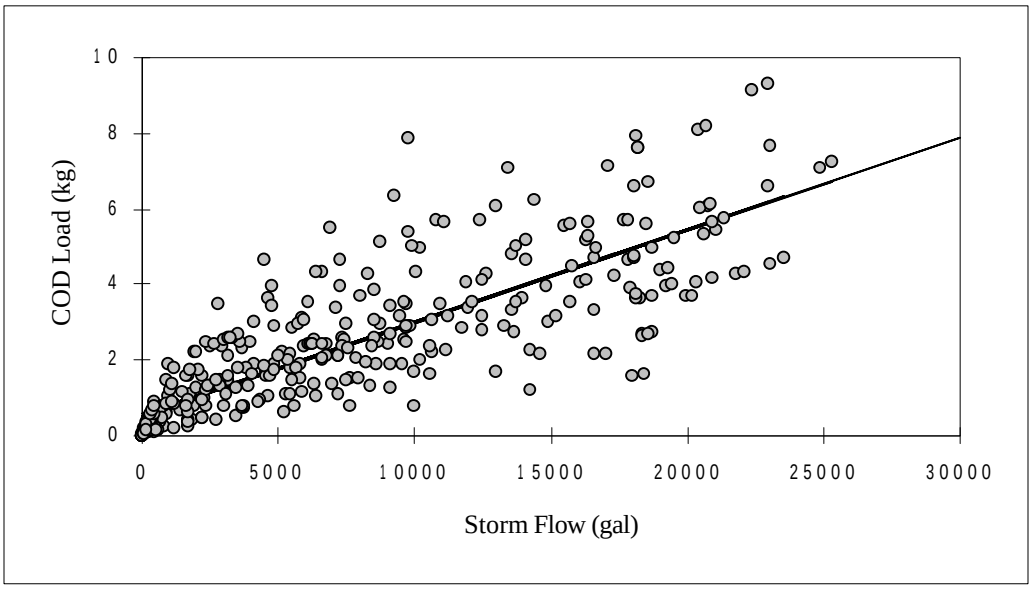

Figure G-1

Second, it is possible that the COD load measured during the storm was measured in error. This error could result from any number of reasons, including mishandling of the sample, mishap in the laboratory analysis, or a simple recording error, just to name a few.

Third, the disturbance could be the result of an inherently random component in the system under study. Natural systems are notoriously difficult to predict, and there could be any number of explanatory variables that have inherently random components.

Method of Ordinary Least Squares

The method of ordinary least squares (OLS) is the usual way to calculate the coefficients of a regression equation. OLS provides a simple procedure for calculating the coefficients of an inexact linear function by minimizing the sum of the squared differences, e^2, between the observed values of the dependent variable Y and the estimated values $\hat{Y}$. Furthermore, the OLS coefficients computed from a sample are the minimum-variance, linear, unbiased estimators of the population regression coefficients only if certain assumptions are satisfied. Mathematically, the OLS procedure is defined as

$$\text{minimize } \sum e_i^2 = \sum (Y_i - \hat{Y}_i)^2 \qquad \text{(G-3)}$$

where expression G-3 is often referred to as the error sum of squares (ESS) or the residual sum of squares.

Although OLS guarantees the "best" linear fit of the sample data, it is not necessarily the "best linear and unbiased estimator" (BLUE) for the population regression coefficients. Unlike the sample disturbance term *e*, the population disturbance term, denoted as *U*, is not observable. Consequently, the following assumptions must be made regarding the statistical properties of the population disturbance term *U* to complete the specification of the OLS model:

1. The disturbance term is normally distributed, and therefore the expected value, or mean, of all *U*'s for any given value of *Y* is zero.
2. All values of *U*, associated with different values of an independent variable *X*, have the same variance (homoscedastic assumption).
3. Each value of *U* is independent of all other values of *U* (uncorrelated residuals).
4. The value of any independent variable *X* is independent of the value of *U*.

The complete OLS model specifies both the population regression equation and the parameters of the distribution of the population disturbance term. The population regression equation derived from the data in Figure G-1 contains two distinct statements: a scientific statement $[0.548 + 0.0002(Flow_i)]$ and a statistical statement (U and its distribution).

If any of the assumptions regarding the distributional properties of the disturbance terms are violated, the OLS coefficients will not be BLUE. Unfortunately, the highway runoff data collected during the course of this research exhibit the characteristics of both heteroscedasticity and autocorrelation, which are two of the most common violations of the disturbance term assumptions. The procedures used to identify misspecified disturbance terms, the consequences of applying OLS procedures in the presence of a misspecified disturbance term, and the remedies used to correct for such misspecifications, are discussed in the remainder of this appendix.

Heteroscedasticity

Heteroscedasticity is the formal name that describes the condition in that the variance of the residuals is not uniform across the range of an explanatory variable X. This condition is common in cross-sectional data where the observations of variables of differing magnitudes are collected at a single point in time. Re-consider the data plotted in Figure G-1. It is apparent that the variance for the COD load increases as the storm flow increases. One possible explanation for this phenomenon is that the COD loads may vary with storm intensity. For example, low-intensity storms might produce smaller COD loads than higher intensity storms, regardless of the duration, and consequently the storm volume. In any case, the values for COD load are not as variable for low storm flows as they are for the higher volume flows. This is a classic illustration of heteroscedasticity in cross-sectional data.

It can be shown that the OLS estimate of the population regression coefficients is an unbiased estimator regardless of the distributional properties (i.e., the variance or correlation) of the population disturbance term. However, the OLS coefficients are not the minimum variance estimators if the homoscedastic assumption of the disturbance

term is violated. This is because the most inaccurate observations, or the observations with the largest variances, will dominate the ESS calculation. In other words, OLS will minimize an ESS that is heavily influenced by the observations that have the largest variances. Furthermore, this same calculation will lead to a biased estimate of the population variance (e.g., on average, the variance will be either underestimated or overestimated), which in turn will lead to a biased estimate of the variance of the population regression coefficients. The result is that conventionally computed confidence intervals and the conventionally employed *t* and *F* tests are no longer valid. If the population variance is underestimated (there is no theoretical basis for determining the direction of the bias), the computed confidence intervals will be narrower than they should be, providing an ill-founded belief in the precision of the model. A complete mathematical justification regarding the effects of misspecified disturbance terms is found in Johnson et. al., 1987.

Method of Generalized Least Squares

The ideal regression estimating scheme should give less importance, or "weight," to those observations coming from populations with greater variability than those that come from populations of smaller variability. Unfortunately, OLS does not follow this strategy, as it assigns equal weight to each observation. But a method known as generalized least squares (GLS) does follow this strategy and is capable of producing estimators that are BLUE. To illustrate GLS, re-consider the COD-storm flow model:

$$COD_i = 0.548 + 0.0002(Flow_i) + U_i \qquad \text{(G-4)}$$

Assume that the heteroscedastic variances σ_i^2 are known (i.e., $E(U_i^2) = \sigma_i^2$). If equation G-4 is divided through by σ_i to obtain:

$$\frac{COD_i}{\sigma_i} = 0.548\left(\frac{1}{\sigma_i}\right) + 0.0002\left(\frac{Flow_i}{\sigma_i}\right) + \left(\frac{U_i}{\sigma_i}\right) \qquad \text{(G-5)}$$

The purpose of this transformation is found in the following feature of the transformed disturbance term:

$$\text{var}\left(\frac{U_i}{\sigma_i}\right) = E\left(\frac{U_i}{\sigma_i}\right)^2$$

$$= \frac{1}{\sigma_i^2} E(U_i^2) \text{ since } \sigma_i^2 \text{ is known}$$

$$= \frac{1}{\sigma_i^2}(\sigma_i^2) \text{ since } E(U_i^2) = \sigma_i^2$$

$$= 1, \text{ which is a constant} \qquad \text{(G-6)}$$

The variance of the transformed disturbance term U is now constant, or homoscedastic. But also note that the effect of this transformation is to weight each variable by a value that is inversely proportional to its standard deviation, σ_i. If OLS is applied to the transformed variables, the COD observations from populations with large σ_i will be given proportionately less weight than the COD observations from populations with smaller σ_i during the minimizing of the ESS. Since all other OLS assumptions are retained, the OLS coefficients calculated from the transformed data will be BLUE.

To summarize, the method of GLS is merely OLS performed with a set of transformed variables that satisfy the OLS assumptions. Unfortunately, GLS is difficult in practice because the heteroscedastic variances σ_i^2, and subsequently the correct heteroscedastic transformations, are not known. Furthermore, there is no method to directly determine the best transformation. The procedure is strictly trial and error. A transformation is made, the equation is re-estimated using OLS procedures with the transformed variables, and a statistical test is used to determine if the new disturbance term is homoscedastic.

Tests for Heteroscedasticity

Heteroscedasticity can be expected in any cross-sectional analysis involving the relationship between highway runoff constituents and runoff volume, duration, antecedent dry period, traffic counts, etc., if a wide range of storm sizes are sampled. The identification of suspect variables, however, involves considerable judgment and knowledge regarding the data at hand. Although statistical tests are available for detecting the presence of heteroscedasticity, the decision as to that variables to test is strictly ad hoc.

Graphical methods, such as plotting the OLS residuals versus an independent variable, are often used to identify suspect independent variables. The heteroscedastic pattern displayed by the variable can suggest the appropriate GLS transformation (e.g., does the variance increase linearly, exponentially, etc., with the increase in the independent variable). There is no assurance, however, that two or more variables are not jointly the cause of the problem. The determination of heteroscedasticity more often depends upon the statistical evaluation of hypothesis testing. Several tests are available including the Park test, Glejser test, Spearman's rank correlation test, Goldfeld-Quandt test, and others.

A two-step procedure was used during this research to determine the degree of heteroscedasticity in the data set. The first step used the Goldfeld-Quandt test to determine heteroscedasticity among *individual* variables. If two are more variables failed the Goldfeld-Quandt test, which was the case for every runoff constituent, a second step was performed using the Breusch-Pagan test to confirm the existence of a general case of heteroscedasticity in the model. The Breusch-Pagan test was also used to confirm the presence or absence of heteroscedasticity following a GLS transformation.

The Goldfeld-Quandt Test

The Goldfeld-Quandt test is a popular method used to determine heteroscedasticity caused by a single independent variable in the model. The test is valid only if the heteroscedastic variance is positively related to an explanatory variable in the model. The degree of heteroscedasticity is calculated as the ratio of variability exhibited in the largest values of the explanatory variable, typically the upper 30 to 40% of the

range of X, to the variability exhibited in the smallest values of the explanatory variable, the lowest 30 to 40% of the range of X. If the disturbance terms are assumed to be normally distributed and if the assumption of homoscedasticity is valid, it can be shown that this ratio follows the F distribution with numerator and denominator degrees of freedom equal to $(n-d-2K)/2$, where n is the sample size, d is the number of observations deleted to calculate the ratio, and K is the number of regression coefficients estimated (including the intercept). As a hypothesis test, if the computed F-ratio is greater than the critical F-ratio at the chosen level of significance, the null hypothesis of homoscedasticity is rejected.

Specifically, the Goldfeld-Quandt test was performed on each explanatory variable as follows:

1) All observations (423) are sorted by increasing value of the suspect variable.
2) The middle portion of the observations are deleted. In this study, 131 observations were deleted, leaving 146 "low" values and 146 "high" values.
3) The OLS equation is estimated for each of the two subgroups.
4) The computed test statistic is calculated by dividing the error sum of squares (ESS) of the high group by the ESS of the low group.
5) The computed test statistic is compared to the critical F-statistic. The critical F-statistic for 139 degrees of freedom (n = 423, d = 131, and K = 7) in the numerator and 139 degrees of freedom in the denominator at the 0.05 level is approximately 1.3. If the computed F-statistic is greater than the critical F-statistic, the null hypothesis of no heteroscedasticity is rejected.

In summary, if the ESS of the upper range is 1.3 times the ESS of the lower range, the variance across the range of X is considered heteroscedastic.

The structure of the Goldfeld-Quandt test limits the test to identifying heteroscedasticity caused by a single variable. If the model contains more than one independent variable, the test should be applied to as many of the variables as possible. If two or more independent variables are identified as heteroscedastic, it must be assumed that they jointly contribute heteroscedasticity to the model. In this case, a more general test should be used to confirm the presence of heteroscedasticity in the model.

Table G-1 summarizes the results of the Goldfeld-Quandt test. The results indicate that storm duration, storm flow, storm vehicle count, and antecedent traffic count are all suspected of causing heteroscedasticity in each short model. The previous storm flow is an additional suspect only in the COD short model.

Table G-1 Calculated Test Statistic in Goldfeld-Quandt Test

Constituent	Duration	Flow	Vehicle Count	Antecedent Traffic	Previous Traffic	Previous Flow
COD	3.1	9.3	3.6	3.2	0.8	1.6
Nitrate	4.5	8.0	4.5	4.0	1.0	0.7
Oil and Grease	12.5	8.3	26.0	3.3	0.4	1.0
TSS	3.0	17.0	5.1	1.9	0.8	0.5
Phosphorous	4.0	9.1	4.0	3.0	0.5	0.9
Copper	9.0	32.9	20.5	3.0	0.1	0.3
Iron	2.5	13.8	4.3	2.9	0.4	0.2
Lead	2.3	22.9	4.8	5.7	0.4	0.1
Zinc	10.0	43.5	22.0	55.0	0.04	0.5

(Critical value of $F = 1.3$)

The Breusch-Pagan Test

The Breusch-Pagan test is a more general test that examines a model for heteroscedasticity caused by one or more independent variables. Like the Goldfeld-Quandt test, a set of suspect variables must be identified prior to application of the test. In this research, each independent variable that failed the Goldfeld-Quandt test is assumed to jointly contribute to heteroscedasticity in the model.

The Breusch-Pagan test standardizes each OLS residual by dividing by the variance of the residuals. This set of standardized residuals is then regressed against the suspect explanatory variables. A test statistic is calculated as one half of the total sum of squares minus the ESS. The total sum of squares (SS) is defined as the sum of the squared deviations of the sample values of the dependent variable about the sample mean of the dependent variable. This test statistic is distributed as chi-squared with k degrees of freedom, where k is the number of suspect explanatory variables. Because the

condition of homoscedasticity is assumed, the null hypothesis of homoscedasticity is rejected if the test statistic is larger than the critical value of the chi-square statistic.

Specifically, the Breusch-Pagan test was conducted during this research as follows:

1) Compute the OLS residuals ($e_i = Y_i - \hat{Y}_i$) for the model, where Y is the observed value of the dependent variable and $\hat{Y}$ is the regression value.
2) Calculate e_i^2 / S_e^2, where $S_e^2 = \sum e_i^2 / n$ and n = number of observations.
3) Regress the standardized OLS residuals, e_i^2 / S_i^2, on the suspect independent variables.
4) Calculate the test statistic as (SS - ESS) / 2 where SS is the Total Sum of Squares $\left(R^2 = 1 - \frac{ESS}{SS} \right)$
5) If the test statistic is greater than the critical value of the chi-square statistic, the null hypothesis of homoscedasticity is rejected. The critical value of chi-square distribution at the 0.05 level with 4 degrees of freedom (e.g., 4 suspect variables) is 9.49.

Heteroscedasticity Transformations

Consider the structure of the following highway runoff model estimated by OLS:

$$Y_i = \beta_0 + \beta_1 D_i + \beta_2 F_i + \beta_3 V_i + \beta_4 A_i + \beta_5 PV_i + \beta_6 PF_i + U_i \qquad \text{(G-7)}$$

where Y_i = dependent variable (kg/m2);

β_i = regression coefficients;

D_i = storm duration (min);

F_i = storm flow (L/m2);

V_i = average # of vehicles per lane during the storm;

A_i = average # of vehicles per lane during the antecedent dry period;

PV_i = average # of vehicles per lane during the previous storm;

PF_i = flow during the previous storm (L/m2)

U_i = disturbance term

As shown in Table G-1, the Goldfeld-Quandt test determined that each of the explanatory variables, with the exception of PV and PF, contributed heteroscedasticity in the base model (PF only contributed in the COD data set). Furthermore, the Breusch-Pagan test also confirmed a general case of heteroscedasticity in the base model. Therefore, a GLS transformation must be found such that the disturbance term of the transformed equation is homoscedastic. As noted above, there is no automatic method for determining the "best" transformation. The process is purely trial and error until an acceptable transformation is found. The obvious starting point is to assume that the heteroscedastic variances are directly related to each variable that failed the Goldfeld-Quandt test. Other possibilities include heteroscedastic variances that are related to the estimated values of the dependent variable, or related to the OLS residuals themselves. In all, 13 transformations were performed for the purpose of correcting for heteroscedasticity. The logic behind each transformation is described below.

Transformation I-a: Assumes that the heteroscedastic variance is a linear function of storm duration (i.e., $E(U_i^2) = D_i\sigma^2$). The transformed equation to be estimated by OLS is:

$$\frac{Y_i}{\sqrt{D_i}} = \beta_o \frac{1}{\sqrt{D_i}} + \beta_1 \frac{D_i}{\sqrt{D_i}} + \beta_2 \frac{F_i}{\sqrt{D_i}} + \beta_3 \frac{V_i}{\sqrt{D_i}} + \beta_4 \frac{A_i}{\sqrt{D_i}} + \beta_5 \frac{PV_i}{\sqrt{D_i}} + \beta_6 \frac{PF_i}{\sqrt{D_i}} + \frac{U_i}{\sqrt{D_i}}$$

Transformation I-b: Assumes that the heteroscedastic variance is a linear function of storm flow (i.e., $E(U_i^2) = F_i\sigma^2$). The transformed equation to be estimated by OLS is:

$$\frac{Y_i}{\sqrt{F_i}} = \beta_o \frac{1}{\sqrt{F_i}} + \beta_1 \frac{D_i}{\sqrt{F_i}} + \beta_2 \frac{F_i}{\sqrt{F_i}} + \beta_3 \frac{V_i}{\sqrt{F_i}} + \beta_4 \frac{A_i}{\sqrt{F_i}} + \beta_5 \frac{PV_i}{\sqrt{F_i}} + \beta_6 \frac{PF_i}{\sqrt{F_i}} + \frac{U_i}{\sqrt{F_i}}$$

Transformation I-c: Assumes that the heteroscedastic variance is a linear function of vehicle intensity (i.e., $E(U_i^2) = V_i\sigma^2$). The transformed equation to be estimated by OLS is:

$$\frac{Y_i}{\sqrt{V_i}} = \beta_o \frac{1}{\sqrt{V_i}} + \beta_1 \frac{D_i}{\sqrt{V_i}} + \beta_2 \frac{F_i}{\sqrt{V_i}} + \beta_3 \frac{V_i}{\sqrt{V_i}} + \beta_4 \frac{A_i}{\sqrt{V_i}} + \beta_5 \frac{PV_i}{\sqrt{V_i}} + \beta_6 \frac{PF_i}{\sqrt{V_i}} + \frac{U_i}{\sqrt{V_i}}$$

Transformation Id: Assumes that the heteroscedastic variance is a linear function of antecedent traffic count changes (i.e., $E(U_i^2) = A_i\sigma^2$). The transformed equation to be estimated by OLS is:

$$\frac{Y_i}{\sqrt{A_i}} = \beta_o \frac{1}{\sqrt{A_i}} + \beta_1 \frac{D_i}{\sqrt{A_i}} + \beta_2 \frac{F_i}{\sqrt{A_i}} + \beta_3 \frac{V_i}{\sqrt{A_i}} + \beta_4 \frac{A_i}{\sqrt{A_i}} + \beta_5 \frac{PV_i}{\sqrt{A_i}} + \beta_6 \frac{PF_i}{\sqrt{A_i}} + \frac{U_i}{\sqrt{A_i}}$$

Transformation I-e: Assumes that the heteroscedastic variance is a linear function of the previous storm flow (i.e., $E(U_i^2) = PF_i\sigma^2$). The transformed equation to be estimated by OLS is:

$$\frac{Y_i}{\sqrt{PF_i}} = \beta_o \frac{1}{\sqrt{PF_i}} + \beta_1 \frac{D_i}{\sqrt{PF_i}} + \beta_2 \frac{F_i}{\sqrt{PF_i}} + \beta_3 \frac{V_i}{\sqrt{PF_i}} + \beta_4 \frac{A_i}{\sqrt{PF_i}} + \beta_5 \frac{PV_i}{\sqrt{PF_i}} + \beta_6 \frac{PF_i}{\sqrt{PF_i}} + \frac{U_i}{\sqrt{PF_i}}$$

Transformation II-a: Assumes that the heteroscedastic variance changes at an increasing rate as storm duration changes (i.e., $E(U_i^2) = D_i^2\sigma^2$). The transformed equation to be estimated by OLS is:

$$\frac{Y_i}{D_i} = \beta_o \frac{1}{D_i} + \beta_1 + \beta_2 \frac{F_i}{D_i} + \beta_3 \frac{V_i}{D_i} + \beta_4 \frac{A_i}{D_i} + \beta_5 \frac{PV_i}{D_i} + \beta_6 \frac{PF_i}{D_i} + \frac{U_i}{D_i}$$

Transformation II-b: Assumes that the heteroscedastic variance changes at an increasing rate as flow changes (i.e., $E(U_i^2) = F_i^2\sigma^2$). The transformed equation to be estimated by OLS is:

$$\frac{Y_i}{F_i} = \beta_o \frac{1}{F_i} + \beta_1 \frac{D_i}{F_i} + \beta_2 + \beta_3 \frac{V_i}{F_i} + \beta_4 \frac{A_i}{F_i} + \beta_5 \frac{PV_i}{F_i} + \beta_6 \frac{PF_i}{F_i} + \frac{U_i}{F_i}$$

Transformation II-c: Assumes that the heteroscedastic variance changes at an increasing rate as vehicle intensity changes (i.e., $E(U_i^2) = V_i^2\sigma^2$). The transformed equation to be estimated by OLS is:

$$\frac{Y_i}{V_i} = \beta_o \frac{1}{V_i} + \beta_1 \frac{D_i}{V_i} + \beta_2 \frac{F_i}{V_i} + \beta_3 + \beta_4 \frac{A_i}{V_i} + \beta_5 \frac{PV_i}{V_i} + \beta_6 \frac{PF_i}{V_i} + \frac{U_i}{V_i}$$

Transformation II-d: Assumes that the heteroscedastic variance changes at an increasing rate as antecedent traffic count (i.e., $E(U_i^2) = A_i^2\sigma^2$). The transformed equation to be estimated by OLS is:

$$\frac{Y_i}{A_i} = \beta_o \frac{1}{A_i} + \beta_1 \frac{D_i}{A_i} + \beta_2 \frac{F_i}{A_i} + \beta_3 \frac{V_i}{A_i} + \beta_4 + \beta_5 \frac{PV_i}{A_i} + \beta_6 \frac{PF_i}{A_i} + \frac{U_i}{A_i}$$

Transformation II-e: Assumes that the heteroscedastic variance changes at an increasing rate as the previous storm flow changes (i.e., $E(U_i^2) = PF_i^2\sigma^2$). The transformed equation to be estimated by OLS is:

$$\frac{Y_i}{PF_i} = \beta_o \frac{1}{PF_i} + \beta_1 \frac{D_i}{PF_i} + \beta_2 \frac{F_i}{PF_i} + \beta_3 \frac{V_i}{PF_i} + \beta_4 \frac{A_i}{PF_i} + \beta_5 \frac{PV_i}{PF_i} + \beta_6 + \frac{U_i}{PF_i}$$

Transformation III: Assumes that the heteroscedastic variance is proportional to the estimated values of Y obtained from the OLS estimation of the base model (i.e., $E(U_i^2) = \hat{Y}_i^2\sigma^2$). The transformed equation to be estimated by OLS is:

$$\frac{Y_i}{\hat{Y}_i} = \beta_o \frac{1}{\hat{Y}_i} + \beta_1 \frac{D_i}{\hat{Y}_i} + \beta_2 \frac{F_i}{\hat{Y}_i} + \beta_3 \frac{V_i}{\hat{Y}_i} + \beta_4 \frac{A_i}{\hat{Y}_i} + \beta_5 \frac{PV_i}{\hat{Y}_i} + \beta_6 \frac{PF_i}{\hat{Y}_i} + \frac{U_i}{\hat{Y}_i}$$

Transformation IV-a and IV-b: Assumes the heteroscedastic variance is a linear function of the OLS residuals (i.e., $E(U_i^2) = |e_i|\sigma^2$). Model IV-a uses the residuals from regressing Y on the suspect independent variables only. Model IV-b uses the residuals

from regressing *Y* on all independent variables in the base model. In either case, the equation to be estimated by OLS is:

$$\frac{Y_i}{\sqrt{|e_i|}} = \beta_o \frac{1}{\sqrt{|e_i|}} + \beta_1 \frac{D_i}{\sqrt{|e_i|}} + \beta_2 \frac{F_i}{\sqrt{|e_i|}} + \beta_3 \frac{V_i}{\sqrt{|e_i|}} + \beta_4 \frac{A_i}{\sqrt{|e_i|}} + \beta_5 \frac{PV_i}{\sqrt{|e_i|}} + \beta_6 \frac{PF_i}{\sqrt{|e_i|}} + \frac{U_i}{\sqrt{|e_i|}}$$

Transformation IV-b was the best transformation for the data collected during this research.

Autocorrelation

Autocorrelation (or autoregression) refers to the presence of correlation among the disturbance terms. Autocorrelation is commonly associated with time-series data where the value of a given observation may be dependent upon the value of the preceding observation. In this case, a plot of the residuals will show a pronounced pattern.

Autocorrelation is unavoidable if all of the observations recorded during each storm event are included in the highway runoff data base since each observation recorded for the same storm will be related. Although there is no correlation *between* storms, the observations *within* each storm will be correlated. A hypothetical pattern of residuals that might be expected from a data set containing four storm events is plotted in Figure G-2.

A major rationale for including the disturbance term is to measure the combined effects of all variables not included in the regression equation. Many of the variables that affect highway runoff quality are autocorrelated. For example, every observation recorded during a particular storm will be dependent upon the amount of material that resided on the highway surface at the start of the rainfall. It follows that if any of the omitted variables are autocorrelated, the disturbance term will also be autocorrelated.

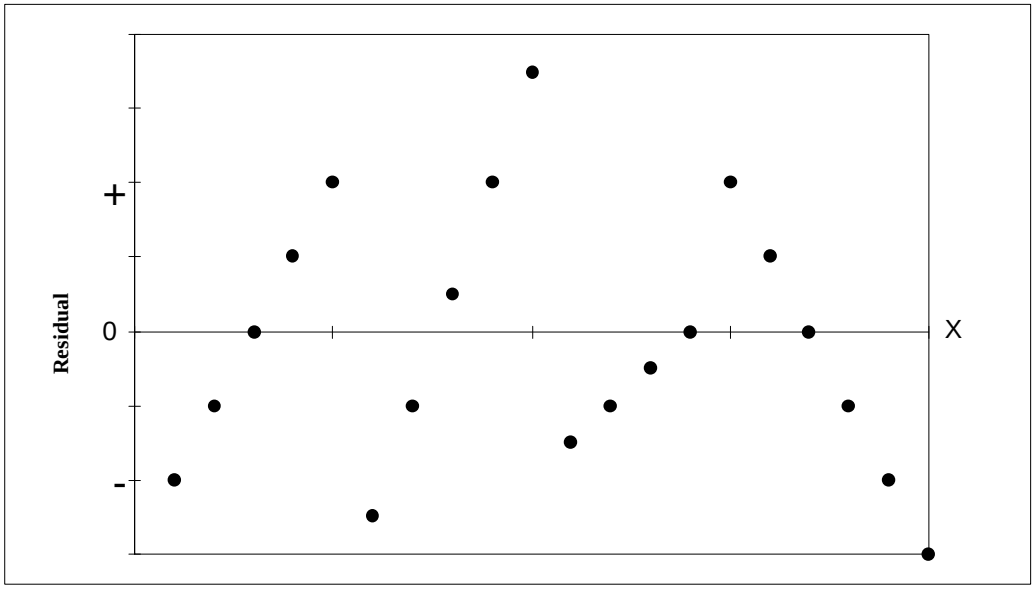

Figure G-2

The Test for Autocorrelation

Autocorrelation is defined as a disturbance term U_t whose value is dependent upon its immediately preceding value U_{t-1}, plus a random variable V_t. The subscript *t* is used to denote time because autocorrelation is typically a time series problem. If the relationship between U_t and U_{t-1} is linear, the autoregression is described as "first-order" and takes on the form:

$$U_t = \rho U_{t-1} + V_t \qquad \text{(G-8)}$$

The term rho (ρ) is called the autoregressive coefficient and is interpreted as the change in U_t for a 1-unit change in U_{t-1}. It should also be noted that the random variable V_t (that is a disturbance term) has the classical statistical specifications and is uncorrelated with U_t.

The Durbin-Watson *d* statistic is commonly used to detect the presence of autocorrelation. The test is valid only for first-order autoregression and where a "lagged," or previous value of the dependent variable does not appear as an explanatory variable. The *d*-statistic is calculated as:

$$d = \frac{\sum_{t=2}^{T} (e_t - e_{t-1})^2}{\sum_{t=1}^{T} e_t^2} \qquad \text{(G-9)}$$

where the *e*'s are the OLS residuals computed from the sample. The relationship between the *d* statistic and the autoregression coefficient rho can be shown by expanding G-9 to obtain:

$$d = \frac{\sum_{t=2}^{T} e_t^2 - 2\sum_{t=2}^{T} e_t e_{t-1} + \sum_{t=2}^{T} e_{t-1}^2}{\sum_{t=1}^{T} e_t^2} \qquad \text{(G-10)}$$

Because the squared terms summed over $t = 1$ and $t = 2$ will be nearly the same, G-10 can be rewritten as:

$$\begin{aligned} d &\approx \frac{\sum e_t^2 - 2\sum e_t e_{t-1} + \sum e_t^2}{\sum e_t^2} \\ &\approx \frac{2\sum e_t^2 - 2\sum e_t e_{t-1}}{\sum e_t^2} \\ &\approx 2\left(1 - \frac{\sum e_t e_{t-1}}{\sum e_t^2}\right) \end{aligned}$$

By definition, $\sum e_t e_{t-1} / \sum e_t^2 = \rho$, therefore

$$d \approx 2(1 - \rho) \qquad \text{(G-11)}$$

The distribution of the *d* statistic is based on this approximation. If there is no first-order autocorrelation, rho is equal to zero and the *d* statistic is *approximately* equal to 2. But because of the approximation, there is an "inconclusive" range of values for that the *d* statistic can neither confirm nor deny the presence of autocorrelation. In regard

to hypothesis testing, there are three critical ranges: (1) values of d for that the null hypothesis of no autocorrelation is rejected, (2) values of d for that the null hypothesis of no autocorrelation is not rejected, and (3) an inconclusive range of d values. For this reason, a Durbin-Watson table shows two critical values: the lower value (d_L) and the upper value (d_U) of the inconclusive range.

The formal hypothesis test for autocorrelation is stated as follows:

H_0: no autocorrelation.

H_a: autocorrelation

The decision rules are:

1) Reject H_0 if $d < d_L$ (positive) or if $d > 4 - d_L$ (negative).

2) Do not reject H_0 if $d_U < d < 4 - d_U$.

3) Test inconclusive if $d_L < d < d_U$, or, $4 - d_U < d < 4 - d_L$.

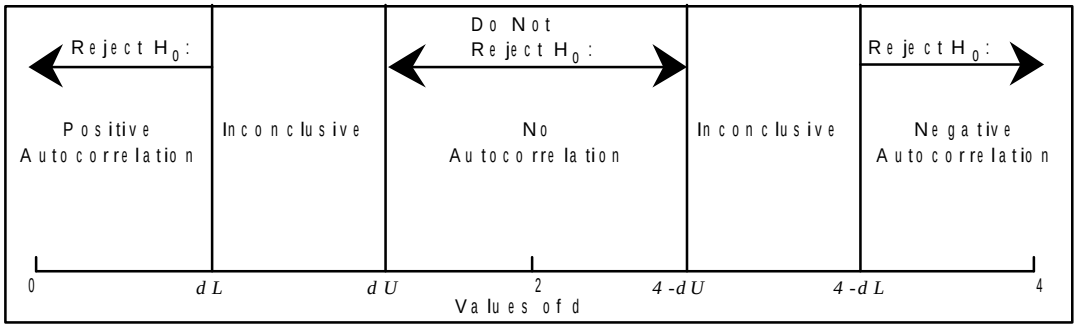

Figure G-3 Acceptance and Rejection Regions for the Durbin-Watson Statistic (after Johnson et. al., 1987)

The approximate values for d_L and d_U for 423 observations, 6 explanatory variables, and an intercept term is 1.57 and 1.78, respectively.

Autocorrelation Transformations

The solution to the autocorrelation misspecification is similar to that of heteroscedasticity. The procedure is to transform the misspecified equation into one with a uncorrelated disturbance term to permit the use of OLS procedures. The consequences of ignoring autocorrelation are the same as with heteroscedasticity, that is, OLS procedures will yield unbiased estimates of the population regression coefficients, but these estimates will not be minimum-variance estimates. As explained earlier, the OLS estimate of the population variance will be biased, that will nullify the *t* and *F* tests.

If the autoregressiveness in the sample is assumed to be first-order, equation G-8 suggests the following two-step transformation procedure:

1) Create a new set of variables Y_t^* and X_t^* (for all X) where:

$$Y_2^* = Y_2 - \rho Y_1 \qquad X_2^* = X_2 - \rho X_1$$

$$Y_3^* = Y_3 - \rho Y_2 \qquad X_3^* = X_3 - \rho X_2$$

$$\vdots \qquad\qquad \vdots$$

2) Re-estimate the OLS equation using the transformed variables.

Although the theoretical solution is straightforward, the practical solution is not simple since (1) the value of rho is not known and (2) the first observation is lost in the transformation.

The latter problem is solved by using the following transformations for the first observation:

$$Y_1^* = Y_1\sqrt{1-\rho^2} \qquad X_1^* = X_1\sqrt{1-\rho^2}$$

The appropriate value of rho is determined by using the Hildreth-Lu, or grid procedure. This is an iterative search procedure in which rho is incremented from -1 to +1 in small increments such as 0.1, 0.05, 0.01, etc. The data is transformed using each value of rho, the OLS equation is estimated, and the ESS recorded. The "best" value of

rho is the one that yields the smallest ESS. Table G-2 shows the results of the grid search for rho in a COD model.

Table G-2

COD Rho Search

r	**ESS**
0.55	144
0.60	140
0.65	137
0.70	**135.4**
0.75	135.5
0.80	136
0.85	140
0.90	144
0.95	150

Once a value is determined for rho, the GLS method can be applied. The formal transformation is stated below:

Transformation V: Assumes that first-order autoregression is present in the base model. The transformed equation to be estimated by OLS is:

$$Y_i^* = (1-\rho)\beta_0 + \beta_1 D_i^* + \beta_2 F_i^* + \beta_3 V_i^* + \beta_4 A_i^* + \beta_5 PV_i^* + \beta_6 PF_i^* + \nu_i$$

Dual Transformations

All of the transformations described thus far treat the problem of heteroscedasticity and autocorrelation separately. However, both problems can occur simultaneously, and both sets of transformations can be made to the OLS equation in an attempt to remedy the problem. An OLS equation estimated using a heteroscedastic transformation, for example, can be re-estimated using a first-order autoregression transformation. Likewise, the OLS equation estimated using the first-order

autoregression transformation can subsequently be re-estimated using each of the heteroscedastic transformations. Note that the result of the dual transformation is dependent upon the sequence in which the transformations are performed. Again, there is no hard and fast rule to determine the correct transformation.

During this study, two dual transformations were performed. The logic for each transformation is described below:

Transformation VI: Assumes the proper heteroscedasticity correction for Model V is the "best" transformation of Models I - IV. For example, if Model IV-b resulted in the lowest Breusch-Pagan value, the transformed equation to be estimated by OLS is:

$$\frac{Y_i^*}{\sqrt{|e_i|}} = \frac{(1-\rho)\beta_0}{\sqrt{|e_i|}} + \beta_1 \frac{D_i^*}{\sqrt{|e_i|}} + \beta_2 \frac{F_i^*}{\sqrt{|e_i|}} + \beta_3 \frac{V_i^*}{\sqrt{|e_i|}} + \beta_4 \frac{A_i^*}{\sqrt{|e_i|}} + \beta_5 \frac{PV_i}{\sqrt{|e_i|}} + \beta_6 \frac{PF_i}{\sqrt{|e_i|}} + \frac{v_i}{\sqrt{|e_i|}}$$

Transformation VII: Assumes that the proper correction for autoregression in the "best" transformation of Models I - IV is the first-order model. For example, if Model IV-b resulted in the lowest Breusch-Pagan value, the transformed equation to be estimated by OLS is:

$$\left(\frac{Y_i}{\sqrt{|e_i|}}\right)^* = (1-\rho)\frac{\beta_0}{\sqrt{|e_i|}} + \beta_1\left(\frac{D_i}{\sqrt{|e_i|}}\right)^* + \beta_2\left(\frac{F_i}{\sqrt{|e_i|}}\right)^* + \beta_3\left(\frac{V_i}{\sqrt{|e_i|}}\right)^* + \beta_4\left(\frac{A_i}{\sqrt{|e_i|}}\right)^*$$
$$+ \beta_5\left(\frac{PV_i}{\sqrt{|e_i|}}\right)^* + \beta_6\left(\frac{PF_i}{\sqrt{|e_i|}}\right)^* + \frac{v_i}{\sqrt{|e_i|}}$$

Summary

Transformation VII was determined to be the best transformation of the data collected during this research. Table G-3 lists the values of the Durbin-Watson statistic for the final model of each constituent.

Table G-3

Values of the Durbin-Watson Statistic

Constituent	Durbin-Watson Statistic
TSS	1.79
VSS	1.99
BOD_5	1.89
COD	1.74
Total Carbon	1.81
Dis. Total Carbon	1.79
Nitrate	1.94
Total Phosphorus	1.71
Oil and Grease	1.61
Copper	1.99
Iron	1.78
Lead	2.00
Zinc	1.98

$d_L = 1.57$
$d_U = 1.78$

Appendix H

Residual Histograms

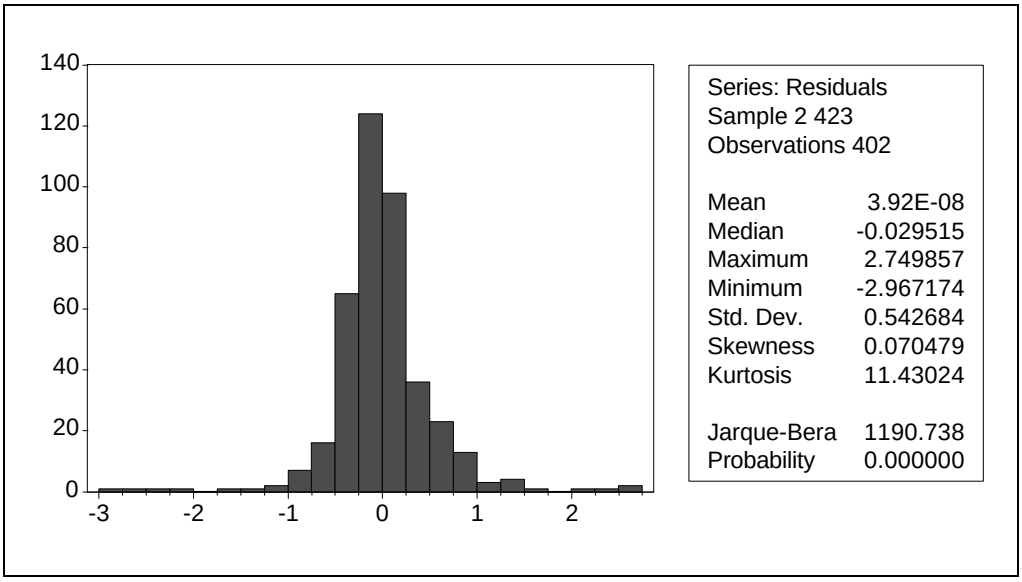

Figure H-1 TSS

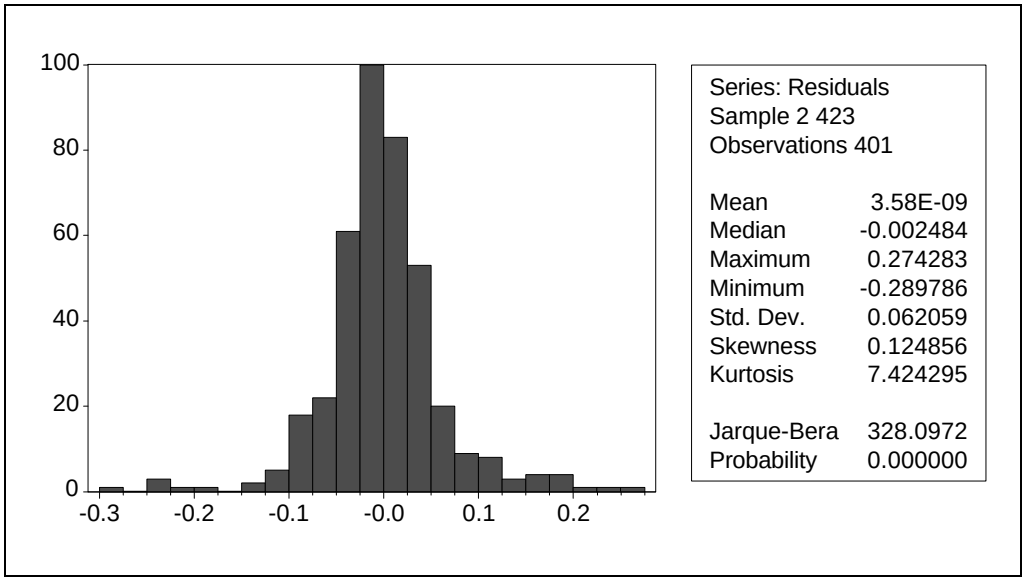

Figure H-2 VSS

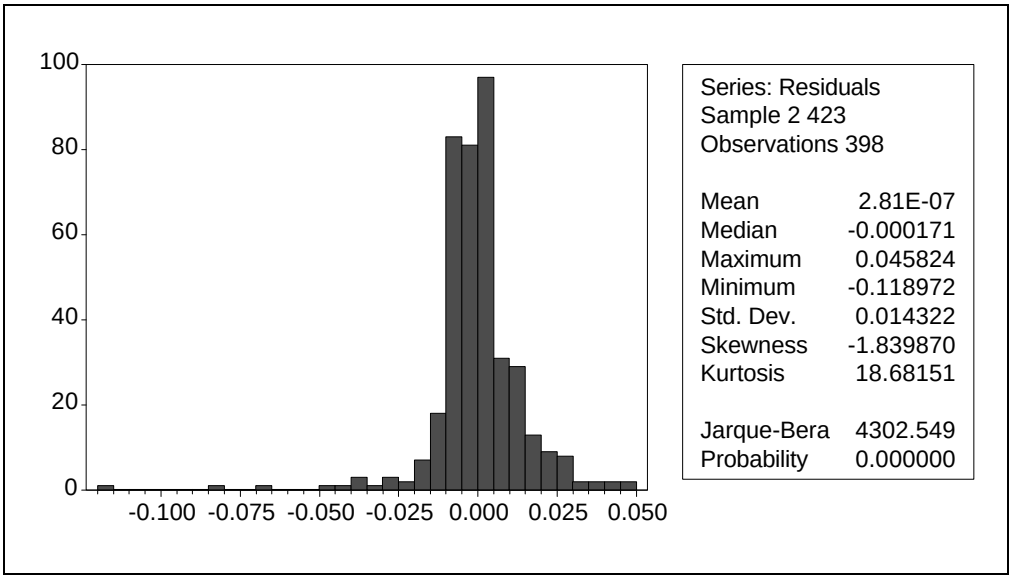

Figure H-3 BOD_5

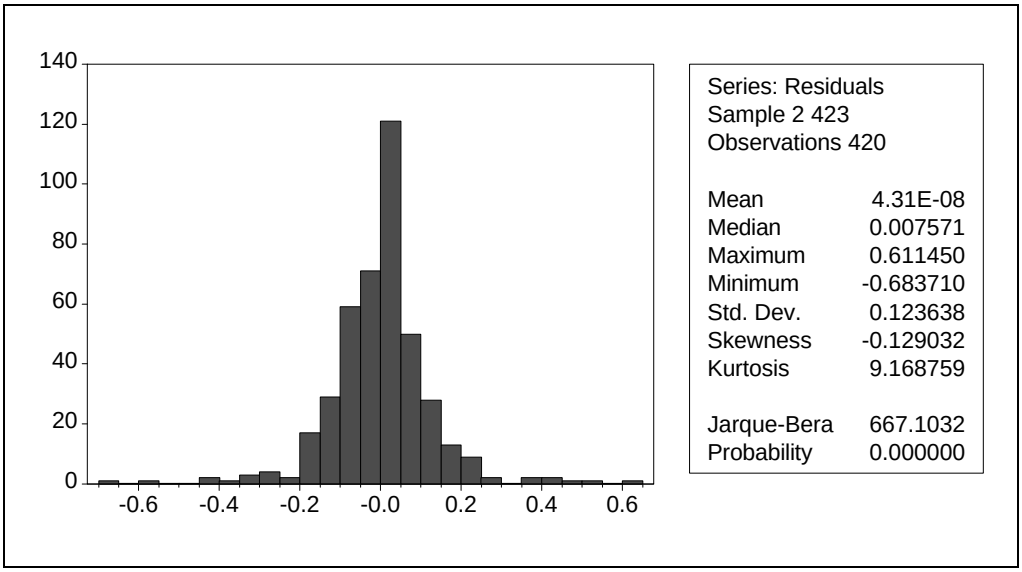

Figure H-4 COD

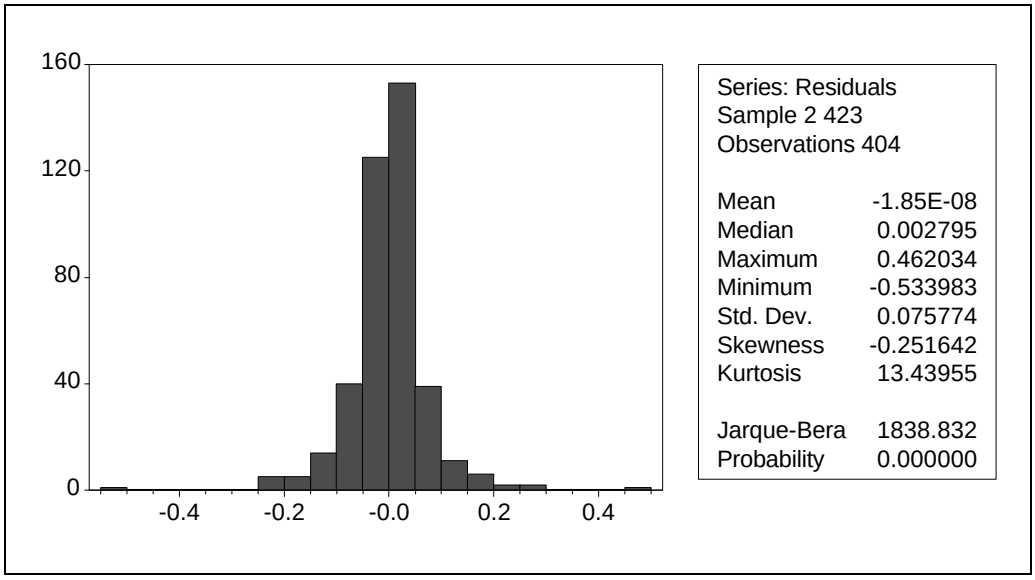

Figure H-5 Total Carbon

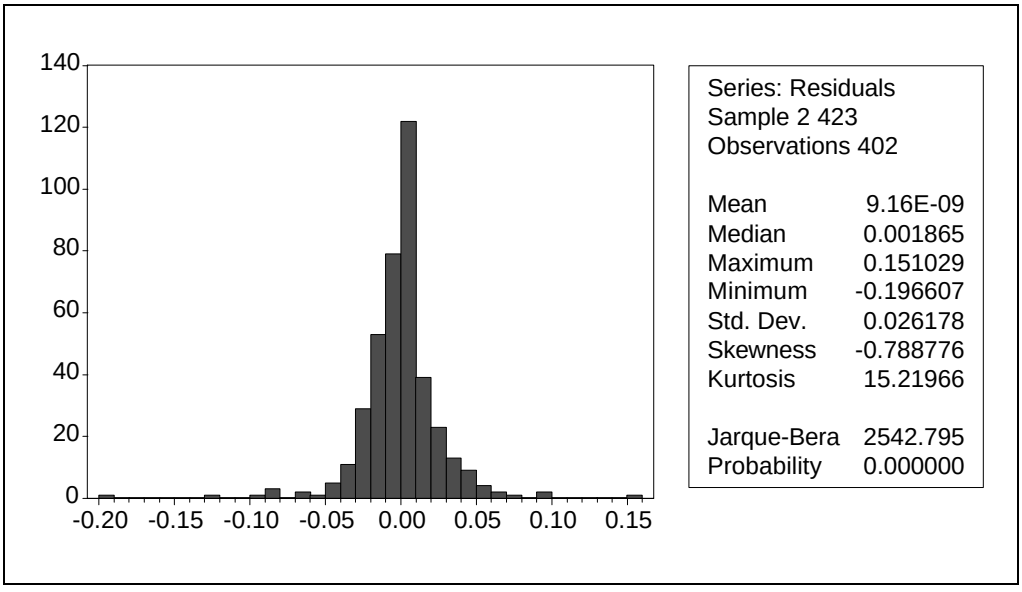

Figure H-6 Dissolved Total Carbon

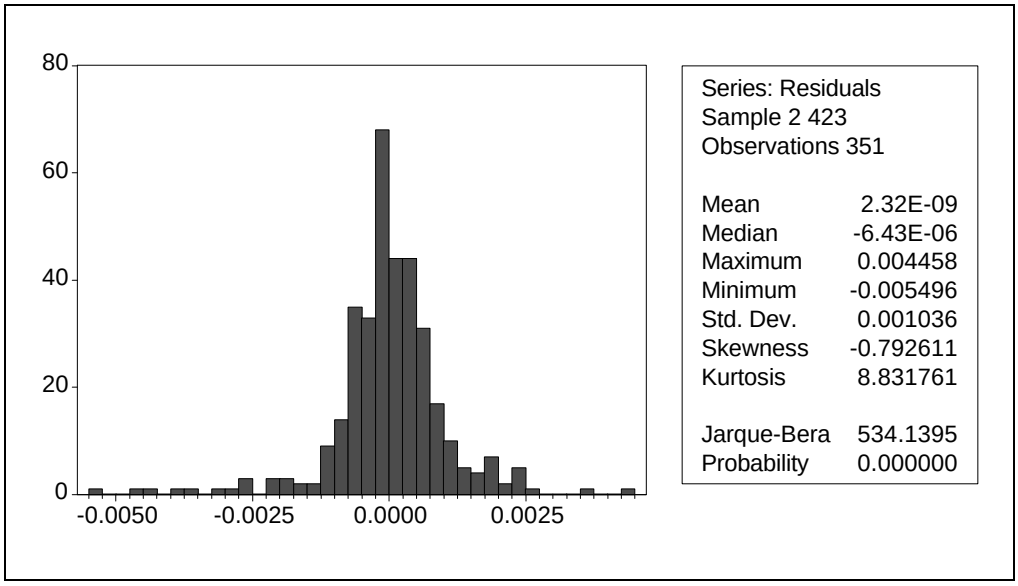

Figure H-7 Nitrate

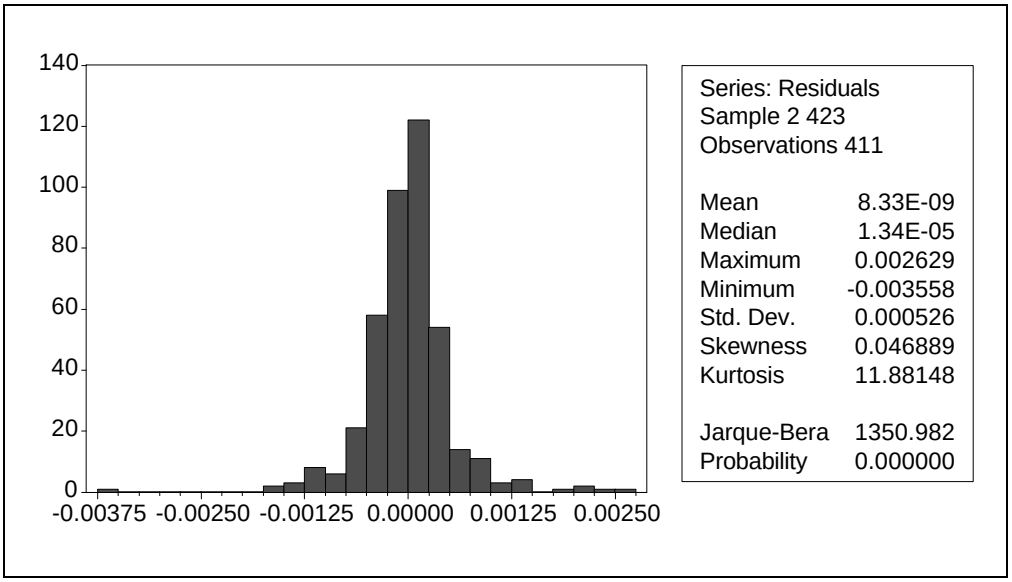

Figure H-8 Total Phosphorus

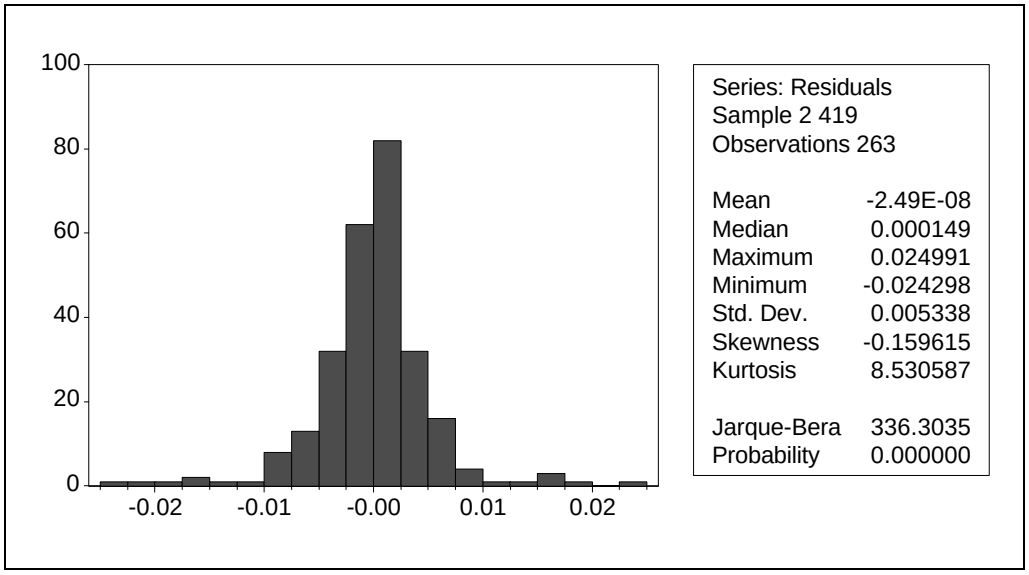

Figure H-9 Oil and Grease

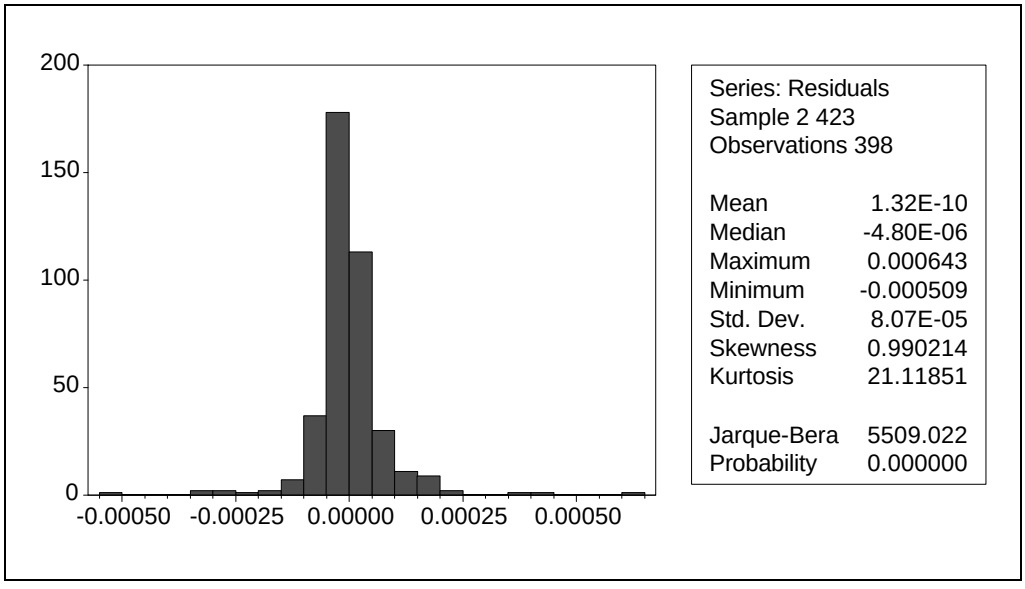

Figure H-10 Copper

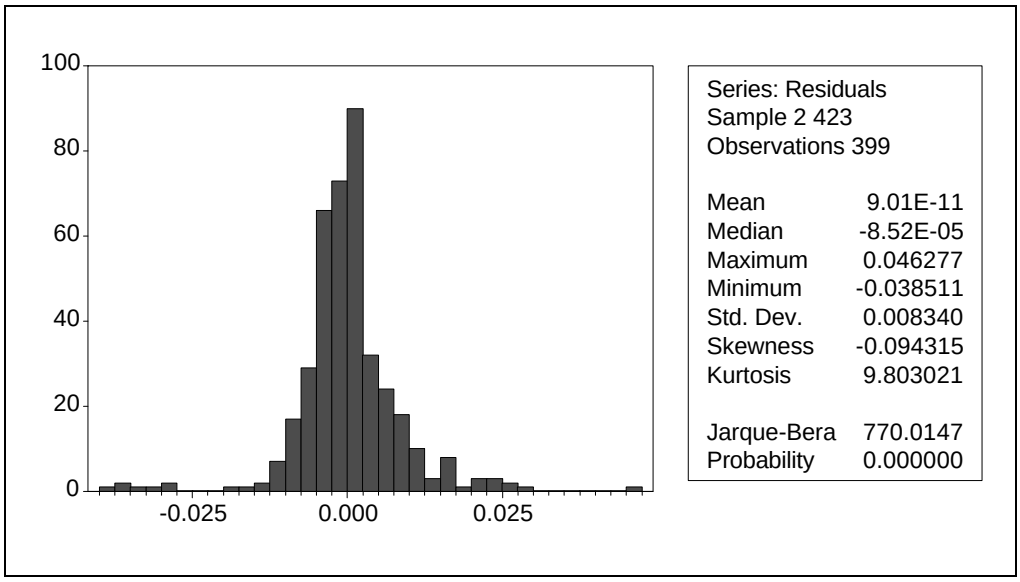

Figure H-11 Iron

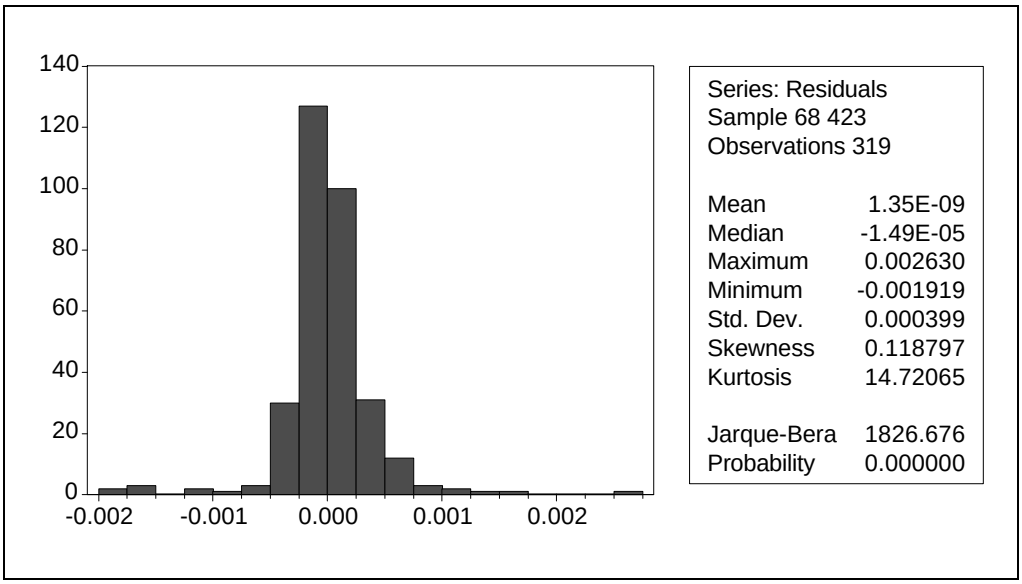

Figure H-12 Lead

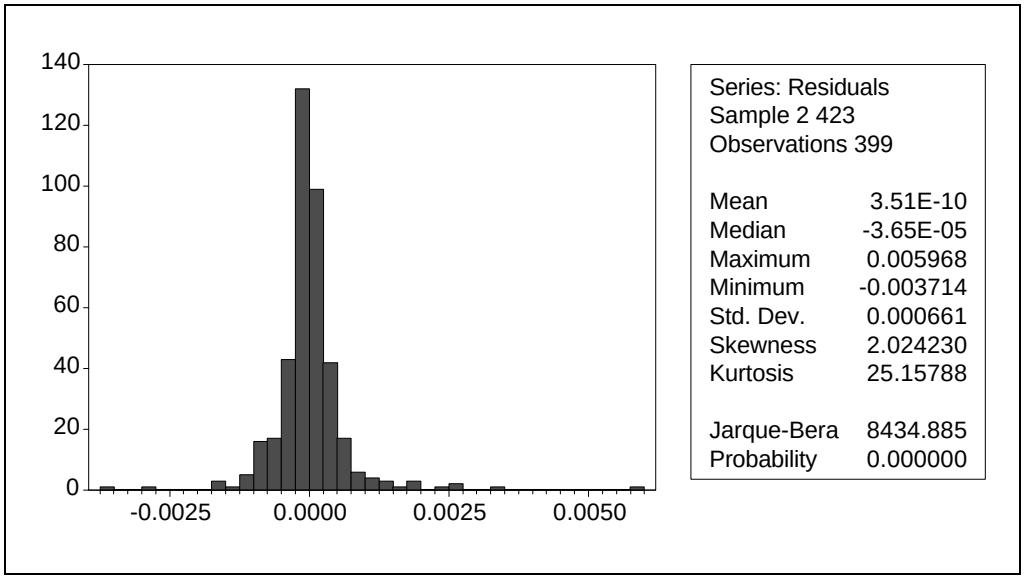

Figure H-13 Zinc

Appendix I
Regression Results

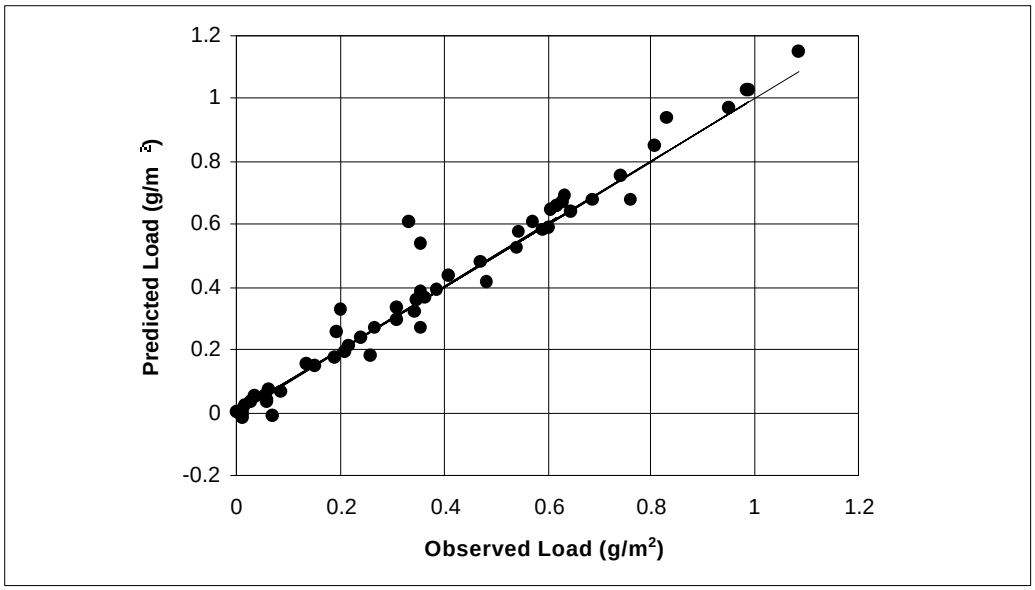

(a) Fit of Data from West 35th Street Site

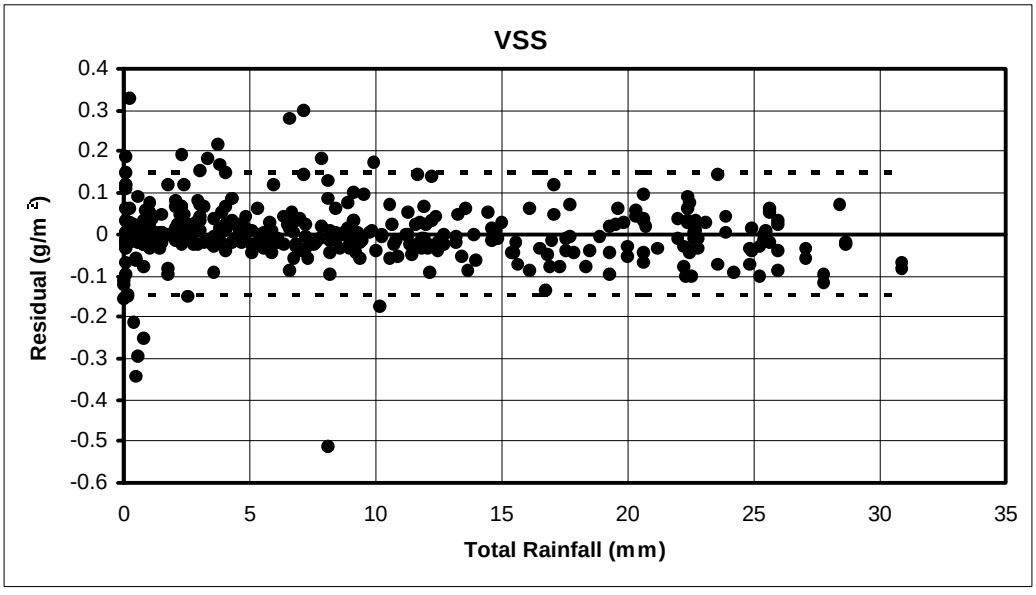

(b) Model Residuals vs. Total Rainfall (Dashed Lines Indicate ± 2 Std. Error)

Figure I-1 VSS Model Results

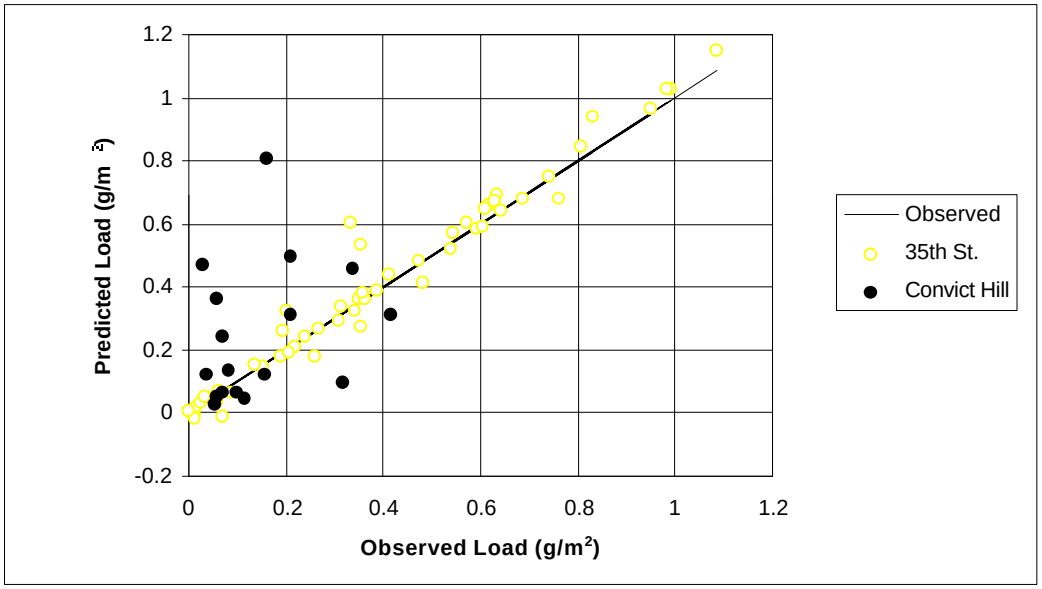

(a) Model Predictions at the Convict Hill Site

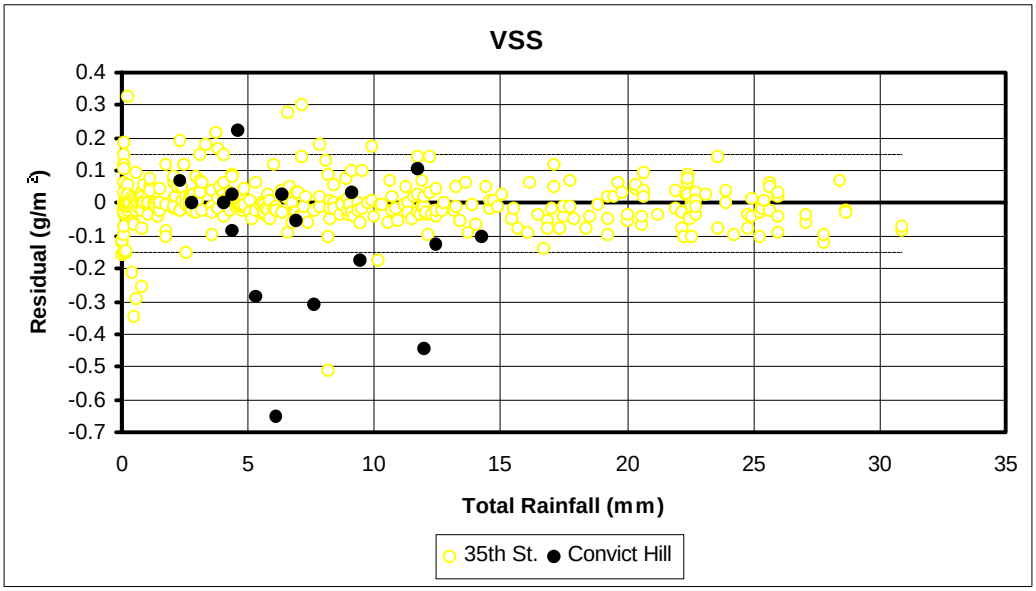

(b) Prediction Error vs. Total Rainfall

Figure I-2 VSS Model Predictions

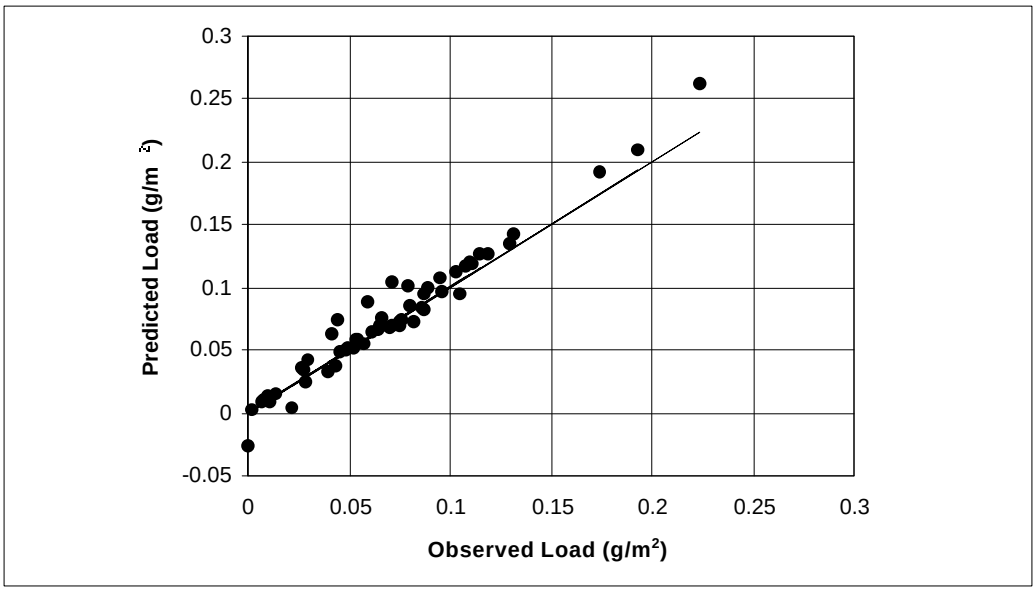

(a) Fit of Data from West 35th Street Site

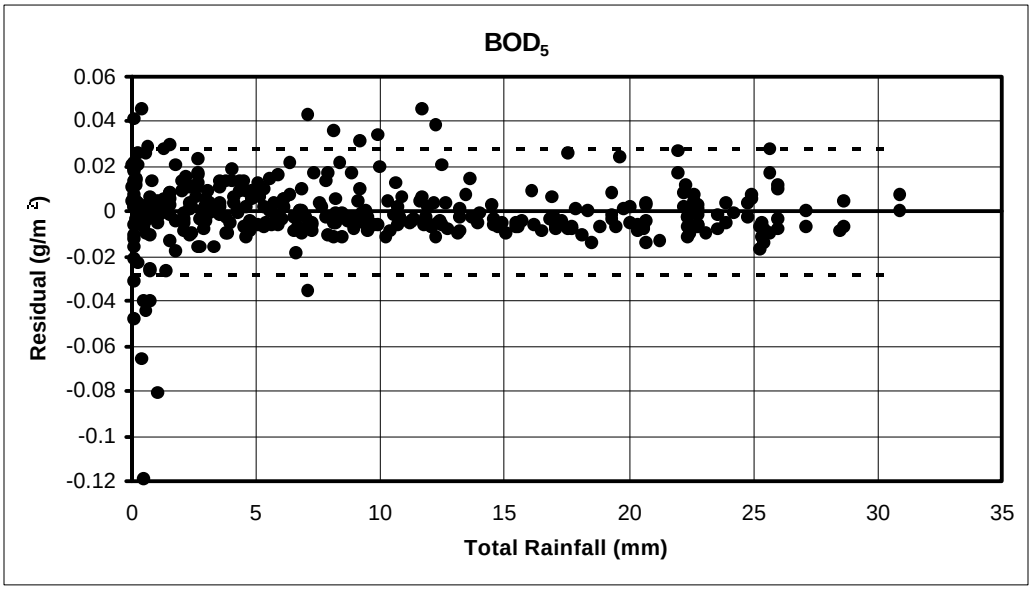

(b) Model Residuals vs. Total Rainfall (Dashed Lines Indicate ± 2 Std. Error)

Figure I-3 BOD_5 Model Results

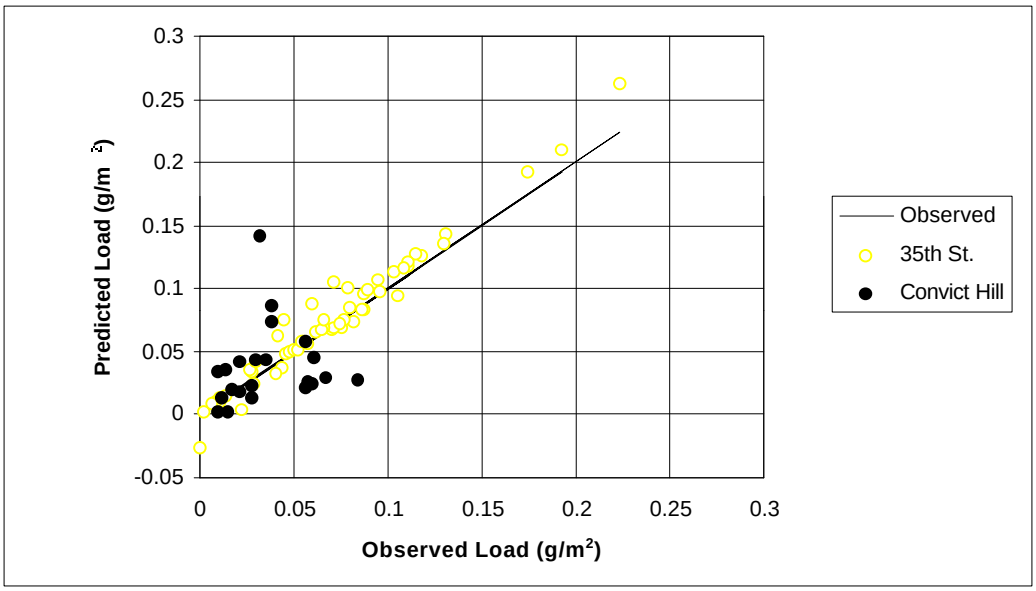

(a) Model Predictions at the Convict Hill Site

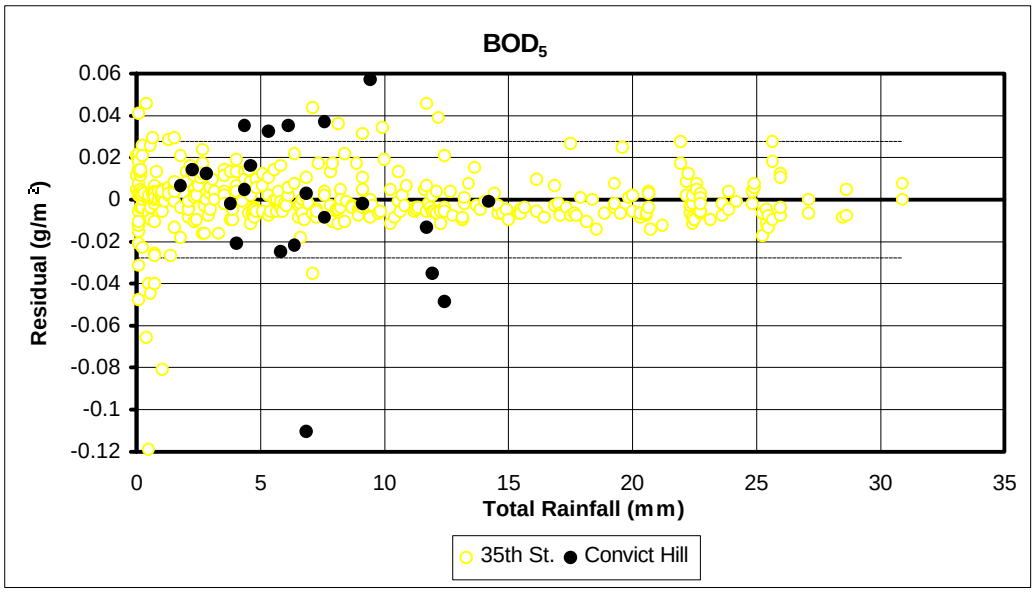

(b) Prediction Error vs. Total Rainfall

Figure I-4 BOD_5 Model Predictions

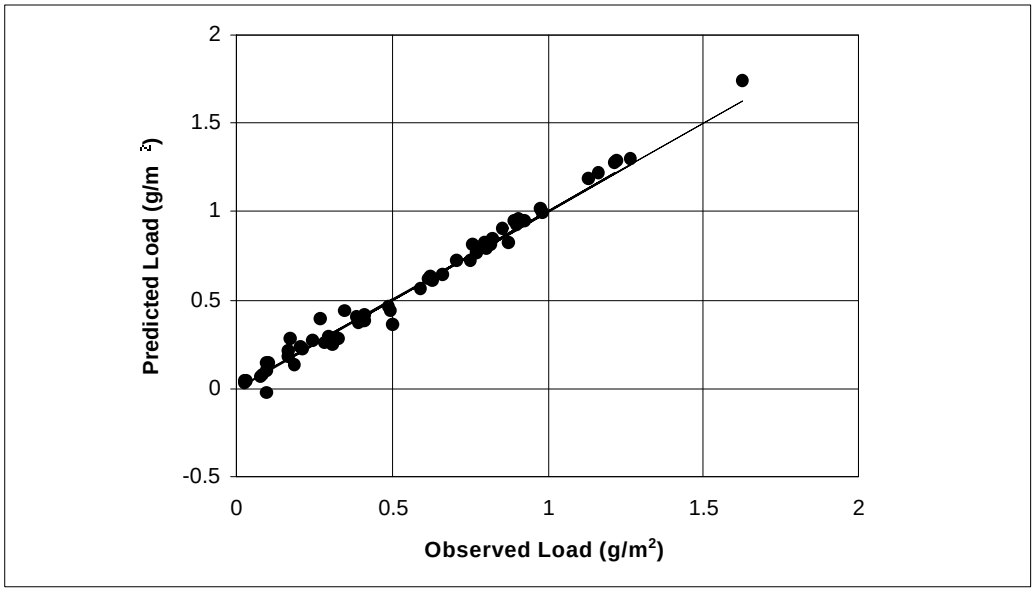

(a) Fit of Data from West 35th Street Site

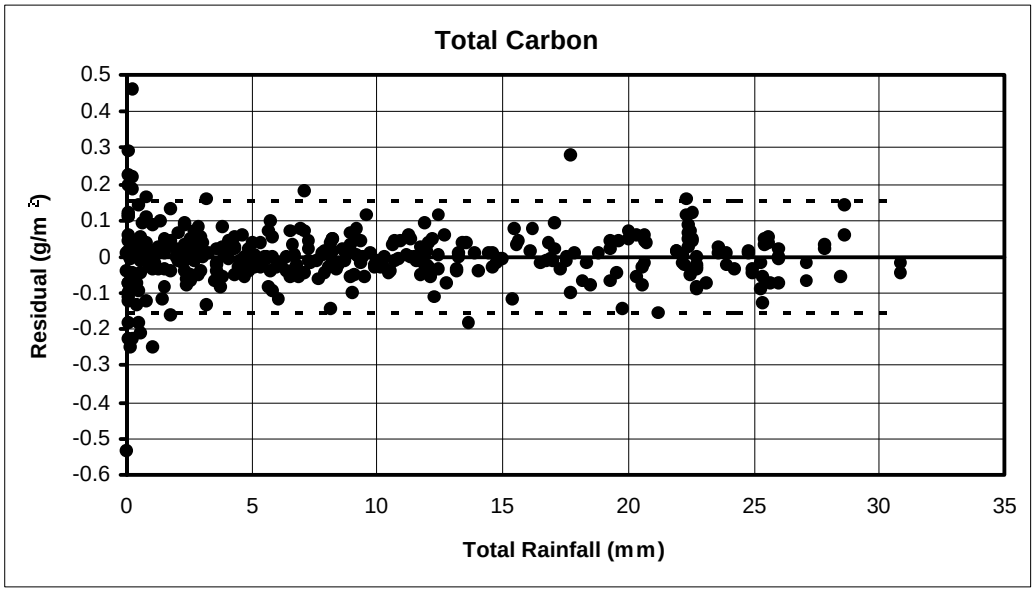

(b) Model Residuals vs. Total Rainfall (Dashed Lines Indicate ± 2 Std. Error)

Figure I-5 Total Carbon Model Results

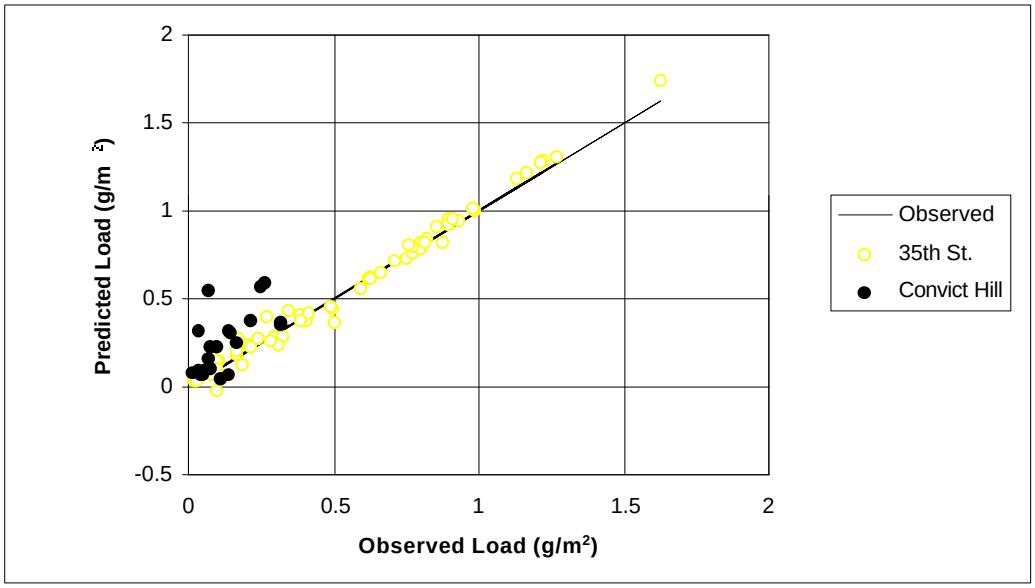

(a) Model Predictions at the Convict Hill Site

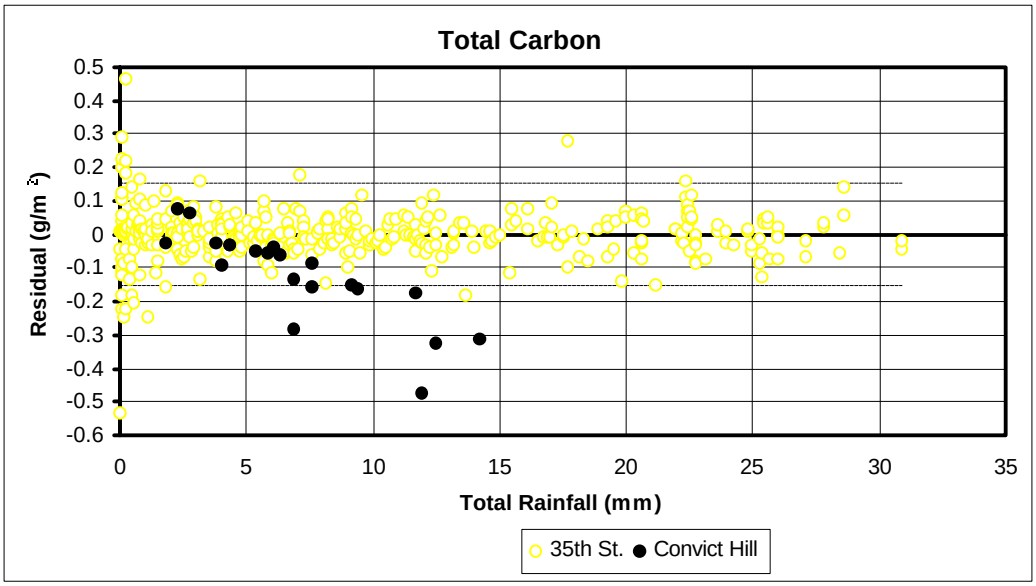

(b) Prediction Error vs. Total Rainfall

Figure I-6 Total Carbon Model Predictions

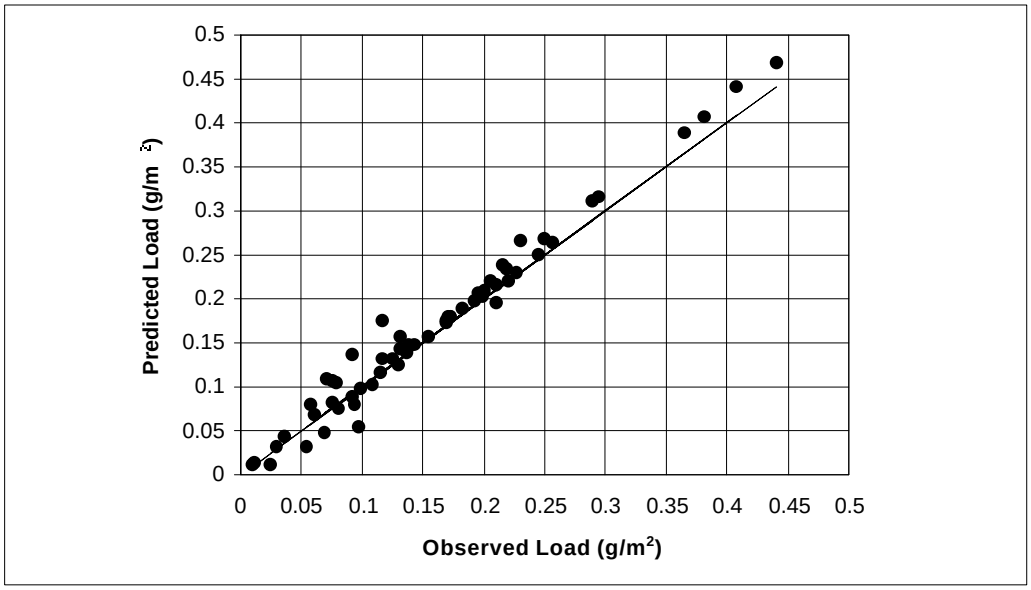

(a) Fit of Data from West 35th Street Site

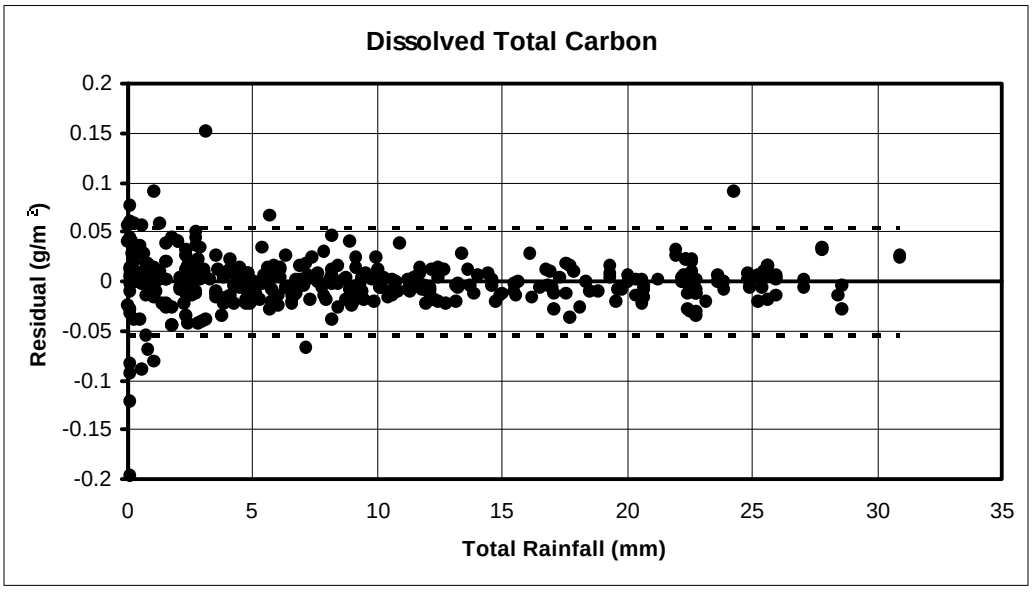

(b) Model Residuals vs. Total Rainfall (Dashed Lines Indicate ± 2 Std. Error)

Figure I-7 Dissolved Total Carbon Model Results

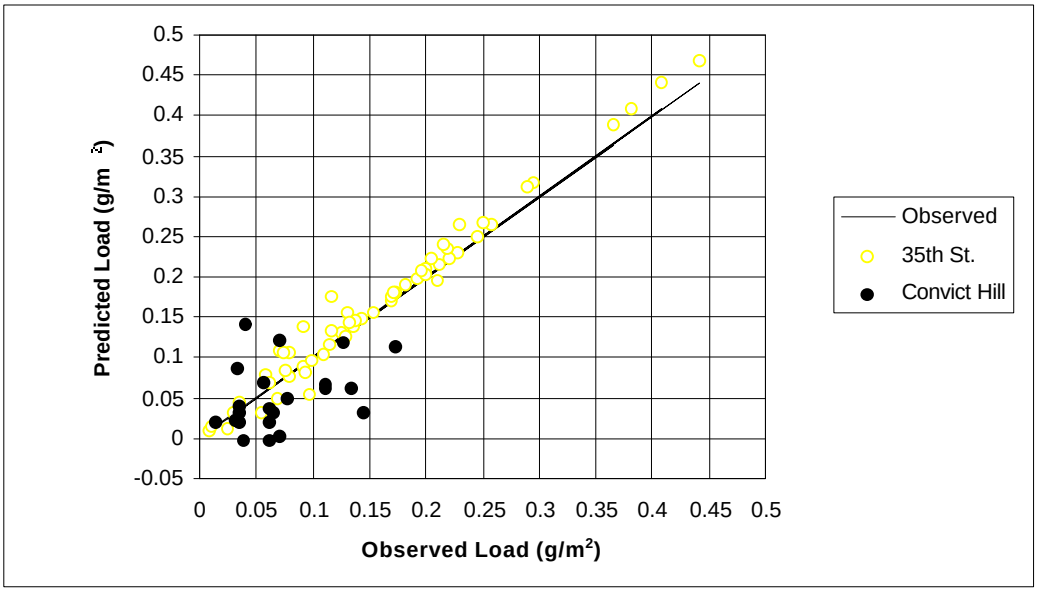

(a) Model Predictions at the Convict Hill Site

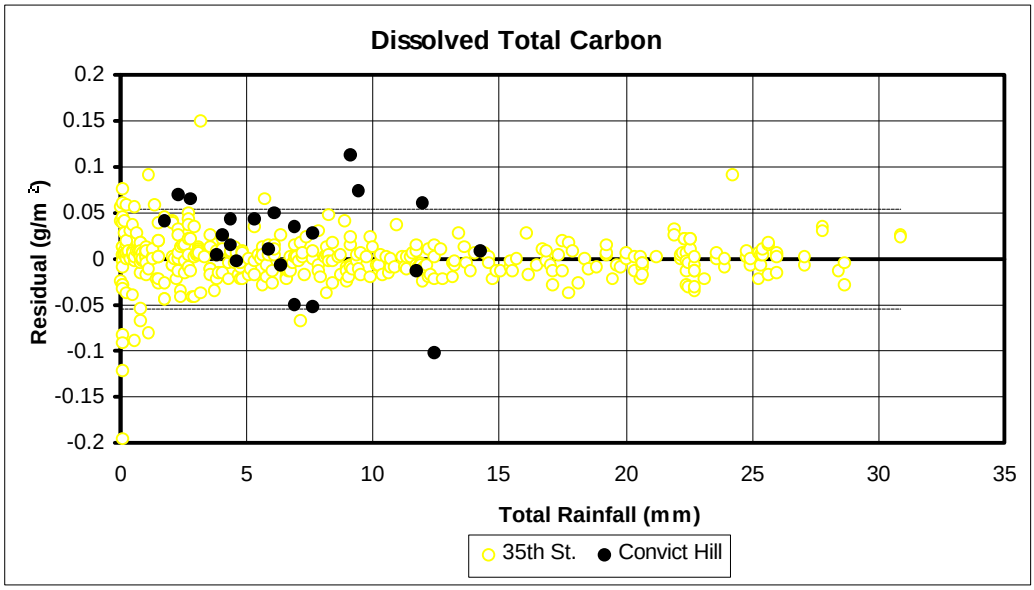

(b) Prediction Error vs. Total Rainfall

Figure I-8 Dissolved Total Carbon Model Predictions

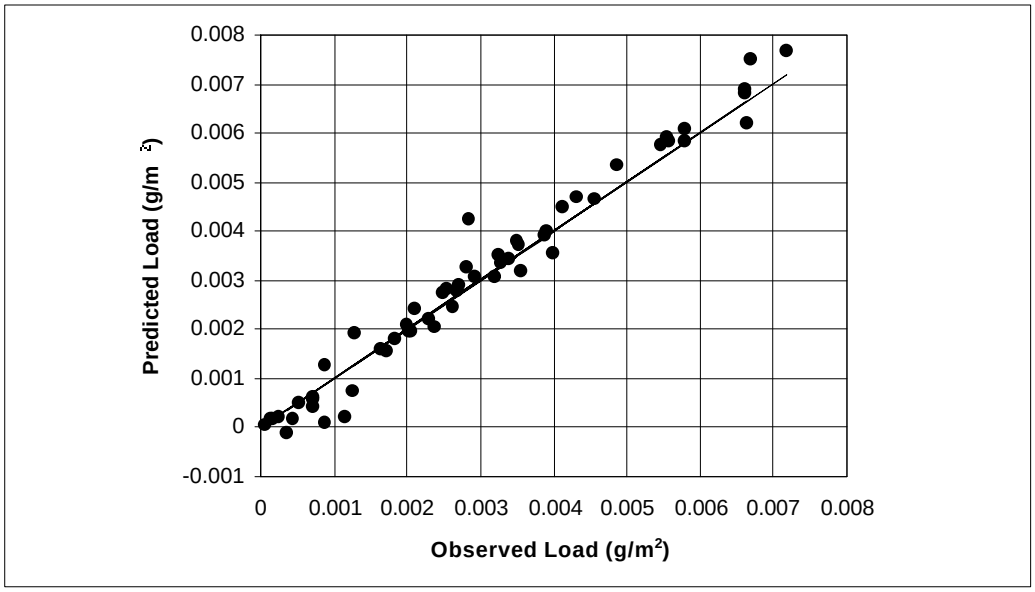

(a) Fit of Data from West 35th Street Site

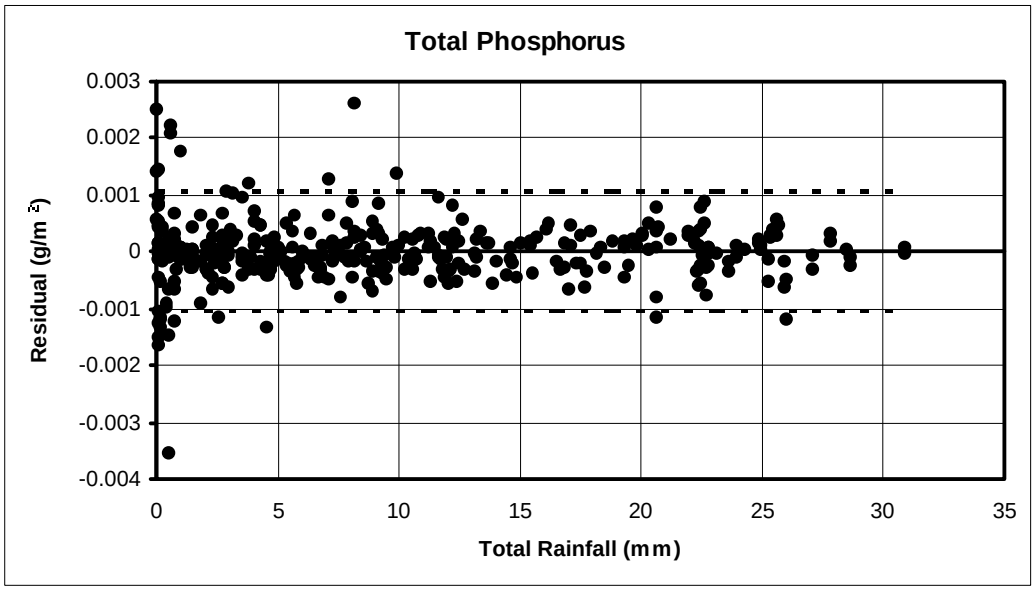

(b) Model Residuals vs. Total Rainfall (Dashed Lines Indicate ± 2 Std. Error)

Figure I-9 Total Phosphorus Model Results

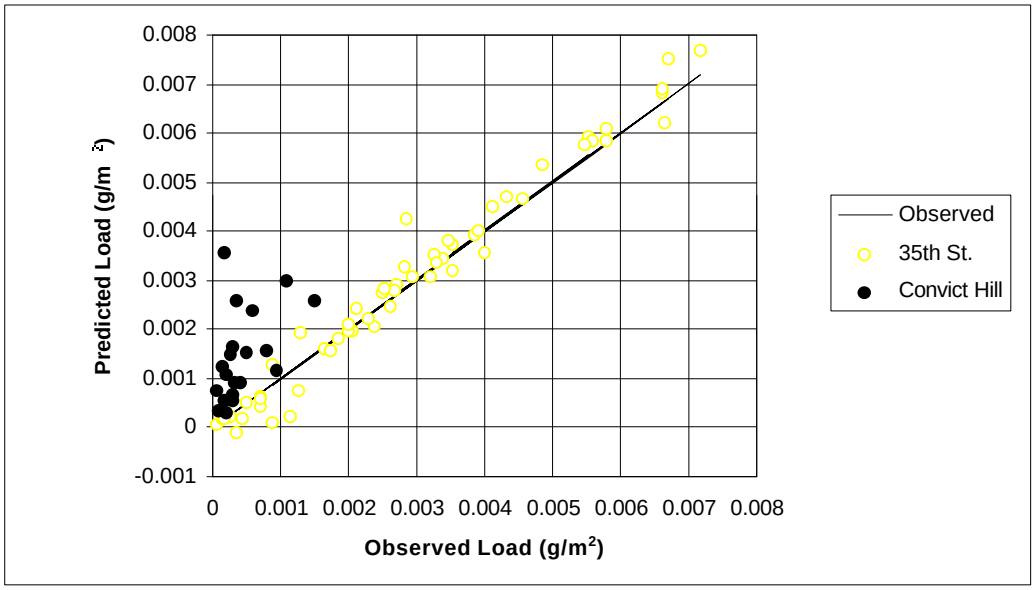

(a) Model Predictions at the Convict Hill Site

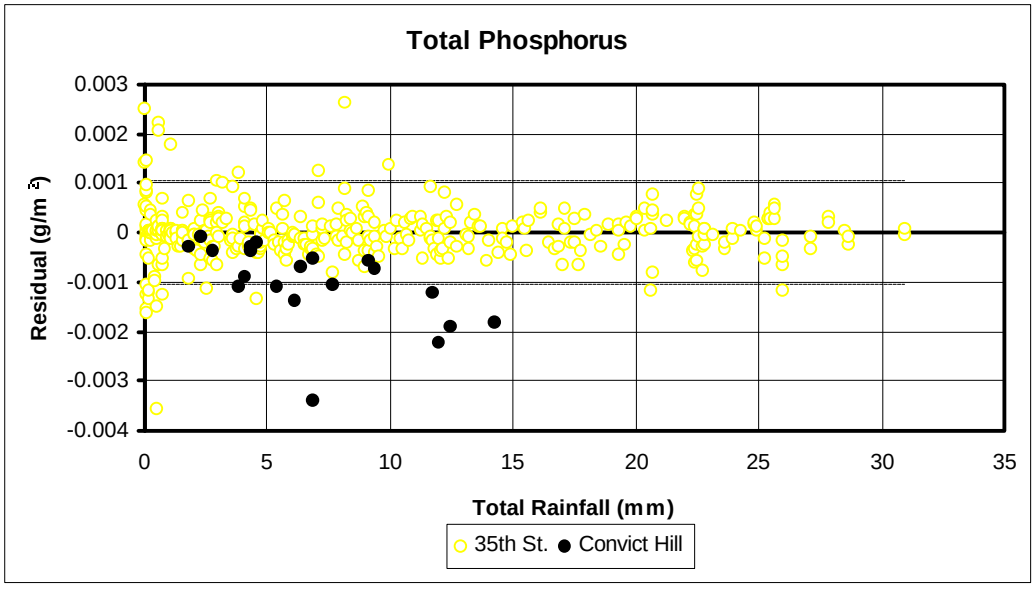

(b) Prediction Error vs. Total Rainfall

Figure I-10 Total Phosphorus Model Predictions

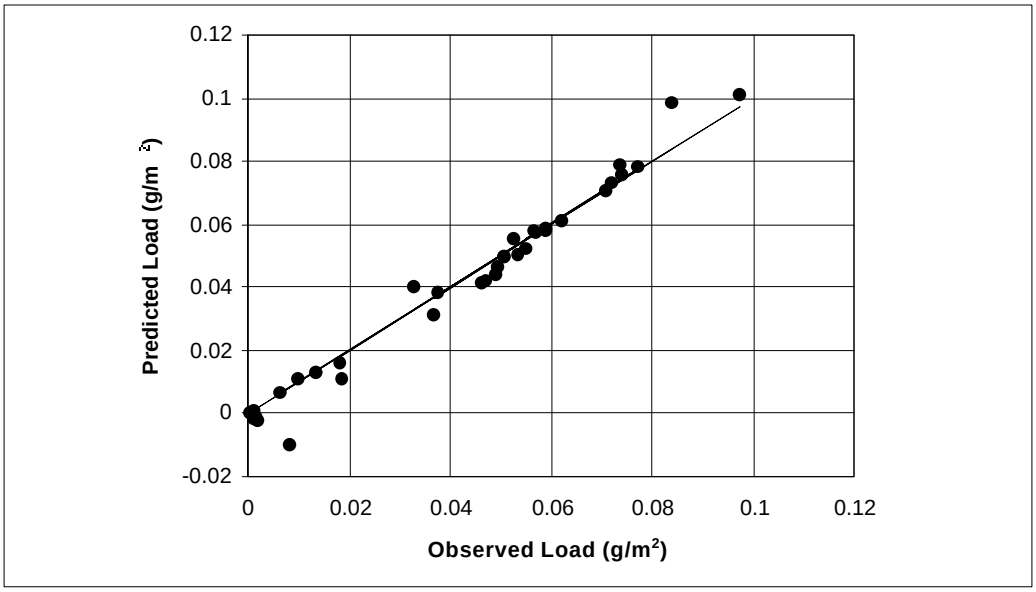

(a) Fit of Data from West 35th Street Site

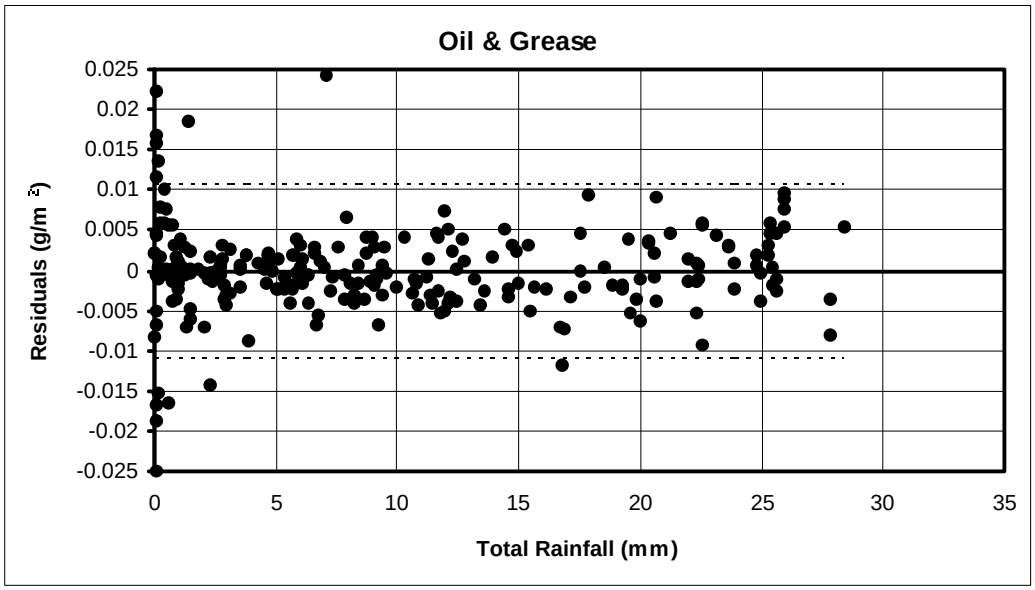

(b) Model Residuals vs. Total Rainfall (Dashed Lines Indicate ± 2 Std. Error)

Figure I-11 Oil and Grease Model Results

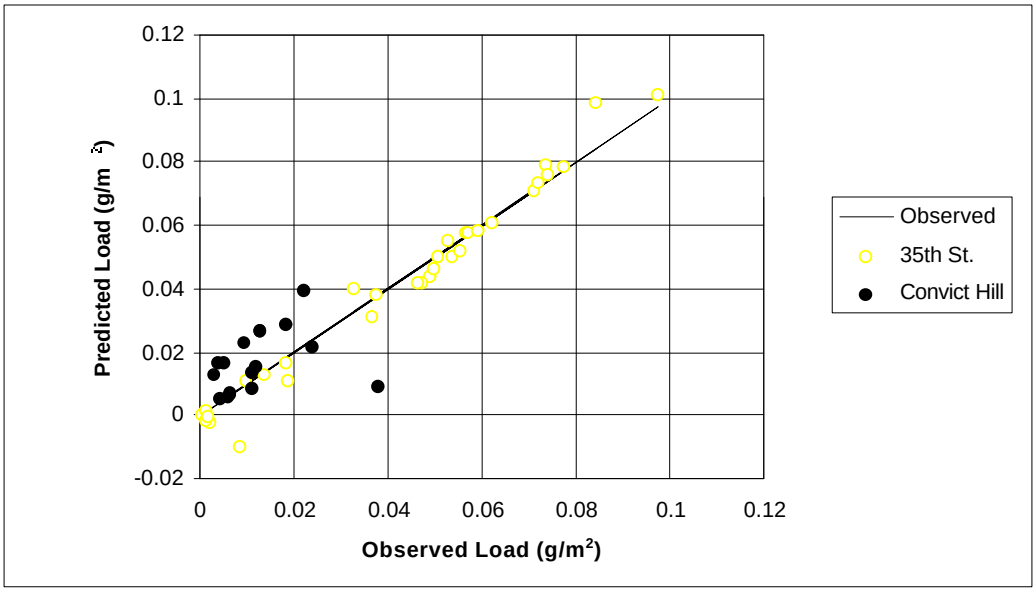

(a) Model Predictions at the Convict Hill Site

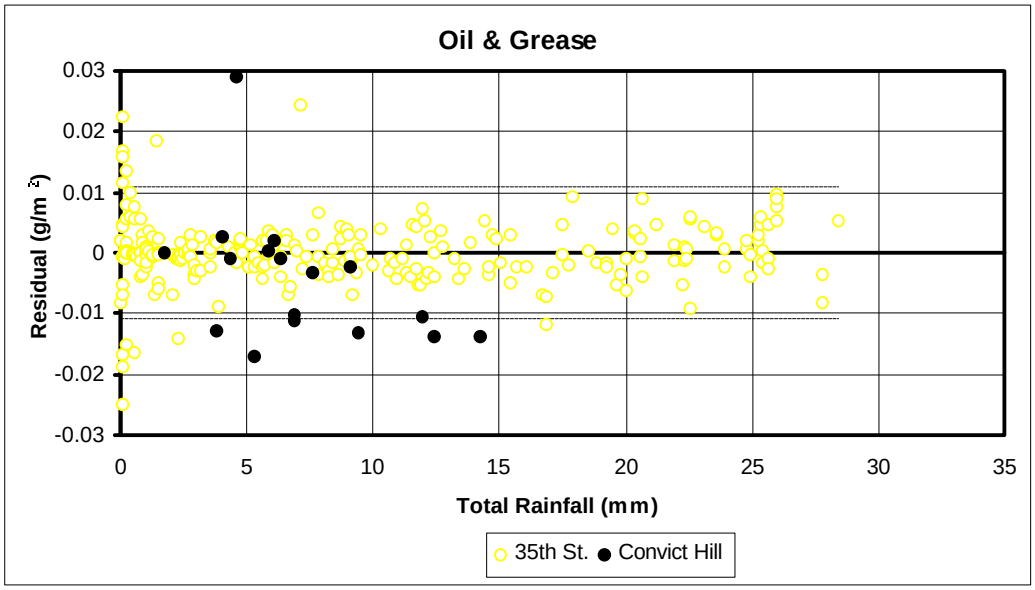

(b) Prediction Error vs. Total Rainfall

Figure I-12 Oil and Grease Model Predictions

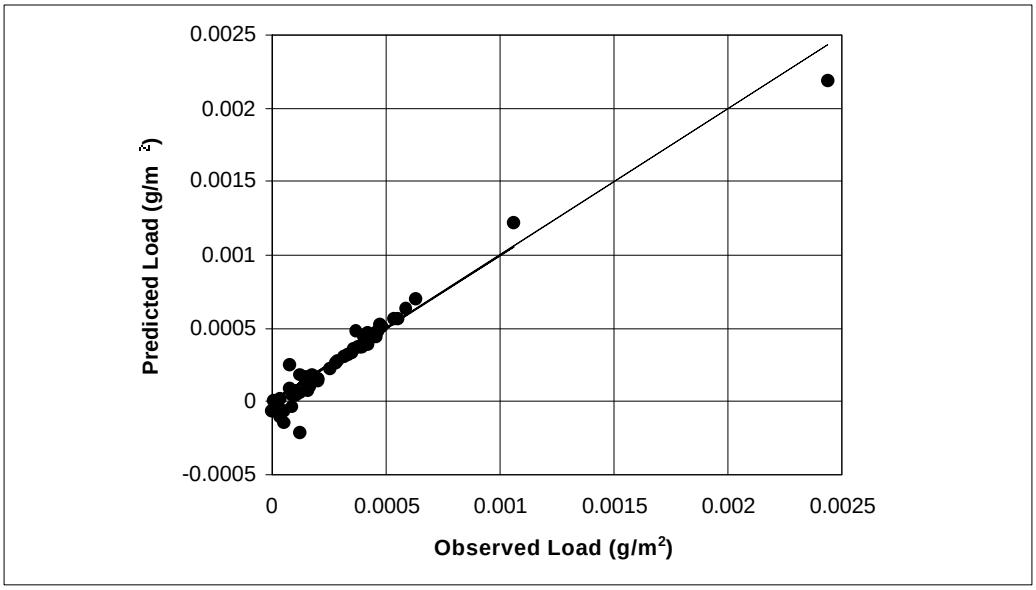

(a) Fit of Data from West 35th Street Site

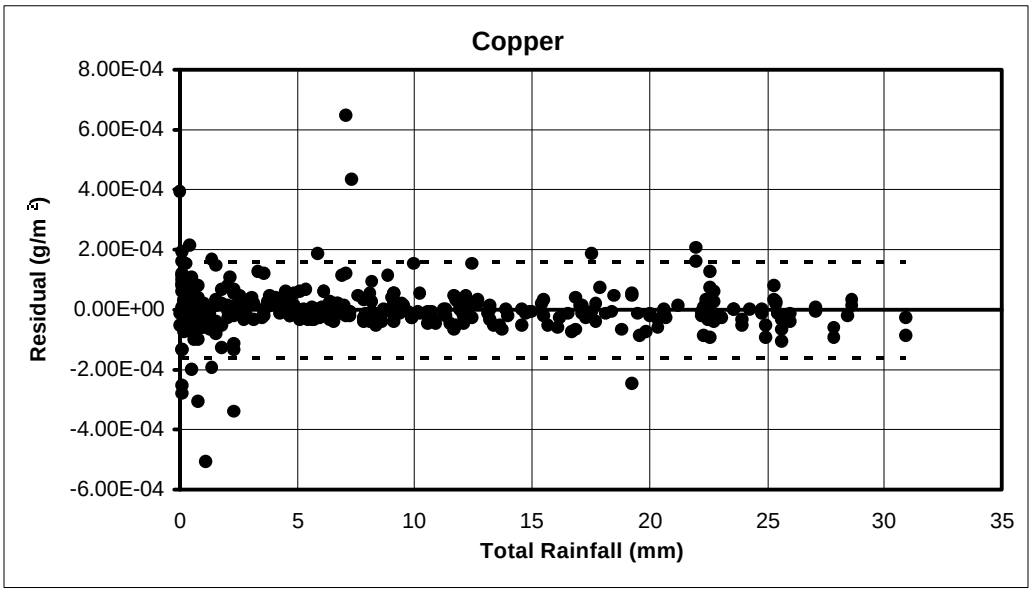

(b) Model Residuals vs. Total Rainfall (Dashed Lines Indicate ± 2 Std. Error)

Figure I-13 Copper Model Results

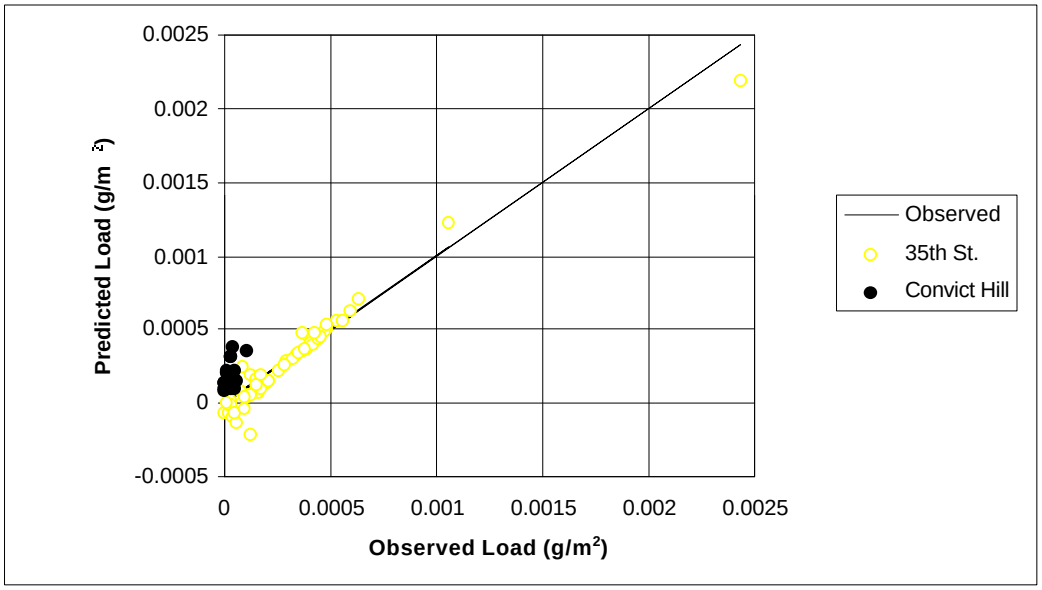

(a) Model Predictions at the Convict Hill Site

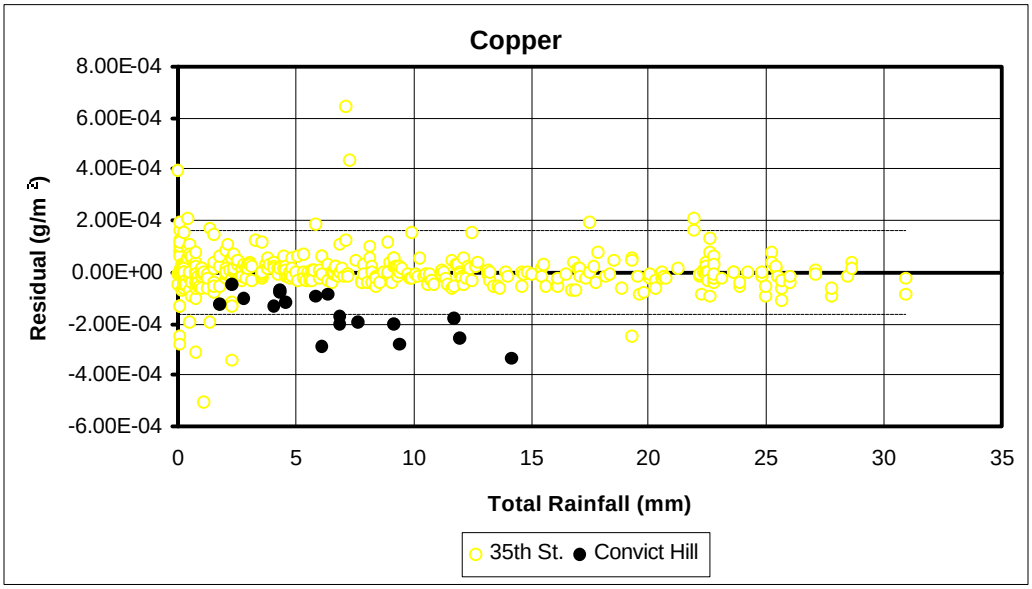

(b) Prediction Error vs. Total Rainfall

Figure I-14 Copper Model Predictions

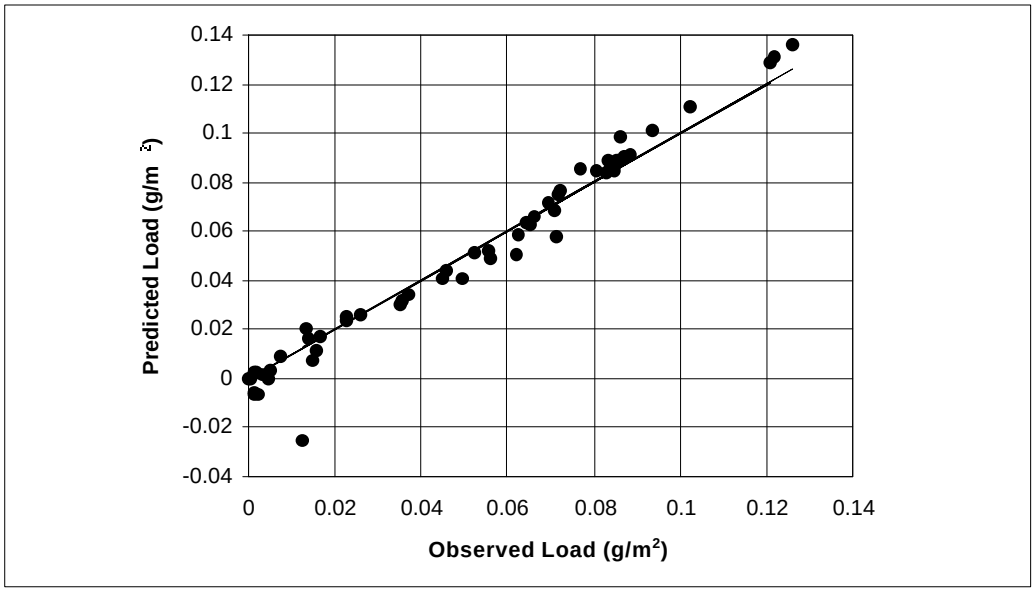

(a) Fit of Data from West 35th Street Site

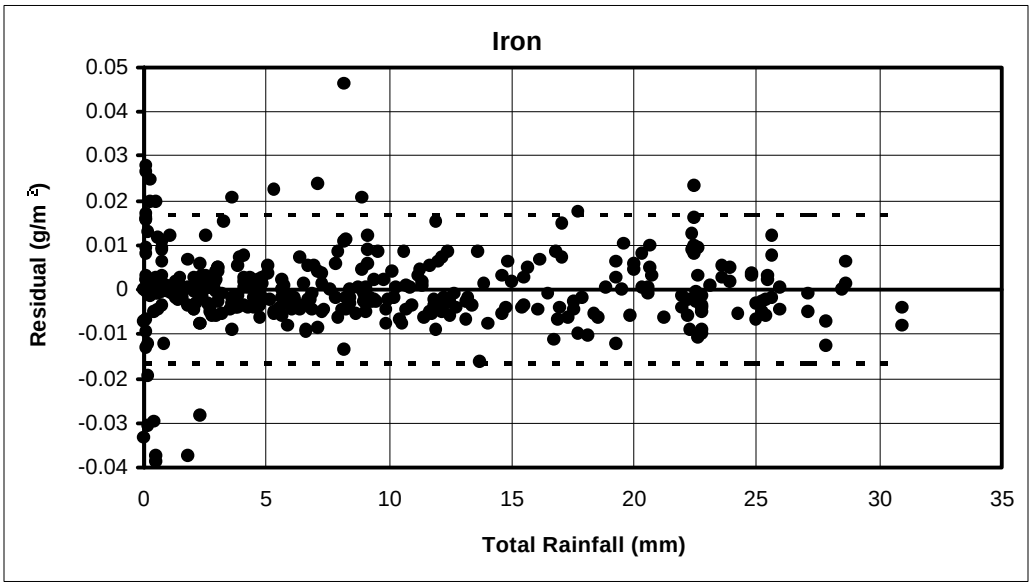

(b) Model Residuals vs. Total Rainfall (Dashed Lines Indicate ± 2 Std. Error)

Figure I-15 Iron Model Results

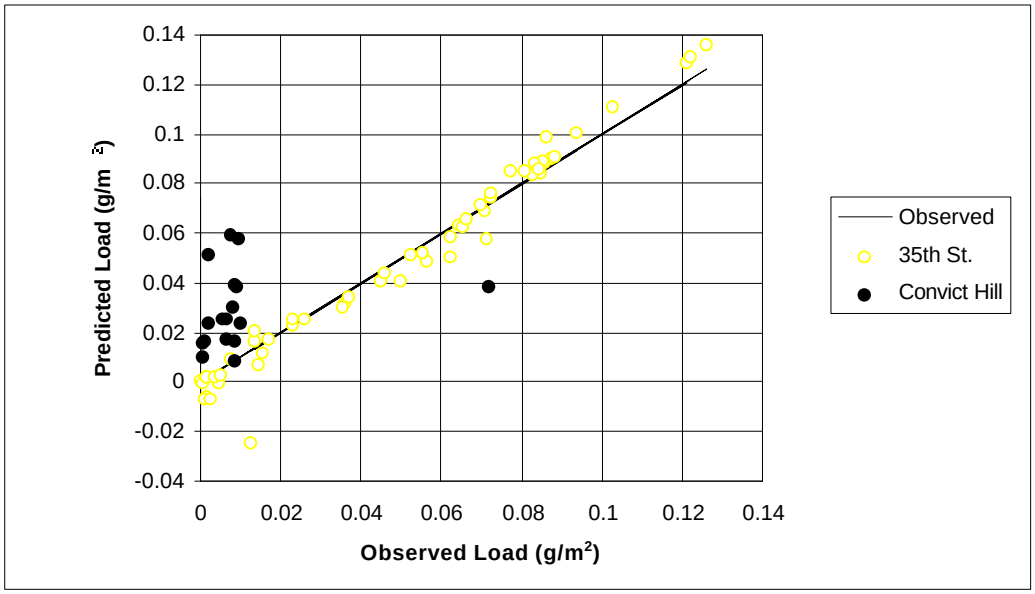

(a) Model Predictions at the Convict Hill Site

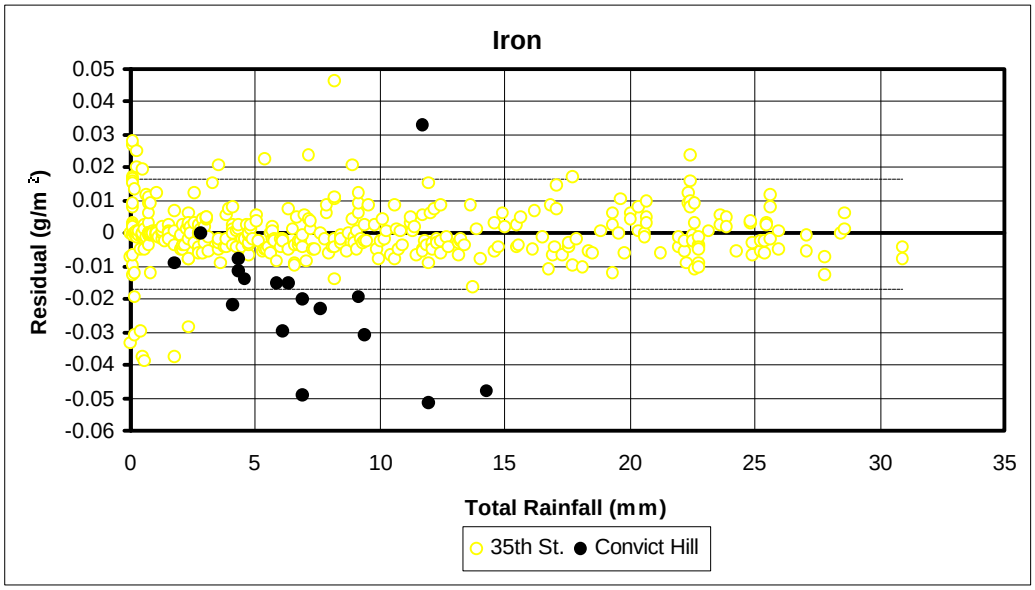

(b) Prediction Error vs. Total Rainfall

Figure I-16 Iron Model Predictions

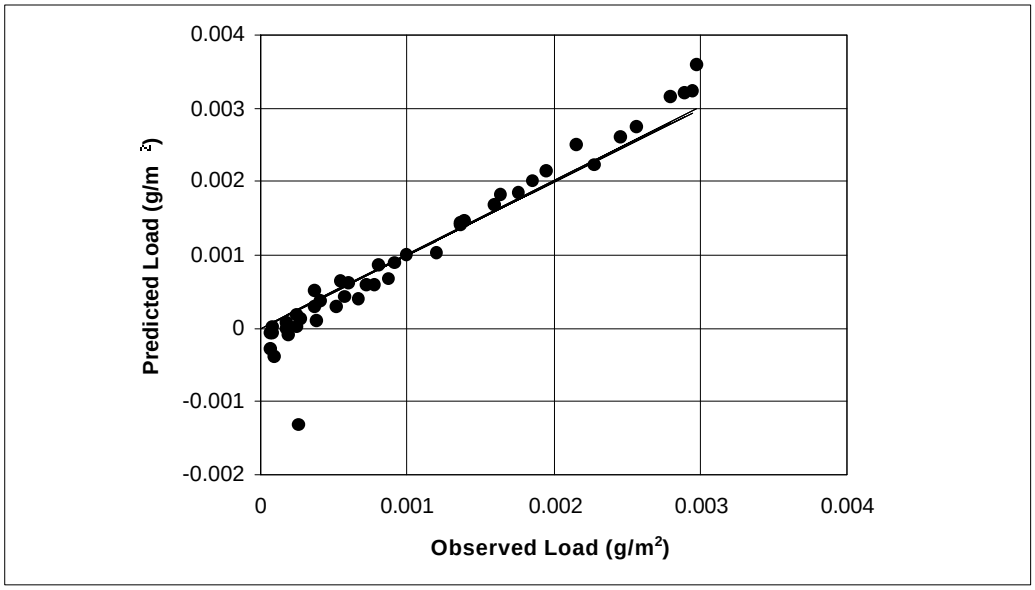

(a) Fit of Data from West 35th Street Site

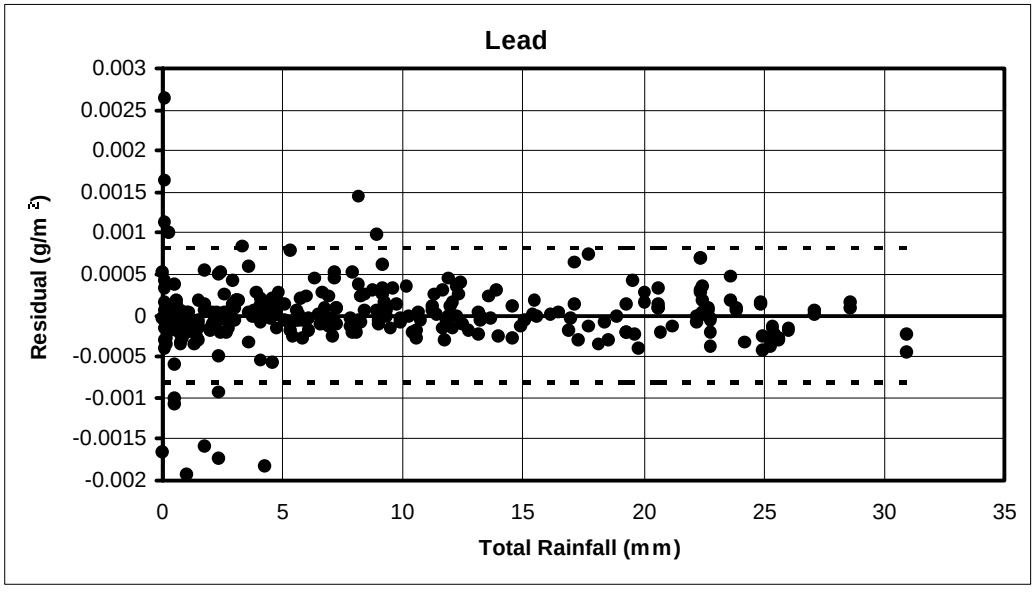

(b) Model Residuals vs. Total Rainfall (Dashed Lines Indicate ± 2 Std. Error)

Figure I-17 Lead Model Results

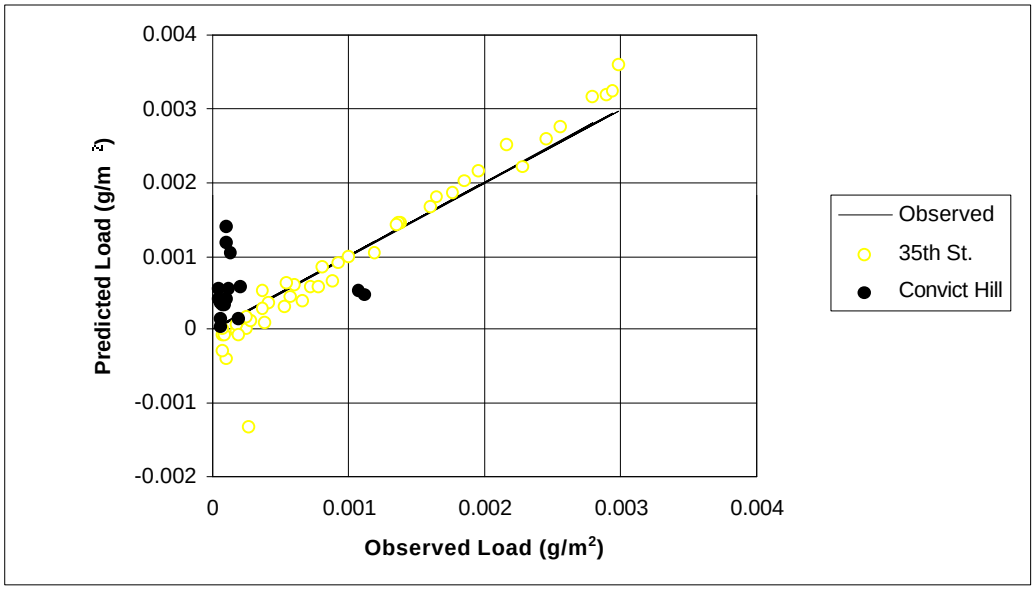

(a) Model Predictions at the Convict Hill Site

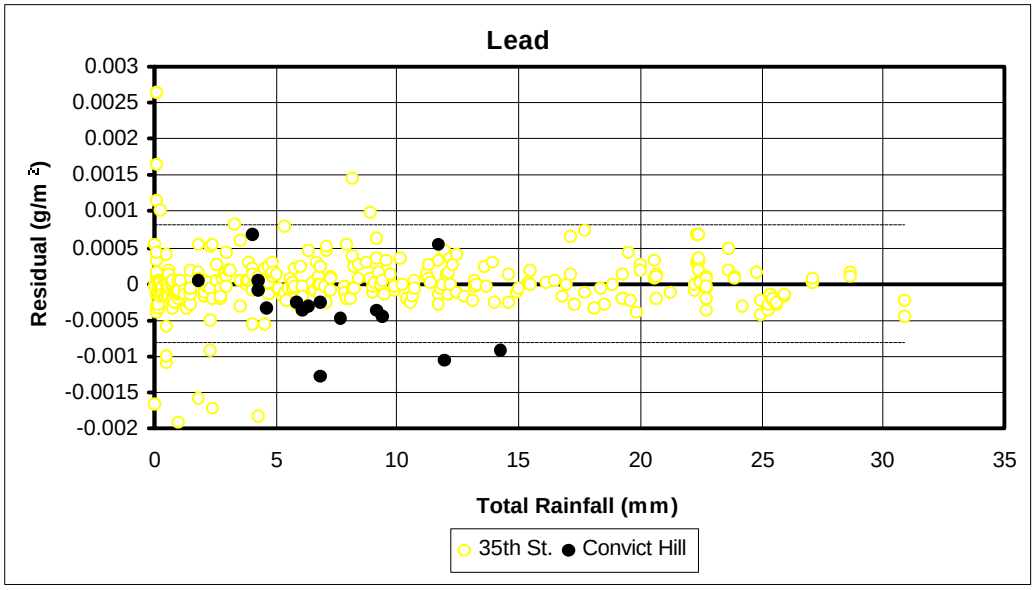

(b) Prediction Error vs. Total Rainfall

Figure I-18 Lead Model Predictions